UNIVERSITÀ DEGLI STUDI DI MILANO

Facoltà di Medicina e Chirurgia

Dipartimento di Biotecnologie Mediche e Medicina Traslazionale

DOTTORATO DI RICERCA IN

BIOTECNOLOGIE APPLICATE ALLE SCIENZE MEDICHE – CICLO XXVIII

Scuola di Dottorato in Scienze Biomediche Cliniche e Sperimentali

TESI DI DOTTORATO DI RICERCA

CO-TARGETING OF ONCOGENIC AND DEATH RECEPTORS PATHWAYS in HUMAN MELANOMA: PRE-CLINICAL RATIONALE FOR A PRO-APOPTOTIC AND ANTI-ANGIOGENIC STRATEGY

Settore BIO/13 – Biologia Applicata

DOTTORANDO

Dott.ssa Giulia Grazia

Matr. R10098

RELATORE

Prof. Carmelo Carlo-Stella

CORRELATORE

Dott. Andrea Anichini

Anno Accademico 2014-2015

Abstract

INTRODUCTION: Resistance to cell death is one of the well-known hallmarks of cancer. Metastatic melanoma is an aggressive disease whose treatment has significantly improved thanks to the recent development of either target-specific or immune-modulating agents. Since the FDA approval of the BRAFV600E inhibitor Vemurafenib in 2011, several other inhibitors, targeting relevant oncogenic signalling pathways (i.e. the MEK/ERK or the PI3K/Akt/mTOR pathways) have been used to treat melanoma patients. However intrinsic or acquired resistance limits the efficacy of these compounds, with relapses in most of the patients within 6 months. Therefore, there is an immediate necessity for new therapeutic strategies to face this issue, and one option could be represented by combinatorial treatments associating different anti-tumor agents able to target not only tumor cells but also to counteract pro-tumoral mechanisms in melanoma microenvironment.

HYPOTHESIS: Our goal was to obtain pre-clinical evidence for the efficacy of an anti-tumor approach based on the combination of MEK, PI3K inhibitors and TRAIL; building upon the hypothesis that these agents should:
1) be able to overcome melanoma intrinsic resistance to programmed cell death by the concomitant targeting of both the extrinsic (mainly through TRAIL activity) and the intrinsic (mainly due to the activity of MEK and PI3K pathway inhibitors) apoptosis pathways;
2) be able to promote an anti-angiogenic effect combining the well-known vascular disrupting activity of TRAIL and the effects of inhibition of pro-angiogenic pathways in tumor and in tumor-associated vasculature due to targeting of ERK and AKT cascades.

METHODS: A large panel of patient-derived melanoma cell lines was used to test the *in vitro* efficacy of the association between AZD6244/Selumetinib (a MEK1/2 inhibitor), the dual PI3K/mTOR inhibitor BEZ235, and soluble TRAIL. Chou-Talalay drug interaction analysis was used to determine Combination Indexes and Fraction Affected values for all the possible combinations of anti-tumor agents. Whole-genome gene expression profiling, flow cytometry experiments, western blot analysis, proteomic arrays and ELISAs were used to clarify the mechanism behind the synergy shown for the AZD6244+TRAIL and AZD6244+BEZ235+TRAIL associations. Moreover, xenografts in SCID mice were used to confirm the *in vivo* efficacy and mechanism of action of the combination between the MEK inhibitor and TRAIL, using tumor growth rates and immunohistochemistry on tumor nodules to evaluate effects of the association. Human Umbilical Vein Endothelial Cells (HUVEC) were chosen to model the endothelial-melanoma cell interaction in order to analyze its effects on response to the combinatorial treatment, both in terms of apoptosis induction and endothelial differentiation/activation status.

RESULTS: While half of the melanoma cell lines we tested were resistant to the death receptor ligand TRAIL, several were susceptible either to AZD6244 or to BEZ235, evidencing independent susceptibility profiles to these drugs and setting the rationale for their association. The combination of the MEK inhibitor, with or without the PI3K/mTOR inhibitor, and TRAIL achieved synergistic anti-tumor activity in 20/21 melanoma cell lines tested, including tumors resistant to either one of the agents.

Mechanistically, an increment in induction of caspase-dependent cell death and of mitochondrial depolarization was evidenced for the association, and a significant modulation of key regulators of extrinsic and intrinsic apoptosis pathways including c-FLIP, BIM, BAX, clusterin, Mcl-1 and several IAP family members was confirmed. Moreover, silencing experiments defined Apollon downmodulation as a central event for the promotion of the melanoma apoptotic response to our combinatorial treatments.

SCID mice bearing melanoma xenografts were treated with the MEK inhibitor and TRAIL, alone or in combination, obtaining a more significant tumor growth inhibition by the combinatorial treatment, with no detectable adverse events on mice body weight and tissue histology. TUNEL staining on tissues sections indicated also *in vivo* an increased promotion of tumor apoptosis, which was associated with suppression of several pro-angiogenic molecules like HIF1α, VEGFα, IL-8 and TGF1β as well as a marked reduction in CD31 positive cells.

Furthermore, initial results on HUVECs pointed at a possible effect of the interaction between endothelial and melanoma cells, affecting responsiveness of HUVECs to combinatorial treatments, as documented by increased endothelial cell apoptosis, in response to MEK inhibitor and TRAIL treatment, after co-culture with melanoma cells. The modulatory effect of melanoma on endothelial cells was evidenced not only by “activation” markers (upregulation of ICAM-1/CD54) but also the “differentiation” status of endothelial cells, indicated by increased alpha-SMA levels, reduction in the expression of vascular cadherin CD144 and downmodulation of the endothelial marker CD31.

CONCLUSIONS: Results of this work suggest that concomitant targeting of melanoma oncogenic signalling pathways and the TRAIL receptor cascade can not only overcome *in vitro* tumor resistance to different anti-tumor agents, but can also have *in vivo* effects on tumor microenvironment, promoting pro-apoptotic effects and inhibition of tumor angiogenesis. Moreover, this could be associated to a modulation of endothelium responsiveness to anti tumor agents by direct interaction with melanoma cells.

1. INTRODUCTION

1.1 METASTATIC MELANOMA: AN AGGRESSIVE DISEASE WITH A POOR PROGNOSIS

1.1.1 Incidence, origin and classification

Melanoma is one of the most aggressive human cancers, representing less than 4% of all skin neoplasms, yet being responsible for more than 75% of deaths related to cutaneous malignancies. Its incidence is still increasing, with more than 160000 new cases per year worldwide.[1,2]

Cutaneous melanomas origin from aberrant transformations occurring in melanocytes, the melanin-producing cells of the body, responsible for skin pigmentation and sun protection.[3] Exposure to UV light increases skin pigmentation through the activity of the α-melanocyte stimulating hormone (α-MSH) secreted by keratinocytes after a p53-dependent induction of proopiomelanocortin (POMC) and its post-translational cleavage.[4] Melanocytes express the melanocortin 1 receptor (MC1R) [5] that, upon binding to α-MSH, promotes pigment synthesis and melanin production through the activation of the microphthalmia-associated transcription factor (MITF), which is considered the "master regulator" of melanocyte biology and whose levels determine the activation of different sets of target genes. [3]

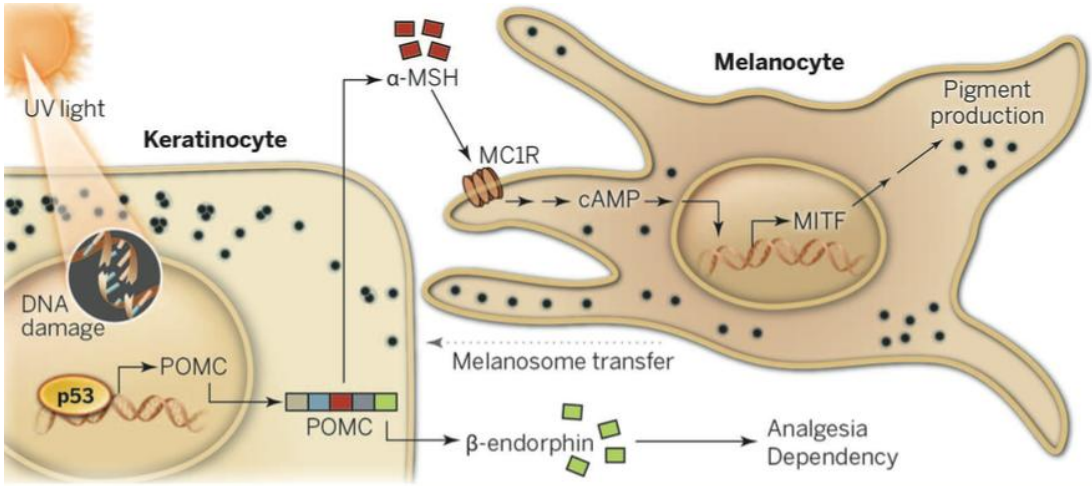

Figure 1.1: UVR response in melanocytes. UVR-induced DNA damage induces p53 activation in keratinocytes and consequant up-regulation of proopiomelanocortin (POMC). β-endorphin and α-MSH are produced by post-translational cleavage of POMC and the secreted α-MSH is the ligand for MC1R on melanocytes. Its activation results in melanin synthesis and transfer to keratinocytes.

Melanomas can occur de novo or progress from pre-existing benign nevi through different and subsequent histological phases. [6]

The Clark model was the first to describe morphological changes that characterize melanomagenesis and progression from normal skin to malignant melanoma. [7]

The first phenotypic change is the onset of a benign nevus: here the control of cell growth is disrupted but aberrant proliferation is still limited. At molecular level we can find abnormal activation of the mitogen-activated protein-kinases (MAPK) pathway, possibly due to somatic mutation in N-RAS or BRAF, key components of the MAPK cascade. The next event gives rise to a dysplastic nevus, associated with abnormalities in mechanisms that control cell cycle progression after DNA repair (i.e. deletion in cyclin-dependent kinase inhibitor 2A (CDKN2A)) and susceptibility to cell death (i.e. deletions of the phosphatase and tensin homologue (PTEN)). Further progression generates *in situ* melanoma, characterized by a radial growth phase (RGP) were melanoma cells spread in the upper epidermis; this step can be associated with decreased activity of MITF and consequent decrease in differentiation and expression of melanoma markers. Malignant melanoma is marked by more rapid vertical growth phase (VGP) were neoplastic cells invades the dermis and deeper structures and can metastasize and spread throughout the body. [7]

Not all melanomas pass through each of these phases but can arise directly from isolated melanocytes.

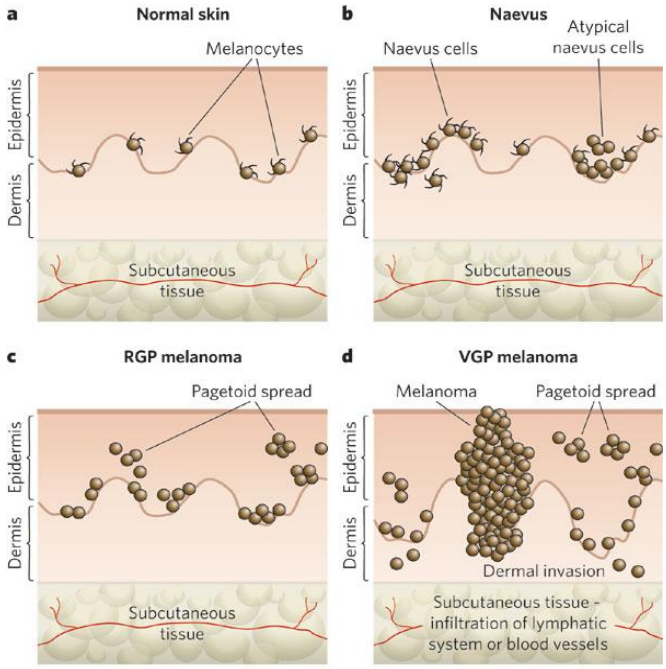

Figure 1.2: Melanomagenesis. A) Skin composition under physiological conditions; **B**) Nevi are characterized by atypical growth of melanocytes and can become dysplastic; **C**) Radial-growth-phase (RGP) melanoma is the first malignant stage; **D**) Vertical-growth-phase (VGP) melanoma, at this stage melanoma cells acquire metastatic potential and can infiltrate the vascular and lymphatic systems.

A more recent study by Hunter Shain *et al.* [8] has proposed a model for the genetic evolution of melanoma. As shown in Figure 1.3, they have reported that all benign lesions harbor BRAF V600E pathogenic alteration, therefore demonstrating that this mutations is sufficient to form a nevus. The progression towards a malignant lesion is then initiated by other

mutations that affect the MAPK cascade (NRAS or other BRAF mutations), followed by TERT mutations, characteristics that have been proposed to define “intermediate lesions”. The presence of TERT mutations at these early stages suggests that precursors cells (naevus cells) that exhaust their replicative potential proceed toward a replicative senescence [9], while other precursors can bypass this mechanism, keep on dividing, and acquire new mutations progressing toward the melanoma stage.

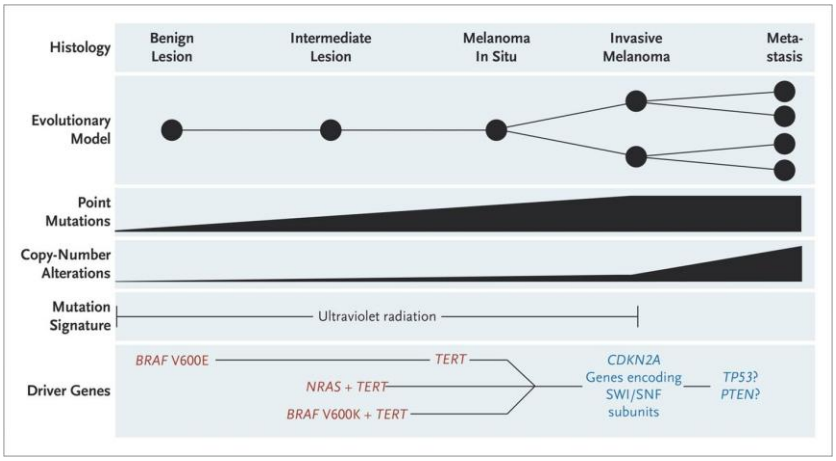

Figure 1.3: Proposed model for melanoma progression and corresponding genetic alterations.

Melanomas can be classified based on site of origin, tumor thickness and histologic subtype. More than 90% of all melanomas are from cutaneous origin, but other primary sites of onset include mucosal, uveal and leptomeningeal.

Classification of cutaneous melanomas defines four major subtypes, with different patterns of growth and anatomic locations: superficial spreading (SSM), lentigo maligna (LM), acral lentiginous and nodular. [10]

Figure 4: **Different type of cutaneous melanoma**. **A)** Superficial spreading melanoma. **B)** Nodular melanoma. **C)** Lentigo maligna melanoma. **D)** Acral lentiginous melanoma

While superficial spreading melanoma can be found in any part of the skin but is most frequent on sites with acute-intermittent sun exposure, NM (nodular melanoma) is the

second most common subtype and is particularly localized on the trunk, head and neck. Different types have distinct biological and clinical behaviors: for example lentigo maligna are indolent tumors that develop over decades on chronically sun-exposed area such as the face, while, on the other hand, acral lentigenous melanoma is usually found on palms, soles and nails (sun-protected regions) and tend to be more aggressive [11]

Subtype	Frequency	Common site	Key distinguishing features
Superficial spreading melanoma	70%	Trunk of men Legs of women	RGP, 1–5 years
Nodular melanoma	10–25%	Trunk of men Legs of women	RGP, 6–18 months
Acral lentiginous melanoma	5%	Palms, soles, nails	Not related to sun damage All races affected Accounts for 30–70% of melanoma in dark-skinned individuals
Lentigo maligna melanoma	<1%	Head and neck of elderly	Associated with chronic sun exposure RGP, 3–15 years
Noncutaneous melanoma	5%	Ocular, mucosal	Not associated with sun exposure Prognostic features and treatment differ from that of cutaneous subtypes

Table 1.1: **Classification of melanoma**.

The TNM Classification of Malignant Tumours (TNM) is a globally used system that describes the stage of a solid tumor based on three main parameters[12]:

- T describes the size of the primary tumor and whether it has invaded other tissues,
- N describes involvement of regional lymph nodes,
- M describes presence/absence of distant metastasis.

Guidelines of the American Joint Committee on Cancer (AJCC) and the Union for International Cancer Control (UICC) determine the classification of melanomas on the bases of tumor thickness, mitotic rate and ulceration, histological features that indicate prognosis and define staging, paralleled by number and extent of metastases (summarized in table 2).[13] Classification should be done after the initial excisional biopsy of the lesion, followed by a sentinel lymph node biopsy if needed.

Of note, as tumor thickness increases there is a significant decline in survival rates: for patients with T1 melanomas (thickness <1 mm) 10-year survival rates is 92%; 80% for patients with T2 melanomas (thickness 1.01-2.00 mm); 63% for T3 staged patients (thickness 2.01-4.00 mm) and for patients with melanomas more than 4.00 mm thick (T4) the survival rate dropped to less than 50%. [13] Moreover, survival of patients with an ulcerated melanoma is significantly lower than for patients with equivalent T stage but with no ulceration. Furthermore, tumor mitotic rate, defined as the threshold of 1/mm^2, is a powerful and, most important, independent prognostic factor.

Classification	Thickness (mm)	Ulceration Status/Mitoses
T		
Tis	NA	NA
T1	≤ 1.00	a: Without ulceration and mitosis < 1/mm²
		b: With ulceration or mitoses ≥ 1/mm²
T2	1.01-2.00	a: Without ulceration
		b: With ulceration
T3	2.01-4.00	a: Without ulceration
		b: With ulceration
T4	> 4.00	a: Without ulceration
		b: With ulceration
N	No. of Metastatic Nodes	Nodal Metastatic Burden
N0	0	NA
N1	1	a: Micrometastasis*
		b: Macrometastasis†
N2	2-3	a: Micrometastasis*
		b: Macrometastasis†
		c: In transit metastases/satellites without metastatic nodes
N3	4+ metastatic nodes, or matted nodes, or in transit metastases/satellites with metastatic nodes	
M	Site	Serum LDH
M0	No distant metastases	NA
M1a	Distant skin, subcutaneous, or nodal metastases	Normal
M1b	Lung metastases	Normal
M1c	All other visceral metastases	Normal
	Any distant metastasis	Elevated

Abbreviations: NA, not applicable; LDH, lactate dehydrogenase.
*Micrometastases are diagnosed after sentinel lymph node biopsy.
†Macrometastases are defined as clinically detectable nodal metastases confirmed pathologically.

	Clinical Staging*				Pathologic Staging†		
	T	N	M		T	N	M
0	Tis	N0	M0	0	Tis	N0	M0
IA	T1a	N0	M0	IA	T1a	N0	M0
IB	T1b	N0	M0	IB	T1b	N0	M0
	T2a	N0	M0		T2a	N0	M0
IIA	T2b	N0	M0	IIA	T2b	N0	M0
	T3a	N0	M0		T3a	N0	M0
IIB	T3b	N0	M0	IIB	T3b	N0	M0
	T4a	N0	M0		T4a	N0	M0
IIC	T4b	N0	M0	IIC	T4b	N0	M0
III	Any T	N > N0	M0	IIIA	T1-4a	N1a	M0
					T1-4a	N2a	M0
				IIIB	T1-4b	N1a	M0
					T1-4b	N2a	M0
					T1-4a	N1b	M0
					T1-4a	N2b	M0
					T1-4a	N2c	M0
				IIIC	T1-4b	N1b	M0
					T1-4b	N2b	M0
					T1-4b	N2c	M0
					Any T	N3	M0
IV	Any T	Any N	M1	IV	Any T	Any N	M1

Table 1.2: Guidelines for primary tumor and regional lymph node staging.

Clinical staging identifies five classes, from 0 to IV, with increasing degrees of invasiveness and worsening prognosis. In the absence of known distant metastasis, the extent of regional lymph node involvement and number of lymph nodes invaded by the disease become other prognostic indicators. (Table 2)

Melanoma at its early stages is generally cured by excisional surgery with good results, while metastatic melanoma is extremely difficult to treat and has a way worst prognosis.[14](Figure 5)

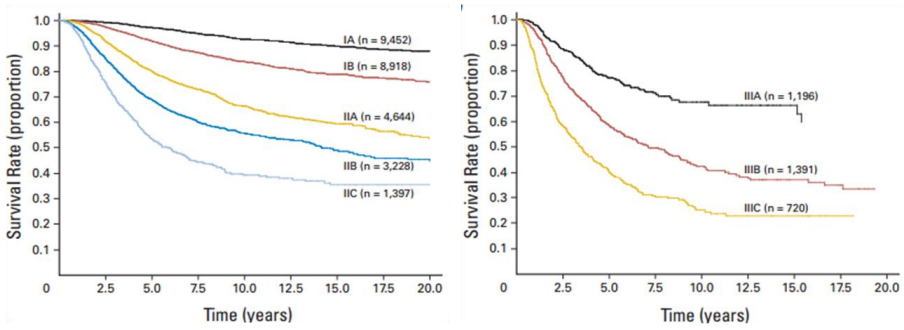

Figure 1.5: **Survival rates for the different staging groups of melanoma patients.**

1.1.2 Melanoma risk factors

Melanoma is a multi- factorial disease and its development depends on both environmental and genetic contributions.

UV exposure

Several epidemiological studies have firmly established that the major melanoma risk factor is ultraviolet (UV) radiation, with the highest risk associated to an intermittent and intense UVR exposure, along with sunburns during childhood. [15,16]

The effects on the skin of ultraviolet radiation are diverse and include, besides to genetic changes that account for the high mutation rate of melanoma, also an induction of reactive oxygen species (ROS), alterations in cutaneous immune function, and production of several growth factors.[15]

Both UVA and UVB can induce DNA damage, UVB through direct mutagenesis at dipyrimidine sites that can result in C>T mutations, while UVA indirectly inducing the formation of reactive oxygen species (ROS) and subsequently G>T transversion mutations due to oxidative damage.[3] In 2012 a whole-exome sequences study defined that about 50% of melanoma driver mutations can be attributed to C>T and G>T transitions (UV-signature), most of which occurring in tumor suppressor genes such as CDKN2A, PTEN and TP53.[17] Recent studies involving mouse models have demonstrated plural links between UV exposures and melanomagenesis; specifically, Zaidi *et al*. showed that UVB can induce melanocyte activation through an interferon-γ dependent inflammatory response.[18] Moreover, Viros et al. demonstrated that in mice, UVR can accelerate BRAF-driven melanomagenesis through alterations in TP53 gene.[19] Furthermore, UV exposure has been shown to promote melanoma metastatic progression enhancing perivascular invasion of tumor cells and increasing the number of lung metastasis through recruitment and activation of neutrophils.[20]

Genetic susceptibility

Heritable phenotypic risk factors include phototype (a fair skin, blue or green eyes, blonde or red hair are associated with an incremented incidence of melanomas), sun sensitivity, an inability to tan[18-20]. A high number of melanocytic naevi, or the presence of clinically atypical naevi are also connected to an augmented risk of melanoma onset.

Moreover, somatic mutations randomly acquired by melanocytes and accumulation of genomic changes can influence melanoma onset: candidate-gene studies and genome-wide association studies (GWAS) for melanoma and these melanoma-associated phenotypes have identified sever variants associated with melanoma risk in the general population.[21-24]

Nevertheless, the presence of germ line variants can be predisposing and family history is among the strongest risk factors.

Indeed, about 10% of melanoma cases occur in families where patients report close relatives affected, and mutations in cyclin-dependent kinase inhibitor 2A (CDKN2A) are present in 20-40% of familial melanoma, being therefore the most common. [25] The CDKN2A gene encodes for two transcripts generated by two different splicing variants: p16 inhibitor of cyclin-dependent kinase 4 (p16INK4A) and the alternate reading frame (p14ARF). The latest controls positively p53 activity, therefore a loss of function impacts on proliferation control of DNA damaged cells. p16INK4A, instead, regulates the phosphorylation status of the oncosuppressor retinoblastoma protein (RB) through the inhibition of CDK4 and CDK6. [26]
Other high penetrance melanoma predisposition genes are CDK4, whose mutations impact on the same pathway affected by CDKN2A mutations [27], inactivating alterations in BRACA1-associated protein-1 (BAP1) [28] or substitutions in MITF gene sequence and alterations in the gene encoding for α-MSH and MCR1. [29]

1.1.3 Molecular classification of sporadic melanoma

Interestingly, a recent paper published by the "cancer genome atlas network" has defined a framework for the genomic classification of cutaneous melanomas, through an integrated analysis of DNA, RNA and proteins from a large collection of 333 samples from melanoma patients. [30] Referring to the most mutated genes, they identified 4 different melanoma subtypes: mutant BRAF, mutant RAS, mutant NF1, and Triple-WT (wild-type), linking the genomic setting to possible response to targeted therapies, therefore proposing a guide for clinical decision.

Mutation Subtypes	*BRAF*	*RAS*	*NF1*	Triple Wild-Type
[1]MAPK pathway	[1]*BRAF* V600, K601	[1]*(N/H/K) RAS* G12, G13, Q61	[1]*NF1* LoF mut; (*BRAF* non-hot-spot mut)	[1]*KIT* COSMIC mut/amp, *PDGFRa* amp, *KDR* (*VEGFR2*) amp; rare COSMIC *GNA11* mut, *GNAQ* mut
[2]Cell-cycle pathway	*CDKN2A* mut/del/h-meth (~60%); [2](CDK4 COSMIC mut)	*CDKN2A* mut/del/h-meth (~70%); *CCND1* amp (~10%), [2](*CDK4* COSMIC mut)	*CDKN2A* mut/del/h-meth (~70%); *RB1* mut (~10%)	*CDKN2A* mut/del/h-meth (~40%); *CCND1* amp (~10%), [2]*CDK4* amp (15%)
[3]DNA damage response and cell death pathways	*TP53* mut (~10%); [3](note: *TP53* wild-type in ~90% of *BRAF* subtype)	*TP53* mut (20%)	*TP53* mut (~30%)	[3]*MDM2* amp (~15%); [3]BCL2 upregulation
[4]PI3K/Akt pathway	[4]*PTEN* mut/del (~20%); [4](rare *AKT1/3* and *PIK3CA* COSMIC mut)	[4]AKT3 overexpression (~40%); [4](rare *AKT1/3* and *PIK3CA* COSMIC mut)	[4]AKT3 overexpression (~30%)	[4]AKT3 overexpression (~20%)
[5]Epigenetics	[5]*IDH1* mut, [5](rare *EZH2* COSMIC mut); [5]*ARID2* mut (~15%)	[5]*IDH1* mut, [5](rare *EZH2* COSMIC mut); [5]*ARID2* mut (~15%)	[5]*IDH1* mut, [5](*EZH2* mut); [5]*ARID2* mut (~30%)	[5]*IDH1* mut, [5](rare *EZH2* COSMIC mut)
Telomerase pathway	Promoter mut (~75%)	Promoter mut (~70%)	Promoter mut (~85%)	Promoter mut (< 10%); *TERT* amp (~15%)
Other pathways	*PD-L1* amp, *MITF* amp, *PPP6C* mut (~10%)	*PPP6C* mut (~15%)		
[6]High immune infiltration (pathology)	~30%	~25%	~25%	~40%

Class 1: Clinically actionable	[1]BRAF inhibitors; [1]MEK inhibitors	[1]MEK inhibitors		[1]C-KIT inhibitors (imatinib, dasatinib, nilotinib, sunitinib); PKC inhibitors (AEB071)
	[2]CDK inhibitors	[1,2]CDK inhibitors		[2]CDK inhibitors
	[3]MDM2/p53 interaction inhibitors			[3]MDM2/p53 interaction inhibitors
	[4]PI3K/Akt/mTOR inhibitors	[4]PI3K/Akt/mTOR inhibitors	[4]PI3K/Akt/mTOR inhibitors	[4]PI3K/Akt/mTOR inhibitors
	[6]immunotherapies (mAb against immune checkpoint proteins, high dose bolus IL-2, interferon-α2b)			
Class 2: Translationally actionable	[1]ERK inhibitors	[1]ERK inhibitors	[1]MEK inhibitors; [1]ERK inhibitors	
	[5]IDH1 inhibitors	[5]IDH1 inhibitors	[5]IDH1 inhibitors	[5]IDH1 inhibitors
	[5]EZH2 inhibitors	[5]EZH2 inhibitors	[5]EZH2 inhibitors	[5]EZH2 inhibitors
	(PPP6C) Aurora kinase inhibitors	(PPP6C) Aurora kinase inhibitors		
Class 3: Pre-clinical	[5]ARID2 chromatin remodelers (synthetic lethality)	[5]ARID2 chromatin remodelers (synthetic lethality)	[5]ARID2 chromatin remodelers (synthetic lethality)	[3](BCL2) BH3 mimemitcs

Table 1.3: Mutational subtypes and clinical implications.

Table 3 summarizes the four identified subtypes and the predicted genetic alterations are indicated; in each one of the genomic classes a subset of melanomas expresses significant immune infiltration markers.

The different extent of immune infiltration, which is independent from the specific subtype, has been associated with improved survival and has obvious potential implications for immunotherapy.

1.2 ONCOGENIC SIGNALLING PATHWAYS IN MELANOMA

Most if not all genetic alterations present in melanoma cells have as a consequence the constitutive activation of either the MAPK pathway or the PI3K/AKT/mTOR pathway. To better understand the molecules involved, I will briefly describe the main components of the two cascades.

1.2.1 The Mitogen Activated Protein Kinase (MAPK) cascade

Mitogen-activated protein kinases (MAPK) are serine, threonine, and tyrosine specific protein kinases, involved in responses to multiple stimuli and that regulate a wide variety of cellular functions, such as proliferation, survival, gene expression and resistance to therapies.[31]

Mammalian cells possess four main MAPKs cascades, activated by distinct signals. Each cascade is a hierarchical pathway built on three protein kinases that act one after the other using phosphorylation to activate their substrates: the upstream elements are the MAPK kinase kinase (MAPKKK), then the intermediate MAPK kinase (MAPKK) and then the "effector" kinases, the MAPK. [32] (Figure 7)

The four different terminal kinases are the ERK1/2, the c-Jun amino terminal kinases (JNK1/2/3), p38 kinases and ERK5/BMK1. Each cascade can be activated by different stimuli, both internal, such as DNA damage or metabolic stress, and extrinsic like cell-matrix interactions or growth factors response. The most known and studied is the "canonical" pathway, the RAS-RAF-MEK-ERK. [33]

Normally, when a ligand (i.e. the Epidermal Growth Factor (EGF)) binds to its receptor on the plasma membrane RAS GTPases activity is stimulated. Active RAS interacts with the MAPKKK of the RAF family inducing membrane translocation, dimerization and activation. RAF kinases then phosphorylate in serine-threonine residues the MEK kinases, which subsequently activate ERK. [34]

All components of this pathway are present in different isoforms: two subtypes of ERK (ERK1 and ERK2), two subtypes of MEK (MEK1 and MEK2), three subtypes of RAF (ARAF, BRAF and CRAF) and three subtypes of RAS (HRAS, NRAS and KRAS) have been described and characterize, increasing the complexity of this pathway.[35]

Active ERK has substrates both in the cytoplasm, where it can phosphorylate cytoskeletal proteins affecting cell movement, or many other substrates such as ribosomal S6 kinases [36](RSKs); or ERK can translocate into the nucleus activating several transcription factors.[37]

In immune cells it induces the expression of tumor necrosis factor alpha (TNFα) and inducible nitric oxide synthase (iNOS). [38]

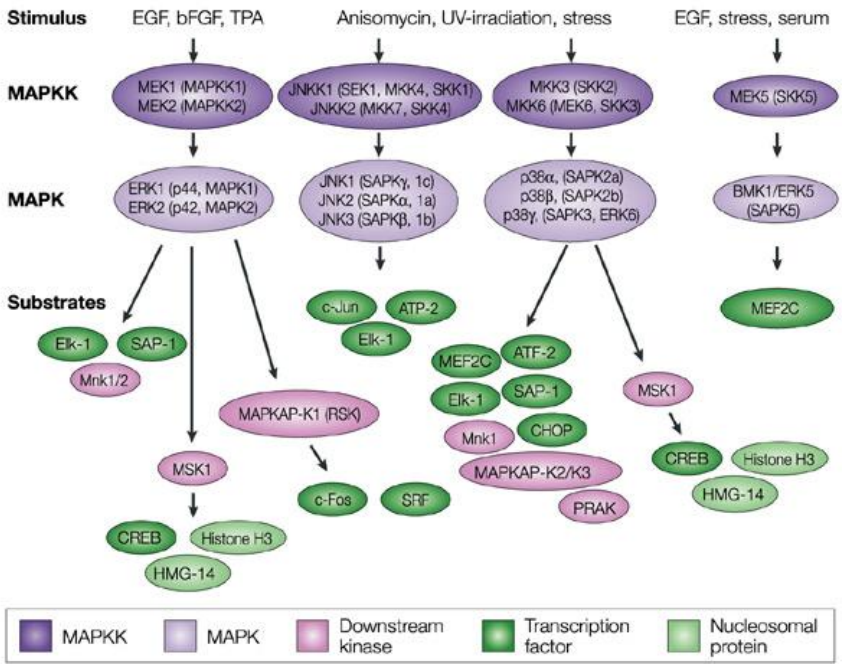

Figure 1.6: **The mammalian MAPK cascade**.

Several studies have demonstrated that the ERK1/2 MAPK pathway is a key controller of cell proliferation and survival. [39] Both ERK1 and ERK2 are activated in response to mitogenic stimuli and multiple line of evidence have reported the correlation between mitogenic response to growth factors and the ability to activate ERK1/2 [40] as well as the fact that silencing these proteins is able to inhibit proliferation of different type of cells.[41] Findings confirmed by the evidence that small molecules inhibitors targeting MEK are able to inhibit cell proliferation [42] and, conversely, the induced expression of MEK is sufficient to stimulate cell replicative potential. [43] Furthermore, activation of signalling mediated by ERK1/2 has been shown to induce cell cycle progression [44], to activate cell cycle regulators such as cyclin D1 [45] and c-Myc [46] and to down regulate several proteins such as p21. Moreover, the activation of MAPK/ERK signalling induces biosynthesis of nucleotide and proteins. [47] Interestingly, several studies have shown that ERK1/2 activity promotes cell proliferation and survival acting on the expression of both pro-survival molecules such as Bcl-2 and Mcl-1 as well as on pro-apoptotic members of the Bcl-2 family (like Bim and Bad).[48]

1.2.2 The PI3K-AKT-mTOR signalling pathway

The phosphoinositide-3 kinase (PI3K)/ v-Akt murine thymoma viral oncogene (AKT) mammalian target of rapamycin (mTOR) signalling pathway is among the most important pathways that regulate cell proliferation and survival as well as transcription and motility. [49]

PI3K cascade is usually activated by receptor tyrosin kinases (RTKs) engagement, but it can also respond to several type of cytokines.[50]

Class I PI3 kinases are present in different isoforms α, β, and γ and formed by heterodimers of a regulatory subunit (p85/p55/p50) and a catalytic subunit (p100), whose activation induces phosphorylation of the phosphatidylinositol-4,5-biphosphate (PIP2), generating phosphatidylinositol-3,4,5-triphosphate (PIP3). [51] The latest recruits several adaptor and effector proteins to cellular membrane and leads to the activation, through the phosphorylating activity of the phosphoinositide-dependent kinase 1 (PDK1), of protein kinase B (AKT), the main node in PI3K pathway. [52]

AKT is a serine/threonine-specific protein kinase involved in multiple cellular processes; once activated it is able to phosphorylate a high number of target proteins, regulating their activity either positively or negatively. [53]

The phosphatase and tensin homolog deleted on chromosome 10 (PTEN) is one of the key molecules that negatively regulate the PI3K pathway through a dephosphorylating activity on PI3K, thereby acting as a tumor suppressor and controlling cellular division, migration and apoptosis.[54]

Akt activity is implicated in cell cycle progression and protein synthesis through the regulation of several proteins such as the glycogen synthase kinase-3α (GSK-3α), the forkhead transcription factors, cyclin kinase inhibitors p21 and p27 and mTOR. [55] Moreover, Akt contributes to the stabilization of cyclin D1 and c-Myc through the inhibition of GSK3α. [56]

Also, Akt can promote the degradation of the oncosuppressor p53 by phosphorylating and thereby activating its negative regulator Mdm2. [57]

Furthermore, several studies have demonstrated that PI3K/Akt signalling is anti-apoptotic through different activities on multiple proteins. For example, Akt can inhibit caspase-9 activity, a crucial initiator of the apoptotic cascade [58]; similarly, PKB/Akt phosphorylates BAD and thus releases the anti-apoptotic members of the Bcl-2 family. [59] Moreover, Akt can activate and phosphorylate I-kB kinase, finally leading to the activation of the transcription factor NF-kB, which has among its targets Bcl-2 and Bcl-XL. [60]

Activation of mTOR is able to control cell growth through the activation of p70S6K and inhibition of 4E-BP1, two molecules that control protein translation. [61]

Besides melanoma, the activation of PI3K/Akt signalling pathway has been found in many other different type of human cancer; among them breast cancers, tumors of the lung, ovary, thyroid, pancreas and stomach, as well as glioblastoma and several hematological

malignances. [62] Moreover, similar studies have highlighted correlations between Akt activation and advanced stage, histological grade or poor prognosis. [62]

Specifically, Akt activation in human cancer can be due to several different mechanisms; with the most common being alterations in PI3K (through amplification of PI3KCA gene [63], or somatic mutations [64]) as well as alterations in PTEN (usually loss of function via gene mutation, deletion or promoter methylation. [65]

Of note, constitutive or residual PI3K pathway activation has been found in cells that have developed resistance to conventional chemotherapy and radiation, as well as resistance to other target-specific therapies. [66]

Importantly, MAPK and PI3K pathways often cross-interact, usually through reciprocal regulation with positive or negative feedbacks, and the activation of either one of the two cascades can converge in the activation of common downstream target proteins (i.e several transcription factors or protein kinases). For instance, hyper-activated RAS can induce, aside from MAPK pathway induction, also the PI3K cascade [67]; similarly, PI3K pathway inhibition can induce a rebound effect and can induce phosphorylation of ERK or of other components of the MAPK pathway. [68]

1.3 COMMON GENETIC ALTERATIONS IN MELANOMA

The development of human cancers is a multi-step process during which normal cells acquire, through accumulation of genetic and epigenetic alterations, several “malignant” characteristics (or “hallmarks”) that render them able to evade proliferation control. [69]

The hallmarks of cancer first described by Hanahan and Weinberg in 2000, [69] comprise self-sufficiency from growth signals, insensitivity to growth-inhibitory signals, evasion of programmed cell death, limitless replicative potential, sustained angiogenesis and tissue invasion and metastasis.

Melanoma cells acquire these characteristics mainly through alterations in signalling molecules, cell cycle and proliferation regulators, and transcription factors/ epigenetic regulators; all of which have as a consequence an hyperactivation of either the MAPK or the PI3K cascades.[70] (**Figure 7**)

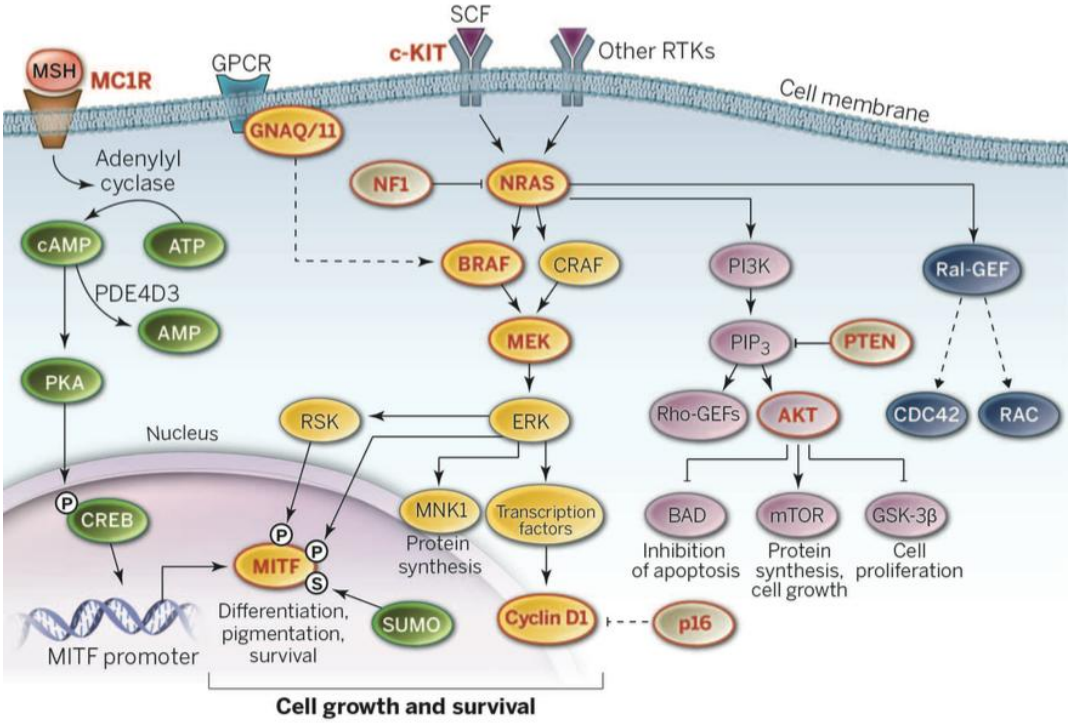

Figure 1.7: Signalling pathways in melanoma. MAPK signalling promotes cell growth and survival and is constitutively active in most melanomas. RAS family members are activated by RTKs and signal through effector proteins, including RAF kinases, PI3K, and Ral-GEFs. Oncogenic BRAF and NRAS are found in 40 to 60% and 10 to 30% of melanomas, respectively. c-KIT signalling is essential for melanocyte development and is associated with melanomas arising on acral, mucosal, and chronically sun-damaged skin. Mutations in GNAQ and GNA11, two G protein a subunits involved in MAPK signalling, are the dominant genetic lesions in uveal melanomas.. Known melanoma oncogenes and tumor suppressors are labeled in red. Dotted lines represent omitted pathway components.

Signalling molecules

Activating mutations of relevant components of the MAPK pathway, such as BRAF and NRAS oncogenes have been identified respectively in 63% and 26% of primary melanomas [71] The most common mutation in BRAF gene is a missense mutation with a valine-to-glutamic acid substitution in position 600 ($BRAF^{V600E}$) in the kinase domain that renders RAF constitutively active, enabling it to bind its substrate as a monomer and leading to a constant MEK-ERK signalling.[71] NRAS mutations are usually gain-of function alterations [with the most common being leucine for glutamine at position 61 ($NRAS^{Q61L}$)] that maintain RAS in the GTP-bound state, the active form.[72] Both of these alterations result in MAPK pathway hyperactivation.

Melanoma cells can also be characterized by AKT3 [73] amplification; insertions and deletions in the coding region PTEN [74] and also other somatic mutations (i.e. $Akt1/3^{E17K}$, $Akt1^{Q79K}$) in different of its components (including mTOR, IRS4, PIK3R1, PIK3R4, and PIK3R5), leading to a constitutive signalling of the phosphatidylinositol 3-kinase pathway. [75,76]

Moreover, the receptor tyrosine kinase (RTK) c-Kit is activated by somatic mutations in 17% of melanomas from chronic sun-damaged skin, and in 11% of acral and 21% of mucosal melanomas and it can signal through both the MAPK and the PI3K/AKT pathway. [77]

Cutaneous melanomas may also constitutively express several RTKs such as EGFR, PDGFR, AXL and VEGFRs , whose activation by autocrine or paracrine mechanisms can sustain main intracellular signalling pathways, including the RAS-RAF-MEK-ERK and the PI3K-AKT cascades. [78]

Furthermore, mutation in NF1 gene determine loss of the GTPase activating protein, causing a reduction in RAS inactivation and consequent aberrant MAPK signalling. [79]

Cell cycle and proliferation regulators

Deletions or mutations in CDKN2A or TP53, as well as amplifications in MDM2, can determine loss of cell cycle checkpoint function. Moreover, the RB pathway can be altered due to p16INK4a lesions or mutations in either CDK4 or retinoblastoma 1 (RB1), as well as cyclin D1 (CCND1) amplifications. [80]

Transcription factors and epigenetic regulators

The melanocyte specific transcription factor MITF, can be amplified in many melanomas and act as a lineage-specific oncogene; furthermore, germ-line variants that induce constitutive activity are associated with familial melanoma. [81]

The main target of MITF, the oncogene MYC, can also be amplified, inducing an activation of the canonical Wnt pathway.[81]

1.4 TARGET-SPECIFIC INHIBITORS in MELANOMA

The discovery, by Davies et al in 2002 [71] that 40% - 60% of melanomas carry a somatic missense mutation in BRAF gene, has prompted the development of a large number of small molecule inhibitors specific for BRAF mutant, and, some years later, for other molecules along the MAPK or the PI3K pathways.

1.4.1 FDA- approved drugs

The first inhibitor to be clinically tested was Vemurafenib (PLX4032), a selective BRAF V600E inhibitor which in an initial phase I study in melanoma patients led to a response rate of 81% [82] impressive results that were then confirmed in a randomized phase III clinical trial were OS at 6 months was 84% in the vemurafenib group and 64% in the dacarbazine group, while the progression free survival (PFS) rates were 5.3 versus 1.6 months [83,84] Due to these striking data, in 2011 the Federal Drug Agency (FDA) approved the use of Vemurafenib for the first-line treatment of BRAF mutant melanomas.

Further studies led to the development and testing of other target-specific inhibitors: the BRAF inhibitor Dabrafenib (GSK2118436) and the MEK1/2 inhibitor Trametinib (GSK1120212). Phase II and III clinical trials showed improved response rates of both these compounds if compared to chemotherapy with increment in both median PFS and OS. Specifically, Dabrafenib reached an increment in median progression free survival from 2.7 months of dacarbazine group to 5.1 months [84]. Moreover, in patients with BRAF V600E or V600K mutant metastatic melanoma, Trametinib, as compared with chemotherapy, improved rates of both progression-free (4.8 vs 1.5 months) and overall survival (81% vs 67% at six months). [85]

As a consequence of these results between 2012 and 2013 Dabrafenib and Trametinib were approved by FDA for melanoma treatment.

Starting from the demonstration of efficacy of the BRAF inhibitors Vemurafenib and Dabrafenib and the MEK inhibitor Trametinib as monotherapies for the treatment of metastatic melanoma, more recent studies have explored the activity of the combination of BRAFi with MEKi in BRAF mutant melanomas in the hypothesis to improve clinical outcomes by preventing or delaying the onset of resistance observed with single therapy regimens.[86]

A study from Larkin [87] et al. published last year demonstrated a significant improvement in progression-free survival (12.3 vs 7.2 months) of patients with BRAF mutant metastatic melanoma by the combination of Vemurafenib with the MEK inhibitor Cobimetinib, paralleled by a non-significant but present increment in treatment-related adverse events.[88]

In a more recent open-label, phase 3 trial conducted on previously untreated patients with BRAF V600E or V600K mutations, the association of Dabrafenib and Trametinib significantly

improved overall survival compared with Vemurafenib monotherapy and no increased overall toxicity was seen. [89]

Based on these results, in November 2015, the FDA approved the MEK inhibitor Cobimetinib for BRAF mutant metastatic melanoma in combination with Vemurafenib.

Nevertheless, despite impressive clinical benefits the onset of intrinsic or acquired resistance is a major hurdle also for the double-drug approach that need to be faced with novel anti-tumor strategies.[87,88]

1.4.2 Compounds in pre-clinical and clinical testing

Besides to the FDA-approved drugs, many novel inhibitors of RAF, MEK1/2 and PI3K/mTOR are being tested in a lot of of pre-clinical and clinical studies. (Figure 9)

RAF inhibition

Among the novel ATP-competitive RAF inhibitors that are undergoing evaluation in clinical trials there are:

Encorafenib (LGX818): highly potent BRAF inhibitor with specificity against the BRAF V600E. Monotherapy with Encorafenib is currently being tested in a phase I clinical trial on patients with advanced or metastatic $BRAF^{V600E}$ melanoma (NCT01436656), while other phase II trials are ongoing in patients with other solid or hematological tumors (NCT01981187) [90]

XL281 (BMS-908662): CRAF, $BRAF^{V600}$ and ^{V600E} selective RAF inhibitor with potent *in vivo* antitumor activity against several human tumor models. [91] A phase I study to determine the safety, tolerability, pharmacodynamics and bioavailability was undertaken in 48 patients with advanced solid tumors including melanoma.[91]

RAF265: small-molecule multi-kinase inhibitor against multiple kinases, including $BRAF^{V600E}$, CRAF and others. [92] A phase Ib clinical trial combining RAF265 with the MEK1/2 inhibitor MEK162 has been completed (NCT01352273) and a phase II clinical trial is ongoing to evaluate efficacy of monotherapy with RAF265 in patients with advanced or metastatic melanoma (NCT00304525). [93]

MEK inhibition

There are two major classes of MEK inhibitors, ATP competitive and non-competitive inhibitors (see Table 4 for a complete list of currently tested molecules).

Most of the currently used compounds are the so-called noncompetitive MEK inhibitors, indicating that instead of competing for the binding to the ATPbinding site, they go to an adjacent allosteric site, achieving a high specificity.[94]

Among the more promising second and third generation inhibitors that are being developed for MEK1/2 targeting and that are already tested in phase III clinical trials there is Selumetinib (AZD6244) by AstraZeneca.

Selumetinib is a highly selective, ATP non-competitive inhibitor of MEK1/2 with no activity on other kinases; several pre-clinical studies showed that AZD6244 effectively reduced the growth of melanoma cells by inducing G1-phase cell cycle arrest.[95,96]

Selumetinib has been tested in phase I clinical trials and its administration resulted in disease stabilization and ERK phosphorylation reduction in tumor biopsies of patients with metastatic melanoma. [97] In a phase II trial, therapy with selumetinib or temozolomide was given to metastatic melanoma patients with unknown NRAS/BRAF status; despite results showed no significant differences in PFS, all the patients that responded had BRAF mutant tumors. [98] Further studies, therefore, selected patients with BRAF mutant melanoma and in a randomized phase II clinical trial, the combination of dacarbazine and Selumetinib showed an improved median PFS if compared to dacarbazine monotherapy (5.6 vs 3.0 months) but no beneficial result was seen for OS. [73]

MEK1/2 inhibitor	Year reported	Developer or owner	*In vitro* IC_{50} for MEK1 (nM)*	Ability to disrupt MEK phosphorylation	Clinical progression	$T_{0.5}$ (hours or days)
PD098059	1995	Pfizer	2000 ‡	Weak	Pre-clinical	Not relevant
U0126	1998	DuPont	72‡	Weak	Pre-clinical	Not relevant
PD184352 (CI-1040)	1999	Pfizer	17‡	Weak	Phase II	20.9+/–4.8 h
PD0325901	2004	Pfizer	1‡	Weak	Phase II	7.8 h
Binimetinib (MEK162, ARRY-438162)	2006	Novartis/Array Biopharma	12	Weak	Phase III	3.63–7.4 h
Selumetinib (AZD6244, ARRY-142886)	2007	AstraZeneca/ Array Biopharma	14‡	Weak	Phase III	5.33 h
Refametinib (RDEA119, BAY 869766)	2009	Bayer AG	19§	Weak	Phase II	12 h
CH4987655 (RO4987655)	2009	Chugai Pharmaceutical Co	5.2	Moderate	Phase I	4 h
Pimasertib (AS703026, MSC1936369)	2010	Merck KGaA	52‡	Not available	Phase II	5 h
TAK-733	2011	Takeda	3.2‡	Weak	Phase I	48–56 h
Trametinib (GSK1120212)	2011	GlaxoSmithKline	0.7	Moderate	Approved for $BRAF^{V600E/K}$-mutant melanoma	~4 days
CH5126766 (RO5126766)	2012	Chugai Pharmaceutical Co	160‡	Strong	Phase I	60 h
Cobimetinib (GDC-0973, XL518)	2012	Genentech (Roche)	4.2	Weak	Phase III	40 h
GDC-0623	2013	Genentech (Roche)	5	Strong	Phase I	4–10 h

Table 1.4: MEK1/2 inhibitors.

PI3K-AKT-mTOR inhibition

Many human cancers have been successfully treated with agents that inhibit mTOR; [99] in melanoma PI3K signalling targeting has been tested with either first generation agent rapamycin and the second-generation agents, everolimus and temsirolimus. [100]

Unfortunately, clinical trials with these compounds have shown no objective responses neither as single agents nor in combination with BRAF inhibitors. [101] [102]

All these molecules inhibit mTORC1 and their efficacy is limited due to lack of activity on mTORC2. To face this issue both dual mTORC1/2 and dual PI3K-mTOR inhibitors (NVP-BEZ235) are been tested. [103] Both *in vitro* and *in vivo* studies have demonstrated that dual PI3K-mTOR inhibition has a remarkable anti-proliferative activity and exerts a durable suppression of AKT phosphorylation.[104]

1.5 MECHANISMS OF RESISTANCE TO TARGET THERAPIES

Despite impressive clinical results obtained by FDA-approved drugs such as Vemurafenib, Dabrafenib, Trametinib and Cobimetinib, alone or in combinations, there is still a significant percentage of patients that do not respond to these inhibitors, used either in monotherapy or in combined treatments. Moreover, quite rapid relapses (within 6 months from the starting of treatment) are seen not only in patients undergoing single treatments, but also for the two-drugs combinatorial regimens. [82-85,87-89]

A high number of studies have been carried on to define mechanisms of resistance to target-specific therapies (mainly with BRAF V600E and MEK inhibitors), and according to its temporal occurrence, therapeutic resistance can be classified in either primary, or intrinsic, and acquired resistance. [105]

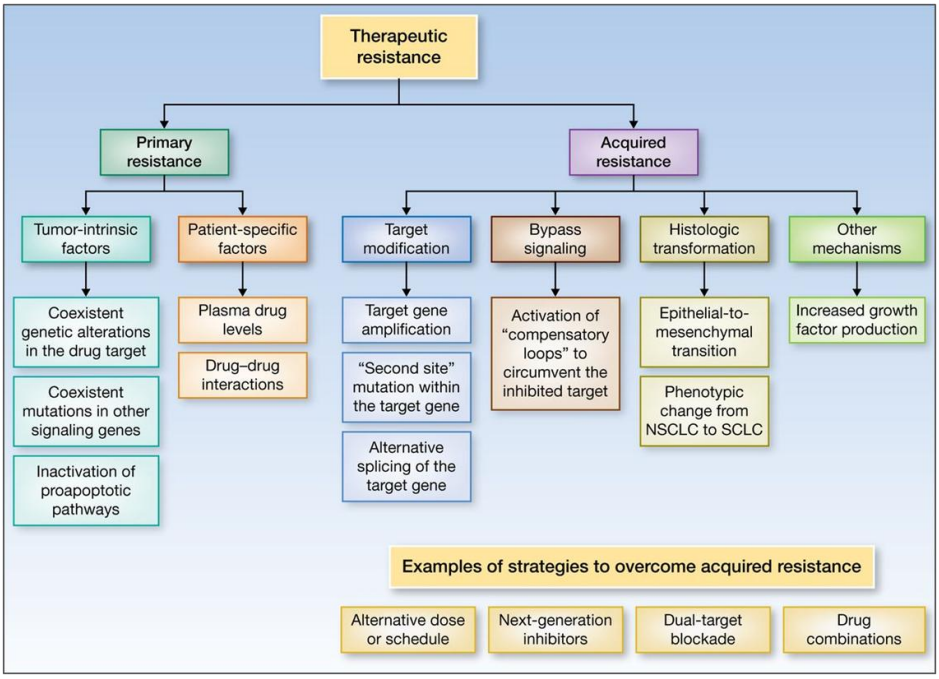

Figure 1.8: Mechanisms of therapeutic resistance to kinase inhibitors.

1.5.1 Intrinsic resistance

Primary or intrinsic resistance is defined as a lack of treatment response that is seen early at starting of treatment. It can be mediated by either tumor intrinsic factors (i.e.genetic alterations within the drug target) and by patient-specific factors.

Melanoma intrinsic resistance to target-specific therapy is not infrequent: 10% to 20% of patients never achieve meaningful responses, showing no tumor shrinkage or only limited tumor reduction (innate or intrinsic resistance). [106-108]

Melanoma insensitivity to therapies has been linked to alterations in molecules belonging to the pathway of programmed cell death with both defects in proapoptotic signalling and enhancement of antiapoptotic inputs, synergistically contributing to an apoptosis deficiency.[109]

Moreover, interesting recent studies have addressed the question of whether molecular features of the subset of intrinsically-resistant melanomas might mediate insensitivity to MAPK inhibition. In 2013 Garraway et al demonstrated that a dysregulation of a melanocytic signalling network that comprises GPCR/PKA/AC and MITF can cause resistance to RAF/MEK/ERK inhibition.[110] Moreover, in BRAF mutant melanomas, a low MITF expression and activity and higher levels of NF-kB and of the receptor tyrosine kinase AXL have been linked to resistance to MAPK pathway inhibitors. [111]

Furthermore, a low MITF/AXL ratio has been proved to predict resistance to several target-specific therapies both in BRAF mutant and NRAS mutant melanoma cell lines. [112]

Of note, parallel oncogenic pathway activation due to mutations in BRAF, RAS, or MEK1 is an reason of intrinsic resistance to inhibitors for either MEK1/2 or BRAF mutant respectively.

1.5.2 Acquired resistance

When disease progresses after an initial response to the targeted therapy, there is usually a development of acquired resistance, implying that the tumor has refined a mechanism of “escape” to evade blockade of the target.

As already explained, melanoma acquired resistance to target-specific inhibitors is a major hurdle in melanoma therapy because, despite good percentage of initial response, quite all patients relapse within 5-7 months. [82-85,89]

Several mechanisms of acquired resistance to RAF inhibition have been elucidated and can be classified in a MAPK-dependent resistance, which all involve a re-activation of the MAPK signalling; a MAPK-independent resistance through the activation of other parallel signalling pathways (especially the PI3K/AKT/mTOR cascade) and an adaptive RTK-driven resistance[113].

MAPK-dependent resistance is characterized by a re-activation of ERK signalling that can be RAF dimerization -dependent or -independent.

To the first group belong mechanisms that involve secondary BRAF alterations, such as the amplification of the number of BRAF copies [114], the expression of alternatively spliced variants [115] of BRAF that dimerize in a RAS-independent manner, as well as acquired RAS mutation (i.e. NRAS Q61K) [113], identified both in inhibitor-resistant cell lines and in clinical samples, or CRAF overexpression.

RAF- independent mechanisms of resistance include mutations either in MEK1 or MEK2 [116]; over expression of other MAPKs, such as COT [117]; and loss in the tumor suppressor protein NF1. [118,119]

MAPK-independent mechanisms of resistance, on the other hand, bypass the re-activation of ERK signalling through, for example, activation of the PI3K/AKT pathway[113,119], RTK activity upregulation, as well as repression of important apoptotic BH3-only genes such as Bim-EL and Bmf.

Of note, not all acquired resistance to MAPKi can be explained by genomic mechanisms and a recent paper from Hugo et al. [120] demonstrated a high recurrence of trascriptomic alterations in melanoma resistant to single drug (BRAFi) or duble drug therapies (BRAFi+MEKi), specifically with a enhanced c-MET and a reduced LEF1 expression, as well as with a YAP1 signal activation. [121]

1.5.3 Overcoming melanoma resistance to targeted therapies

The majority of the inhibitors used for the treatment of metastatic melanoma (i.e. MEK and $BRAF^{V600E}$ inhibitors) achieve anti-tumor effects inducing cancer cell death, mainly through the modulation of several molecules in the apoptotic cascade.[122,123]

Based on this knowledge, on the notion of the interplay between the MAPK and the PI3K pathways and on the recently elucidated mechanisms underlying melanoma acquired resistance to target-specific inhibitors, many pre-clinical studies have been conducted to explore whether an option to overcome primary and secondary resistance to cell death could be represented by combinations of multiple anti-tumor agents.

The most promising drug associations tested at pre-clinical level include (extensively reviewed in [124]):

I) simultaneous targeting of two components of either the MAPK or the PI3K cascades

II) parallel targeting of MEK and PI3K/mTOR pathways;

II) RTKs blockade combined with other pro-apoptotic strategies;

III) death receptors activation in association with MEK-, PI3K/mTOR - or histone deacetylase (HDAC)-inhibitors;

IV) simultaneous targeting of multiple anti-apoptotic molecules.

Probably, the most successful drug-combination tested has been the association between BRAF inhibitors (such as Vemurafenib or Dabrafenib) and MEK inhibitors like Selumetinib, Trametinib or Cobimetinib. The simultaneous treatment of melanoma cell lines or xenografts with associations of these drugs leaded to reduced proliferation, tumor growth inhibition and increment in cancer cell apoptosis. [125,126]

Another promising approach is represented by the simultaneous inhibition of MEK and PI3K/mTOR pathways. Several studies have analyzed effects of the combination between MEKi and BRAFi (i.e. Selumetinib, Dabrafenib, Trametinib, U0126) with compounds targeting PI3K or mTOR (i.e. Wortmannin, BEZ235, AZD8055, Rapamycin). In vitro and in vivo testing confirmed beneficial results in terms of reduction in tumor cell viability, increment in cancer cell apoptosis and reduce tumor incidence/growth. [127,128]

1.6 TRAIL: A TUMOR-SELECTIVE, PRO-APOPTOTIC LIGAND

Tumor necrosis factor (TNF) related apoptosis inducing ligand, also known as TRAIL, is a type II transmembrane protein of 32-33 kDa that was initially cloned based on its homology with FasL/Apo1L/CD95L e TNF. [129] TRAIL gene maps on chromosome 3, in position 3q26 and it is formed by 5 exons and 4 introns. [130]

TRAIL is expressed as a 281 amino acids long transmembrane protein with a short intracellular domain (N-terminal) of 17 amino acids, an hydrophobic transmembrane portion of 21 aa and the carboxi-terminal region (C-terminal) that, following proteolytic cleavage, can form the soluble and biologically active form (sTRAIL). [130]

TRAIL is a pro-apoptotic member of the TNF superfamily of death receptor ligands and acts forming omotrimeric structures stabilized by a Zn ion, essential for its stability. [131]

At physiological level TRAIL protein is mainly expressed as a membrane-bound molecule by immune cells, specifically by $CD4^+$ T cells, monocytes, and dendritic cells. [132-134] It plays a key role on NK or T-cell mediated killing of infected or tumor cells. TRAIL can be up-regulated on immune cells by interferon (INF-α2 and INF-γ), interleukin-2 (IL-2) and IL-15 [135] and its role in melanoma surveillance is confirmed by studies showing that it can mediate *in vivo* tumor rejection and prevent liver metastasis in melanoma mouse models. [133]

1.6.1 TRAIL receptors

TRAIL has a complex system of receptors, each with a different affinity for the ligand and different ability to transduce the associated signal.

Five receptors for TRAIL are known: TRAILR1/ DR4/APO-2, TRAIL-R2/DR5/TRICK2/Killer, TRAILR3/DcR1/TRID/LIT, TRAILR4/ DcR2/TRUNDD and osteoprotegerin (OPG); all codified by genes mapping on chromosome 8.[136]

TRAIL receptors belong to the Tumor-necrosis factor receptor (TNFR) family and four of them are type I transmembrane proteins, while OPG is a soluble protein. All receptors share common features: the ligand binding sites have 65% of sequence homology and they all bind the ligand through two specific sytes: the CDR3, conserved in all the family components and responsible for the ligand affinity, and the CDR2 that defines the selectivity of the interaction.[137]

Two of the receptors, the DR4 (TRAIL-R1) and DR5 (TRAIL-R2), are transmembrane proteins with a cytoplasmic “death domain” (DD) that share with other family members (such as Fas/CD95 and TNFR1) and that is responsible for the activation, upon ligand binding, of the apoptotic machinery.

DcR1 (TRAIL-R3) and DcR2 (TRAIL-R4), on the other hand, are known as decoy receptors (DcRs), and behave as antagonist receptors: while DcR2 has an incomplete DD, the DcR1

completely lacks the cytoplasmic region, rendering them, therefore, not able of triggering apoptosis. The fifth receptor, osteoprotegerin is a soluble protein with lower affinity for TRAIL, with no known pro-apoptotic potential lacking all the cytoplasmic region. [136] The role of DcRs is still controversial: they are thought to compete with the pro-apoptotic TRAIL receptors for ligand binding but they have also been shown to be able to activate cell survival pathways through NF-κB (nuclear factor κ-light-chain-enhancer of activated B cells), ERK or p38 activity. [138,139]

Altered expression of TRAIL-R is frequently observed in tumors, but contrasting results have been obtained when correlation between TRAIL receptors expression and tumor susceptibility to TRAIL and tumor stages has been evaluated [140,141]

Of note, in melanoma cells some studies have found a correlation between the level of expression of the death receptors and levels of apoptosis in response to TRAIL[142]: higher levels of TRAIL-R2 were usually present in more susceptible cells.[143]

Interestingly, freshly isolated melanoma cells have been found relatively resistant to TRAIL-induced cell death, and this was associated with a low expression of TRAIL receptors

1.6.2 TRAIL -induced signalling pathways

The mechanism of TRAIL dependent apoptosis induction is a well-characterized pathway whose cascade of events corresponds to the “classical” extrinsic (death receptors-dependent) pathway of apoptosis. [144]

After engagement of DR4 or DR5 by TRAIL, the receptors homotrimerize and this in turn induces the aggregation of the death domains, that mediate the recruitment at the plasma membrane of the adaptor protein FADD (Fas- associated Death Domain).[145] The Death Effector Domain of FADD recruits the pro-caspase-8 in its inactive form, allowing the assembly of the death-inducing signalling complex (DISC). In the DISC, pro-caspase 8 is cleaved and therefore activated.[144]

Two different mechanisms of response to TRAIL have been identified in distinct cell types. Accordingly, cells are classified as type I or type II. The TRAIL-DISC chain of events in type I cells is able to recruits a high number of initiator caspases (caspase -8 and -10) and is sufficient to activate apoptosis program through the cleavage of other downstream substrates, eventually leading to activation of the effector caspase -3 and -7. [146]

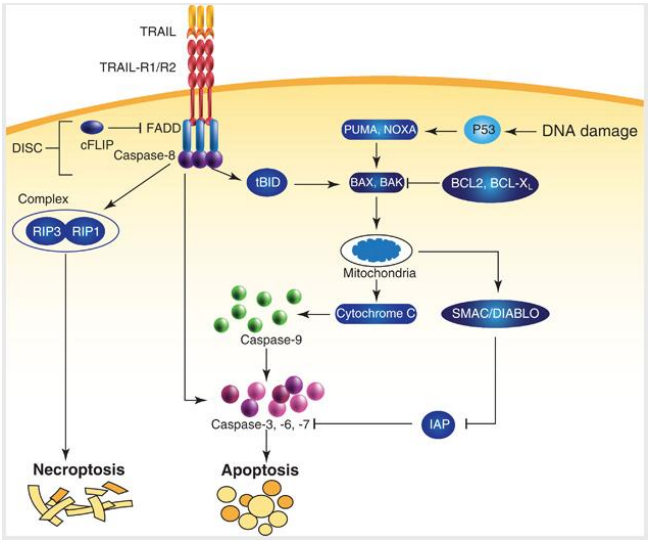

Figure 1.9: **Intrinsic and extrinsic apoptosis pathways.**

In type II cells, on the contrary, the response to TRAIL requires amplification of the extrinsic signal by activation of the intrinsic (mitochondrial - dependent) apoptosis pathway.[147] In these cells, initiator caspases cleave the pro-apoptotic BCL-2 family protein BH3 interacting-domain death agonist (BID) through the cleavage af its inactive form (p22) to a truncated and active t-Bid. After cleavage, the activated BID translocates to the mitochondrial membrane, where it interacts with the pro-apoptotic Bcl-2 family members BAX and BAK [148], allowing these proteins to form pores and to induce MOMP (permeabilization of the mitochondrial membrane) [147]. MOMP promotes the release of the pro-apoptotic proteins cytochrome c (cyt-c) , of the Second Mitochondrial -Derived Activator of Caspase (SMAC/DIABLO), and of tha Apoptosis Inducing Factor (AIF).

At this level apoptosis can be regulated through the activity of several molecules, among which anti-apoptotic Bcl-2 family members (Bcl-2, Bcl-X_L, Mcl-1, Bcl2-A1 and Bcl-w) that inhibit the activity of Bax and Bak, and pro-apoptotic regulators such as the BH3-only proteins Bim, Bik, Bad, Bid, Bmf, Puma, Noxa and Hrk. [149]

In the cytosol, cyt-c and Apaf-1 (Apoptotic protease activating factor-1) bind and recruit pro caspase -9, forming a complex known as Apoptosome. [150] Inside the apoptosome the pro caspase-9 is activated and in turn it activates effector caspases -3 and -7. Among the multiple targets of caspases activity there is PARP (Poly-ADP-ribose Polymerase), an enzyme with key roles in the DNA repair. [146]

SMAC/DIABLO promotes apoptosis by inhibiting the binding between caspases and the IAP [cellular inhibitor of apoptosis (cIAP)-1, cIAP-2, X-linked inhibitor of apoptosis (XIAP), Survivin, Apollon, IAP-like protein-2 (ILP-2) and ML-IAP/Livin] family proteins, which inhibit caspase enzymatic activity.[149]

Another important, regulator protein at the DISC level is the FLICE-like inhibitory protein (c-FLIP) that can inhibit activation of caspases-8 and -10. [151] c-FLIP has three splicing variants

that generate 3 isoforms with different molecular weight: c-$FLIP_S$ (26KDa), c-$FLIP_L$ (55KDa) and the c-$FLIP_R$ (24KDa).
Moreover, caspases activity can be directly inhibited by other intracellular molecules such as X-inhibitor of apoptosis protein (XIAP). [150]

NON APOPTOTIC TRAIL SIGNALLING

In addition to the canonical apoptosis pathway, TRAIL binding to its receptors was recently shown to trigger the formation of a secondary complex that can activate different signalling pathways such as JNK, p38 or NF-κB and that results in non-apoptotic stimuli [152].Upon TRAIL binding, TRAIL-R1 and TRAIL-R2 receptors can recruit the protein RIP leading to formation of a secondary complex, different from DISC and containing TRAF2 and TRADD. RIP phosphorylates and activates IkB-kinase (IKK); this in turn leads to IkB phosphorylation and degradation that result in release and activation of transcription factor NF-kB. The secondary complex is even responsible for the activation of additional pathways by TRAIL, including MAPK, JNK and Akt/PKB signalling [152]. Although not fully understood, signalling from the secondary complex through these different pathways, contributes in different cell types to regulation of several functions, including proliferation, cell migration, and invasion and production of pro-inflammatory factors [152].

1.6.3 TRAIL: a promising anti-tumor agent

Normally, DNA damage induces the apoptotic cascade through the activation of the onco-suppressor protein p53, whose alterations concur in tumor onset and resistance to therapies. For this reason the death receptors represent an appealing therapeutic target, being able to activate the programmed cell death program.[143]
Interest for TRAIL therapeutic potential came from the demonstration that injection of soluble TRAIL in animals with different tumor xenografts induced tumor regression with no apparent systemic toxicity[140,141] that instead characterized the usage of other members of the TNF superfamily (like Fas/FasL and TNFα/TNFR1). Pre-clinical and clinical studies are currently ongoing in different cancer types to assess activity and safety of TRAIL and TRAIL receptors agonist antibodies[153 154]
Despite some encouraging results in selected malignancies[154], a major limitation to the targeting of TRAIL pathway is represented by resistance.

TRAIL pathway has been pre clinically and clinically targeted through recombinant soluble forms of TRAIL (developed by Genentech , USA and Amgen, USA) or with monoclonal antibodies targeting TRAIL receptors (i.e. Mapatumomab, Conatumomab, Lexatumomab).

Mapatumomab (Human Genome Sciences, USA) is a fully human agonistic monoclonal antibody directed against TRAIL-R1 and it is in phase II clinical trial on non-small lung cancer patients and colorectal cancer patients.[155]

Conatumomab, Laxatumomab (HGS-ETR-2) are instead agonistic antibodies for the TRAIL-R2 and are currently under clinical testing for different type of cancers [156]

1.6.4 Mechanisms of resistance to TRAIL -induced apoptosis

Different type of cancers, including melanoma, display frequent resistance to TRAIL, achieved through several mechanisms.

The level of expression of the agonist receptors (and of the decoy receptors) is key one determinant of susceptibility/resistance to TRAIL in cancer cells, together with the extent of expression of the initiator caspase-8. Indeed, some TRAIL resistant melanoma cells have been shown to have low levels of DR4 and of caspase-8.[157]

Moreover, one of the main mechanisms of resistance to TRAIL acts at the level of the DISC and is mediated by the cellular FLICE-inhibitory protein (c-FLIP). Indeed, c-FLIP has structural homology with pro-caspase-8 and its structure allows it to be recruited to the DISC where it inhibits the processing and activation of pro-caspase-8. c-$FLIP_L$ and c-$FLIP_S$ can compete with pro-caspase-8 for association with FADD [158] and c-FLIP is thus considered a major inhibitor of the extrinsic pathway of apoptosis.

Furthermore, another key determinant of resistance to TRAIL, in melanoma and other tumors, is the expression of a large set of anti-apoptotic proteins. For example, an overexpression of XIAP can block the activation of effector caspase-3. [149]

In several tumor types, including melanoma, constitutive or receptor-induced activation of MAPK and PI3K pathways promotes TRAIL resistance. The different mechanisms linking signalling pathways activation to TRAIL resistance share a common strategy: MAPK or PI3K activation tends to shift the balance of pro- and anti- apoptotic proteins in favor of the latter. [159] [160] Some examples: IGF-1 can trigger resistance to TRAIL by upregulating expression of anti-apoptotic proteins Bcl-2, Bcl-XL and surviving. [159] In nasopharyngeal carcinoma, inhibition of Akt with LY294002 prevents upregulation of FLIP expression and rescue TRAIL susceptibility[161]. In melanocytes, stem cell factor (SCF), a melanocyte growth factor that activates both the PI3K and the ERK pathways, is protective for TRAIL-induced apoptosis [162] In neuroblastoma cells, the PI3K/AKT inhibitor PI103 rescues TRAIL susceptibility by shifting the balance toward proapoptotic Bcl-2 family members and increased mitochondrial apoptosis. [163]

1.7 ANGIOGENESIS AND ANGIOGENIC SIGNALLING PATHWAYS

Angiogenesis is a complex process that consist in formation of new capillaries from pre-existing vassels, requiring interaction between cytokines, growth factors, the extracellular matrix and different type of cells; angiogenesis is fundamental for tissue maintenance, development and survival. [164]

Hypoxia is one of the key drivers of angiogenesis because cells respond to reduced levels of oxygen stimulating the Hypoxia-inducible factors (HIFs) and other molecules (including mTOR) that respond promoting the formation of new vascuature to guarantee oxygen supply. [165] During the angiogenic process endothelial cells interact with pericytes, stromal cells and the extracellular matrix.

Endothelial cells respond to hypoxia inducing HIF-1a, which in turn upregulates the expression of endothelial growth factor A (VEGFA) and vascular endothelial growth factor receptor 2 (VEGFR2). VEGFA binds to two tyrosine kinase receptors: VEGFR1 and VEGFR2 stimulating endothelial cell mitogenesis and vascular permeability and resulting in triggering of endothelial signalling cascades responsible for cytoskeleton reorganization and sprouting. [166]

Besides the interaction between VEGF and VEGFR families, other pathways known to play important roles in the angiogenic process are the Notch pathway, the Platelet-derived growth factor (PDGF) pathway, the angiopoietin (ANGPT1 and ANGPT2) and TIE2/TEK interactions, and the transforming growth factor β (TGF β) activity on its receptors. All of these pathways and the molecules that they include concur at inducing a remodeling of the extracellular matrix, recruitment proliferation and maturation of pericytes and endothelial cells.

Tumor angiogenesis is based on processes similar to the one of physiological angiogenesis, both driven by hypoxia, but in case of neoplastic cells, with a persistent stimulation of the angiogenic cascade by tumor-produced pro-angiogenic factors. [164]

For instance, while ANGPT-2 normally antagonizes activity of ANGPT-1 on TIE2, in tumor contexts ANGPT-2 can mediate the recruitment of TIE2-expressing tumor-associated macrophages (TEM) that can produce pro-angiogenic factors. [167]

Moreover, tumor vessels are different from normal ones, being more disorganized, leaky and tortuous and tumor endothelial cells have been reported to have cytogenetic alterations. [168]

Melanoma is an highly aggressive disease and its progression from the initial phases to the more invasive vertical growth phase is paralleled by the acquisition of a rich vascular network. Melanoma neovascularization has been correlated with overall survival, poor prognosis and increased relapse rates.[169,170]

Secretion by melanoma cells of various pro-angiogenic cytokines, such as VEGF-A, PGF-1 and -2, IL-8, or TGF-1 promotes the so-called “angiogenic switch”, meaning the particular

state of the tumor in which the balance between pro-angiogenic molecules and inhibitors is impaired in favor of the first. [171]

Moreover, HIF1 expression and activity is increased in melanoma and is associated with a decreased differentiation of melanoma cells, as well as with VEGF expression (14).

Furthermore, in melanoma cells, BRAFV600E can concur to stabilize HIF1α, the most important subunit of HIF1[172]. Furthermore, also the PI3K pathway is involved in an up-regulation of HIF1α activity through the ribosomal S6 kinase 1 [173] and an accumulation of HIF1α can depend on an increase of reactive oxygen species (ROS) or NF-ĸB. [174] HIF1A is also a target gene of MITF, whose levels are well-known to play key roles in melanoma differentiation and progression.[175]

1.7.1 TRAIL and angiogenesis

Several studies have previously reported the possible anti-angiogenic effects of TRAIL in both the soluble and the membrane-bound form. In 2010 Easton et al [176] demonstrated the inhibition of angiogenesis exerted by TRAIL through the induction of vascular endothelial apoptosis. Moreover, in a study published by Carlo-Stella et al., intravenous injection of mTRAIL-expressing $CD34^+$ cells exerted a potent antitumor activity in NOD/SCID mice bearing systemic multiple myeloma and non-Hodgkin lymphoma xenografts [177,178]. This was due to an efficient homing of CD34+-TRAIL+ cells to the neoplastic tissue where these cells induced a significant anti-tumor activity thanks to the disruption of the tumor vasculature, as evidenced by endothelial cell apoptosis and hemorragic necrosis. These effects were observed only in the tumor-associated vasculature. Interestingly, a recent study by Wilson et al. [179] has provided evidence for the mechanism of the selective effect of TRAIL on tumor-associated endothelial cells. In fact, only these cells, and not the endothelial cells found in normal tissues, upregulate the TRAIL receptor DR5 and become susceptible to apoptosis by TRAIL [179]. Furthermore, Wang et al demonstrated cooperation between TRAIL and doxorubicin to reduce microvessels density through a reduced production of the pro-angiogenic IL-8 and an increment in the anti-angiogenic factor CXCL10 in an in vivo model of soft tissue sarcoma (STS). [180]

1.7.2 MAPK and PI3K cascades: role in angiogenesis and endothelial cell function

Both the MAPK and the PI3K/AKT/mTOR cascades exerted a central role in the biology of endothelial cells [181]: signalling from these pathways is required to prevent endothelial cell apoptosis, as well as to promote angiogenesis and cell survival [181].

Several studies have demonstrated the importance of the PI3K/AKT/mTOR cascade in regulating the VEGF expression and activity. Specifically: Ras expression increases VEGF expression through PI3K activity [182]; and the activation of MEK and PI3K signal has been shown to contributes to IL-8 and VEGF expression in head and neck squamous cell carcinoma [183] and of VEGFR1 and VEGFR3 on bone marrow endothelial cells. [184]

Moreover, Akt has been shown to induce the phosphorilation of the endothelial Nitric Oxyde Synthase (eNOS), a protein involved in the neo-vascularization process and endothelial cell.[185]

Furthermore, the modulation of pro-angiogenic factors, such as HIF-1α, has been demonstrated to be a consequence of AKT activity[186] and the importance of the RAS-RAF-MEK-ERK signalling and the PI3K pathway in melanoma angiogenic switch and aggressive phenotype has been confirmed by a recent study [187] demonstrating that expression of GAB2 and consequent activation of the PI3K cascade induced an incremented angiogenic response through the up-regulation of HIF-1α and VEGF levels in NRAS-driven melanoma cells. Moreover, in the same experiments, the MEK inhibitor PD325901 was able to suppress this pro-angiogenic activity.

AKT activation is known to phospholylate the oncoprotein HDM2, which, consequently translocates from cytoplasm to nucleus, process that is inhibited by PI3K/AKT pathway blockade. On the contrary, AKT overexpression or PTEN loss induce an increment in the expression of HDM2 and HIF-1α, further confirming the role of molecules belonging to the PI3K pathway in the regulation of the HIF activity. [186]

Lastly, a forced expression of PTEN is able to inhibit embryonic angiogenesis and a constitutive activation of Akt is connected to an altered vascularization in mice models.[182]

Also, in hypoxic conditions, the MAPK signalling pathways promotes expression of Bcl-2 in endothelial cells, which in turn promotes angiogenesis, and a MAPK inhibitors blocks Bcl-2 induction in such cells[188]. Similarly, treatment of endothelial cells with the association of mTOR inhibitors and MAPK inhibitors can reduce endothelial cell survival, proliferation, migration and tube formation[189].

Of note, several inhibitors of either the PI3K or the MAPK pathways, used alone or in combinations with other drugs, have been associated with anti-angiogenic effects on tumor models of different type of malignancies: the combination of Sorafenib and Selumetinib

obtained a reduced angiogenesis in renal cell carcinoma xenografts [190] a combined MEK and VEGFR inhibition resulted in an enhanced inhibition of tumor angiogenesis in lung cancer models. [191] Similarly, a combination of AZD6244 and BEZ235 enhanced the anti-angiogenic effects of monotherapy through the reduced expression of matrix metallopeptidase-9 (MMP-9) in tissues from gefitinib-resistant NSCLC xenograft. [192]

2.OBJECTIVES

Metastatic melanoma is an aggressive disease, often resistant to therapies. Despite impressive clinical results achieved in the past 5 years, mainly due to the testing and consequent FDA- approval of target-specific drugs and, more recently, of immune check-point inhibitors, a significant portion of patients is characterized by intrinsic resistance to therapy or experience quite rapid relapses after initial response.
Innovative and effective strategies are therefore needed to overcome insensitivity or resistance to different anti-tumor agents and several preclinical studies have explored the possibility of combinatorial approaches associating pathway- or target-specific inhibitors.

Since apoptosis is a key process involved in the elimination of potentially altered cells, aberrant regulation of apoptosis represents a critical hallmark in cancer, allowing the survival of neoplastic cells. Deficiency in the programmed-cell death control is also at the basis of melanoma chemotherapeutic resistance and a common goal in cancer treatment is represented by induction of apoptosis in tumor cells.[109]
Moreover, effective strategies for cancer treatment should be aimed not only at inducing cancer cell death, but also at targeting other mechanisms in the microenvironment relevant for tumor growth, such as tumor angiogenesis.

TRAIL is a pro apoptotic, vascular- disrupting and tumor- selective agent that has been tested for the treatment of different types of malignancies achieving good safety profiles but unsatisfying results due to frequent resistance of cancer cell to monotherapy targeting TRAIL pathway.

Based on this knowledge, the goal of the present project was to test the anti-tumor efficacy in-vitro and in-vivo of a combinatorial approach associating TRAIL with inhibitors targeting the two main oncogenic signalling pathways often hyperactivated in melanoma cells, the MAPK and the PI3K pathways.

As a MEK inhibitor we decided to use Selumetinib (AZD6244), a compound that is in phase III clinical trials for treatment of solid malignancies and for the targeting of the PI3K cascade we chose NVP-BEZ235 (herein referred to as BEZ235), a dual PI3K-mTOR inhibitor currently under pre-clinical and clinical evaluation.

Our working hypothesis was that these agents should have multiple effects on:

1) tumor cells

exerting synergistic anti-tumor effects possibly combining the pro-apoptotic activities of the different drugs used and activating simultaneously both the the extrinsic (mainly through TRAIL activity) and the intrinsic (mainly due to the activity of MEK and PI3K pathway inhibitors) apoptosis pathways;

this approach should be able to overcome melanoma intrinsic resistance to programmed cell death and will be tested on a panel of melanoma cell lines with known BRAF, NRAS, PTEN and p53 status to evaluate possible dependency of the effects from a specific genetic setting.

2) tumor microenvironment

promoting an anti-angiogenic effect and reducing therefore tumor growth and neovascularization, possibly combining the well-known vascular disrupting activity of TRAIL and the effects of inhibition of pro-angiogenic pathways in tumor and in tumor-associated vasculature due to targeting of ERK and AKT cascades.

Furthermore, since it is well known that tumor-associated vasculature is different from physiological vessels, we sought to test the hypothesis that co-culturing melanoma cells with endothelial cells could render the latest more susceptible to either target-specific therapy or TRAIL and on which mechanistic basis.

The proposed work was therefore aimed at evaluating the *in vitro* and *in vivo* activity and mechanism of action of TRAIL in association with AZD6244 and BEZ235 inhibitors. Expected results should provide a preclinical proof-of-concept for drugs association able to overcome melanoma intrinsic resistance to targeted therapy or biological therapy.

EXPERIMENTAL DESIGN

The aims of the project were pursued through four main steps:

- ***In vitro* analysis of synergism between inhibitors of oncogenic signalling pathway and TRAIL**

  A large panel of melanoma cell lines (n=49) with known genetic background was characterized for susceptibility/resistance profile to small molecules inhibitors targeting the MEK and/or PI3K/mTOR cascades and soluble TRAIL. MTT assay was used to determine IC50 of each cell line and these data were used to evaluate possible co-resistance to the selected drugs. Our findings revealed independent susceptibility profile of melanoma cells to AZD6244, BEZ235 and sTRAIL. Correlation with known relevant mutations in BRAF, NRAS, p53 and PTEN was studied. Chou-Talalay interaction analysis was performed to analyze potential synergism of the drugs used in our experiments.

- ***In vitro* analysis of mechanisms behind the synergism**

  Genome-wide expression profiling of melanoma cells was performed on Illumina platform to get insight into the mechanisms underlying drugs synergism. Annexin/Propidium Iodide (PI) staining, protein arrays, Western blot analysis, caspase activation and mitochondrial membrane depolarization ($\Delta\Psi$) evaluation were used to confirm hypothesized mechanisms. Transient silencing techniques proved the central role of identified molecules.

- ***In vivo* treatment of melanoma xenograft with the MEK inhibitor Selumetinib and sTRAIL**

  Female SCID mice were subcutaneously injected with exponentially growing melanoma cells and mice were treated with AZD6244 and TRAIL at concentrations defined based on literature data. Tumor growth rates were compared between untreated and treated groups and appropriate statistical analysis was performed on growth curves. Treatment-related toxicities were excluded based on haematoxylin-eosin staining of main organs. Immunohistochemistry staining for significant molecules was performed on tumor nodules to define in vivo mechanism of action of drug association.

- ***In vitro* modeling of melanoma-endothelium interaction**

  HUVEC cells were used to set up co-culture experiments with different melanoma cell lines; magnetic separation and multi- parametric flow cytometry was used to determine effects of cell-cell interaction on activation, differentiation status of HUVEC cells and on their response to combinatorial treatment.

3. MATERIAL and METHODS

3.1 REAGENTS

The small molecules inhibitors AZD6244 (MEK1/2), BEZ235 (dual PI3K/mTOR) and PLX4720 (BRAFV600E) were purchased from SelleckChem (Houston, TX, USA); soluble recombinant human TRAIL from AdipoGen (San Diego, CA, USA). The pan-caspase inhibitor z-VAD-fmk and its relative control z-FA-fmk were purchased from R&D Systems (Minneapolis, USA). Tetramethylrhodamine ethyl ester (TMRE) was purchased from Invitrogen-Life Technologies (Carlsbad, CA, USA). All reagents were formulated as recommended by suppliers.

3.2 CELL LINES

Melanoma cell lines were established during several years in the lab starting from surgical specimens of melanoma patients (Stage IIIb to IV following American Joint Committee on Cancer) not previously subjected to chemotherapy and admitted to Fondazione IRCCS Istituto Nazionale dei Tumori, Milan. All lesions were histologically confirmed to be cutaneous malignant melanomas. The study was conducted following institutional guidelines and in accordance to the Declaration of Helsinki Principles. Melanoma cell lines were cultured in RPMI-1640 (Lonza, Basel, Switzerland) supplemented with 2-10% inactivated fetal bovine serum (FBS) (Lonza), 2mM L-glutamine (Lonza), 20mM HEPES buffer (BioWhittaker, Walkersville, USA) in a humified chamber (95% air, 5% CO2) at 37^{o}C.
Human Umbelical Vein Endothelial Cells (HUVEC) were purchased from Invitrogen-Life Technologies and maintained in Medium-200 supplemented with Low Serum Growth Supplemented (LSGS) Kit (Gibco-Life Technologies). For all experiments HUVEC were used before the 10th *in vitro* passage.
All cell lines were regularly screened to ensure absence of mycoplasma contamination by PCR Mycoplasma test kit I/C (PromoKine, Heidelberg, Germany) following manufacturer's intructions.

3.3 CELL VIABILITY ANALYSIS

3.3.1 Cell viability

For evaluation of cell viability the with 3-(4,5)dimethylthiazol-2,5-diphenyltetrazolium bromide (MTT) assay was performed.
In details, cells were seeded at appropriate concentration in 96-wells flat bottom plates with 200 μl RPMI 1640 supplemented with 2% FCS. Next day, drugs were added and cells treated with different concentrations of AZD6244 (0.001μM - 10 μM), BEZ235 (0.001μM - 10 μM), recombinant human TRAIL (5-100 ng/ml. Treatments were performed in quadruplicates. After 48 hours cultures were evaluated for cell viability, by the MTT assay, a

colorimetric metabolic activity indicator of cell viability (it produces a yellow solution that is converted to dark blue, water-insoluble MTT formazan by mitochondrial dehydrogenases of living cells). Briefly, 20 μl of MTT were added to cells and cultures were incubated at 37°C for 4 hours; after this time, supernatant is carefully removed and 100 μl DMSO (Dimethyl sulfoxide) added. The plates are then read for absorbance at 570 nm with reference at 630 nm in a InfiniteM1000 plate reader (Tecan, Männedorf, Switzerland).
Non-linear regression analysis (by PRISM software, Graphpad) was used to calculate IC50 values for melanoma response to AZD6244 and BEZ235, based on dose-response curves by a log(inhibitor) vs. response, variable slope equation.

3.3.2 Drug interaction analysis

Growth inhibition data from MTT assays, performed after 48h of treatment, were analyzed for drug interaction by the Chou and Talalay[193] method through the CompuSyn software (ComboSyn). This is a method for drug combination analysis based on the median-effect equation, and comprises the Michaelis-Menten, Hill, Henderson-Hasselbalch, and Scatchard equations that define interaction between two entities.
The combination index values (CI) calculated through this mathematic result in a quantitative definition of additive effect (CI = 1), synergism (CI < 1) and antagonism (CI > 1) for drug associations. Specific algorithms are also used to calculate fraction affected (FA) values for each combination of compounds, indicating the percentage of cells affected by the treatment.

3.3.3 Assessment of apoptosis

Melanoma cell lines were harvested at exponential growth phase and seeded in 6-weel plates at appropriate concentrations in RPMI with 10% FCS. The day after, culture- medium was changed and cells were treated with AZD6244 and BEZ235 at 0.05 mM and TRAIL at 25 ng/ml or as single agents or in combination in RPMI with FCS 4%. Annexin-V APC and Propidium Iodide (PI) (BD Pharmingen) were used to detect the extent of apoptosis (early, Annexin-V+ PI- and late, Annexin-V+ PI+) and necrosis (Annexin-V- PI+) after 72 hours of treatment. Briefly, cells were detached with Trypsin and washed with cold phosphate-buffered saline (PBS) (BioWhittaker, Lonza, Belgium), resuspended in Binding Buffer (BD Pharmingen) and incubated with Annexin-V APC and PI for 15' at Room Temperature (RT). Samples were acquired on a Gallios Flow Cytometer (Beckman-Coulter), cell debris were excluded gating on forward scatter (FSC) and side scatter (SSC) and data were analyzed by FlowJo software (Tree Star, Inc. Ashland, OR). Each experiment was replicated at least three times.

3.3.4 Measurement of mitochondrial membrane depolarization (ΔΨm)

The extent of mitochondrial membrane depolarization was determined using the fluorescent probe Tetramethylrhodamine Ethyl Ester (TMRE) (Invitrogen, Life Technologies). TMRE is a fluorescent dye that penetrates through cell membrane and is accumulated by mitochondria. In case of mitochondrial membrane depolarization, the integrity of the mitochondrial membrane is disrupted, TMRE is lost and a reduced fluorescence intensity is detected in depolarized cells. Cells were seeded and treated as in 3.4.3, then after 48h harvested, washed with RPMI and incubated for 15 minutes at 37^{o}C with TMRE at final concentration of 50nM. Data were acquired on a Gallios Flow Cytometer (Beckman Coulter) and data were analyzed by FlowJo software gating on forward scatter and side scatter to exclude debris and then evaluating the percentage of cell with a reduced MFI if compared to untreated samples.

3.4 CASPASE ACTIVITY

3.4.1 Caspase activity detection and inhibition

Caspase-3/7 activation was evaluated using the MUSE cell analyzer (Millipore). Briefly, cells were seeded and treated as in 3.4.3 and after 48h the MUSE caspase 3/7 kit was used to stain for the activated form of caspases of interest. The function of the kit is based on a substrate for caspases 3 and 7: if present in the active form they are able to cleave the substrate, that become fluorescent and detectable.

Instead, caspase-8 activation was detected through intracellular staining with an antibody specific for cleaved caspase-8 (Cell Signalling Technologies) after permeabilization of the cells with the Fix and Perm solution (BD Biotecnologies); data were acquired on a Gallios Flow Cytometer.

For caspases-inhibition experiments, melanoma cells were seeded as in 3.4.3 and the day after, before treatments, pre-incubated for 1 hour at 37^{o}C with general caspase inhibitor z-VAD-fmk or control z-FA-fmk (BD Pharmingen) used at 5 μM. Caspases inhibitor and relative control were added every 24 hours and extent of apoptosis was then assessed by annexin-V/PI flow cytometry assay at 72h from treatments.

3.5 GENOME-WIDE EXPRESSION PROFILING

For gene expression experiments, melanoma cells were seeded at appropriate concentration in T75 flasks and, the day after, treated for 8h with AZD6244 (0.1 μM), BEZ235 (0.1 μM) or TRAIL (25 ng/mL), as single drugs or in combinations. Each type of treatment was performed in three biological replicates. Total RNA was then isolated from melanoma cells, using QuiaZol (Invitrogen) reagent, and a clean-up treatment with RNAeasy kit (Qiagen, Valencia, CA) and with RNase-free DNase to remove contaminating genomic

DNA was performed. The Bioanalyzer (Agilent) was used to assess RNA integrity and single-color hybridization of the obtained RNAs was performed on Illumina Bead Chip HumanHT-12_v4 Microarrays (Illumina San Diego, CA) containing more than 48,000 transcript probes.

The expression profiles have been deposited in NCBI's Gene Expression Omnibus (GEO) with GSE accession number GSE55050. The BeadStudio Illumina software was utilized to correct for background, filtering of data, and quantile normalization, while the BRB-array Tools (Vers.4.3.0) software allowed the identification of group of genes significantly modulated by the different types of treatment. Class comparison was carried out by a random-variance F-test with a nominal significance level of 0.001 and the permutation P values for significant genes were computed based on 10,000 random permutations. VENNTURE software[194] was used to carry on a pairwise analysis of significance of gene modulation between any two of the treatments was carried out at P=0.01., and Edwards-Venn diagram were generated in order to categorize all genes significantly modulated by any of the single-treatment as well as by any combination. Upstream regulator analysis and downstream effects analysis on genes significantly modulated by different treatments were done using Ingenuity Pathway Analysis (IPA 8.5, www.ingenuity.com); this software is able to identify, based on the observed changes in the gene expression, which biological functions are expected to be increased or decreased and which modulation in upstream transcriptional regulators can explain the differences seen in the dataset. Results are displayed based on P values and Z score statistics.

P values measures how likely is the association between a set of genes and related function, or the likelihood of the overlap between the changes in gene expression in the dataset and those that are regulated by a predicted transcription factor. The meaning of the Z score statistics is to infer the activation states ("increased" or "decreased") of the identified biological functions and of the predicted transcription factors. Only Z scores greater than 2 or smaller than 2 can be considered significant.

3.6 SURFACE AND INTRACELLULAR STAININGS

3.6.1 Flow cytometry experiments

Expression of surface intracellular molecules was evaluated by flow cytometry, when needed after cell permeabilization with Cytofix/perm (BD Pharmingen). Briefly cells at exponential growth phase were harvested and seeded at appropriate concentrations; the day after treated with AZD6244 and BEZ235 at 0.05mM and TRAIL at 25ng/ml as single drugs or in combinations. At 24-48 hours cells where then harvested again, washed with cold PBS and fixed for 20 minutes on ice with the fixation solution; after the incubation on ice cells were washed twice with Perm-wash and stained with appropriate antibody. Flow cytometry

analyses were carried out with antibodies specific for: cleaved caspase 8, TRAIL-R1/DR4, TRAIL-R2/DR5, CD31(PECAM), CD325 (N-Cadherin) (BioLegend); TRAIL-R3/DCR1 and TRAIL-R4/DCR2 (AdipoGene); CD56 (NCAM), CD54 (ICAM-1) (BD Pharmingen), MCSP, CD202b (TIE-2), CD144 (VE-Cadherin) (Miltenyi Biotec).
When needed FITC conjugated goat anti-mouse secondary antibody (Jackson Lab) was used.

3.7 PROTEIN ANALYSIS

3.7.1 Protein extraction

For protein extraction a total of about $5x10^6$ cells was seeded in T75 flasks and treated with inhibitors or TRAIL at concentrations used for annexin-V/PI experiments. At desired time points cells were collected, washed with ice-cold HBSS (BioWhittaker) and homogenized in lysis buffer (with PMSF and proteases inhibitor) (Invitrogen) or lysis buffer provided with protein arrays (R&D) for 30 minutes on ice. Cells were then centrifuged at high speed and supernatants collected for protein analysis. Protein concentrations in lysates were determined using BCA Protein Assay Kit (Pierce) according to manifacturer's instructions.

3.7.2 Western Blot

Cell lysates (30-60 µg) were loaded in precast 7% NuPAGE Tris-Acetate (for Apollon) or 4% to 12% NuPAGE Bis-Tris polyacrylamide gels (Invitrogen Life Technologies), for other molecules and transferred to nitrocellulose membranes (Amersham). After membrane blocking with Tris-buffered saline solution (0.1% Tween-20 (TBS-T) 5% Bovine Serum Albumine (Sigma-Aldricht), blots were hybridized overnight with the appropriate primary antibody. The next day membranes were washed with T-TBS and hybridized with appropriate horseradish peroxidase (HRP)-conjugated secondary antibody. Signals were detected using the chemiluminescence method and the ECL Western Blotting Detection System (GE Healthcare).
Antibodies used in Western Blot analysis were: livin, clusterin, cIAP-2, BIM, BID, BAX, Mcl-1 and c-Myc (Cell Signalling); survivin (Novus Biologicals); c-IAP1 (R&D Systems); HIF1α and actin (Abcam); Apollon/BIRC6, XIAP, α-SMA (BD Biosciences); cFLIPL/S (Alexis Biochemicals).

3.7.3 Protein arrays specific for apoptosis molecules

The Human Apoptosis Array kit (R&D Systems) was used according to manufacturer's instructions using cells and collected as indicated in the specific data sheets. Arrays were washed and 50 ng of total proteins were hybridized overnight on the arrays. Signals on membranes were detected by chemiluminescence and quantitated by densitometric analysis

with Quantity One software (BioRad Laboratories). Values of protein expression are calculated as percentage of the relative positive controls mean, after background subtraction.

3.7.4 Angogenesis-related protein arrays

Angiogenesis Array kit (R&D Systems) was performed in accordance to manifacturer's instruction with cell supernatants of treated or untreated cells. Supernatants were collected after an O/N of treatment with single drugs or combinations of inhibitors and TRAIL (in order to have as less cell death as possible) and then centrifuged to eliminate any cellular debris. Signals on membranes were detected by chemiluminescence and quantitated by densitometric analysis with Quantity One software (BioRad Laboratories). Values of protein expression are calculated as percentage of the relative positive controls mean, after background subtraction. To assure culture medium was not responsible for signals seen, a control membrane was hybridized with medium-only and developed as the others.

3.8 SILENCING BY SMALL- INTERFERING RNA (siRNA)

For silencing experiments we used an Apollon-specific siRNA that our lab had previously validated (see ref 25) for activity in our melanoma cell lines. The stealth RNAi siRNA sequence is GGGCAUGCUGGAAUGUUGACGUUAA (Invitrogen). Cells were seeded at appropriate concentration in complete medium in 6-well plates and, the day after, transfected with Apollon-siRNA or with its corresponding negative control, at the final concentration of 75nmol/L. Lipofectamine RNAiMAX (Invitrogen) was used as transfecting agent. After 48h from transfection cells were treated with indicated drugs and then evaluated at different time points for extent of apoptosis or mitochondrial depolarization.

3.9 ELISA ASSAYS

TGFβ1 and VEGFα specific Quantikine ELISA kit (R&D Systems) were used according to manufacturer's instructions. Supernatant from treated and untreated melanoma cells were collected as in 3.8.4 and stored at -80^{o}C until use. Absolute concentration was calculated based on a standard curve obtained through serial dilution of a standard sample in the kit. The microplate reader (Tecan Infinite M1000) was used to determine optical density of each plate and then data were elaborated through Microsoft Excel software.

3.10 ANIMAL EXPERIMENTS

In vivo experiments were evaluated and approved by the Institutional Ethical Committee for Animal Experimentation of our Institute and by the Italian Ministry of Health (Project INT_17/2011). Moreover, all projects involving animal experimentation were performed according to the Italian laws (D.L. 116/92 and after additions).

Immunocompromised female mice (severe-combined immunodeficient mice, SCID) 8-10 weeks old were purchased from Charles River Laboratories, housed in the facility at our institute and provided with food and water ad libitum. Exponentially growing melanoma cells were harvested and injected subcutaneously (3 or $5x10^6$) in the left flank of each animal. Mice were then checked every two days for sign of tumor growth. Tumor size was regularly evaluated by measuring the orthogonal diameters (d and D) and calculating tumor volumes with the following formula: $4/3\pi\ d^2\ D\ /2$.

For experiments with drugs treatment, after injection mice were randomly assigned to one of 4 groups (7 animals/group) and when tumors became palpable treatments were started. AZD6244 was administered at 25 mg/kg by oral gavage, TRAIL at 30 mg/kgby intraperitoneal injection. Animals received vehicle, the two drugs as monotherapy or their combination, 7 days per week for two consecutive weeks. Mice were monitored daily for signs of toxicity and were weighed twice a week.

At the end of experiments mice were euthanized and tumor nodules removed for immunohistochemical stainings.

3.11 IMMUNOHISTOCHEMISTRY

Immunohistochemical analysis was performed on formalin-fixed, paraffin-embedded specimens. 4-µm-thick tissue sections were cut, deparaffinized through graded series of ethanol passages and then rehydrated in distilled water. A 30-min incubation in methanol with 0.3% H_2O_2 was used to inhibit endogenous peroxidase and to optimize immune detection, nonenzymatic antigen unmasking was performed: tissue sections heated at 95°C for 6 min in an autoclave in a 5 mM citrate buffer (pH 6). After cooling, tissue sections were incubated with primary antibody overnight at 4°C, then covered with streptavidin–horseradish peroxidase (DAKO Corp.) for 30 min and finally visualized with the use of red 3-amino-9-ethylcarbazole (Sigma Chemical) in 0.05 M acetate buffer containing 0.015% H_2O_2.

Tissue sections from melanoma metastases were characterized by staining for TRAIL-R2/DR5 (Sigma). Neoplastic nodules removed from mice at the end of treatment were characterized by staining with mAbs to human pERK, cleaved caspase-3 (Cell Signalling), Apollon, HIF1α, IL8 (AbCam), VEGFβ (Santa Cruz Biotechnology), as well as to mouse CD31 (Dianova). Apoptosis extent was evaluated by TdT-mediated dUTP nick end-labeling (TUNEL) staining (Roche). Tissue sections subjected to the same treatment but without incubation with primary antibody were used as negative controls. Images were acquired at 20x with an Axiovert 100 microscope (Zeiss) equipped with a digital camera (AxioCam MrC5, Zeiss).

3.12 MELANOMA-ENDOTHELIAL CELLS CO-CULTURES

Exponentially growing melanoma cells were irradiated with 5000 CyG and seeded at the appropriate concentration in RPMI 10%FCS. After 24 hours, co-culture experiments were set up with a 1:1 rate with HUVEC cells in Med200 medium. After 6 days cells were harvested and stained with indicated antibodies (as in 3.7.1) or resuspended in ice-cold PBS buffer with 2mM EDTA and 0.2%FCS and then purified with magnetic separation using anti-MCSP or anti-CD31 microbeads (Miltenyi Biotec) in accordance to manifacturer's instructions and depending on necessities.

3.13 STATISTICAL ANALYSIS

Cluster 3.0 software was used to cluster data from TRAIL susceptibility, TMRE and caspase-8 cleavage assays, as well as results of drug interaction analyses.

GraphPad Prism software was used to generate graphs and statistical analysis for every figure. Spearman correlation analysis was used to determine correlation between melanoma responsiveness to TRAIL and susceptibility to target-specific inhibitors or expression of TRAIL receptors.

One-way or Two-way ANOVA, followed by Bonferroni or Student-Newman-Keul (SNK) multiple comparison test were used to determine significance of differences among treatments in terms of melanoma apoptosis, caspase activation, mitochondrial depolarization, modulation of apoptosis- and angiogenesis-related molecules.

In xenograft experiments, comparison of the antitumor activity of different treatments was carried out by mixed effects model ANOVA [195] by XLSTAT software (Xlstat).

4.RESULTS

DEATH RECEPTORS ENGAGEMENT AND SIGNALLING PATHWAYS INHIBITION

Synergistic anti-tumor activity and inhibition of angiogenesis by co-targeting of oncogenic and death receptor pathways in human melanoma

Giulia Grazia[1], Claudia Vegetti[1], Fabio Benigni[2], Ilaria Penna[1], Valentina Perotti[1], Elena Tassi[1], Ilaria Bersani[1], Gabriella Nicolini[1], Silvana Canevari[3], Carmelo Carlo-Stella[4], Alessandro M. Gianni[6], Roberta Mortarini[1], and Andrea Anichini[1]

[1]Human Tumors Immunobiology Unit, and [3]Functional Genomics Unit, Dept. of Experimental Oncology and Molecular Medicine, [6]Medical Oncology Unit 2, Dept. of Medical Oncology, Fondazione IRCCS Istituto Nazionale dei Tumori, Milan; and Medical Oncology, Università degli Studi di Milano, Milan; [2]San Raffaele Scientific Institute, URI, Milan; [4]Department of Oncology and Hematology, Humanitas Cancer Center, Humanitas Clinical and Research Center, Rozzano; and Department of Medical Biotechnology and Translational Medicine, University of Milan, Italy.

Cell Death and Disease 2014 Oct 2;5:e1434. doi: 10.1038/cddis.2014.410

4.1 TRAIL RECEPTORS ARE EXPRESSED BOTH IN MELANOMA CELL LINES AND IN METASTATIC MELANOMA LESIONS

To confirm the choice of using the pro-apoptotic molecule TRAIL for our association studies, we decided to first evaluate responsiveness to TRAIL in a panel of 49 melanoma cell lines isolated in our laboratory from primary and metastatic tumors (Supplementary Table S1 summarizes known features of cell lines used).

Melanoma response to TRAIL was initially evaluated through MTT assay. 55.6% of cell lines were found to be susceptible (>75% inhibition at the highest dose) to the anti-proliferative and pro-apoptotic activity of TRAIL, while the remaining 44.4% of cell lines showed strong resistance to TRAIL (<25% cell death at 100 ng/mL) (Figure 4.1A). Moreover, responsiveness to TRAIL was not associated with presence of the two most frequent genetic alterations found in cutaneous melanoma ($BRAF^{V600E}$ and $NRAS^{Q61R}$ mutations, Figure 4.1B).

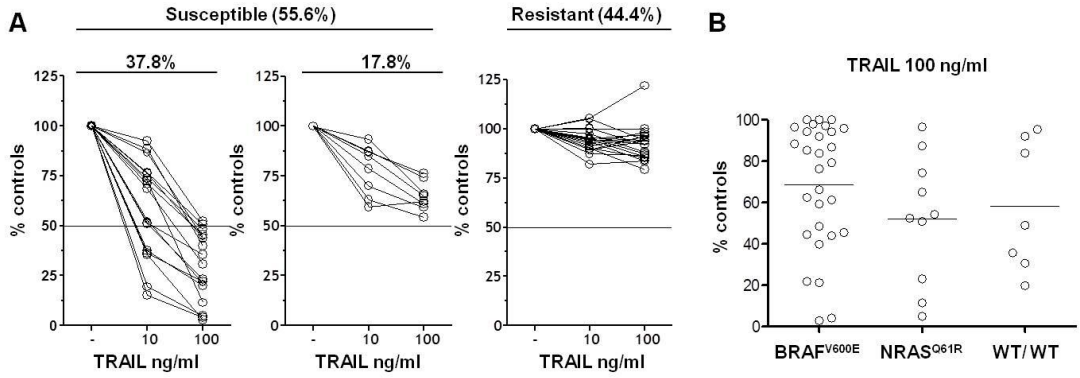

Figure 4.1: Responsiveness to TRAIL and correlation with genetic background. **A**) Susceptibility and resistance to TRAIL (10-100ng/ml) of a panel of melanoma cell lines tested by MTT assay after 48h of treatment. Data are reported as % of growth inhibition over untreated controls. **B**) Lack of association between responsiveness to TRAIL and known mutations in BRAF or NRAS genes.

We then decided to analyze TRAIL receptors expression both *in vitro*, on the same panel of melanoma cell lines, and in tissue sections from lymph nodes or subcutaneous melanoma metastases from 10 patients.

As shown in Figure 4.2A, the analysis of TRAIL receptor expression indicated that TRAIL-R1 (DR4) and TRAIL-R2 (DR5) were always expressed *in vitro*, although with different intensity of staining, and levels of expression of DR5 but not of DR4 were significantly (p= 0.0196) correlated to the responsiveness to TRAIL, pointing to the relevance of this receptor for the pro-apoptotic response to the ligand.

TRAIL-R2/DR5 expression in tissue samples was confirmed by immunohistochemistry staining on neoplastic cells from melanoma metastases (Figure 4.2B), supporting the choice of selecting this pathway as a target in human melanoma.

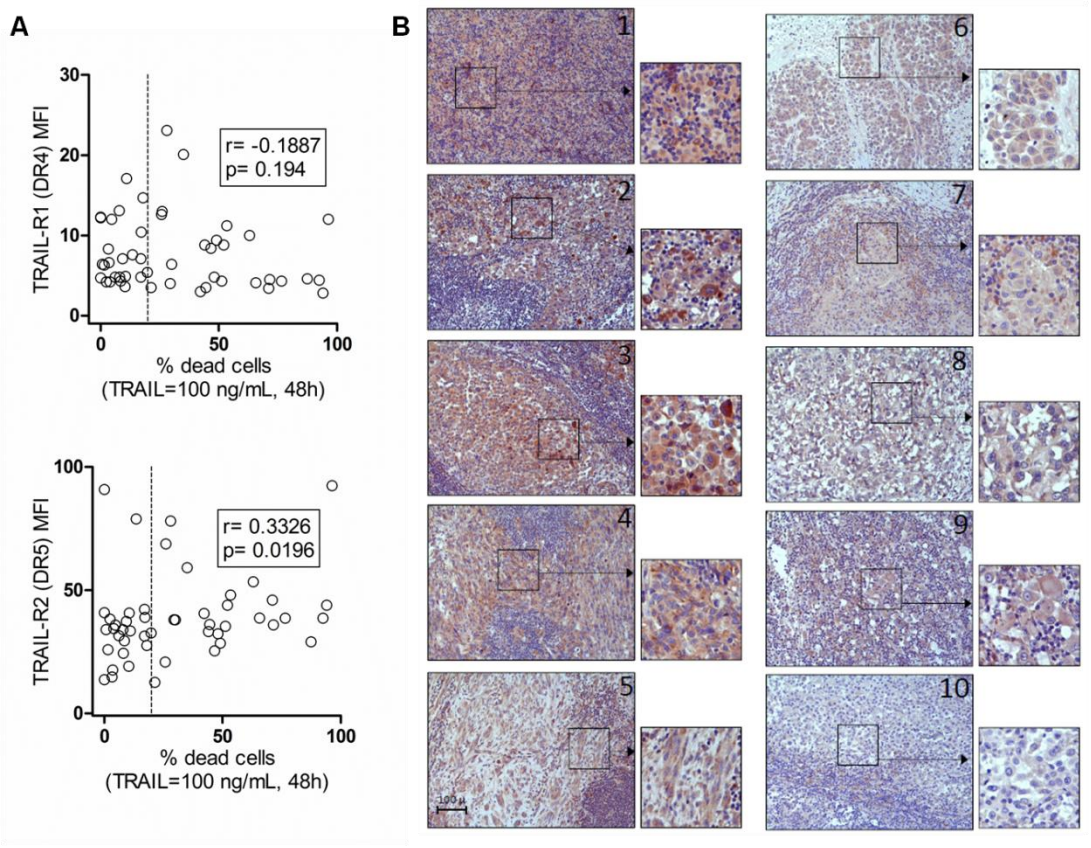

Figure 4.2 TRAIL receptors expression and correlation with response. A) MTT assay at 48h on a panel of melanoma cell lines treated with TRAIL=100 ng/mL; TRAIL-R1 and -R2 expression was assessed by flow cytometry and results are expressed as mean fluorescence intensity (MFI). Statistical analysis by Spearman correlation. **B**) Tissue sections from lymph node (lesions #1-3 and #5-10) or subcutaneous (lesion #4) melanoma metastases from 10 patients were stained with anti-DR5 mAb.

4.2 INDEPENDENT SUSCEPTIBILITY PROFILES OF MELANOMA CELL LINES TO TARGET-SPECIFIC INHIBITORS AND TRAIL

To further confirm the rationale of combining TRAIL with small molecule inhibitors specific for oncogenic signalling pathways, we decided to evaluate whether or not human melanoma cell lines are characterized by frequent intrinsic concomitant resistance to MEK, PI3K/mTOR inhibitors and to the death receptor ligand TRAIL.

To this end we decided to work on the same panel of 49 patient-derived melanoma cell lines with known wild-type or mutant BRAF, NRAS, PTEN and p53 (Supplementary Table S1); to best represent the possible different alterations present in human melanoma. We initially characterized all cell lines for susceptibility to AZD6244 and BEZ235 by MTT assays using a wide range of doses. IC50 for each inhibitor were calculated through non linear regression.

Our data revealed that numerous tumors responsive (with an IC_{50} <0.05 μM) to AZD6244 or BEZ235, were instead TRAIL-resistant (<10% dead cells at TRAIL 100 ng/mL), while several tumors resistant to these inhibitors (with $IC_{50} \geq 0.2$ μM) showed instead high susceptibility to TRAIL (representative data Figure 4.3).

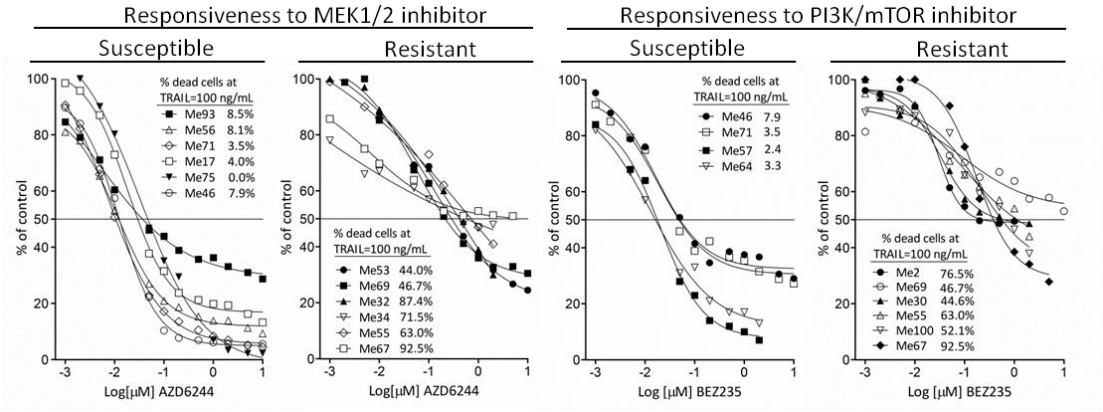

Figure 4.3 Independent susceptibility profiles to MEK and PI3K/mTOR inhibitors and to TRAIL. Dose-response curves and responsiveness of selected melanoma cell lines to AZD6244, BEZ235 and TRAIL assessed by MTT assay after 48h treatment. Data are expressed as % of live cells over untreated controls.

Furthermore, Spearman analysis of growth-inhibition data indicated no significant correlation between susceptibility to the signalling inhibitors and to TRAIL (Figure 4.3). Indeed, concomitant resistance to AZD6244 and TRAIL, or to BEZ235 and TRAIL was found in only 7 and 10 tumors respectively (open circles and squares in Fig 4.4). The relative sporadic presence of cell lines showing cross-resistance to all three drugs supported our choice of evaluating their association for melanoma treatment.

Literature reports that melanoma cells respond to TRAIL receptor engagement as the so-called “type II cells”, activating not only the extrinsic pathway of apoptosis, but also the intrinsic one (mitochondrial dependent).

On these bases, we decided to complete the characterization of our panel of cell lines analyzing caspase-8 cleavage (by flow cytometry) and loss of mitochondrial potential (TMRE assay) in response to TRAIL treatment (100 ng/ml, 48h).

Our data highlighted the expected correlation not only between response to TRAIL (growth inhibition by MTT assay) and caspase-8 cleavage ($p=0.0086$), but also with mitochondrial depolarization ($p<0.0001$, Figure 4.4) confirming that the majority of melanoma cell lines, upon engagement of TRAIL receptors, behave as the type-II cells and require amplification of apoptotic signals through the mitochondrial pathway.

Of note, it is well known that small molecules inhibitors, like AZD6244 and BEZ235, are able to induce melanoma cell death through the activation of the mitochondrial dependent apoptosis cascade. This notion, along with the correlation found between TRAIL susceptibility and mitochondrial depolarization, provided also a mechanistic rationale for the hypothesis of combining oncogenic and death receptor pathways in human melanoma.

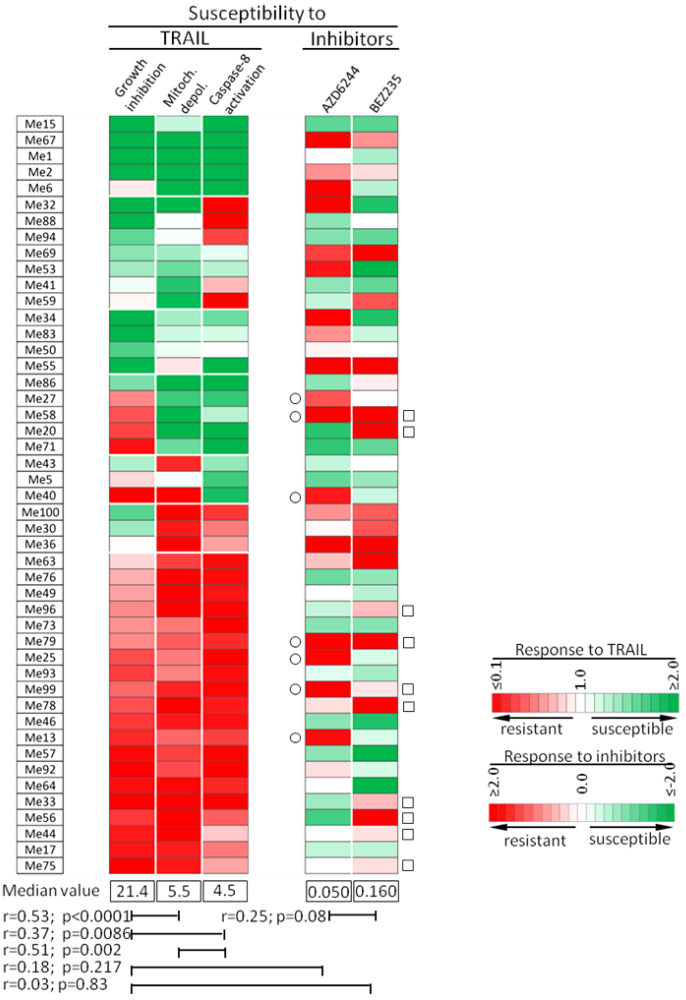

Figure 4.4 Correlation between TRAIL response and mitochondrial depolarization. Cell viability, mitochondrial depolarization and caspase-8 cleavage in response to TRAIL and responsiveness to AZD6244 and BEZ235 (by MTT assay, 48h). Data clustered by the three parameters of response to TRAIL. Statistical analysis by Spearman correlation analysis. TRAIL-resistant tumors with IC50 to AZD6244 (○) or to BEZ235 (□) >0.2 μM. All data represented by a color code indicating the ratio of the values for each tumor to the median value of each parameter in the whole panel.

In fact, the association of TRAIL with small molecules inhibitors like AZD6244 or BEZ235 should be able to increment the level of activation of the apoptotic cascade thanks to: 1) a concomitant targeting of both the extrinsic (mainly due to TRAIL activity) and the intrinsic apoptosis pathways; 2) the convergence of the stimuli on the mitochondrial dependent pathway of cell death; 3) possible effects of the inhibitors on the modulation of pro- and anti-apoptotic molecules responsible for TRAIL resistance in melanoma cells.

The association of TRAIL and target-specific agents should therefore lead to a higher degree of melanoma apoptosis, possibly counteracting mechanisms of melanoma resistance to cell death.

4.3 SYNERGISTIC ANTI- TUMOR EFFECTS through the CONCOMITANT TARGETING of ONCOGENIC and DEATH RECEPTOR PATHWAYS

4.3.1 Chou-Talalay analysis of drug interaction

Two melanoma cell lines susceptible to the inhibitors and TRAIL (Me1 and Me83) and two TRAIL resistant and poorly responsive to AZD6244 (Me13 and Me6), were then selected for the initial analysis of drug interaction. All possible two- and three-drug combinations were evaluated by the Chou and Talalay method using data from MTT assays (see ref.193 and section 3.4.2 for detailed description).

This type of analysis generates a graphical output were fraction affected (FA) values are plotted versus combination index values (CI), giving a quantification of the synergistic interaction between the drugs used. Synergism is defined when CI values are lower than 1.0; a combination index of 1.0 identifies additive effects, while higher values of CI point at antagonism.

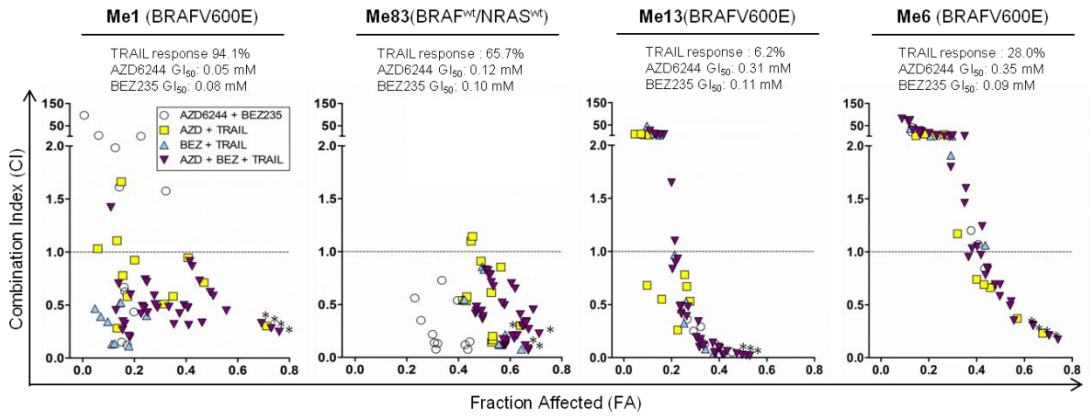

Figure 4.5 Drug interaction analysis by Chou-Talaly method. Fraction affected (Fa) vs Combination index (CI) plots in four melanoma cell lines (Me1, Me83, Me13, Me6) as assessed by a 48 h MTT assay followed by data analysis by Compusyn software. Cells were treated with combinations of AZD6244 (at 0.001, 0.005, 0.01, and 0.05 μM), BEZ235 (at 0.005, 0.01, and 0.02 μM) and TRAIL (at 5, 10 and 25 ng/mL). Note that data points for CI values >150 are not shown.

As shown in Figure 4.5, the outcome of drug interaction, both in terms of synergism/ antagonism and of fraction affected, was dependent not only on the specificity of the combination but also on dosing of each agent. However, two combinations were the best ones in achieving a strong synergism (CI<0.3) with high FA values in all four cell lines: the AZD6244-BEZ235-TRAIL and also the AZD6244-TRAIL combinations; moreover, the lowest CI values were observed when AZD6244 was used at 0.05 μM (asterisks, Figure 4.5).

Western blot analysis of three different melanoma cell lines treated with AZD6244 at 0.05 μM or with BEZ235 at 0.02μM confirmed that the relative targets of these drugs were effectively inhibited (Figure 4.6)

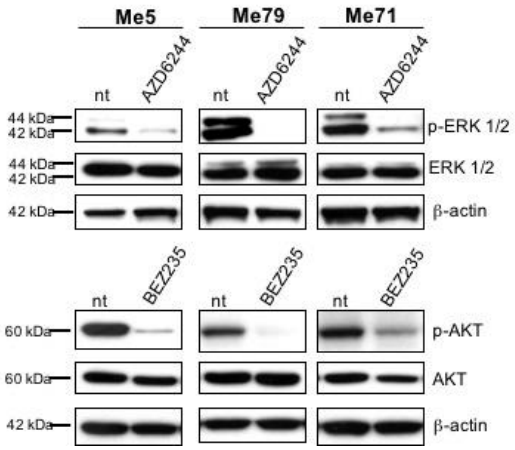

Figure 4.6 AZD6244 and BEZ235 effectively inhibit their targets. Me5, Me79 and Me71 melanoma cells were treated for 18h with at AZD6244 at 0.05 μM or with BEZ235 at 0.02μM and analyzed for the indicated molecules.

4.3.2 Extended drug interaction analysis on a panel of melanoma cell lines

Chou-Talalay drug interaction analysis was then extended to a panel of 21 melanoma cell lines selected for the known profile of susceptibility and resistance to both the inhibitors and TRAIL.

To facilitate the understanding of the results, we created a color code to visualize results of combination indexes and fraction affected data; Figure 4.7 shows the correspondences between colors used and raw data values. Basically, red coloring indicates antagonism while greens shades indicates synergy; additive effects are instead represented in black.

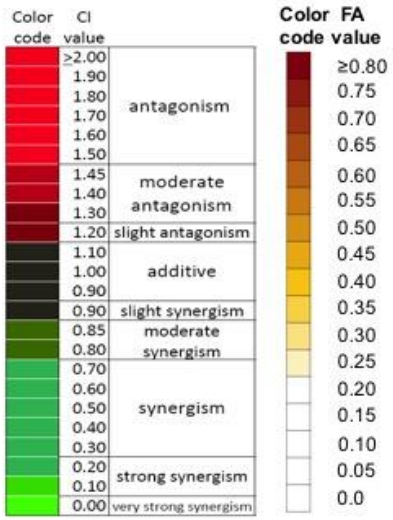

Figure 4.7 Correspondance between color code and raw values for both combination indexes and fraction affected data.

In Figure 4.8 data are reported using the color code described in Figure 4.7 and cell lines used are grouped in AZD6244- resistant (IC_{50} ≥0.2 μM, n=7) and AZD6244- susceptible (IC_{50} ≤0.2 μM, n=14).

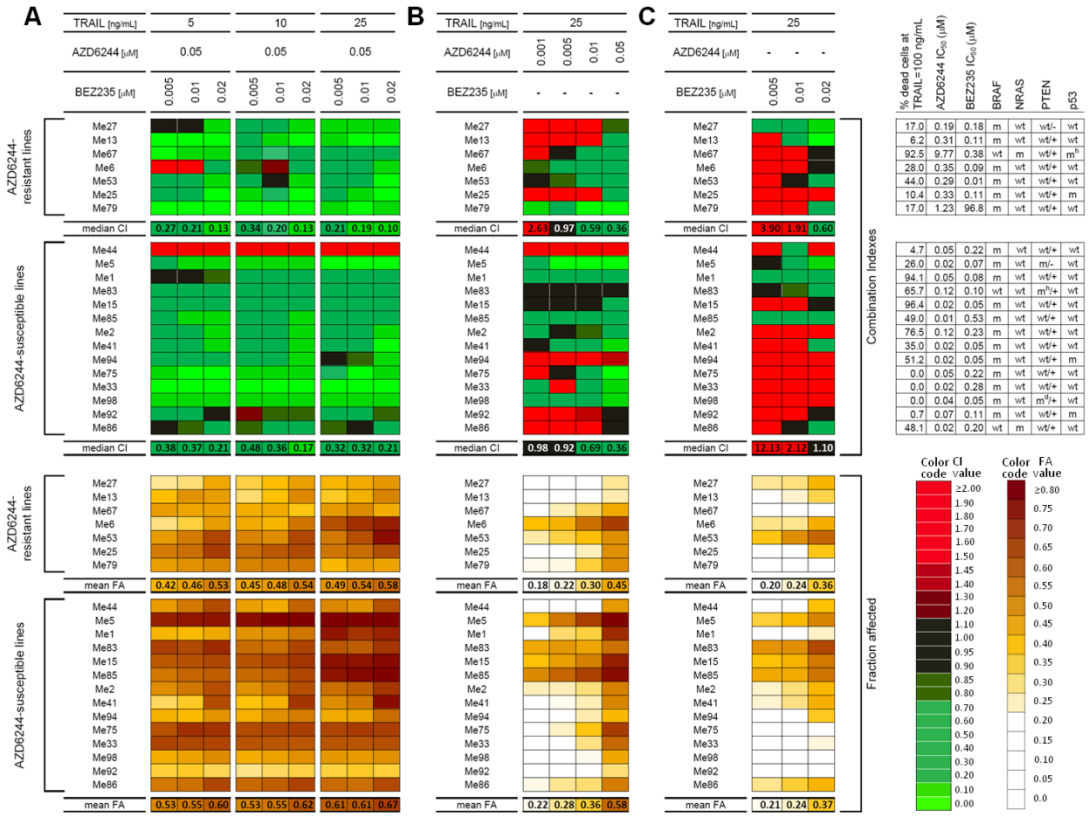

Figure 4.8 Chou and Talalay analysis of drug interaction in two groups of melanoma cell lines with different responsiveness to Selumetinib. Cell lines were treated with the association of AZD6244, BEZ235 and TRAIL (**A**), or AZD6244 and TRAIL (**B**), or BEZ235 and TRAIL (**C**). The right hand side panel summarizes susceptibility profiles and main molecular features of all cell lines. Numbers at the bottom of each panel indicate median CI values and mean FA values for each combination. m: mutant; wt: wild type; +, -: expression/lack of expression of PTEN by western blot.

Results of the Chou-Talalay analysis on the panel of 21 melanoma cell lines confirmed that the AZD6244-BEZ235-TRAIL combinatorial treatment was the best in achieving a strong synergistic interaction between the drugs, with CI<0.3 and high levels of FA in all AZD6244-resistant lines and in 13/14 AZD6244-susceptible lines (Figure 4.8A). Of note, the efficacy of three-drug combination was observed not only in cell lines resistant to the MEK inhibitor, but also in those with high IC50 values for BEZ235, or completely resistant to TRAIL, and was not associated to a particular mutational status of BRAF, NRAS, PTEN and/or p53 (as shown by table at the right hand of the figure).

As expected, increasing doses of BEZ235 and of TRAIL were associated with further improvement in either CI (Figure 4.8A) or FA values (Figure 4.9).

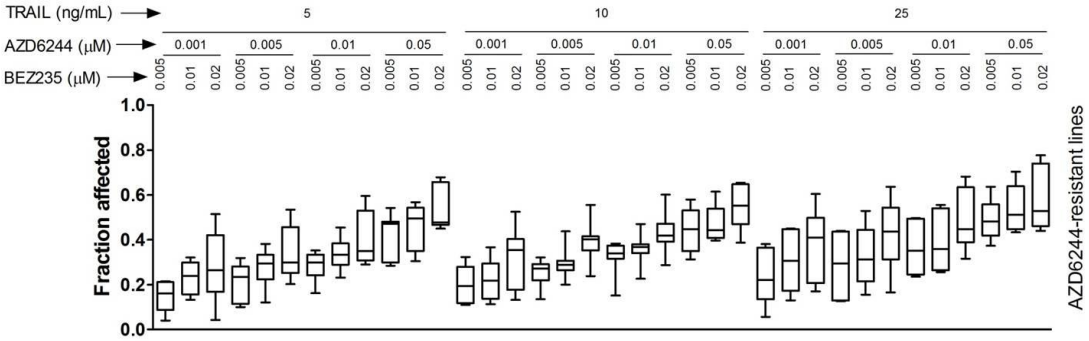

Figure 4.9: Combinatorial treatments increment FA values. Box and whiskers plots of FA (Fraction affected) values by combinatorial treatment of AZD6244-resistant (n=7) melanoma cell lines treated with the association of AZD6244, BEZ235 and TRAIL

Moreover, a detailed statistical analysis of raw FA data (Supplementary Table S2) indicated that a significant increment in FA values were achieved using TRAIL at the highest dose (25ng/ml) as well as if BEZ235 was added to AZD6244+TRAIL or TRAIL was added to the AZD6244+BEZ235 combinations.

In the same panel of tumors, also the AZD6244-TRAIL combination achieved strong synergism values, again when AZD6244 was used at 0.05 μM (Figure 4.8B), while in contrast in most instances the BEZ235-TRAIL combinatorial treatment showed marked antagonism and poor fraction affected (Figure 4.8C).

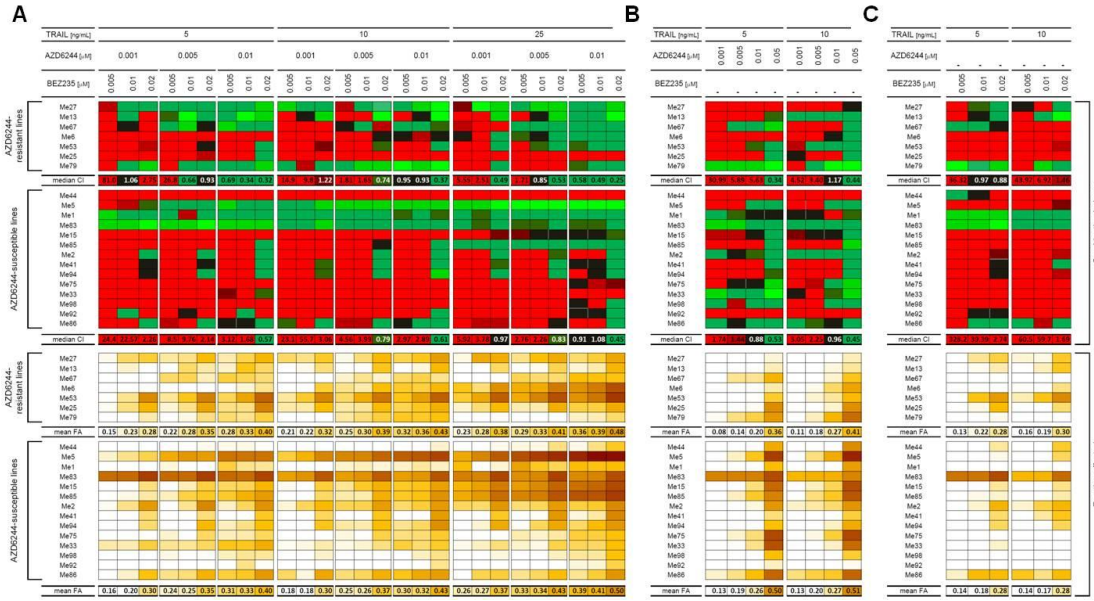

Figure 4.10 Chou and Talalay analysis of drug interaction in two groups of melanoma cell lines with different responsiveness to Selumetinib. The same panel of cell lines (as in Figure 4.8) was treated with the association of AZD6244, BEZ235 and TRAIL (**A**), or AZD6244 and TRAIL (**B**), or BEZ235 and TRAIL (**C**). Numbers at the bottom of each panel indicate median CI values and mean FA values for each combination.

Based on the results summarized in Figure 4.10 (where data are reported with color code used in Figure 4.7) at an AZD6244 dosage lower than 0.05 μM (ranging from 0.001 μM to 0.01 μM) CI values for both the AZD6244+TRAIL and AZD6244+BEZ235+TRAIL association indicated, in the vast majority of cell lines, antagonism and the BEZ+TRAIL combination was confirmed to exert antagonistic effects; also, at these conditions the percentage of cells affected, represented by the FA values, was significantly low (Figure 4.10).

Taken together, these results indicated that association of MEK inhibitors, with or without PI3K/mTOR blockade, with TRAIL leads to synergistic anti-tumor effects, when AZD6244 is used at 0.05μM, on most melanomas, both independently from their intrinsic resistance to inhibitors or to TRAIL and irrespective from the genetic background of the cell lines analyzed.

4.5 COMBINATORIAL TREATMENTS RESCUE SUSCEPTIBILITY OF MELANOMA CELLS TO CASPASE-DEPENDENT APOPTOSIS

4.5.1 Gene expression profiling of melanoma cells treated with inhibitors and TRAIL

To gain insight into the main biological processes behind the positive association of MEK, PI3K/mTOR inhibitors and TRAIL, we decided to carry out a whole genome gene expression analysis.

Since our goal was to identify the possible mediators of the activity our association, we selected for this type of experiment Me13 cells. This line was both resistant to TRAIL and poorly responsive to AZD6244 and BEZ235, but responded significantly (CI <0.01) to the combinatorial treatment. Whole genome gene expression studies were carried out on Illumina Bead Chip HumanHT-12_v4 Microarrays by the facility at our Institute.

Class comparison analysis helped us to first identify the set of genes specifically modulated by the AZD6244-BEZ235-TRAIL association (examples visualized by Edwards-VENN diagrams, Figure 4.11A), and we subjected them to analysis by IPA (Ingenuity Pathway Analysis) software.

We used the “downstream effects analysis”, a computational tool that, starting from observed changes in a dataset of gene expression, identifies which biological functions are expected to be either decreased or increased.

A significant up-regulation of the functions “cell death” and “apoptosis” and a down-regulation of the functions “tumorigenesis”, “cell migration” and “proliferation” were identified (Figure 4.11B and Supplementary Table S3).

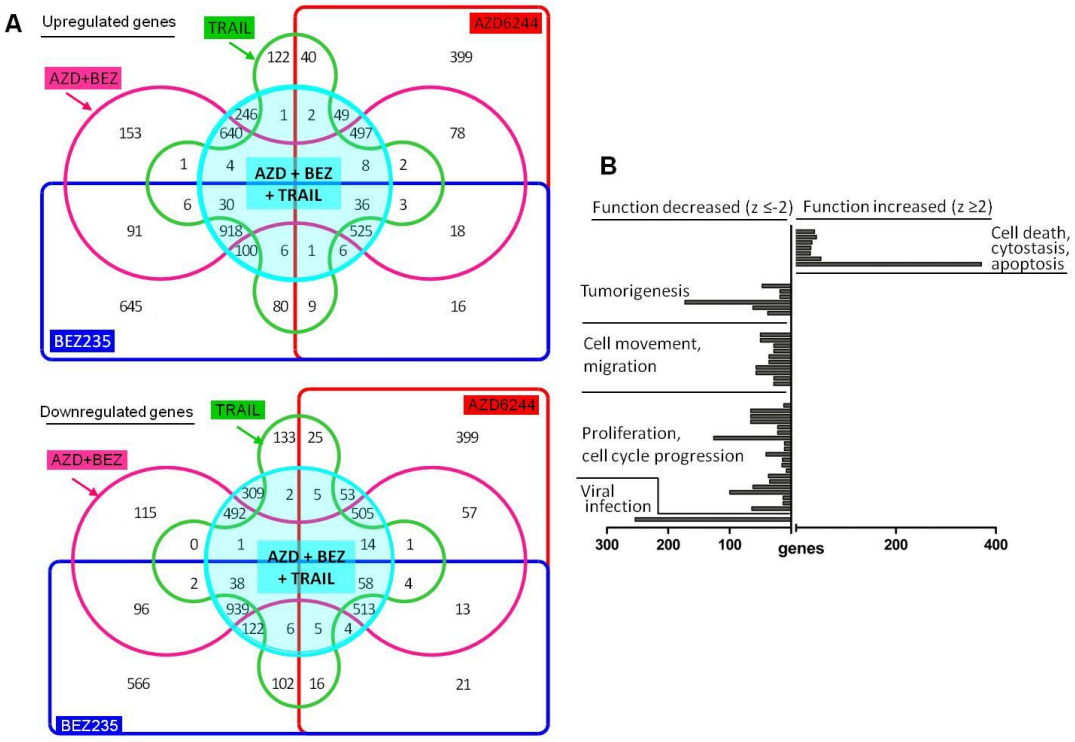

Figure 4.11 Combinatorial treatments induce modulation of the functions related to cell death. **A**) schematic representation of the subsets of genes modulated by different combinatorial treatments. **B**) Data from the gene expression profiling on melanoma cells treated with AZD6244+BEZ235+TRAIL were used to identify the specific set of genes affected by the three-drugs treatment (identified by light blue color) and these were then subjected to downstream effect analysis (by IPA). Only biological functions with significant z score statistic (>2, indicating increase of biological function, or <-2, indicating decrease of biological function).

The same analysis was performed on genes modulated by the AZD6244-TRAIL association. Similarly, we used IPA to identify biological processes associated with the modulation of specific genes by combinatorial treatment (Figure 4.12A) and our results confirmed an increment of the functions “cell death” and “apoptosis” also for this two-drug combination (Figure 4.12B and Supplementary Table S4).

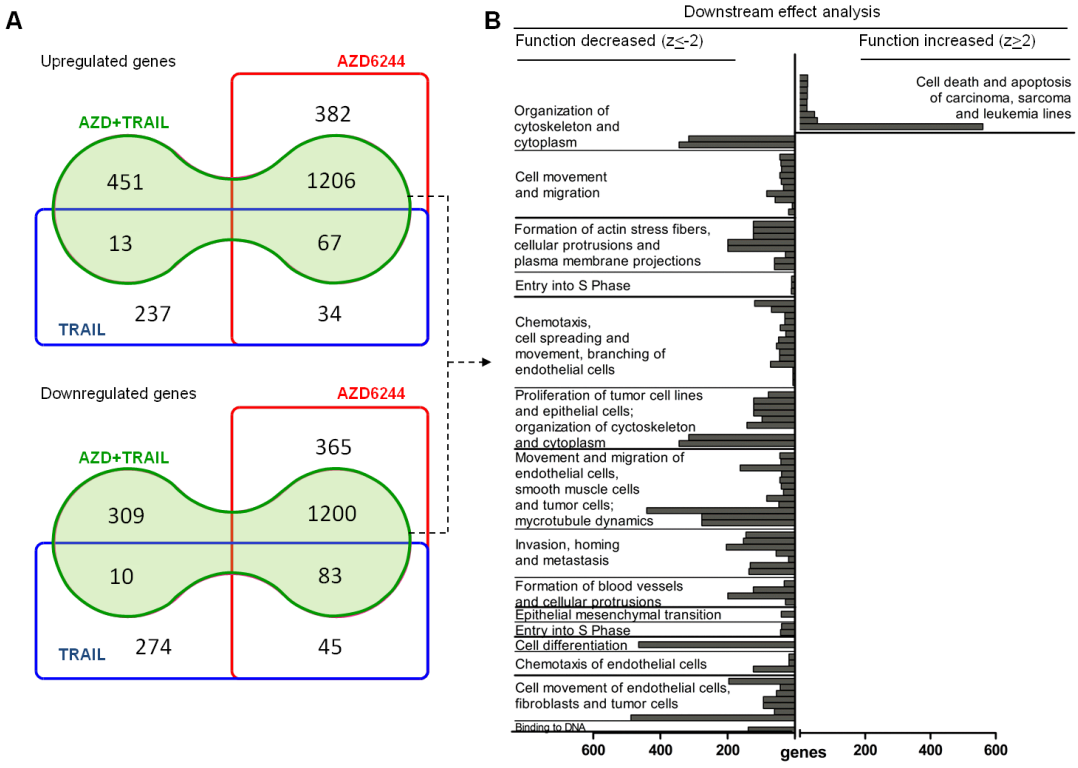

Figure 4.12 Treatments with AZD6244 and TRAIL modulate genes related to cell death. A) Edwards-VENN diagram representation of significantly modulated genes in Me13 cells treated with AZD6244 (red), TRAIL (blue) or their association (green). **B**) Downstream effect analysis on the subsets of genes identified by the green shape in panel a. Only biological functions with significant Z score statistic (>2, indicating increase of biological function, or <-2, indicating decrease of biological function) and significant overlap P value are shown.

4.5.2 Apoptotic cell death and caspase activation

To confirm results of gene expression profile and therefore the induction of melanoma cell death by the association, we performed annexin-V/PI flow cytometry assays to discriminate between apoptosis and necrosis.

Figure 4.13 shows results of our experiments in terms of the sum of early (annexin-V+ PI-) and late (annexin-V+ PI+) apoptosis. Significantly higher levels of apoptotic cell death, compared to single agents, were observed in 5/8 tumors by AZD6244-TRAIL ($p<0.01$ by ANOVA followed by SNK test), and in 8/8 tumors by the three-drug combination ($p<0.01$ in 7/8 tumors and $p<0.05$ in 1/8 tumors).

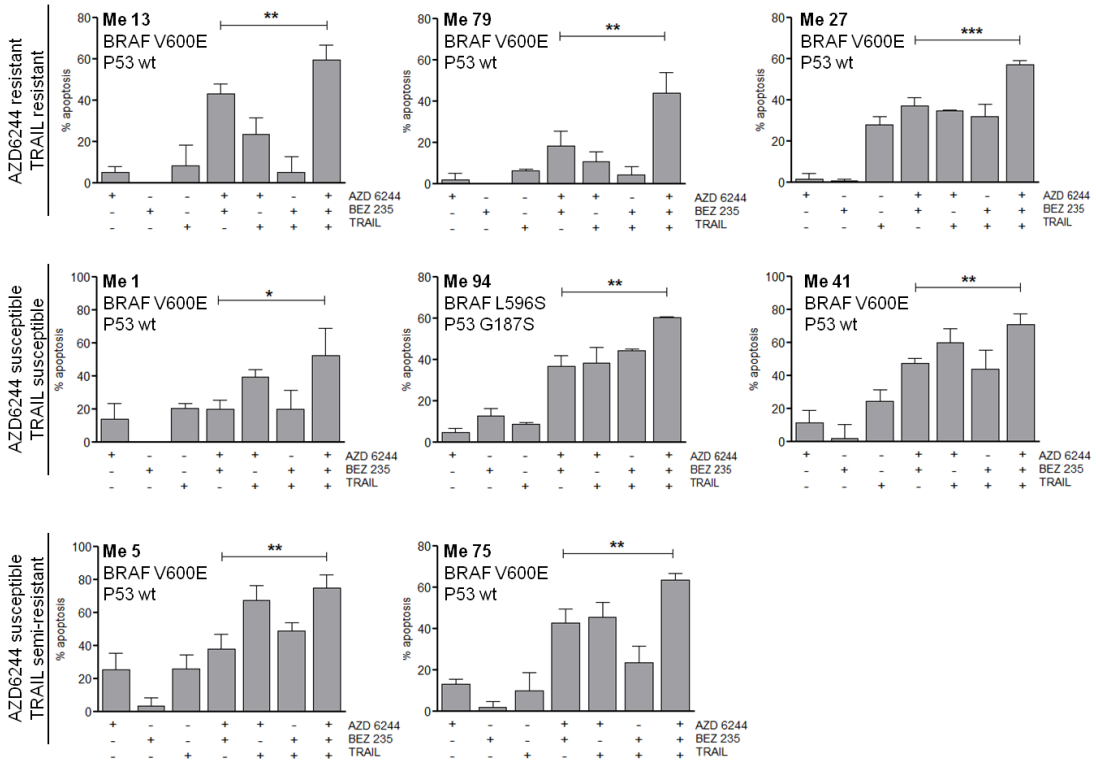

Figure 4.13 Combinatorial treatment induce melanoma apoptosis. Melanoma cells were treated with AZD6244 (0.05 μM), BEZ235 (0.05 μM), and TRAIL (25 ng/mL) and their combinations for 72 h, and apoptosis was assessed by Annexin-V/PI assay. Results shown as sum of early (annexin-V^+ PI^-) and late (annexin-V^+ PI^+) apoptosis values. Statistical analysis by ANOVA followed by SNK test. ***: p<0.001, **: p<0.01; *: p<0.05

Data reported in Figure 4.14 highlight that the increment in melanoma cell death achieved by combinatorial treatment is not dependent on the specific inhibitor used, but on the pathway being targeted, as the association of a different inhibitor of the MEK/ERK pathway (PD0325901) with TRAIL exerts similar effects in terms of apoptotic cell death if compared to single agents. Also in this case the addition of Rapamycin (an inhibitor of the PI3K/mTOR/AKT pathway) determines a further increment in melanoma cell death.

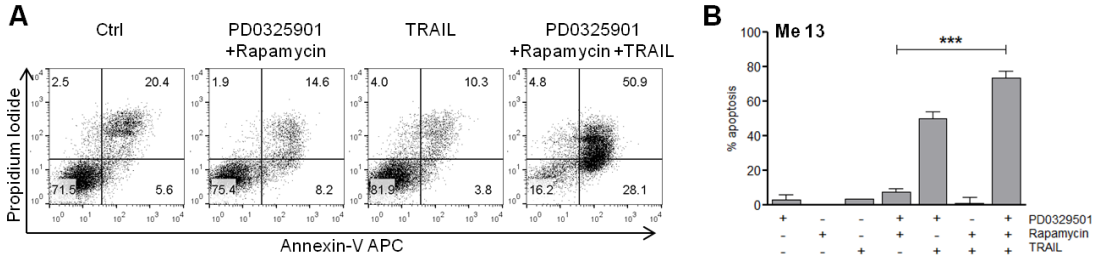

Figure 4.14 Enhanced melanoma apoptosis by association of TRAIL with PD0325901 and Rapamycin. Me13 cells were treated with TRAIL (10 ng/mL), PD0325901 (5 nM), rapamycin (10 nM) or their combinations. Apoptosis was assessed at 72 h by flow cytometry (representative plots in **A** and mean values (± S.D.) for three independent experiments in **B**) p<0.001 for all comparisons, by ANOVA and SNK test.

Since the two pathways of apoptosis converge on the cleavage and induction of effector caspase-3/7, we then performed a caspase activation assays.

Results, shown in Figure 4.15, indicated the AZD6244-BEZ235-TRAIL and AZD6244-TRAIL as the combinations to achieve a significantly higher activation of caspase 3/7, if compared to single agents ($p<0.01$) or to the association of the two target-inhibitors ($p<0.01$).

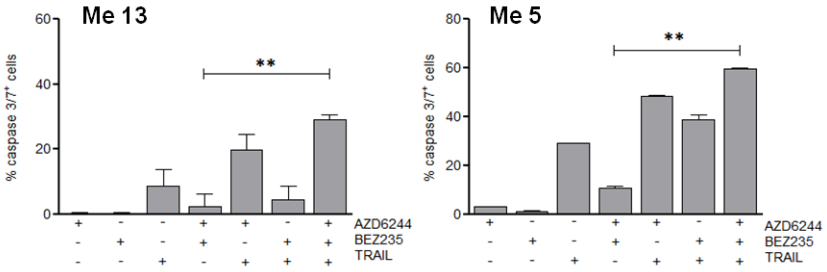

Figure 4.15 Induction of caspase activity by combinatorial treatments. Caspase 3/7 activation in two melanoma cell treated with AZD6244 (0.05 μM), BEZ235 (0.05 μM), and TRAIL (25 ng/mL) and their combinations for 24 h. Mean values (± S.D.) for three independent experiments. Statistical analysis by ANOVA followed by SNK test. **: $p<0.01$

To confirm the functional relevance of caspase activation for cell death induction by our association of drugs, we performed more annexin-V/Propiudium Iodide experiments with a pre-treatment of cells with a pan caspase inhibitor (z-VAD-fmk) and its relative control (z-FA-fmk).

As attended, the blockade of caspases activation completely abolished the increase in apoptosis induced by the addition of TRAIL to the AZD6244-BEZ235 combination, even in TRAIL-resistant (Me13) or in weakly susceptible (Me5) melanomas. No impact on cell death promoted by the two inhibitors together was seen (Figure 4.16).

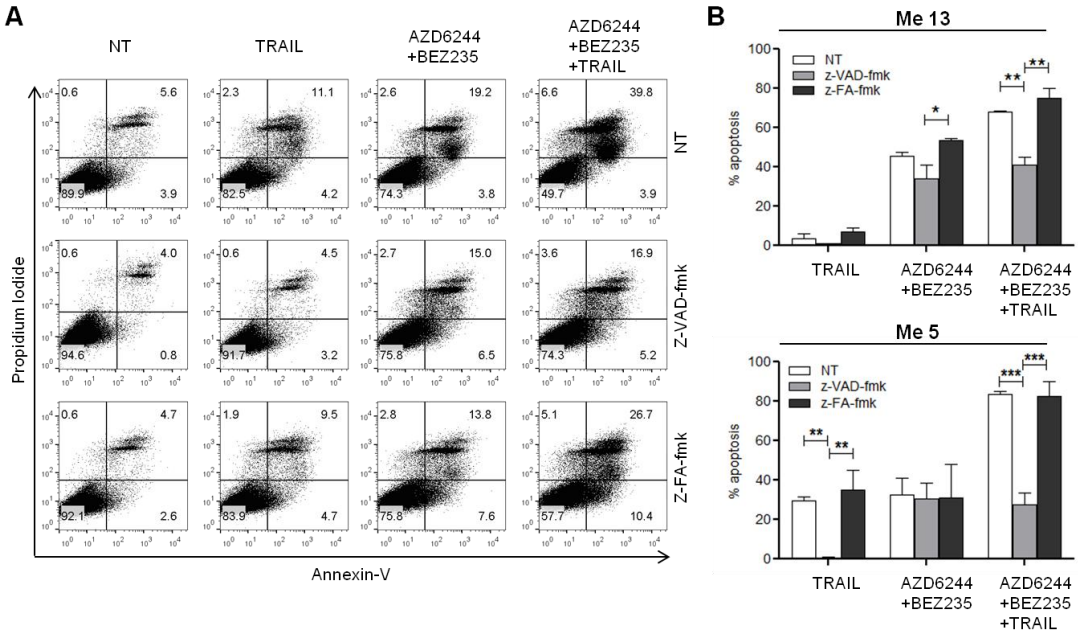

Figure 4.16 Apoptosis induced by combinatorial treatments is caspase- dependent. Annexin-V/PI assays (**A**, single experiment; **B**, average of three experiments) in melanoma cells (Me 5, Me13) treated with AZD6244 (0.05 μM), BEZ235 (0.05 μM), and TRAIL (25 ng/mL) and their combinations for 72h in the presence of the pancaspase inhibitor z-VAD-fmk or of the negative control peptide z-FA-fmk. Statistical analysis by ANOVA followed by SNK test. ***: p<0.001, **: p<0.01; *: p<0.05.

As shown in Figure 4.17 we obtained similar results with the two-drug association (AZD6244 +TRAIL), with apoptotic levels that, in the presence of caspase inhibition, go back to the ones obtained by Selumetinib treatment only.

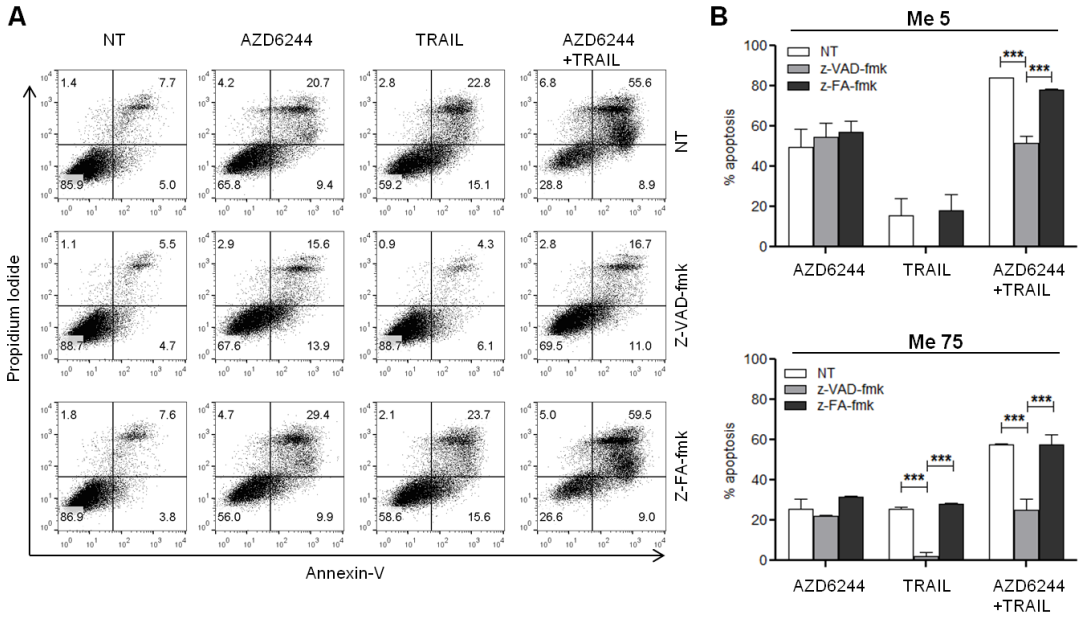

Figure 4.17 Apoptosis induced by the association of Selumetinib and TRAIL is caspase-dependent. Me5 and Me75 were treated with AZD6244 (0.05 mM) or TRAIL (25 ng/mL) or their combinations for 72 h, in the presence of the pancaspase inhibitor z-VAD-fmk or of the negative control peptide z-FA-fmk, and apoptosis was assessed by Annexin-V/PI assay (**A** representative plots, **B** mean of three independent experiments). Results shown as sum of early and late apoptosis. Mean values (± S.D.) for three independent experiments. Statistical analysis by ANOVA followed by SNK test. ***: p<0.001, **: p<0.01.

Taken together these results indicated that the concomitant targeting of MEK, with or without PI3K/mTOR inhibition, and of the TRAIL pathway has a synergistic anti-melanoma activity likely mediated by an enhancement of caspase-dependent apoptosis.

Our hypothesis, therefore, was that the inhibitors used for our combinatorial treatment could operate at some level in TRAIL receptor cascade, modulating molecules responsible for melanoma intrinsic resistance to TRAIL-induced apoptosis.

4.6 COMBINATORIAL TREATMENTS MODULATE SEVERAL PRO AND ANTI-APOPTOTIC MOLECULES

To further dissect the mechanisms leading to the positive interaction demonstrated for our association of drugs, we decided to test whether combinatorial treatments had any impact on the expression of several pro- and anti-apoptotic molecules in both the extrinsic and intrinsic pathways of cell death.

Western blot analysis of cells treated with the AZD6244-BEZ235-TRAIL combination revealed that this treatment significantly affected the expression of the caspase-8 inhibitor c-FLIP, inducing a marked down-regulation seen on both c-FLIP$_L$ and/or c-FLIP$_S$ (Figure 4.18A).

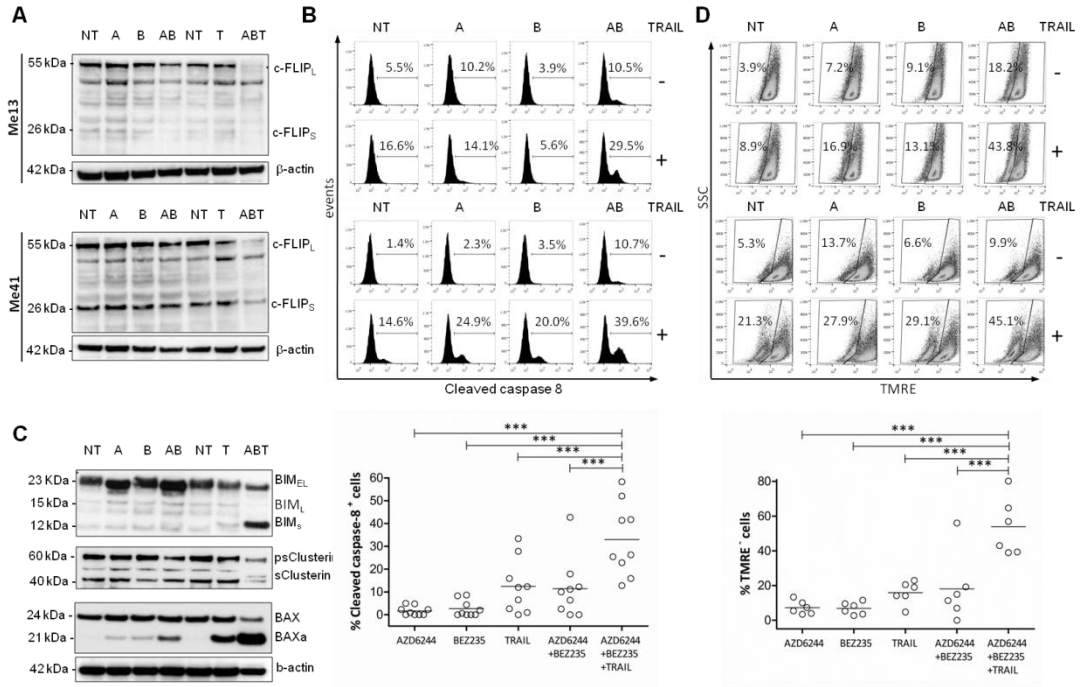

Figure 4.18 Combinatorial treatments modulate several pro and anti-apoptotic molecules and induce caspase-8 activation and mitochondrial depolarization. A) Western blot analysis for c-FLIP expression in two melanoma cell lines (Me13 and Me41) treated with AZD6244 (A), BEZ235 (B), TRAIL (T) or the indicated combinations. **B**) flow-cytometry analysis for cleaved caspase-8 (representative histograms and results in a panel of 9 cell lines). **C**) western blot analysis for expression of BIM, clusterin and BAX in Me13 cells treated as in (a). **D**)TMRE analysis for mitochondrial depolarization (representative histograms and results in a panel of 6 cell lines). Statistical analysis by ANOVA followed by SNK test; ***, p<0.001.

This was demonstrated in two melanoma cell lines with different susceptibility profiles to the anti-tumor agents used: reduced levels of cFLIP were seen not only in Me41, partially responsive to TRAIL and susceptible to the inhibitors, but also in Me13 cells, less responsive to AZD6244 and resistant to TRAIL.

As expected, the same association induced also the most significant increment in caspase-8 cleavage, as evidenced by flow cytometry experiments and confirmed in a panel of 9 other cell lines (Figure 4.18B).

The efficacy of our treatment was documented also by analysis of several Bcl-2 family members: western blots showed an up-regulation of the pro-apoptotic isoforms BIMs and BAXα, a down-regulation of two isoforms (ps and s) of the Bax inhibitor Clusterin (Figure 4.18C), as well as a down-modulation of Mcl-1 and BID (Figure 4.19 and data not shown).

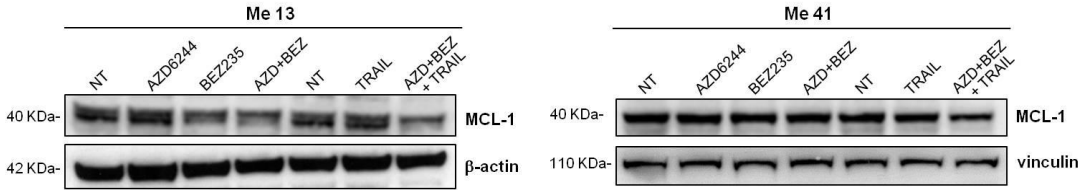

Figure 4.19 Combinatorial treatments down-regulate MCL-1. Western blot analysis of two melanoma cell lines (Me 13 and Me 41) treated or not with the indicated associations of AZD6244, BEZ235 (0.05μM) and TRAIL (25 ng/ml)

Moreover, as expected, the strongest increase in mitochondrial depolarization was exerted by the three-drug association if compared to single agents and to the AZD6244-BEZ235 combination (Figure 4.18D), in agreement with the notion that Bcl-2 family members have a central role in the mitochondrial pathway of cell death. [196]

Enhanced modulation of c-FLIP, and up-regulation of BIMs and BAXα, but not of Clusterin, compared to single agents, as well as caspase-8 cleavage and mitochondrial depolarization were confirmed also for the AZD6244-TRAIL association (Figure 4.20).

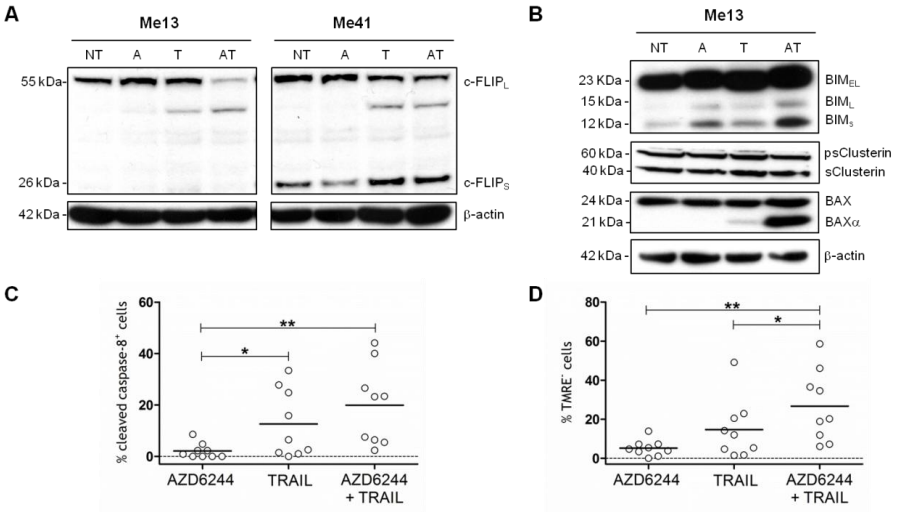

Figure 4.20 The association of Selumetinib and TRAIL modulates several proteins and induces caspase-8 activation and mitochondrial depolarization. A, B) Western blot analysis for c-FLIP, BIM, clusterin and BAX in melanoma cell lines treated with AZD6244 (A), TRAIL (T) or their combination (AT). **C**) Cleaved caspase-8 and **D**) TMRE assay for mitochondrial depolarization in a panel of 9 melanoma cell lines. Statistical analysis in **C,D** by ANOVA followed by SNK test; ** p<0.01; * p<0.05.

Since the Inhibitor of Apoptosis Proteins (IAP) is another group of molecules with important roles in programmed cell death, we also evaluated the expression of several members of this family.

Treatment of the same two melanoma cell lines (Me13 and Me41) with AZD6244-BEZ235-TRAIL induced a strong down-modulation of c-IAP1, c-IAP2, XIAP and Bruce/Apollon/BIRC6, but not of Survivin and Livin, if compared to the effects of single agents or to AZD6244-BEZ235 treatment (Figure 4.21).

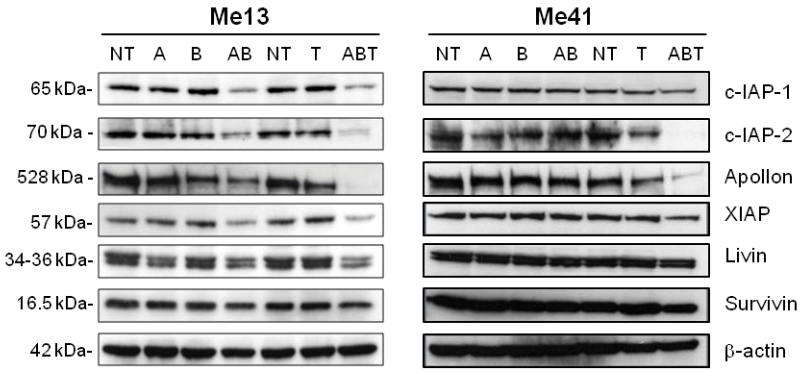

Figure 4.21 Combinatorial treatments modulate IAPs. Western blot modulation of IAP proteins by treatment of two melanoma cells lines (Me13 and Me41) with AZD6244 (A), BEZ235 (B) TRAIL (T) and their combinations (AB, ABT); NT: untreated

Similarly, the AZD6244-TRAIL association was able to down-modulate IAP-2, XIAP and, specially, Apollon/BIRC6 (Figure 4.22).

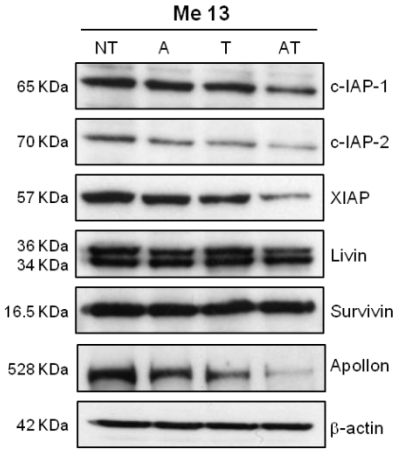

Figure 4.22 The association of Selumetinib and TRAIL modulates the expression of several IAPs. Modulation of the indicated IAP proteins by treatment of melanoma cells (Me13) with AZD6244 (A), or TRAIL (T) or AZD/TRAIL (AT) combination.

Since the giant IAP Apollon/BIRC6 was recently shown by our group to play a relevant role in suppressing melanoma response to several small molecules inhibitors and to TRAIL, and our experiments pointed at a crucial role of this molecule also in in this setting of treatments, we decided to evaluate it through silencing experiments by previously validated siRNA.[197]

As expected, Apollon silencing had no influence on untreated cells, but in cells treated with the MEK inhibitor, with or without BEZ235, and TRAIL, the absence of Apollon significantly reduced the % of live cells (Figure 4.23B).

Correspondingly, Apollon silencing induced a marked increment in mitochondrial depolarization after treatment with AZD6244 and TRAIL or with the three-drugs association. (Figure 4.23C).

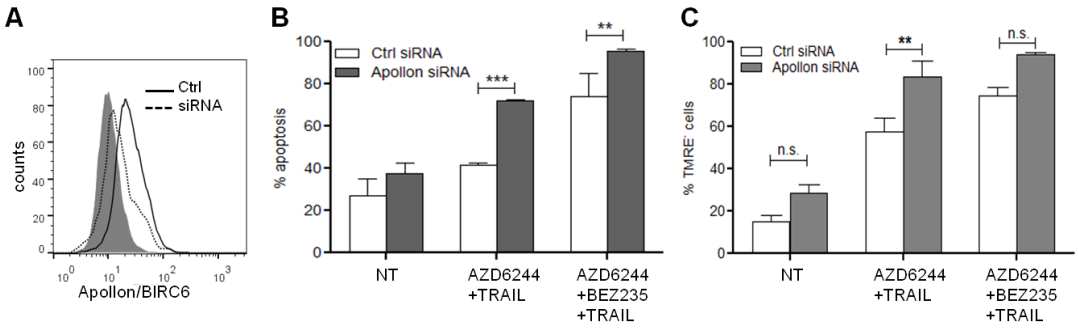

Figure 4.23 Apollon silencing increments melanoma cell death and mitochondrial depolarization. A) Flow cytometry control of Apollon silencing**.** Effect of Apollon silencing on cell death (**B**) and on mitochondrial depolarization (**C**) in Me41 cells treated with the indicated agents and their combinations. Mean values (± S.D.) for three independent experiments; statistical analysis by ANOVA followed by SNK test; ***, p<0.001. **, p<0.01.

Taken together, these results suggest that association of TRAIL with co-targeting of MEK and PI3K/mTOR, or with MEK blockade only, promotes effective melanoma cell death by affecting the expression levels of several molecules involved in the regulation of both the extrinsic and intrinsic apoptosis pathways, with Apollon modulation as a key effect promoted by combinatorial treatment.

4.7 IN VIVO ANTI-TUMOR ACTIVITY OF THE COMBINATORIAL TREATMENT THROUGH PROMOTION OF MELANOMA CELL DEATH AND INHIBITION OF ANGIOGENESIS

4.7.1 Tumor growth inhibition *in vivo*

Based on our positive *in vitro* results, we decided to verify if co-targeting of oncogenic and death receptor pathways could exert significant anti-tumor effects also *in vivo*.

To this end, since both the three-drug (AZD/BEZ/TRAIL) and two-drug (AZD/TRAIL) associations shared synergistic anti-melanoma activity *in vitro* and similar mechanisms of apoptosis induction, we decided to investigate the effects of two-drug treatment with Selumetinib and TRAIL on melanoma xenografts.

We started testing three melanoma cell lines selected to have different susceptibility to TRAIL, for their ability to grow subcutaneously in immune-compromised mice.

All the three lines tested grew *in vivo*, with no sign of toxicity on mice results of increment in tumor volume over time are showed in Figure 4.24.

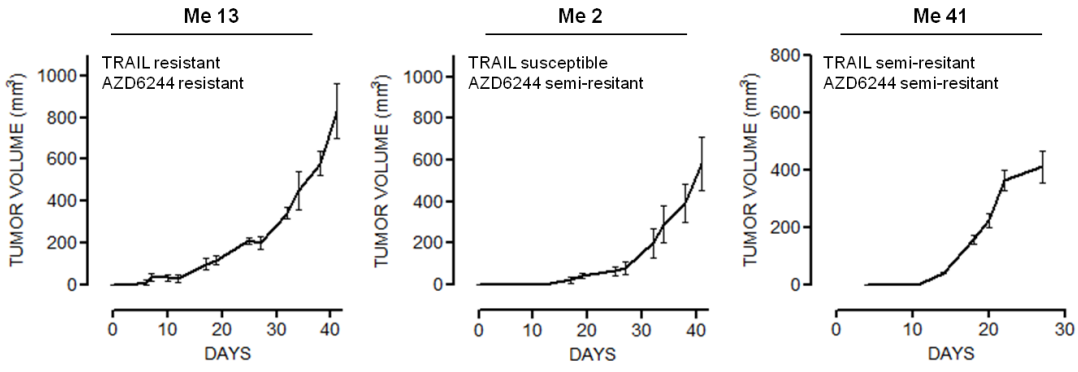

Figure 4.24 Growth curves of 3 melanoma cell lines subcutaneously injected in female SCID mice.

To evaluate the efficacy of our combination we then selected, among the cell lines tested for the ability to grow *in vivo*, the one that was TRAIL- resistant (Me13) and poorly responsive to AZD6244 and for which we already had good *in vitro* data on the response to drug association.

Female SCID mice were injected with exponentially growing melanoma cells and, when tumors became palpable, were treated the MEK inhibitor or soluble TRAIL for two consecutive weeks. AZD6244 treatment of SCID mice bearing s.c. Me13 xenografts exerted a moderate tumor inhibition effect, while as expected TRAIL had no impact on tumor growth, confirming the resistance of this cell line also *in vivo*.

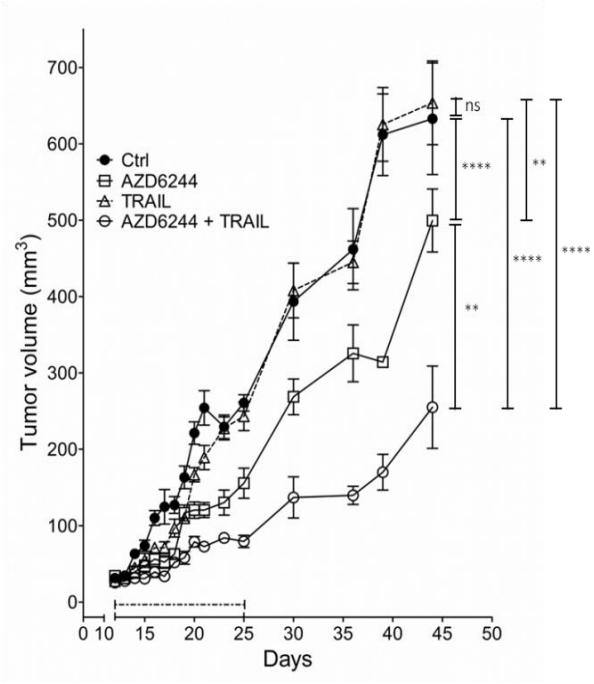

Figure 4.25 The association of Selumetinib and TRAIL significantly reduces tumor growth. Female SCID mice (n=7/group) bearing Me13 xenografts were treated between day 11 and day 25 (dotted line) with AZD6244, TRAIL, or their combination. Statistical analysis by mixed models ANOVA; ****: p<0.0001; ***: p<0.001; **: p<0.01.

However, the AZD6244-TRAIL combination achieved a significant anti-tumor activity compared to single treatments, with a reduced tumor volume (Figure 4.25) and no associated sign of treatment-related toxicity as shown by histological analysis of main organs (Figure 4.26A) and monitoring of mouse body weight (Figure 4.26B).

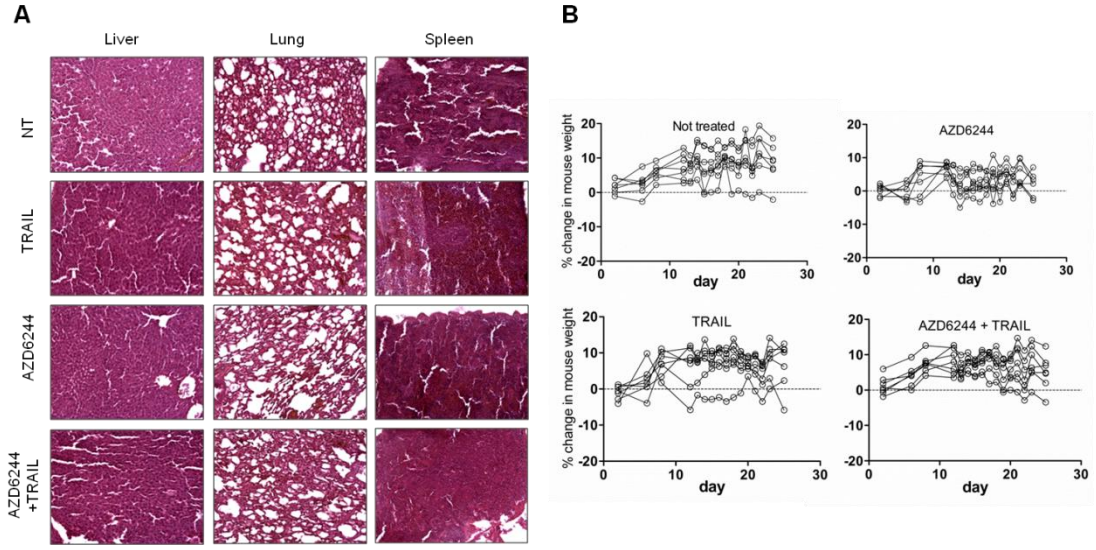

Figure 4.26 A) representative EE stainings of tissue sections from liver, lung and spleen of control and treated mice. **B**) body weight analysis of individual mice (n=7/treatment group) during treatments. Results shown as % change in body weight compared to pre-treatment values of each mouse.

4.7.2 Enhanced tumor cell death *in vivo*

To confirm an increment in promotion of melanoma cell death also *in vivo*, neoplastic nodules were removed at the end of treatment and analyzed for the presence of apoptotic cells by immunohistochemistry.

Deoxynucleotidyl transferase-mediated dUTP nick-end labeling (TUNEL) staining revealed an enhanced positivity in the AZD6244-TRAIL association group, compared to single treatments.

Moreover, higher levels of cleaved caspase 3 and a more pronunced down-modulation of pERK and Apollon were present in nodules from animals treated with combination of drugs if compared to vehicle treated, or single agent treated mice. (Figure 4.27).

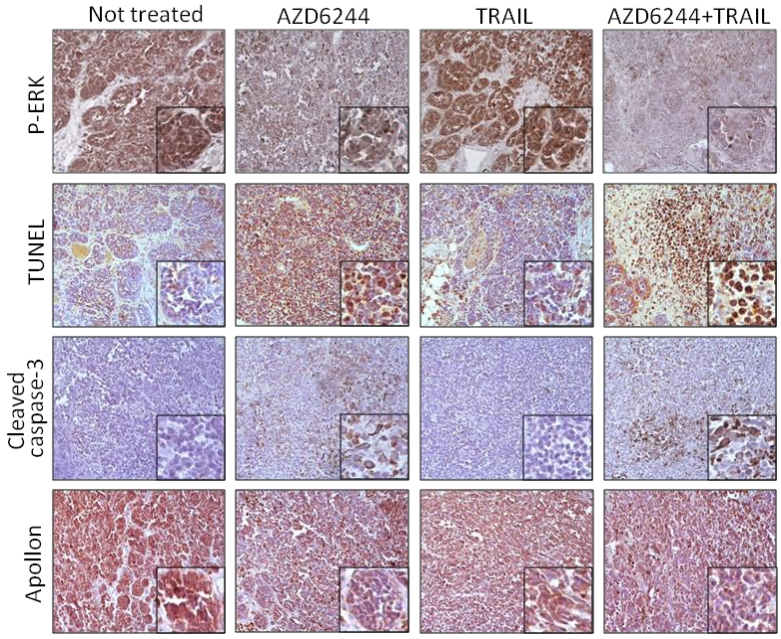

Figure 4.27 Immunohistochemistry analysis of tumor nodules from animals treated with combination of AZD6244 and TRAIL. Insets, higher magnification of a representative area of each panel. Original magnification, 20x.

These results confirmed an effective inhibition of the ERK pathway, possibly more significant with combinatorial treatment than with single agents, and a synergistic promotion of melanoma cell death also *in vivo* by the two-drug regimen.

4.7.3 Inhibition of angiogenesis by the concomitant targeting of MEK and TRAIL receptor

Among the functions that downstream effect analysis evidenced as inhibited by the AZD6244-TRAIL association, “migration and proliferation of endothelial cells” was of particular interest for the possible indication of indirect effects of combinatorial treatment also on tumor microenvironment (Figure 4.12B).

We therefore subjected data to the “upstream regulator analysis”, a tool able to identify transcriptional regulators that can explain observed changes in gene expression of a dataset. As expected, the analysis on genes modulated by the association of AZD6244 and TRAIL, predicted a highly significant inhibition of several master regulator genes related to angiogenic processes, including TGFβ1, HGF, EGF, Myc, HIF1α and VEGFα (Supplementary Table S5), in addition to MITF activation, which is a common consequence of ERK pathway inhibition. [198]

To confirm this hypothesis, we initially performed experiments on Me13 cells with protein array specific for angiogenesis-related molecules. As expected we found a strong down-modulation of several molecules with key roles in the angiogenic process by the AZD6244-TRAIL association (Figure 4.28).

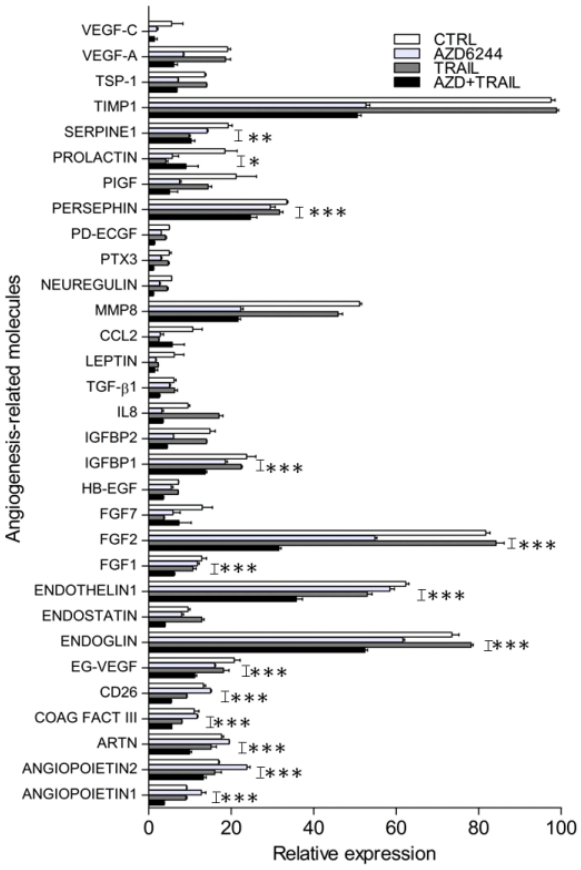

Figure 4.28 Protein array screening at 24 h after melanoma treatment. AZD6244, and TRAIL were used at 0.1 μM, and 25 ng/mL respectively. All molecules shown in the figure were significantly modulated, compared to control untreated cells, by the AZD6244+TRAIL combination (P at least <0.05, by ANOVA and SNK test). ***: p<0.001, **: p<0.01; *: P<0.05.

A decreased expression of Myc and HIF1α levels upon treatment of Me13 cells with AZD6244-TRAIL, or with AZD6244 only was confirmed by western blot analysis (Figure 4.29A).

Moreover, to further confirm our results we decided to carry on ELISA experiments on supernatants from cells treated overnight with AZD6244-TRAIL and we found a significant suppression of VEGFα and TGFβ1 secretion, in absence of melanoma cell death (Figure 4.29B-E). Inhibition of VEGFα secretion by the association of MEK inhibitor and TRAIL was confirmed in 4 out of 5 additional melanoma cell lines (Fig. 4.29C).

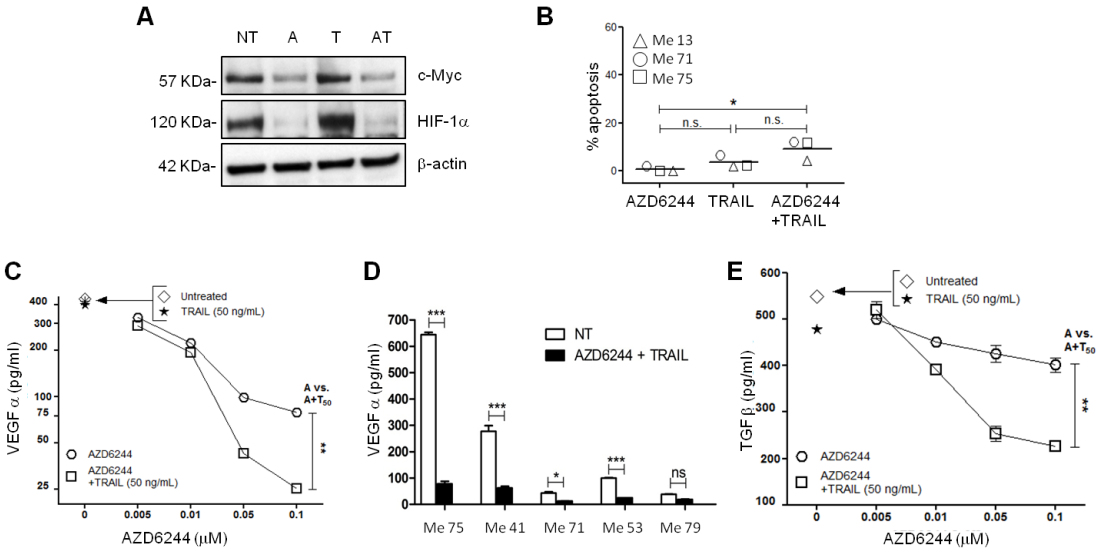

Figure 4.29 AZD6244 and TRAIL treatment modulates the production by melanoma cell lines of angiogenesis related molecules. A) Western blot analysis for Myc and HIF-1α in Me13 cells treated for 18 h in-vitro with AZD6244 (A), TRAIL (T) or their combination. **B**) Percentage of apoptosis in three different melanoma cell lines after treatment with Selumentinib, TRAIL or their combination for 18h. **C,E**) Secretion of VEGFα and TGFβ1 by Me13 treated in-vitro for 18 h with AZD6244, or TRAIL or their association. **D**) Inhibition of VEGFα secretion in five melanoma cell lines by AZD6244+TRAIL treatment for 18 h Statistical analysis by ANOVA and SNK test; ***: p<0.001; **: p<0.01; *: p<0.05.

Based on this preliminary *in vitro* evidence, we then analyzed the nodules from treated animals to confirm our hypothesis of effects of the AZD6244 and TRAIL combination also on tumor microenvironment.

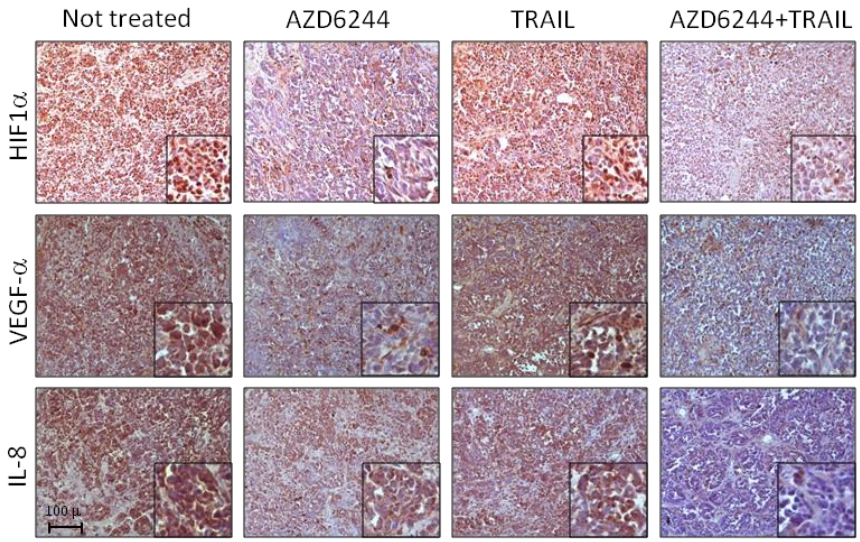

Figure 4.30 The association of Selumetinib and TRAIL reduces tumor production of angiogenesis mediators. Me13 tumor nodules removed from control and treated mice were stained with antibodies for HIF-1α, VEGFα and IL-8. Insets, higher magnification of a representative area of each panel. Original magnification, 20x.

Immunohistochemistry staining for HIF-1α, VEGFα, and IL-8, a well-known target of HIF-1α, showed that the concomitant treatment with MEK inhibitor and TRAIL was more effective than single agents alone in reducing the expression of these molecules also *in vivo* (Figure 4.30).

Moreover, analysis of very wide microscopy fields on HE stained sections (Figure 4.31A) showed a markedly reduced density of both large and small blood vessels; a result confirmed also by staining for murine CD31, a well known endothelial cell marker (Figure 4.31B).

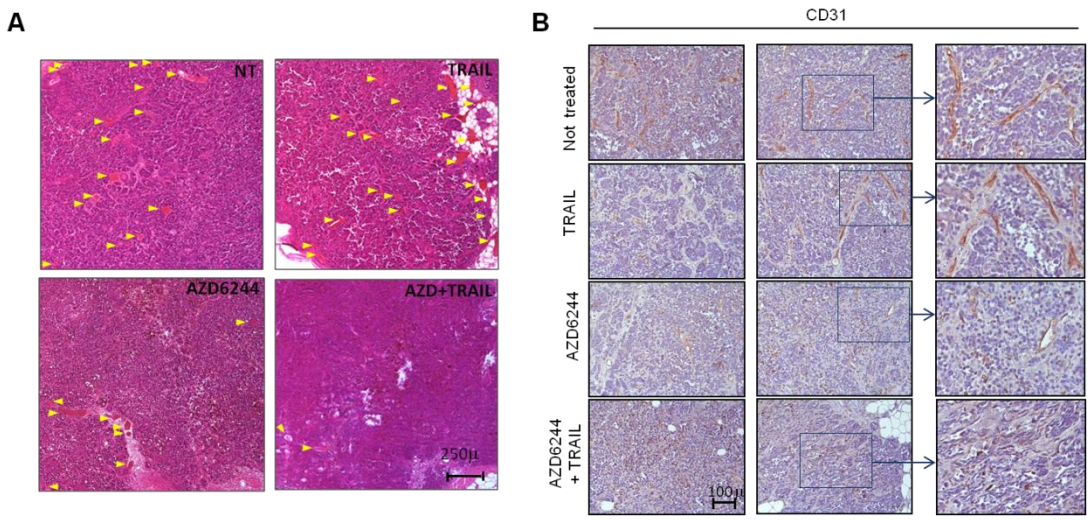

Figure 4.31 Combinatorial treatment reduces number of tumor vessels. A) Haematoxilin eosin staining of neoplastic nodules from mice treated with AZD6244, TRAIL and their combination. Arrows: large blood vessels. **B**) staining of Me13 nodules for murine CD31 endothelial cell marker. Two

representative fields (left and middle panel) and a higher magnification area (inset, right panel) are shown for each treatment group.

Taken together, these data indicate that a combinatorial treatment approach that targets at least one relevant melanoma survival pathway (MEK-ERK) and the TRAIL signalling cascade has a positive anti-tumor activity *in vivo* not only with direct effects on tumor cells, but also with indirect activity on tumor micro-environment through inhibition of angiogenesis.

4.8 EFFECTS OF COMBINATORIAL TREATMENT ON ENDOTHELIAL CELLS

Since one of the main effects of *in vivo* treatment with the combination of AZD6244 and TRAIL was a reduction in the expression of angiogenesis-related molecules (i.e. HIF-1α, VEGF-α, IL-8), associated with a marked decrease in density of blood vessels (CD31+ cells/ hematoxilin-eosin staining) in tumor nodules, we decided to test whether these two dugs affected vitality or phenotype of endothelial cells.

As a model for endothelium we decided to use Human Umbilical Vein Endothelial Cells (HUVEC) and on these cells we initially evaluated TRAIL receptors expression and response to treatment with different doses of soluble TRAIL.

As shown in Figure 4.32 although HUVECs expressed moderate levels of TRAIL-R1 and high levels of TRAIL-R2, treatment with their ligand had no effects on cell viability at any of the doses used.

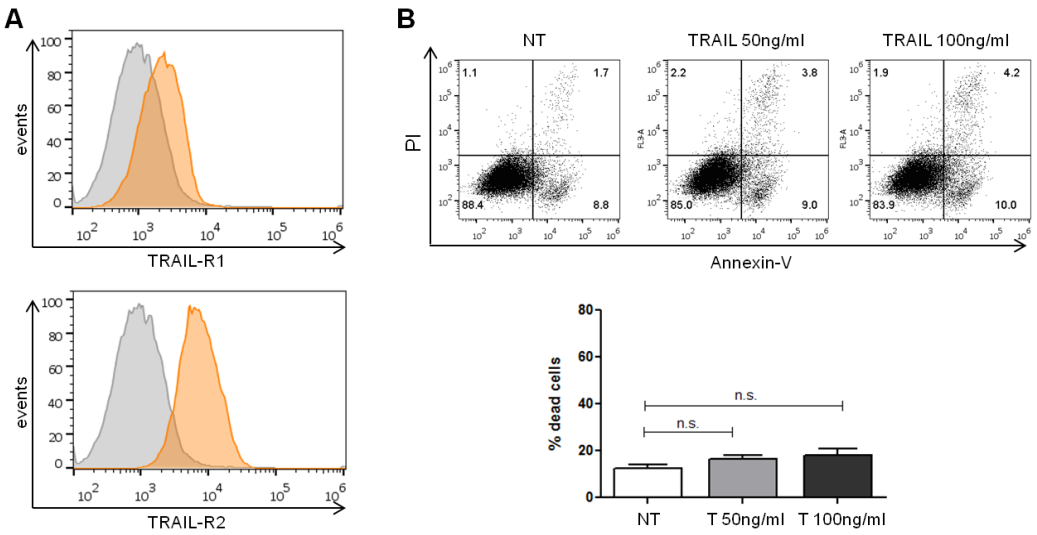

Figure 4.32 TRAIL activity on HUVEC cells. A) TRAIL receptors expression on Huvec cells. **B**) Annexin-V and Propidium Iodide staining of Huvec cells treated or not with sTRAIL at 50-100ng/ml for 72h. Representative dot plots and mean of three independent experiments. Statistical analysis by one-way ANOVA followed by Newman-Kewls post test.

We then decided to evaluate HUVEC response to AZD6244 as single agent and, despite the fact that already at the lowest dose used (0.01μM) the phosphorilation of ERK was inhibited (Figure 4.33 A), no correspondent effects were seen on HUVEC cell death through annexin-V/propidium Iodide stainings (Figure 4.33 B).

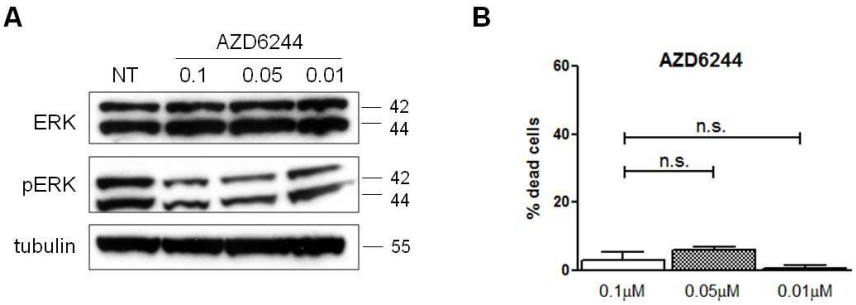

Figure 4.33 AZD6244 activity on HUVEC cells. A) Western blot analysis of Huvec cells for expression of total ERK and pERK after treatment with AZD6244 at 0.01-0.05-0.1 μM. **B**) Annexin-V and Propidium Iodide staining of Huvec cells treated or not with AZD6244 at the same doses for 72h. Mean of three independent experiments. Statistical analysis by one-way ANOVA followed by Newman-Kewls post test.

Interestingly, as shown in Figure 4.34, total cell death (by Annexin-V/Propidium Iodide) staining in HUVECs treated with the association of the MEK inhibitor and TRAIL was significantly incremented when AZD6244 was used at 0.05 μM and TRAIL at 50ng/ml.

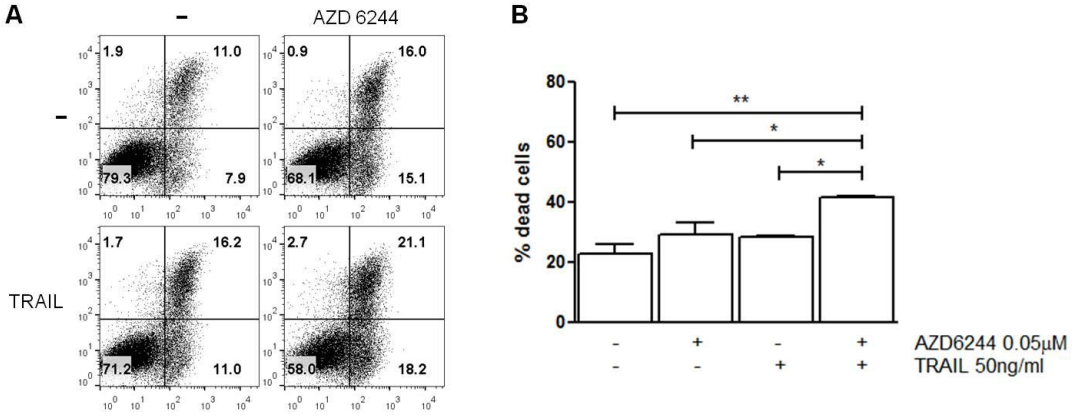

Figure 4.34 Treatment with Selumtinib and TRAIL induces Huvec cells apoptosis. Annexin-V and Propidium Iodide staining of Huvec cells treated or not with AZD6244 0.05 μM, TRAIL 50 ng/ml or their association for 72h. Representative plots (**A**) and mean of three independent experiments (**B**).

A significant increment in apoptosis was obtained by the combinatorial treatment if compared to untreated cells or to single treatment, suggesting a positive interaction between the two drugs also on endothelial cells.

Nevertheless, since the increment in endothelial cell death achieved by treatment with the association of Selumetinib and TRAIL was, although significant, not sufficient in our opinion to justify the reduction of $CD31^+$ cells seen *in vivo* experiments, we hypothesized that the anti-angiogenic effect of the MEK inhibitor-TRAIL association could be the result of a melanoma-induced modulation of the responsiveness of the tumor-associated vasculature to these agents. To prove our hypothesis we set up co-culture experiments where endothelial cells are in direct contact with melanoma cells for up to 5/6 days.

Interestingly, if HUVEC were previously co-cultured with different melanoma cell lines, there was a tendency toward an increase in susceptibility to the association of Selumetinib and TRAIL in terms of apoptotic cell death (Figure 4.35). For co-culture experiments melanoma cells were identified using CD56, a molecule always expressed on the membrane of our melanoma cell lines; while endothelial cells were identified through the expression of CD31.

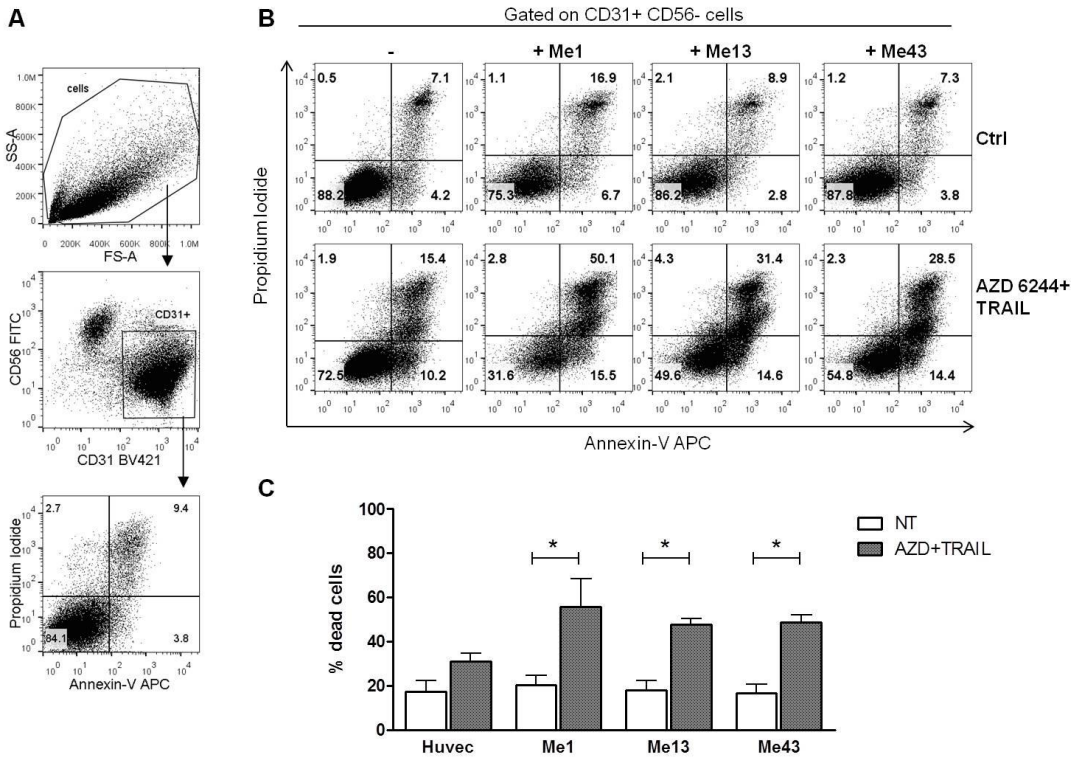

Figure 4.35 Pre-conditioning with melanoma cells renders HUVEC more susceptible to AZD6244+TRAIL treatment. A) Gaiting strategy for the identification of endothelial cells (CD31+CD56-) and melanoma cells (CD56+CD31-). Annexin-V/PI stainings on Huvec cells after 5/6 days of co-cultures with the indicated melanoma cell lines (Me1, Me13, Me43) and 48h hours of treatment with AZD6244 0.05uM and TRAIL 50ng/ml (**B** representative dot plots; **C** mean of three independent experiments). Statistical analysis by Two-way Anova analysis of variance followed by Bonferroni post test. * P< 0.05.

These initial experiments confirmed our hypothesis that melanoma cells can alter the susceptibility of endothelial cells to TRAIL and MEK inhibitor.

It is well-known that tumor-associated vasculature is different from normal one [199] and, based on this notion, we hypothesized that the melanoma-HUVEC co-cultures could lead to a significant shift in the phenotypic profiles of the endothelial cells.

As shown in Figure 4.36 A, and in agreement with the current literature, melanoma-HUVEC co-culture led to an upregulation of ICAM-1 (CD54) on endothelial cells, a finding that could be explained as “activation” of endothelial cells through the PKCα-p38-SP-1 pathway.[200]

Interestingly, we also found evidence for modulation of molecules that are related to endothelial cell “differentiation” rather than to “activation”: in fact, two different melanoma cell

lines induced a reduction in expression of vascular cadherin (CD144, cadherin 5). Notably, other molecules tested (i.e TRAIL-R2, CD202b) were not significantly affected by the co-cultures (Figure 4.36 B)

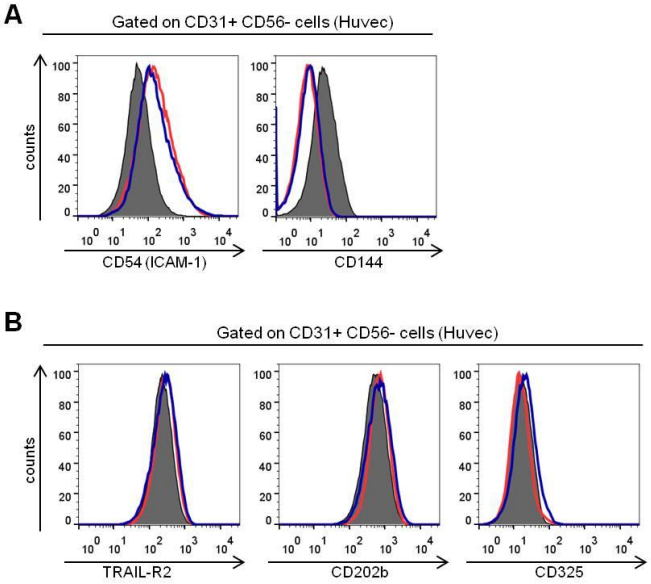

Figure 4.36: Co-cultures with melanoma cell lines induce modulation of ICAM-1 and CD144 on endothelial cells. Staining with the indicated antibodies on Huvec cells not treated (filled gray hystogram) or isolated after 5/6 days of co-cultures with Me1 (red hystograms) or Me43 (blu hystograms).

Moreover, we noticed that two different melanoma cell lines (red and blu lines in Figure 4.37) were different in inducing a down-modulation of the endothelial marker CD31 and the marker of EMT alpha smooth muscle actin (α-SMA); furthermore, both melanoma cell lines induced an up-regulation of the receptor tyrosine kinase AXL.

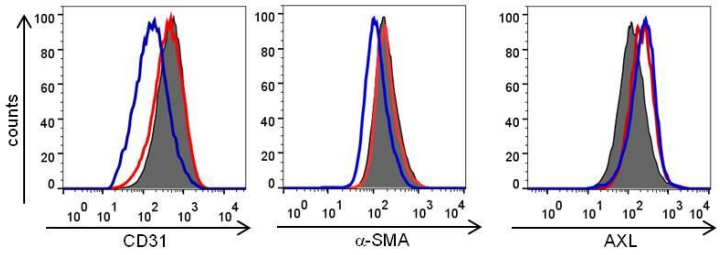

Figure 4.37 Staining with the indicated antibodies on Huvec cells not treated (filled gray hystogram) or isolated after 5/6 days of co-cultures with Me1 (red hystograms) or Me43 (blu hystograms).

Based on these result we hypothesized that different melanoma cells (possibly depending on their own gene expression profile) may differentially regulate HUVEC differentiation stage and this in turn may impact on the endothelium responsiveness to drugs.

To this end we have characterized 5 different melanoma cell lines for their gene expression profile and we have classified these tumors according to available melanoma classes

previously defined in the literature as “invasive” and “proliferative”. [111] Results indicated that while Me 1 belongs to the “invasive” family of tumors, Me 43 is instead in the “proliferative” group (data not shown).

Starting from the observation that Me1 and Me43 not only belong to the two opposite family (proliferative and invasive) but also induce opposite effects on the expression of several molecules on endothelial cells, we further hypothesized that these melanoma can also differ for their expression of angiogenesis-related factors.

We therefore selected a list of genes related to the angiogenic process and clustered our 5 melanoma cell lines on the bases of their expression of these molecules.

Interestingly, as shown in Figure 4.38, these two tumors are very different in terms of expression of this list of genes.

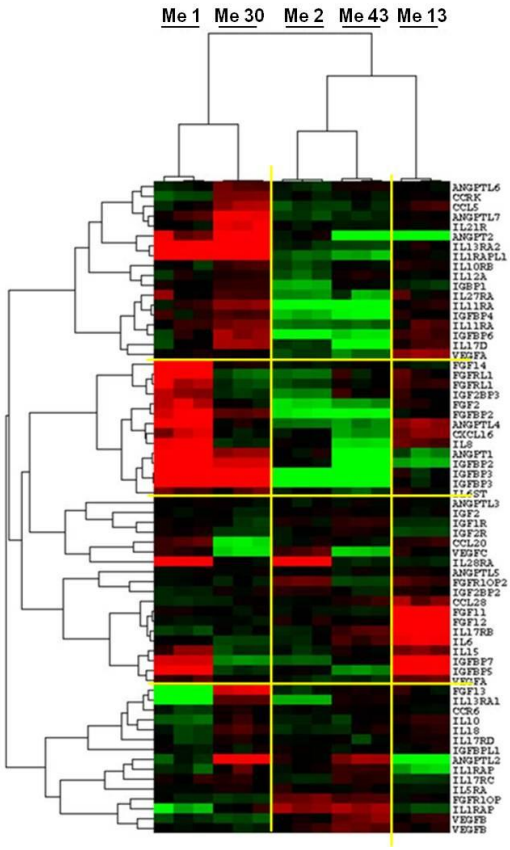

Figure 4.38: Clustering of melanoma cell lines based on gene expression of angiogenesis related factors.

Based on this evidence we decided to gain more insight into the changes to gene expression in endothelial cells if co-cultured with melanoma cell lines that belong to different classes (i.e. invasive vs proliferative).

To this end we decided to perform long-term (>5 days) co-culture experiments between Me1 or Me43 melanoma cells and HUVEC, aimed at analyze the gene expression profile of pre-conditioned endothelial cells.

We have therefore developed an assay that allows the isolation of pure endothelial cells after co-culture with melanoma cell lines using negative magnetic separation with anti melanoma beads (Miltenyi Biotec) (Figure 4.39).

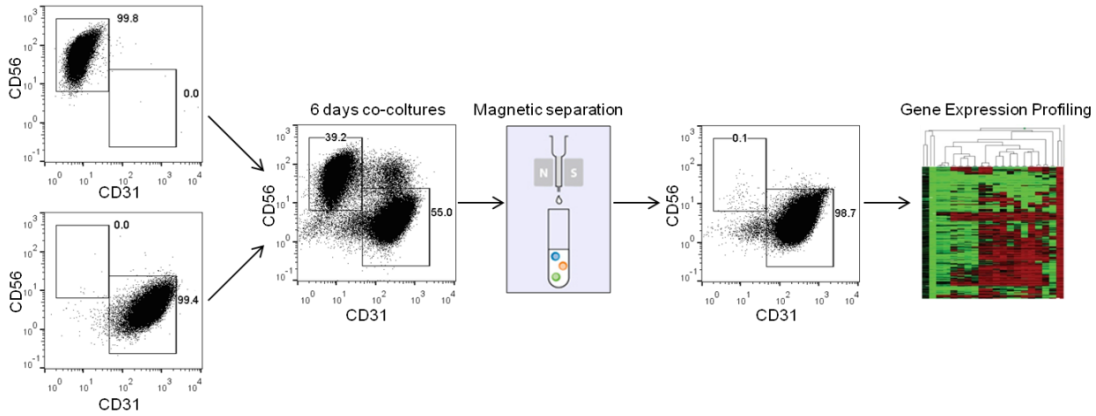

Figure 4.39: Magnetic beads allow separation of pure endothelial cells from co-cultures with melanoma cell lines. Melanoma cells and Huvec cells co-cultured for 6 days. Endothelial cells are purified through magnetic separation with anti-melanoma beads (anti-MCSP beads Miltenyi Biotec) and stained for CD56 and CD31. Purity over 97%.

Gene expression profiling of HUVEC cells previously co-cultured with melanoma cell lines belonging to the two different classes are ongoing and results will be analyzed in the next months.

5.DISCUSSION

Melanoma is an aggressive disease with an always increasing incidence and hardly curable when in advanced stage. Despite recent and impressive improvements achieved in melanoma treatment due to the development of target specific drugs (i.e. Vemurafenib, Dabrafenib and Trametinib) as well as of monoclonal antibodies targeting immune checkpoints (i.e. Ipilimumab, Nivolumab), there is still a fraction of patients that do not respond to this type of approaches or that relapse quickly after treatments, for which other alternatives are urgently required.

Different strategies are being investigated to face the need of new therapeutic options, one of which is the possibility to overcome melanoma resistance to different anti-tumor agents and to rescue tumor susceptibility to cell death through combinatorial treatments.
Recent pre-clinical studies have investigated several options, such as the co-targeting of MAPK and PI3K/mTOR intracellular pathways [201,202] the association of Vemurafenib with inhibitors of autophagy [203], ER-stress inducers [204], or combination of other anti-tumor agents that trigger the extrinsic and the intrinsic pathway of apoptosis.[205-207]

Based on the knowledge that target specific inhibitors are being widely tested in clinical trials for melanoma treatment, and building upon the hypothesis that a good therapeutic strategy should not only target tumor cells, but also relevant pro-tumoral mechanisms in melanoma microenvironment, such as angiogenesis, we decided to test, in melanoma cell lines and in melanoma xenografts, the effects of the co-targeting of MAPK, PI3K and death receptors cascades.
In this work we have collected evidence demonstrating that the association of TRAIL and a MEK inhibitor such as AZD6244, with or without the addition of a PI3K pathway inhibitor, exerts synergistic anti- melanoma effects both *in vitro* and *in vivo*. This was shown to be due to a dual activity affecting not only tumor cells, but also tumor microenvironment.
The first, direct effect of the association between TRAIL and the signalling pathway inhibitors used, was the possibility to overcome melanoma intrinsic resistance to each agent and to achieve significantly low values of Combination Indexes, even in cell lines completely resistant to one of both of the drugs.
Importantly, synergism was observed not only in BRAF mutant cell lines, but also in NRAS mutant or wild-type ones; indicating that this combinatorial approach could potentially be widely used and not limited to a sub-group of patients. Moreover, a synergistic interaction between the drugs was seen independently from the mutational status of p53 or PTEN, two genes known to be involved in melanoma resistance to target therapy [121,208]
In contrast, the association between TRAIL and BEZ235 only, without the addition of the MEK inhibitor, was characterized by a marked antagonism, suggesting that the effects seen for the AZD6244-TRAIL combination are peculiar and cannot be achieved by the inhibition of a different well known oncogenic signalling pathway.

Gene expression experiments, analysis of caspases activation and cell death assays in the presence of the pan-caspase inhibitor z-VAD-fmk, indicated that both the two- drug (AZD6244+TRAIL) and the three-drug associations achieved anti-tumor effects through a direct induction of caspase-dependent melanoma apoptosis. This evidence supported us in the hypothesis that combinatorial treatments could counteract apoptosis- resistance mechanisms behind melanoma intrinsic resistance to monotherapy with TRAIL or target specific inhibitors.

Analysis of the expression of several components of the intrinsic and extrinsic pathway of apoptosis confirmed our idea. Several studies report that cFLIP, the main caspase-8 inhibitor, is overexpressed in human melanoma lesions and is one of the main mechanisms of melanoma resistance to TRAIL-induced cell death: indeed, as shown by Ivanov *et al.* [209], cFLIP down-regulation is sufficient to revert resistance to TRAIL of TRAL-R2+ melanoma cells. In our experiments we found that the association of AZD6244 and TRAIL, with or without BEZ235, induced a strong down-regulation in the expression of cFLIP long and short isoforms, associated with caspase-8 activation.

Furthermore, we hypothesized that the rescue of caspase-8 activation through reduction in cFLIP-L/s levels could not be sufficient to explain the overall pro-apoptotic effect of the combinatorial treatments but that additional effects on molecules belonging to mitochondrial pathway of apoptosis were likely to be present.

Recent works by Eberle *et al* indicate that Bax direct or indirect targeting could represent an applicable strategy to overcome resistance of melanoma cells to TRAIL-induced apoptosis[109,206] ; moreover, in melanoma, inhibition of Bim by siRNA was found to attenuate conformational changes of Bax [210] and clusterin is known to specifically interact with conformation-altered Bax in response to chemotherapeutic drugs [211]. Based on this knowledge, we decided to evaluate modulation of these molecules by our treatments; as expected, we found a strong up-regulation of the pro-apoptotic BIMs and BAXα isoforms and a parallel reduction in clusterin and Mcl-1 by drugs association. Interestingly, BIM is not only a key mediator of TRAIL-induced cell death, but in diffuse large B cell lymphoma BIM was demonstrated to mediate the apoptotic response to AZD6244 and to BEZ235 in KRAS-mutant colorectal cancer cells. [206] [212] These results, therefore, suggest that the association of AZD6244+/- BEZ235 and TRAIL targets a BIM-BAX axis, inducing mitochondrial depolarization and contributing to melanoma cell death.

The over-expression of several IAPs, through the inhibition of both the initiator and the effector caspases, is well known to contribute to apoptosis resistance in different tumor types, including melanoma. [197] [213] Our lab previously reported the central role of the giant IAP Apollon/BIRC6 in modulating melanoma response to several signalling inhibitors [197] and interestingly here we found that, among all IAPs, the one that was most significantly modulated by the association of AZD6244+/- BEZ235 and TRAIL was BIRC6/Apollon, whose central role was confirmed by silencing experiments.

Mechanistically, therefore, we could conclude that the association of target specific inhibitors and TRAIL had synergistic effects in terms of incremented melanoma apotosis likely mediated by the reduction of cFLIP expression, BIM and BAX activation, and the down-regulation of Apollon expression.
These results were confirmed also in an *in vivo* model, were tumor growth of melanoma xenografts was significantly reduced by the combined treatment along with an increment in TUNEL and cleaved caspase-3 staining and a reduced expression of Apollon in tumor nodules.

Previous reports demonstrated that TRAIL treatment *in vivo* is able to disrupt tumor vasculature through induction of TRAIL receptor up-regulation on endothelial cells [214]; moreover, TRAIL can negatively regulate VEGF-induced angiogenesis [215] and TRAIL and concomitant inhibition of MEK and VEGFR has been reported to reduce tumor angiogenesis in lung cancer models. [191] Based on these evidences we decided to evaluate effects of combining TRAIL and AZD6244 on tumor microenvironment.
Initial *in vitro* experiments confirmed inhibitory effects of AZD6244+TRAIL on master regulators of angiogenesis, such as TGFβ, HIF-1α and Myc, as well as on production of pro-angiogenic molecules such as VEGFα, in absence of melanoma cell death.
The evaluation of CD31+ cells in nodules from melanoma xenografts after mice treatment with the MEK inhibitor and TRAIL confirmed also *in vivo* the effects of reduced angiogenesis, that was paralleled by a reduced staining for HIF-1α, VEGF and IL-8.
These results confirmed the presence of an indirect effect of the association studied, mediated by the activity of the two drugs on tumor microenvironment through a reduced promotion of angiogenesis.

The next goal was then to identify mechanisms behind the evidence of a reduced number of vessels in nodules after combinatorial treatment.
Our first hypothesis was a direct effect of AZD6244 and TRAIL on endothelial cells; but no induction of cell death was evidenced on an endothelial cell line after treatment with single agents, despite the expression of TRAIL receptors on HUVECs and the inhibition on MEK/ERK signalling pathway by AZD6244 at the doses used.
The association of MEK inhibitor and the pro-apoptotic ligand was able to slightly increase the extent of endothelial apoptosis, but although significant, in our opinion it was not sufficient to justify the reduction of CD31+ cells seen in vivo experiments. Based on these results we hypothesized that the anti-angiogenic effect of the MEK inhibitor-TRAIL association could be the result of a melanoma-induced modulation of the responsiveness of the tumor-associated vasculature to these agents.

Initial experiments confirmed our hypothesis evidencing a tendency toward an increase in endothelial cell death, upon AZD6244+TRAIL combinatorial treatment, after co-culture with melanoma cell lines.

Subsequent experiments, aimed at clarify mechanisms behind the effects seen, demonstrated a modulation of several molecules in endothelial cells after the co-cultures with different melanoma cell lines.

Notably, data demonstrated not only an incremented “activation” of endothelium by direct interaction with tumor, seen through an up-regulation of ICAM-1 and expected by previous reports, but also a modulation of molecules known to play significant roles in endothelial cell differentiation (such as an increment in cadherin-5 and a reduced expression of CD31). This evidence could suggests us that melanoma cells induce a “re-programming” of endothelial cells.

Moreover, we noticed that two melanoma cell lines seem to differentially induce modulation of the expression of αSMA as well of CD31. This observation suggested us that different melanoma cell lines could differentially influence endothelial cells.

To test this hypothesis we selected 5 melanoma cell lines and clustered them on the basis of their expression of a set of genes known to play key roles in the angiogenic process.

In 2011, Hoek at al showed that melanoma cells with a “proliferative” phenotype were responsive to MAPK inhibition and a recent paper published by Garraway et al. demonstrated that melanoma cells with different sensitivity to MAPK pathway inhibitors, display distinct transcriptional profiles and are characterized by differential expression of MITF, NF-κB and the receptor tyrosine kinase AXL (“invasive” vs “proliferative”).

Interestingly, the two melanoma cell lines found to be opposite for the expression of several group of angiogenesis-related factors, belong to two different classes if we divide the same melanoma cell lines on the bases of the classification proposed by Garraway.

Starting from this notion, and in order to clarify if different melanoma cell lines (invasive vs proliferative) could differentially influence endothelial cell proliferation/maturation/phenotype, we decided to set-up gene-expression experiments on endothelial cells previously co-cultured with melanoma cell lines and purified through magnetic separation. Results will be available shortly and further experiments with the same aims are still ongoing.

6.CONCLUSIONS

Aim of the presented project was to obtain pre-clinical evidence for a possible strategy to overcome melanoma resistance to apoptosis could be represented by the concomitant targeting of oncogenic signalling pathways and the TRAIL receptors, pro-apoptotic pathway.

The chosen drugs (Selumetinib, BEZ235 and TRAIL) were tested *in vitro* in a large panel of short-term melanoma cell lines for synergistic interactions and the best combination identified was verified for anti-tumoral effects also *in vivo*.

Results of this work suggest that concomitant targeting of melanoma oncogenic signalling pathways and the TRAIL receptor cascade:

1) is able to overcome *in vitro* tumor resistance to either agent with irrespective from the main genetic alteration present in melanoma cells;
2) has synergistic effects in terms of induction of melanoma cell death by promoting a caspase-dependent apoptosis through the modulation of pro and anti-apoptotic molecules such as BIM, BAX, c-FLIP and Clusterin, along with a reduction in several members of the IAP family;
3) has a key mediator of the effects Apollon/BIRC6; indeed its silencing is sufficient to sensitize melanoma cells to inhibitors or TRAIL –induced cell death
4) reduces the production of key mediators of tumor-promoted angiogenesis (i.e. VEGFα, TGFβ, IL-8)

In addition the association of Selumetinib and TRAIL *in vivo*:

5) reduces tumor growth of melanoma xenografts through induction of cancer cell death (increment in TUNEL positive cells), likely through the same mechanisms demonstrated for the in vitro synergy (i.e. Apollon/BIRC modulation)
6) reduces the presence of main mediators of angiogenesis in tumor sections from xenografted mice
7) reduces number of CD31+ cells in tumor nodules
8) changes the structure and integrity of tumor vessels (Hematoxylin-eosine staining)

Moreover, initial/preliminary results conducted on a model of endothelial cells suggest that there is a possible modulation of endothelial differentiation status and responsiveness to combinatorial therapy fuelled by direct interaction with melanoma cells and evidenced by:

9) upregulation of ICAM-1/CD54 on endothelial cells after co-culture with melanoma cell lines, indicating an endothelial “activation”;

10) a modulation of the “differentiation” status of endothelial cells, indicated by reduced levels of alpha-SMA, a reduction in the expression of vascular cadherin CD144 and a downmodulation of the endothelial marker CD31 after co-cultures between melanoma and HUVEC cells.

All these data represent a pre-clinical rationale for a pro-apoptotic and anti-angiogenic strategy for melanoma treatment based on the association between inhibitors of main oncogenic signalling pathway and the anti-tumor agent TRAIL.

FUTURE PLANS

On the bases of the results just summarized, we are currently performing experiments aimed at:

1) evaluating changes in the gene expression profile (Illumina array) of HUVEC cells after co-culture with melanoma cell lines;

2) verifying if melanomas with different AXL/ MITF status could be different in affective responsiveness of endothelial cells after co-culture experiments;

3) indentifying mechanisms behind the reduced production by melanoma cells of VEGFα, TGFβ and IL-8 after combinatorial treatment.

REFERENCES

1. Siegel, R., Ma, J., Zou, Z. & Jemal, A. Cancer statistics, 2014. *CA Cancer J Clin* **64**, 9-29.
2. Eggermont, A.M., Spatz, A. & Robert, C. Cutaneous melanoma. *Lancet* **383**, 816-827 (2014).
3. Lo, J.A. & Fisher, D.E. The melanoma revolution: from UV carcinogenesis to a new era in therapeutics. *Science* **346**, 945-949 (2015).
4. Cui, R.*, et al.* Central role of p53 in the suntan response and pathologic hyperpigmentation. *Cell* **128**, 853-864 (2007).
5. Raimondi, S.*, et al.* MC1R variants, melanoma and red hair color phenotype: a meta-analysis. *Int J Cancer* **122**, 2753-2760 (2008).
6. Elder, D.E. Precursors to melanoma and their mimics: nevi of special sites. *Mod Pathol* **19 Suppl 2**, S4-20 (2006).
7. Miller, A.J. & Mihm, M.C., Jr. Melanoma. *N Engl J Med* **355**, 51-65 (2006).
8. Shain, A.H.*, et al.* The Genetic Evolution of Melanoma from Precursor Lesions. *N Engl J Med* **373**, 1926-1936 (2015).
9. MacKie, R.M., English, J., Aitchison, T.C., Fitzsimons, C.P. & Wilson, P. The number and distribution of benign pigmented moles (melanocytic naevi) in a healthy British population. *Br J Dermatol* **113**, 167-174 (1985).
10. Palmieri, G.*, et al.* Multiple Molecular Pathways in Melanomagenesis: Characterization of Therapeutic Targets. *Front Oncol* **5**, 183 (2015).
11. Chudnovsky, Y., Khavari, P.A. & Adams, A.E. Melanoma genetics and the development of rational therapeutics. *J Clin Invest* **115**, 813-824 (2005).
12. Piris, A., Lobo, A.C. & Duncan, L.M. Melanoma staging: where are we now? *Dermatol Clin* **30**, 581-592, v.
13. Balch, C.M.*, et al.* Final version of 2009 AJCC melanoma staging and classification. *J Clin Oncol* **27**, 6199-6206 (2009).
14. Improta, G.*, et al.* New developments in the management of advanced melanoma - role of pembrolizumab. *Onco Targets Ther* **8**, 2535-2543.
15. Garibyan, L. & Fisher, D.E. How sunlight causes melanoma. *Curr Oncol Rep* **12**, 319-326.
16. Whiteman, D.C., Whiteman, C.A. & Green, A.C. Childhood sun exposure as a risk factor for melanoma: a systematic review of epidemiologic studies. *Cancer Causes Control* **12**, 69-82 (2001).
17. Hodis, E.*, et al.* A landscape of driver mutations in melanoma. *Cell* **150**, 251-263 (2012).
18. Zaidi, M.R.*, et al.* Interferon-gamma links ultraviolet radiation to melanomagenesis in mice. *Nature* **469**, 548-553.
19. Viros, A.*, et al.* Ultraviolet radiation accelerates BRAF-driven melanomagenesis by targeting TP53. *Nature* **511**, 478-482.
20. Bald, T.*, et al.* Ultraviolet-radiation-induced inflammation promotes angiotropism and metastasis in melanoma. *Nature* **507**, 109-113.
21. Bishop, D.T.*, et al.* Genome-wide association study identifies three loci associated with melanoma risk. *Nat Genet* **41**, 920-925 (2009).
22. Falchi, M.*, et al.* Genome-wide association study identifies variants at 9p21 and 22q13 associated with development of cutaneous nevi. *Nat Genet* **41**, 915-919 (2009).
23. Duffy, D.L.*, et al.* IRF4 variants have age-specific effects on nevus count and predispose to melanoma. *Am J Hum Genet* **87**, 6-16.
24. Gudbjartsson, D.F.*, et al.* ASIP and TYR pigmentation variants associate with cutaneous melanoma and basal cell carcinoma. *Nat Genet* **40**, 886-891 (2008).
25. Goldstein, A.M.*, et al.* Features associated with germline CDKN2A mutations: a GenoMEL study of melanoma-prone families from three continents. *J Med Genet* **44**, 99-106 (2007).
26. Read, J., Wadt, K.A. & Hayward, N.K. Melanoma genetics. *J Med Genet* (2015).
27. Puntervoll, H.E.*, et al.* Melanoma prone families with CDK4 germline mutation: phenotypic profile and associations with MC1R variants. *J Med Genet* **50**, 264-270 (2013).

28. Testa, J.R.*, et al.* Germline BAP1 mutations predispose to malignant mesothelioma. *Nat Genet* **43**, 1022-1025 (2011).
29. Pasquali, E.*, et al.* MC1R variants increased the risk of sporadic cutaneous melanoma in darker-pigmented Caucasians: a pooled-analysis from the M-SKIP project. *Int J Cancer* **136**, 618-631 (2015).
30. network, t.c.g.a. Genomic Classification of Cutaneous Melanoma. *Cell* **161**, 1681-1696 (2015).
31. Johnson, G.L. & Lapadat, R. Mitogen-activated protein kinase pathways mediated by ERK, JNK, and p38 protein kinases. *Science* **298**, 1911-1912 (2002).
32. Raman, M., Chen, W. & Cobb, M.H. Differential regulation and properties of MAPKs. *Oncogene* **26**, 3100-3112 (2007).
33. Yoon, S. & Seger, R. The extracellular signal-regulated kinase: multiple substrates regulate diverse cellular functions. *Growth Factors* **24**, 21-44 (2006).
34. Hazzalin, C.A. & Mahadevan, L.C. MAPK-regulated transcription: a continuously variable gene switch? *Nat Rev Mol Cell Biol* **3**, 30-40 (2002).
35. Pylayeva-Gupta, Y., Grabocka, E. & Bar-Sagi, D. RAS oncogenes: weaving a tumorigenic web. *Nat Rev Cancer* **11**, 761-774.
36. Gogl, G.*, et al.* Structural basis of Ribosomal S6 Kinase 1 (RSK1) inhibition by S100B Protein: modulation of the Extracellular Signal-regulated Kinase (ERK) signalling cascade in a calcium-dependent way. *J Biol Chem*.
37. Roskoski, R., Jr. ERK1/2 MAP kinases: structure, function, and regulation. *Pharmacol Res* **66**, 105-143.
38. Rochette, L.*, et al.* Nitric oxide synthase inhibition and oxidative stress in cardiovascular diseases: possible therapeutic targets? *Pharmacol Ther* **140**, 239-257.
39. Meloche, S. & Pouyssegur, J. The ERK1/2 mitogen-activated protein kinase pathway as a master regulator of the G1- to S-phase transition. *Oncogene* **26**, 3227-3239 (2007).
40. Meloche, S., Pages, G. & Pouyssegur, J. Functional expression and growth factor activation of an epitope-tagged p44 mitogen-activated protein kinase, p44mapk. *Mol Biol Cell* **3**, 63-71 (1992).
41. Liu, X., Yan, S., Zhou, T., Terada, Y. & Erikson, R.L. The MAP kinase pathway is required for entry into mitosis and cell survival. *Oncogene* **23**, 763-776 (2004).
42. Sebolt-Leopold, J.S.*, et al.* Blockade of the MAP kinase pathway suppresses growth of colon tumors in vivo. *Nat Med* **5**, 810-816 (1999).
43. Brunet, A., Pages, G. & Pouyssegur, J. Constitutively active mutants of MAP kinase kinase (MEK1) induce growth factor-relaxation and oncogenicity when expressed in fibroblasts. *Oncogene* **9**, 3379-3387 (1994).
44. Roovers, K. & Assoian, R.K. Integrating the MAP kinase signal into the G1 phase cell cycle machinery. *Bioessays* **22**, 818-826 (2000).
45. Lavoie, J.N., L'Allemain, G., Brunet, A., Muller, R. & Pouyssegur, J. Cyclin D1 expression is regulated positively by the p42/p44MAPK and negatively by the p38/HOGMAPK pathway. *J Biol Chem* **271**, 20608-20616 (1996).
46. Sears, R.*, et al.* Multiple Ras-dependent phosphorylation pathways regulate Myc protein stability. *Genes Dev* **14**, 2501-2514 (2000).
47. Chambard, J.C., Lefloch, R., Pouyssegur, J. & Lenormand, P. ERK implication in cell cycle regulation. *Biochim Biophys Acta* **1773**, 1299-1310 (2007).
48. Balmanno, K. & Cook, S.J. Tumour cell survival signalling by the ERK1/2 pathway. *Cell Death Differ* **16**, 368-377 (2009).
49. Brazil, D.P., Park, J. & Hemmings, B.A. PKB binding proteins. Getting in on the Akt. *Cell* **111**, 293-303 (2002).
50. Wymann, M.P., Zvelebil, M. & Laffargue, M. Phosphoinositide 3-kinase signalling--which way to target? *Trends Pharmacol Sci* **24**, 366-376 (2003).
51. Cantley, L.C. The phosphoinositide 3-kinase pathway. *Science* **296**, 1655-1657 (2002).
52. Satyamoorthy, K. & Herlyn, M. Cellular and molecular biology of human melanoma. *Cancer Biol Ther* **1**, 14-17 (2002).

53. Kihara, A., Noda, T., Ishihara, N. & Ohsumi, Y. Two distinct Vps34 phosphatidylinositol 3-kinase complexes function in autophagy and carboxypeptidase Y sorting in Saccharomyces cerevisiae. *J Cell Biol* **152**, 519-530 (2001).
54. Stambolic, V*., et al.* Negative regulation of PKB/Akt-dependent cell survival by the tumor suppressor PTEN. *Cell* **95**, 29-39 (1998).
55. Blume-Jensen, P. & Hunter, T. Oncogenic kinase signalling. *Nature* **411**, 355-365 (2001).
56. Alt, J.R., Cleveland, J.L., Hannink, M. & Diehl, J.A. Phosphorylation-dependent regulation of cyclin D1 nuclear export and cyclin D1-dependent cellular transformation. *Genes Dev* **14**, 3102-3114 (2000).
57. Mayo, L.D. & Donner, D.B. The PTEN, Mdm2, p53 tumor suppressor-oncoprotein network. *Trends Biochem Sci* **27**, 462-467 (2002).
58. Cardone, M.H*., et al.* Regulation of cell death protease caspase-9 by phosphorylation. *Science* **282**, 1318-1321 (1998).
59. Datta, S.R*., et al.* Akt phosphorylation of BAD couples survival signals to the cell-intrinsic death machinery. *Cell* **91**, 231-241 (1997).
60. Ozes, O.N*., et al.* NF-kappaB activation by tumour necrosis factor requires the Akt serine-threonine kinase. *Nature* **401**, 82-85 (1999).
61. Wendel, H.G*., et al.* Survival signalling by Akt and eIF4E in oncogenesis and cancer therapy. *Nature* **428**, 332-337 (2004).
62. Altomare, D.A. & Testa, J.R. Perturbations of the AKT signalling pathway in human cancer. *Oncogene* **24**, 7455-7464 (2005).
63. Pedrero, J.M*., et al.* Frequent genetic and biochemical alterations of the PI 3-K/AKT/PTEN pathway in head and neck squamous cell carcinoma. *Int J Cancer* **114**, 242-248 (2005).
64. Bertelsen, B.I., Steine, S.J., Sandvei, R., Molven, A. & Laerum, O.D. Molecular analysis of the PI3K-AKT pathway in uterine cervical neoplasia: frequent PIK3CA amplification and AKT phosphorylation. *Int J Cancer* **118**, 1877-1883 (2006).
65. Hennessy, B.T., Smith, D.L., Ram, P.T., Lu, Y. & Mills, G.B. Exploiting the PI3K/AKT pathway for cancer drug discovery. *Nat Rev Drug Discov* **4**, 988-1004 (2005).
66. West, K.A., Castillo, S.S. & Dennis, P.A. Activation of the PI3K/Akt pathway and chemotherapeutic resistance. *Drug Resist Updat* **5**, 234-248 (2002).
67. Mendoza, M.C., Er, E.E. & Blenis, J. The Ras-ERK and PI3K-mTOR pathways: cross-talk and compensation. *Trends Biochem Sci* **36**, 320-328.
68. Shi, H., Kong, X., Ribas, A. & Lo, R.S. Combinatorial treatments that overcome PDGFRbeta-driven resistance of melanoma cells to V600EB-RAF inhibition. *Cancer Res* **71**, 5067-5074.
69. Hanahan, D. & Weinberg, R.A. The hallmarks of cancer. *Cell* **100**, 57-70 (2000).
70. Lo, J.A. & Fisher, D.E. The melanoma revolution: from UV carcinogenesis to a new era in therapeutics. *Science* **346**, 945-949.
71. Davies, H*., et al.* Mutations of the BRAF gene in human cancer. *Nature* **417**, 949-954 (2002).
72. Albino, A.P., Le Strange, R., Oliff, A.I., Furth, M.E. & Old, L.J. Transforming ras genes from human melanoma: a manifestation of tumour heterogeneity? *Nature* **308**, 69-72 (1984).
73. Stahl, J.M*., et al.* Deregulated Akt3 activity promotes development of malignant melanoma. *Cancer Res* **64**, 7002-7010 (2004).
74. Wu, H., Goel, V. & Haluska, F.G. PTEN signalling pathways in melanoma. *Oncogene* **22**, 3113-3122 (2003).
75. Shull, A.Y*., et al.* Novel somatic mutations to PI3K pathway genes in metastatic melanoma. *PLoS One* **7**, e43369.
76. Dankort, D*., et al.* Braf(V600E) cooperates with Pten loss to induce metastatic melanoma. *Nat Genet* **41**, 544-552 (2009).
77. Davies, M.A. & Samuels, Y. Analysis of the genome to personalize therapy for melanoma. *Oncogene* **29**, 5545-5555.
78. Bardeesy, N*., et al.* Role of epidermal growth factor receptor signalling in RAS-driven melanoma. *Mol Cell Biol* **25**, 4176-4188 (2005).

79. Maertens, O.*, et al.* Elucidating distinct roles for NF1 in melanomagenesis. *Cancer Discov* **3**, 338-349.
80. Tsao, H., Chin, L., Garraway, L.A. & Fisher, D.E. Melanoma: from mutations to medicine. *Genes Dev* **26**, 1131-1155.
81. Yokoyama, S.*, et al.* A novel recurrent mutation in MITF predisposes to familial and sporadic melanoma. *Nature* **480**, 99-103.
82. Flaherty, K.T.*, et al.* Inhibition of mutated, activated BRAF in metastatic melanoma. *N Engl J Med* **363**, 809-819.
83. Chapman, P.B.*, et al.* Improved survival with vemurafenib in melanoma with BRAF V600E mutation. *N Engl J Med* **364**, 2507-2516.
84. Hauschild, A.*, et al.* Dabrafenib in BRAF-mutated metastatic melanoma: a multicentre, open-label, phase 3 randomised controlled trial. *Lancet* **380**, 358-365.
85. Flaherty, K.T.*, et al.* Improved survival with MEK inhibition in BRAF-mutated melanoma. *N Engl J Med* **367**, 107-114.
86. Flaherty, K.T.*, et al.* Combined BRAF and MEK inhibition in melanoma with BRAF V600 mutations. *N Engl J Med* **367**, 1694-1703.
87. Larkin, J.*, et al.* Combined vemurafenib and cobimetinib in BRAF-mutated melanoma. *N Engl J Med* **371**, 1867-1876.
88. Long, G.V.*, et al.* Combined BRAF and MEK inhibition versus BRAF inhibition alone in melanoma. *N Engl J Med* **371**, 1877-1888.
89. Robert, C.*, et al.* Improved overall survival in melanoma with combined dabrafenib and trametinib. *N Engl J Med* **372**, 30-39.
90. Mandal, R., Becker, S. & Strebhardt, K. Stamping out RAF and MEK1/2 to inhibit the ERK1/2 pathway: an emerging threat to anticancer therapy. *Oncogene*.
91. Dickson, M.A.*, et al.* Phase I study of XL281 (BMS-908662), a potent oral RAF kinase inhibitor, in patients with advanced solid tumors. *Invest New Drugs* **33**, 349-356.
92. Su, Y.*, et al.* RAF265 inhibits the growth of advanced human melanoma tumors. *Clin Cancer Res* **18**, 2184-2198.
93. Hertzman Johansson, C. & Egyhazi Brage, S. BRAF inhibitors in cancer therapy. *Pharmacol Ther* **142**, 176-182.
94. Wallace, E.M., Lyssikatos, J.P., Yeh, T., Winkler, J.D. & Koch, K. Progress towards therapeutic small molecule MEK inhibitors for use in cancer therapy. *Curr Top Med Chem* **5**, 215-229 (2005).
95. Yeh, T.C.*, et al.* Biological characterization of ARRY-142886 (AZD6244), a potent, highly selective mitogen-activated protein kinase kinase 1/2 inhibitor. *Clin Cancer Res* **13**, 1576-1583 (2007).
96. Haass, N.K.*, et al.* The mitogen-activated protein/extracellular signal-regulated kinase kinase inhibitor AZD6244 (ARRY-142886) induces growth arrest in melanoma cells and tumor regression when combined with docetaxel. *Clin Cancer Res* **14**, 230-239 (2008).
97. Adjei, A.A.*, et al.* Phase I pharmacokinetic and pharmacodynamic study of the oral, small-molecule mitogen-activated protein kinase kinase 1/2 inhibitor AZD6244 (ARRY-142886) in patients with advanced cancers. *J Clin Oncol* **26**, 2139-2146 (2008).
98. Kirkwood, J.M.*, et al.* Phase II, open-label, randomized trial of the MEK1/2 inhibitor selumetinib as monotherapy versus temozolomide in patients with advanced melanoma. *Clin Cancer Res* **18**, 555-567.
99. Liu, P., Cheng, H., Roberts, T.M. & Zhao, J.J. Targeting the phosphoinositide 3-kinase pathway in cancer. *Nat Rev Drug Discov* **8**, 627-644 (2009).
100. Markman, B., Dienstmann, R. & Tabernero, J. Targeting the PI3K/Akt/mTOR pathway--beyond rapalogs. *Oncotarget* **1**, 530-543.
101. Margolin, K.*, et al.* CCI-779 in metastatic melanoma: a phase II trial of the California Cancer Consortium. *Cancer* **104**, 1045-1048 (2005).
102. Davies, M.A.*, et al.* Phase I study of the combination of sorafenib and temsirolimus in patients with metastatic melanoma. *Clin Cancer Res* **18**, 1120-1128.
103. Maira, S.M.*, et al.* Identification and characterization of NVP-BEZ235, a new orally available dual phosphatidylinositol 3-kinase/mammalian target of rapamycin inhibitor with potent in vivo antitumor activity. *Mol Cancer Ther* **7**, 1851-1863 (2008).

104. Aziz, S.A., *et al.* Vertical targeting of the phosphatidylinositol-3 kinase pathway as a strategy for treating melanoma. *Clin Cancer Res* **16**, 6029-6039.
105. Lovly, C.M. & Shaw, A.T. Molecular pathways: resistance to kinase inhibitors and implications for therapeutic strategies. *Clin Cancer Res* **20**, 2249-2256.
106. Sosman, J.A., *et al.* Survival in BRAF V600-mutant advanced melanoma treated with vemurafenib. *N Engl J Med* **366**, 707-714.
107. Kugel, C.H., 3rd & Aplin, A.E. Adaptive resistance to RAF inhibitors in melanoma. *Pigment Cell Melanoma Res* **27**, 1032-1038.
108. Aplin, A.E., Kaplan, F.M. & Shao, Y. Mechanisms of resistance to RAF inhibitors in melanoma. *J Invest Dermatol* **131**, 1817-1820.
109. Eberle, J., Fecker, L.F., Hossini, A.M., Kurbanov, B.M. & Fechner, H. Apoptosis pathways and oncolytic adenoviral vectors: promising targets and tools to overcome therapy resistance of malignant melanoma. *Exp Dermatol* **17**, 1-11 (2008).
110. Johannessen, C.M., *et al.* A melanocyte lineage program confers resistance to MAP kinase pathway inhibition. *Nature* **504**, 138-142.
111. Konieczkowski, D.J., *et al.* A melanoma cell state distinction influences sensitivity to MAPK pathway inhibitors. *Cancer Discov* **4**, 816-827.
112. Muller, J., *et al.* Low MITF/AXL ratio predicts early resistance to multiple targeted drugs in melanoma. *Nat Commun* **5**, 5712.
113. Nazarian, R., *et al.* Melanomas acquire resistance to B-RAF(V600E) inhibition by RTK or N-RAS upregulation. *Nature* **468**, 973-977.
114. Shi, H., *et al.* Melanoma whole-exome sequencing identifies (V600E)B-RAF amplification-mediated acquired B-RAF inhibitor resistance. *Nat Commun* **3**, 724.
115. Poulikakos, P.I., *et al.* RAF inhibitor resistance is mediated by dimerization of aberrantly spliced BRAF(V600E). *Nature* **480**, 387-390.
116. Van Allen, E.M., *et al.* The genetic landscape of clinical resistance to RAF inhibition in metastatic melanoma. *Cancer Discov* **4**, 94-109.
117. Johannessen, C.M., *et al.* COT drives resistance to RAF inhibition through MAP kinase pathway reactivation. *Nature* **468**, 968-972.
118. Nathanson, K.L., *et al.* Tumor genetic analyses of patients with metastatic melanoma treated with the BRAF inhibitor dabrafenib (GSK2118436). *Clin Cancer Res* **19**, 4868-4878.
119. Nissan, M.H., *et al.* Loss of NF1 in cutaneous melanoma is associated with RAS activation and MEK dependence. *Cancer Res* **74**, 2340-2350.
120. Hugo, W., *et al.* Non-genomic and Immune Evolution of Melanoma Acquiring MAPKi Resistance. *Cell* **162**, 1271-1285.
121. Roesch, A. Tumor heterogeneity and plasticity as elusive drivers for resistance to MAPK pathway inhibition in melanoma. *Oncogene* **34**, 2951-2957.
122. Cragg, M.S., *et al.* Treatment of B-RAF mutant human tumor cells with a MEK inhibitor requires Bim and is enhanced by a BH3 mimetic. *J Clin Invest* **118**, 3651-3659 (2008).
123. Jiang, C.C., *et al.* Apoptosis of human melanoma cells induced by inhibition of B-RAFV600E involves preferential splicing of bimS. *Cell Death Dis* **1**, e69.
124. Grazia, G., Penna, I., Perotti, V., Anichini, A. & Tassi, E. Towards combinatorial targeted therapy in melanoma: from pre-clinical evidence to clinical application (review). *Int J Oncol* **45**, 929-949.
125. Emery, C.M., *et al.* MEK1 mutations confer resistance to MEK and B-RAF inhibition. *Proc Natl Acad Sci U S A* **106**, 20411-20416 (2009).
126. Mitsiades, N., *et al.* Genotype-dependent sensitivity of uveal melanoma cell lines to inhibition of B-Raf, MEK, and Akt kinases: rationale for personalized therapy. *Invest Ophthalmol Vis Sci* **52**, 7248-7255.
127. King, A.J., *et al.* Dabrafenib; preclinical characterization, increased efficacy when combined with trametinib, while BRAF/MEK tool combination reduced skin lesions. *PLoS One* **8**, e67583.
128. Roberts, P.J., *et al.* Combined PI3K/mTOR and MEK inhibition provides broad antitumor activity in faithful murine cancer models. *Clin Cancer Res* **18**, 5290-5303.
129. Wiley, S.R., *et al.* Identification and characterization of a new member of the TNF family that induces apoptosis. *Immunity* **3**, 673-682 (1995).

130. Gong, B. & Almasan, A. Genomic organization and transcriptional regulation of human Apo2/TRAIL gene. *Biochem Biophys Res Commun* **278**, 747-752 (2000).
131. Hymowitz, S.G.*, et al.* Triggering cell death: the crystal structure of Apo2L/TRAIL in a complex with death receptor 5. *Mol Cell* **4**, 563-571 (1999).
132. Griffith, T.S.*, et al.* Monocyte-mediated tumoricidal activity via the tumor necrosis factor-related cytokine, TRAIL. *J Exp Med* **189**, 1343-1354 (1999).
133. Smyth, M.J.*, et al.* Tumor necrosis factor-related apoptosis-inducing ligand (TRAIL) contributes to interferon gamma-dependent natural killer cell protection from tumor metastasis. *J Exp Med* **193**, 661-670 (2001).
134. Nieda, M.*, et al.* TRAIL expression by activated human CD4(+)V alpha 24NKT cells induces in vitro and in vivo apoptosis of human acute myeloid leukemia cells. *Blood* **97**, 2067-2074 (2001).
135. Kayagaki, N.*, et al.* Type I interferons (IFNs) regulate tumor necrosis factor-related apoptosis-inducing ligand (TRAIL) expression on human T cells: A novel mechanism for the antitumor effects of type I IFNs. *J Exp Med* **189**, 1451-1460 (1999).
136. LeBlanc, H.N. & Ashkenazi, A. Apo2L/TRAIL and its death and decoy receptors. *Cell Death Differ* **10**, 66-75 (2003).
137. Trivedi, R. & Mishra, D.P. Trailing TRAIL Resistance: Novel Targets for TRAIL Sensitization in Cancer Cells. *Front Oncol* **5**, 69.
138. Kelley, S.K. & Ashkenazi, A. Targeting death receptors in cancer with Apo2L/TRAIL. *Curr Opin Pharmacol* **4**, 333-339 (2004).
139. Walczak, H.*, et al.* Tumoricidal activity of tumor necrosis factor-related apoptosis-inducing ligand in vivo. *Nat Med* **5**, 157-163 (1999).
140. Kelley, S.K.*, et al.* Preclinical studies to predict the disposition of Apo2L/tumor necrosis factor-related apoptosis-inducing ligand in humans: characterization of in vivo efficacy, pharmacokinetics, and safety. *J Pharmacol Exp Ther* **299**, 31-38 (2001).
141. Lawrence, D.*, et al.* Differential hepatocyte toxicity of recombinant Apo2L/TRAIL versions. *Nat Med* **7**, 383-385 (2001).
142. Fulda, S. Tumor-necrosis-factor-related apoptosis-inducing ligand (TRAIL). *Adv Exp Med Biol* **818**, 167-180.
143. Wajant, H., Gerspach, J. & Pfizenmaier, K. Tumor therapeutics by design: targeting and activation of death receptors. *Cytokine Growth Factor Rev* **16**, 55-76 (2005).
144. Almasan, A. & Ashkenazi, A. Apo2L/TRAIL: apoptosis signalling, biology, and potential for cancer therapy. *Cytokine Growth Factor Rev* **14**, 337-348 (2003).
145. Kischkel, F.C.*, et al.* Cytotoxicity-dependent APO-1 (Fas/CD95)-associated proteins form a death-inducing signalling complex (DISC) with the receptor. *EMBO J* **14**, 5579-5588 (1995).
146. Suliman, A., Lam, A., Datta, R. & Srivastava, R.K. Intracellular mechanisms of TRAIL: apoptosis through mitochondrial-dependent and -independent pathways. *Oncogene* **20**, 2122-2133 (2001).
147. Di Pietro, R. & Zauli, G. Emerging non-apoptotic functions of tumor necrosis factor-related apoptosis-inducing ligand (TRAIL)/Apo2L. *J Cell Physiol* **201**, 331-340 (2004).
148. Deng, Y., Lin, Y. & Wu, X. TRAIL-induced apoptosis requires Bax-dependent mitochondrial release of Smac/DIABLO. *Genes Dev* **16**, 33-45 (2002).
149. Jost, P.J.*, et al.* XIAP discriminates between type I and type II FAS-induced apoptosis. *Nature* **460**, 1035-1039 (2009).
150. MacFarlane, M. TRAIL-induced signalling and apoptosis. *Toxicol Lett* **139**, 89-97 (2003).
151. Zhang, L. & Fang, B. Mechanisms of resistance to TRAIL-induced apoptosis in cancer. *Cancer Gene Ther* **12**, 228-237 (2005).
152. Wilson, N.S., Dixit, V. & Ashkenazi, A. Death receptor signal transducers: nodes of coordination in immune signalling networks. *Nat Immunol* **10**, 348-355 (2009).
153. Herbst, R.S.*, et al.* Phase I dose-escalation study of recombinant human Apo2L/TRAIL, a dual proapoptotic receptor agonist, in patients with advanced cancer. *J Clin Oncol* **28**, 2839-2846.
154. Stuckey, D.W. & Shah, K. TRAIL on trial: preclinical advances in cancer therapy. *Trends Mol Med* **19**, 685-694.

155. Buchsbaum, D.J., Zhou, T. & Lobuglio, A.F. TRAIL receptor-targeted therapy. *Future Oncol* **2**, 493-508 (2006).
156. Mom, C.H.*, et al.* Mapatumumab, a fully human agonistic monoclonal antibody that targets TRAIL-R1, in combination with gemcitabine and cisplatin: a phase I study. *Clin Cancer Res* **15**, 5584-5590 (2009).
157. Kurbanov, B.M., Fecker, L.F., Geilen, C.C., Sterry, W. & Eberle, J. Resistance of melanoma cells to TRAIL does not result from upregulation of antiapoptotic proteins by NF-kappaB but is related to downregulation of initiator caspases and DR4. *Oncogene* **26**, 3364-3377 (2007).
158. Zhang, X.D.*, et al.* Relation of TNF-related apoptosis-inducing ligand (TRAIL) receptor and FLICE-inhibitory protein expression to TRAIL-induced apoptosis of melanoma. *Cancer Res* **59**, 2747-2753 (1999).
159. Hilmi, C.*, et al.* IGF1 promotes resistance to apoptosis in melanoma cells through an increased expression of BCL2, BCL-X(L), and survivin. *J Invest Dermatol* **128**, 1499-1505 (2008).
160. Li, S.S.*, et al.* Latent membrane protein 1 mediates the resistance of nasopharyngeal carcinoma cells to TRAIL-induced apoptosis by activation of the PI3K/Akt signalling pathway. *Oncol Rep* **26**, 1573-1579.
161. Ozturk, S., Schleich, K. & Lavrik, I.N. Cellular FLICE-like inhibitory proteins (c-FLIPs): fine-tuners of life and death decisions. *Exp Cell Res* **318**, 1324-1331.
162. Larribere, L.*, et al.* PI3K mediates protection against TRAIL-induced apoptosis in primary human melanocytes. *Cell Death Differ* **11**, 1084-1091 (2004).
163. Opel, D.*, et al.* Targeting aberrant PI3K/Akt activation by PI103 restores sensitivity to TRAIL-induced apoptosis in neuroblastoma. *Clin Cancer Res* **17**, 3233-3247.
164. Chung, A.S., Lee, J. & Ferrara, N. Targeting the tumour vasculature: insights from physiological angiogenesis. *Nat Rev Cancer* **10**, 505-514.
165. Semenza, G.L. Regulation of oxygen homeostasis by hypoxia-inducible factor 1. *Physiology (Bethesda)* **24**, 97-106 (2009).
166. Davis, G.E. & Senger, D.R. Endothelial extracellular matrix: biosynthesis, remodeling, and functions during vascular morphogenesis and neovessel stabilization. *Circ Res* **97**, 1093-1107 (2005).
167. De Palma, M.*, et al.* Tie2 identifies a hematopoietic lineage of proangiogenic monocytes required for tumor vessel formation and a mesenchymal population of pericyte progenitors. *Cancer Cell* **8**, 211-226 (2005).
168. Hida, K. & Klagsbrun, M. A new perspective on tumor endothelial cells: unexpected chromosome and centrosome abnormalities. *Cancer Res* **65**, 2507-2510 (2005).
169. Vacca, A.*, et al.* Melanocyte tumor progression is associated with changes in angiogenesis and expression of the 67-kilodalton laminin receptor. *Cancer* **72**, 455-461 (1993).
170. Mahabeleshwar, G.H. & Byzova, T.V. Angiogenesis in melanoma. *Semin Oncol* **34**, 555-565 (2007).
171. Ribatti, D., Nico, B., Crivellato, E., Roccaro, A.M. & Vacca, A. The history of the angiogenic switch concept. *Leukemia* **21**, 44-52 (2007).
172. Kumar, P.*, et al.* Bcl-2 protects endothelial cells against gamma-radiation via a Raf-MEK-ERK-survivin signalling pathway that is independent of cytochrome c release. *Cancer Res* **67**, 1193-1202 (2007).
173. Li, Y.M.*, et al.* A hypoxia-independent hypoxia-inducible factor-1 activation pathway induced by phosphatidylinositol-3 kinase/Akt in HER2 overexpressing cells. *Cancer Res* **65**, 3257-3263 (2005).
174. van Uden, P., Kenneth, N.S. & Rocha, S. Regulation of hypoxia-inducible factor-1alpha by NF-kappaB. *Biochem J* **412**, 477-484 (2008).
175. Busca, R.*, et al.* Hypoxia-inducible factor 1{alpha} is a new target of microphthalmia-associated transcription factor (MITF) in melanoma cells. *J Cell Biol* **170**, 49-59 (2005).
176. Chen, P.L. & Easton, A.S. Evidence that tumor necrosis factor-related apoptosis inducing ligand (TRAIL) inhibits angiogenesis by inducing vascular endothelial cell apoptosis. *Biochem Biophys Res Commun* **391**, 936-941.

177. Carlo-Stella, C., Lavazza, C., Carbone, A. & Gianni, A.M. Anticancer cell therapy with TRAIL-armed CD34+ progenitor cells. *Adv Exp Med Biol* **610**, 100-111 (2008).
178. Carlo-Stella, C.*, et al.* Targeting TRAIL agonistic receptors for cancer therapy. *Clin Cancer Res* **13**, 2313-2317 (2007).
179. Wilson, N.S.*, et al.* Proapoptotic activation of death receptor 5 on tumor endothelial cells disrupts the vasculature and reduces tumor growth. *Cancer Cell* **22**, 80-90 (2012).
180. Wang, S.*, et al.* TRAIL and doxorubicin combination induces proapoptotic and antiangiogenic effects in soft tissue sarcoma in vivo. *Clin Cancer Res* **16**, 2591-2604.
181. Roberts, O.L., Holmes, K., Muller, J., Cross, D.A. & Cross, M.J. ERK5 and the regulation of endothelial cell function. *Biochem Soc Trans* **37**, 1254-1259 (2009).
182. Jiang, B.H., Zheng, J.Z., Aoki, M. & Vogt, P.K. Phosphatidylinositol 3-kinase signalling mediates angiogenesis and expression of vascular endothelial growth factor in endothelial cells. *Proc Natl Acad Sci U S A* **97**, 1749-1753 (2000).
183. Dong, G.*, et al.* Hepatocyte growth factor/scatter factor-induced activation of MEK and PI3K signal pathways contributes to expression of proangiogenic cytokines interleukin-8 and vascular endothelial growth factor in head and neck squamous cell carcinoma. *Cancer Res* **61**, 5911-5918 (2001).
184. Mirshahi, P.*, et al.* Malignant hematopoietic cells induce an increased expression of VEGFR-1 and VEGFR-3 on bone marrow endothelial cells via AKT and mTOR signalling pathways. *Biochem Biophys Res Commun* **349**, 1003-1010 (2006).
185. Dimmeler, S., Dernbach, E. & Zeiher, A.M. Phosphorylation of the endothelial nitric oxide synthase at ser-1177 is required for VEGF-induced endothelial cell migration. *FEBS Lett* **477**, 258-262 (2000).
186. Skinner, H.D., Zheng, J.Z., Fang, J., Agani, F. & Jiang, B.H. Vascular endothelial growth factor transcriptional activation is mediated by hypoxia-inducible factor 1alpha, HDM2, and p70S6K1 in response to phosphatidylinositol 3-kinase/AKT signalling. *J Biol Chem* **279**, 45643-45651 (2004).
187. Yang, Y.*, et al.* GAB2 induces tumor angiogenesis in NRAS-driven melanoma. *Oncogene* **32**, 3627-3637.
188. Zhang, C.L., Song, F., Zhang, J. & Song, Q.H. Hypoxia-induced Bcl-2 expression in endothelial cells via p38 MAPK pathway. *Biochem Biophys Res Commun* **394**, 976-980.
189. Dormond-Meuwly, A.*, et al.* The inhibition of MAPK potentiates the anti-angiogenic efficacy of mTOR inhibitors. *Biochem Biophys Res Commun* **407**, 714-719.
190. Yuen, J.S.*, et al.* Combination of the ERK inhibitor AZD6244 and low-dose sorafenib in a xenograft model of human renal cell carcinoma. *Int J Oncol* **41**, 712-720.
191. Takahashi, O.*, et al.* Combined MEK and VEGFR inhibition in orthotopic human lung cancer models results in enhanced inhibition of tumor angiogenesis, growth, and metastasis. *Clin Cancer Res* **18**, 1641-1654.
192. Qu, Y.*, et al.* Antitumor activity of selective MEK1/2 inhibitor AZD6244 in combination with PI3K/mTOR inhibitor BEZ235 in gefitinib-resistant NSCLC xenograft models. *J Exp Clin Cancer Res* **33**, 52.
193. Chou, T.C. Drug combination studies and their synergy quantification using the Chou-Talalay method. *Cancer Res* **70**, 440-446.
194. Martin, B.*, et al.* VENNTURE--a novel Venn diagram investigational tool for multiple pharmacological dataset analysis. *PLoS One* **7**, e36911.
195. Liu, C., Cripe, T.P. & Kim, M.O. Statistical issues in longitudinal data analysis for treatment efficacy studies in the biomedical sciences. *Mol Ther* **18**, 1724-1730.
196. Serasinghe, M.N.*, et al.* Anti-apoptotic BCL-2 proteins govern cellular outcome following B-RAF(V600E) inhibition and can be targeted to reduce resistance. *Oncogene* **34**, 857-867.
197. Tassi, E.*, et al.* Role of Apollon in human melanoma resistance to antitumor agents that activate the intrinsic or the extrinsic apoptosis pathways. *Clin Cancer Res* **18**, 3316-3327.
198. Hartman, M.L., Talar, B., Gajos-Michniewicz, A. & Czyz, M. MCL-1, BCL-XL and MITF Are Diversely Employed in Adaptive Response of Melanoma Cells to Changes in Microenvironment. *PLoS One* **10**, e0128796.

199. Jain, R.K. Normalization of tumor vasculature: an emerging concept in antiangiogenic therapy. *Science* **307**, 58-62 (2005).
200. Zhang, P., Goodrich, C., Fu, C. & Dong, C. Melanoma upregulates ICAM-1 expression on endothelial cells through engagement of tumor CD44 with endothelial E-selectin and activation of a PKCalpha-p38-SP-1 pathway. *FASEB J* **28**, 4591-4609.
201. Greger, J.G.*, et al.* Combinations of BRAF, MEK, and PI3K/mTOR inhibitors overcome acquired resistance to the BRAF inhibitor GSK2118436 dabrafenib, mediated by NRAS or MEK mutations. *Mol Cancer Ther* **11**, 909-920.
202. Kwong, L.N. & Davies, M.A. Targeted therapy for melanoma: rational combinatorial approaches. *Oncogene* **33**, 1-9.
203. Beck, D.*, et al.* Vemurafenib potently induces endoplasmic reticulum stress-mediated apoptosis in BRAFV600E melanoma cells. *Sci Signal* **6**, ra7.
204. Ma, X.H.*, et al.* Targeting ER stress-induced autophagy overcomes BRAF inhibitor resistance in melanoma. *J Clin Invest* **124**, 1406-1417.
205. Berger, A.*, et al.* RAF inhibition overcomes resistance to TRAIL-induced apoptosis in melanoma cells. *J Invest Dermatol* **134**, 430-440.
206. Quast, S.A., Berger, A. & Eberle, J. ROS-dependent phosphorylation of Bax by wortmannin sensitizes melanoma cells for TRAIL-induced apoptosis. *Cell Death Dis* **4**, e839.
207. Zhang, X.D., Borrow, J.M., Zhang, X.Y., Nguyen, T. & Hersey, P. Activation of ERK1/2 protects melanoma cells from TRAIL-induced apoptosis by inhibiting Smac/DIABLO release from mitochondria. *Oncogene* **22**, 2869-2881 (2003).
208. Gembarska, A.*, et al.* MDM4 is a key therapeutic target in cutaneous melanoma. *Nat Med* **18**, 1239-1247.
209. Ivanov, V.N. & Hei, T.K. Sodium arsenite accelerates TRAIL-mediated apoptosis in melanoma cells through upregulation of TRAIL-R1/R2 surface levels and downregulation of cFLIP expression. *Exp Cell Res* **312**, 4120-4138 (2006).
210. Gillespie, S., Borrow, J., Zhang, X.D. & Hersey, P. Bim plays a crucial role in synergistic induction of apoptosis by the histone deacetylase inhibitor SBHA and TRAIL in melanoma cells. *Apoptosis* **11**, 2251-2265 (2006).
211. Zhang, H.*, et al.* Clusterin inhibits apoptosis by interacting with activated Bax. *Nat Cell Biol* **7**, 909-915 (2005).
212. Kim, A.*, et al.* Coexistent mutations of KRAS and PIK3CA affect the efficacy of NVP-BEZ235, a dual PI3K/MTOR inhibitor, in regulating the PI3K/MTOR pathway in colorectal cancer. *Int J Cancer* **133**, 984-996.
213. Fulda, S. & Vucic, D. Targeting IAP proteins for therapeutic intervention in cancer. *Nat Rev Drug Discov* **11**, 109-124.
214. Wilson, N.S.*, et al.* Proapoptotic activation of death receptor 5 on tumor endothelial cells disrupts the vasculature and reduces tumor growth. *Cancer Cell* **22**, 80-90.
215. Na, H.J.*, et al.* TRAIL negatively regulates VEGF-induced angiogenesis via caspase-8-mediated enzymatic and non-enzymatic functions. *Angiogenesis* **17**, 179-194.

FIGURE REFERENCES

Figure 1.1: from Fisher *et al*, Science 2014

Figure 1.2: from Gray-Schopfer *et al*, Nature 2007

Figure 1.3: from Hunter Shain A. *et al*, N Engl J Med 2015

Figure 1.4: from Swetter *et al,* Oncology 2004

Table 1.1: from Chudnovsky *et al*., JCI 2005

Table 1.2 and Figure 1.5: from Balch *et al*, J Clin Oncol 2009

Table 1.3: from t.c.g.a network, Cell 2015

Figure 1.6: from Hazzalin *et al*,Nature Reviews Molecular Cell Biology 2002

Figure 1.7: from Fisher *et al*, Science 2014

Table 1.4: from Caunt *et al*, Nature review 2015

Figure 1.8: from Christine M. *et al*, Clin Cancer Res 2009

Figure 1.9: Image from Azijli *et al*,Cell Death and Differentiation 2013

Figure 4.1- 4.31: Grazia et al, Cell death and Disease 2014

Supplementary

Table S1 **Molecular and biological features of melanoma cell lines used in this study**

		Molecular features of the cell lines[b]			Susceptibility to TRAIL[c] (MTT assay, 100ng/mL, 48h)			Susceptibility to MEK and PI3K/mTOR inhibitors[d] (MTT assay, 48 h)			
Tumor code used in this study	Tissue of origin of cell line[a]	BRAF/NRAS status	PTEN status (gene/protein)	p53 status	Growth inhibition (% dead cells)	Mitochondrial depolarization (% $TMRE^-$ cells)	Caspase-8 activation (% cleaved caspase 8^+ cells)	AZD6244 (IC_{50}, μM)	BEZ235 (IC_{50}, μM)	Tumor code used in previous papers	References
Me1	ln met.	$BRAF^{V600E}$	wt/+	wt	94.1	49.0	28.0	0.050	0.080	Me14464	27, 42, 48
Me2	ln met.	$BRAF^{V600E}$	wt/+	wt	76.5	58.0	32.0	0.120	0.225	Me4023	27, 48
Me5	s.c. met.	$BRAF^{V600E}$	ex.5 $del_{403-409}$/-	wt	26.0	12.2	16.0	0.015	0.070	-	This manuscript
Me6	s.c. met.	$BRAF^{V600E}$	wt/+	wt	28.0	43.6	28.3	0.350	0.088	Me6824	42
Me13	ln met.	$BRAF^{V600E}$	wt/+	wt	6.2	4.7	2.6	0.308	0.109	Me15392	27, 42, 48
Me15	ln met.	$BRAF^{V600E}$	wt/+	wt	96.4	14.2	33.0	0.015	0.045	Me23682	27
Me17	ln met.	$BRAF^{V600E}$	wt/+	$C135W^{Ho}$	4.0	1.7	4.5	0.029	0.092	-	This manuscript
Me20	ln met.	$NRAS^{Q61R}$	wt/+	wt	9.3	26.7	19.0	0.010	2.520	Me18816	42
Me25	local recurrence	$BRAF^{V600E}$	wt/+	Y236H	10.4	5.5	0.0	0.328	0.110	Me1402r	48
Me27	ln met.	$BRAF^{V600E}$	wt/-	wt	17.0	19.6	16.3	0.186	0.178	Me13294	27
Me30	ln met.	$BRAF^{V600E}$	wt/+	wt	44.6	1.6	4.5	0.058	0.586	Me18656	27, 42, 48
Me32	VGP primary me.	$NRAS^{G12S}$	wt/+	wt	87.4	23.9	0.1	0.410	0.030	Me9923p	48
Me33	ln met.	$BRAF^{V600E}$	wt/+	wt	0.0	0.0	0.5	0.023	0.283	-	This manuscript
Me34	ln met.	$NRAS^{Q61R}$	wt/+	$Y126H^{Ho}$	71.5	15.3	14.4	0.560	0.030	-	This manuscript
Me36	ln met.	wt/wt	wt/+	wt	30.0	0.5	5.7	0.780	1.630	Me879	48
Me40	ln met.	$BRAF^{V600E}$	wt/-	wt	1.5	0.1	17.3	0.280	0.100	-	This manuscript
Me41	ln met.	$BRAF^{V600E}$	wt/+	wt	35.0	20.5	6.5	0.020	0.048	Me32562	42
Me43	ln met.	$BRAF^{V600E}$	wt/+	wt	42.2	2.2	13.1	0.029	0.168	Me18732	27, 42, 48
Me44	ln met.	$BRAF^{V600E}$	wt/+	wt	4.7	0.6	7.0	0.050	0.220	Me16938	42
Me46	s.c. met.	$BRAF^{V600E}$	wt/+	wt	7.9	1.5	1.0	0.020	0.030	-	This manuscript
Me49	ln met.	$BRAF^{V600E}$	P246S/+	$S127F^{Ho}$	19.8	0.0	1.1	0.049	0.089	Me2211	27, 42, 48
Me50	ln met.	$BRAF^{V600E}$	$P246S^{He}$/+	$S127F^{Ho}$	53.4	12.6	9.5	0.060	0.160	-	This manuscript
Me53	s.c. met.	$BRAF^{V600E}$	wt/+	wt	44.0	17.6	12.0	0.288	0.012	Me32669	27, 42
Me55	ln met.	wt/wt	wt/+	wt	63.0	9.7	20.0	0.720	1.140	Me3700	42
Me56	ln met.	$BRAF^{V600E}$	P38S/-	S127F	8.1	0.0	3.6	0.012	3.679	Me4686	48
Me57	VGP primary me.	wt/wt	wt/+	R213R	2.4	3.2	0.6	0.020	0.020	Me1007	48
Me58	ln met.	$BRAF^{V600E}$	wt/+	wt	11.0	22.9	12.0	0.387	5.429	Me2559	42
Me59	ln met.	$NRAS^{Q61R}$	wt/+	wt	29.4	21.7	0.0	0.030	0.590	Me4473	42, 48
Me63	ln met.	$BRAF^{V600E}$	$Y223STOP^{He}$ / -	wt	25.8	3.1	0.8	0.085	4.796	-	This manuscript
Me64	ln met.	wt/wt	nd/+	wt	3.3	0.8	1.7	0.050	0.020	Me13923	48
Me67	soft tissue met.	$NRAS^{Q61R}$	wt/+	$R213R^{He}$	92.5	25.5	25.0	9.770	0.380	Me3044	42
Me69	ln met.	$BRAF^{V600E}$	wt/+	Y234C	46.7	15.5	10.5	0.214	12.882	Me17697	48
Me71	ln met.	$BRAF^{V600E}$	wt/+	wt	3.5	17.7	25.0	0.010	0.047	Me21158	27, 42
Me73	ln met.	$BRAF^{V600E}$	$del_{ex3-5-6}$/-	$P128S^{He}$	18.0	5.3	0.0	0.019	0.062	Me1274	42
Me75	VGP primary me.	$BRAF^{V600E}$	wt/+	wt	0.0	1.5	5.8	0.047	0.222	Me10258	42
Me76	ln met.	$BRAF^{V600E}$	wt/+	E258K	21.4	0.0	0.8	0.016	0.067	Me14362	27, 42, 48
Me78	ln met.	$BRAF^{V600E}$	wt/+	wt	10.5	0.0	1.3	0.069	6.098	-	This manuscript
Me79	ln met.	$BRAF^{V600E}$	wt/+	wt	17.0	4.3	1.9	1.224	96.746	Me2934	27, 42, 48
Me83	ln met.	wt/wt	Q171Q / +	wt	65.7	13.8	11.0	0.120	0.100	Me2352	27, 42
Me85	VGP primary me.	$BRAF^{V600E}$	wt/+	wt	49.0	38.9	6.3	0.014	0.525	-	This manuscript
Me86	soft tissue met.	$NRAS^{Q61R}$	wt/+	wt	48.1	23.0	22.0	0.020	0.200	Me15094	27
Me88	ln met.	wt/wt	wt/+	wt	71.1	12.0	0.0	0.020	0.160	Me19410	42
Me92	VGP primary me.	$BRAF^{L596S}$	wt/+	G187S	0.7	3.6	0.0	0.069	0.107	Me20842	27, 42, 48
Me93	ln met.	$BRAF^{L596S}$	wt/+	wt	8.5	5.7	0.9	0.036	0.076	Me20842M1	48
Me94	s.c. met.	$BRAF^{L596S}$	wt/+	G187S	51.2	12.2	2.7	0.018	0.048	Me20842M2	48
Me96	ln met.	$BRAF^{V600E}$	wt/+	wt	17.2	0.0	0.6	0.030	0.280	Me9874	42
Me98	ln met.	$BRAF^{V600E}$	nd/+	wt	0.0	0.5	0.8	0.042	0.048	Me29318	42
Me99	VGP primary me.	$BRAF^{V600E}$	P89S, $del_{ex\ 6-8}$/-	wt	13.5	2.0	0.7	8.697	0.212	Me26635	42
Me100	VGP primary me.	$NRAS^{Q61R}$	wt/+	null	52.1	0.0	2.2	0.120	0.560	Me4405	27, 42, 48

[a] Melanoma cell lines were isolated from: vertical growth phase primary melanomas (VGP primary me.), lymph node metastases (ln met.), subcutaneous metastases (s.c. met.), soft tissues metastases or local recurrences.

[b] Methods for identification of BRAF, NRAS, PTEN and p53 mutations are described in Grazia G. et al. Cell Death and Disease 2014. PTEN data expressed as gene sequence data / protein expression by western blot. He:heterozygous; Ho: homozygous.

[c] Susceptibility to TRAIL was assessed by a 48 h MTT assay. Mitochondrial depolarization (TMRE assay) and caspase-8 cleavage in response to TRAIL were assessed at 24 h by flow cytometry.

[d] Susceptibility to AZD6244 and BEZ235, shown as IC_{50} values, was assessed by a 48 h MTT assay. IC_{50} values were obtained trough non linear regression analysis of dose response curves. See **Fig. 4.3** for representative examples of dose-response plots.

Table S2. Statistical analysis of fraction affected (FA) data.

Comparison 1: High vs. low TRAIL doses in the AZD6244+BEZ235+TRAIL combination: significant FA increase at higher TRAIL doses

		FA values in melanoma cells treated with the association		
		AZD6244 →	**0.05** μM	**0.05** μM
		BEZ235 →	**0.005** μM	**0.005** μM
		TRAIL →	**10** ng/mL	**25** ng/mL
FA values in melanoma cells treated with the association of:	AZD6244 (**0.05** μM) BEZ235 (**0.005** μM) TRAIL (**5** ng/mL)		ns	**
	AZD6244 (**0.05** μM) BEZ235 (**0.005** μM) TRAIL (**10** ng/mL)			**

		treated with the association of:		
		AZD6244 →	**0.05** μM	**0.05** μM
		BEZ235 →	**0.01** μM	**0.01** μM
		TRAIL →	**10** ng/mL	**25** ng/mL
FA values in melanoma cells treated with the association of:	AZD6244 (**0.05** μM) BEZ235 (**0.01** μM) TRAIL (**5** ng/mL)		ns	**
	AZD6244 (**0.05** μM) BEZ235 (**0.01** μM) TRAIL (**10** ng/mL)			**

		FA values in melanoma cells treated with the association		
		AZD6244 →	**0.05** μM	**0.05** μM
		BEZ235 →	**0.02** μM	**0.02** μM
		TRAIL →	**10** ng/mL	**25** ng/mL
FA values in melanoma cells treated with the association of:	AZD6244 (**0.05** μM) BEZ235 (**0.02** μM) TRAIL (**5** ng/mL)		ns	*
	AZD6244 (**0.05** μM) BEZ235 (**0.02** μM) TRAIL (**10** ng/mL)			*

Comparison 2: AZD6244+TRAIL vs. AZD6244+BEZ235+TRAIL: significant FA increase by adding BEZ235

		FA values in melanoma cells treated with the association of:											
		AZD6244 →	**0.05** μM	**0.05** μM	**0.05** μM	AZD6244 →	**0.05** μM	**0.05** μM	**0.05** μM	AZD6244 →	**0.05** μM	**0.05** μM	**0.05** μM
		BEZ235 →	**0.005** μM	**0.01** μM	**0.02** μM	BEZ235 →	**0.005** μM	**0.01** μM	**0.02** μM	BEZ235 →	**0.005** μM	**0.01** μM	**0.02** μM
		TRAIL →	**5** ng/mL	**5** ng/mL	**5** ng/mL	TRAIL →	**10** ng/mL	**10** ng/mL	**10** ng/mL	TRAIL →	**25** ng/mL	**25** ng/mL	**25** ng/mL
FA values in melanoma cells treated with the association of:	AZD6244 (**0.05** μM) TRAIL (**5** ng/mL)		*	**	***								
	AZD6244 (**0.05** μM) TRAIL (**10** ng/mL)						ns	**	***				
	AZD6244 (**0.05** μM) TRAIL (**25** ng/mL)										ns	**	***

Comparison 3: AZD6244+BEZ235 vs AZD6244+BEZ235+TRAIL: Significant FA increase by adding high dose TRAIL

		FA values in melanoma cells treated with the association of:											
		AZD6244 →	**0.05** μM	**0.05** μM	**0.05** μM	AZD6244 →	**0.05** μM	**0.05** μM	**0.05** μM	AZD6244 →	**0.05** μM	**0.05** μM	**0.05** μM
		BEZ235 →	**0.005** μM	**0.005** μM	**0.005** μM	BEZ235 →	**0.01** μM	**0.01** μM	**0.01** μM	BEZ235 →	**0.02** μM	**0.02** μM	**0.02** μM
		TRAIL →	**5** ng/mL	**10** ng/mL	**25** ng/mL	TRAIL →	**5** ng/mL	**10** ng/mL	**25** ng/mL	TRAIL →	**5** ng/mL	**10** ng/mL	**25** ng/mL
FA values in melanoma cells treated with the association of:	AZD6244 **(0.05** μM) BEZ235 (**0.005** μM)		ns	ns	***								
	AZD6244 **(0.05** μM) BEZ235 (**0.01** μM)						ns	ns	***				
	AZD6244 (**0.05** μM) BEZ235 (**0.02** μM)										ns	ns	***

The analysis, carried out by ANOVA followed by SNK test, is based on FA data generated by Compusyn software on a dataset of the 21 melanoma cell lines and treated with the indicated combinations oftarget-specific inhibitors and TRAIL.

***: p<0.05; **: p<0.01; ***: p<0.001**

Table S3. Downstream effect analysis by IPA software of significantly modulated genes by the association of TRAIL, AZD6244 and BEZ235.

Results shown here are based on the set of genes identified by the light blue circles in **Fig.4.11.**
See supplementary methods for the meaning of the p values and of the z score statistics.

Category	Functions Annotation	p-Value	Predicted Activation State	Activation z-score	Molecules	# Molecules	Shown in Fig. S4b
Cell Death and Survival	cell death of melanoma cell lines	6.46E-07	Increased	2.108	ATM,BAG3, BBC3, BIRC5, BMF, CDKN1B, DAB2, DDIT3,DIABLO, EGR1, EPOR, ETS1, FGF2, FOXD3, FOXO3, GADD45A, HSPA5, HSPB8, IL8, MAP2K1, MCL1, MITF,NME1, PAX3, PMAIP1,PPP1R15A, SMOX, SPHK1, STAT2, TFAP2A, TNFRSF1A, TOP1	32	yes
Cell Death and Survival	apoptosis of melanoma cell lines	2.24E-06	Increased	2.188	ATM, BAG3, BBC3, BIRC5, BMF, CDKN1B, DAB2, DDIT3, DIABLO, EGR1, EPOR, ETS1, FGF2, FOXO3, GADD45A, HSPA5, HSPB8, MAP2K1, MCL1, MITF, NME1, PAX3, PMAIP1, PPP1R15A, SMOX, SPHK1, STAT2, TNFRSF1A, TOP1	29	yes
Organismal Survival	organismal death	1.32E-05	Increased	2.819	ABCB6, ABL1, ABL2, ACACA, ACLY, ACTB, ACTG1,ACTN4, ADAM19, ADAMTS1, ADM, ADRB2, ADRBK1, AFG3L1P, AGRN, AHI1, AHR, AIM2, AKAP12, AKT1, ALDH1A3, ANGPTL4, ANK3, ANTXR2, APEX1, ARAP3, ARHGDIA, ARID4B, ARID5B, ARNTL, ARRB1, ASPA, ATF4, ATM, ATP2B1, ATXN3, B3GNT5, BAG3, BBC3, BCL6, BID, BIRC5, BMF, BMPR1A, C1GALT1, C3AR1, C9orf114, CA14, CABIN1, CBFB, CBLB, CBX2, CBY1, CCDC86, CCNB2, CCND1, CCND3, CCNE1, CCNE2, CD151, CD200, CD36, CD44, CDC25A, CDK19, CDK6, CDKN1B, CDKN2C, CEBPB, CEBPD, CEBPG, CHUK, CITED1, CITED2, CLDN1, COL5A2, CPOX,CREB3L2, CREB5, CSK, CSRNP1, CTLA4, CTNNB1, CTSF, CTSL2, CXCR4, CYR61,DAB2, DACT1, DDAH1, DDB2, DDR1, DHCR7, DHX58, DLX5, DMRT2,DNM1L, DUSP1, DYNC2LI1, E2F3, E2F4, E2F5, ECE2, EDNRB, EEF1E1, EGLN1, EGR3, EHD4, EHHADH, EIF2C2, EIF2S1, ELK3, ENDOG, ENG, ENPP2, EPAS1, EPOR, ERRFI1, ETS1, ETS2, EYA4, FABP3, FAIM, FAM20C, FASN, FBXO4, FBXO45, FBXW7, FCER1G, FEN1, FGF2, FGFR3, FGFRL1, FKBP4, FN1, FNDC3B, FOSL1, FOXD3, FOXF2, FOXO3, FOXQ1, FSTL1, FURIN, FXR1, GADD45A, GAS1, GCH1, GCLM, GHR, GJB1, GRN, GSTZ1, H1F0, HAS2, HBEGF, HEXA, HEY1, HEY2, HIF1A, HIPK2, HIST2H2AA3/HIST2H2AA4,HK2, HLX, HMBS, HMGCL, HMGN2, HPGD, HS3ST1, HSPA1A/HSPA1B, HSPA4L, HSPA5, HSPB8, HTR2B, HYAL2, ICMT, ID1, ID2, IDE, IFNAR1, IFNAR2, IFNGR1, IFT122, IGFBP3, IGFBP5, IL12A, IL1B, IL27RA, IL6, IL8, ING4,INSIG1,INSIG2,IP6K2, IRAK1, IRF9, IRS2, ITGA3,ITGA4, ITGA5,ITPKB, JUP, KIF5B, KIT, KLF2, KLF6, KPNA1, KRAS, KRR1, LAMP2, LATS2, LEF1, LFNG, LIF, LIMK1, LMNB2, LMO4, LPL, LRP5, LRP8, LTBR, LYN, MAFB, MAFF, MAP2K1, MAP2K3, MAP2K5, MAP3K12, MARCKS, MARCKSL1, MCL1, MCM10, MEF2C, MEF2D, MET, MGAT1, MITF, MKKS, MNT, MTA2, MTERFD1, MTHFR, MXI1, MYCBP2, NFAT5, NFIB, NFIC, NKX2-5, NKX3-2, NLRP3, NME1, NOA1, NOTCH1, NOTCH2, NOV, NQO1, NR5A2, NRP1, NUMA1, OAT, OPHN1, ORAI1, PAX3, PEX11B, PHB, PHC2, PIK3CB, PISD, PKNOX1, PLAT, PNN,PNPT1, POU3F1, POU3F2, PPAP2B, PPARD, PPARGC1A, PPARGC1B, PPIF, PPIG, PPME1, PPP1R14C, PPP1R15A, PPP3R1, PRNP, PRPF19, PRRX1, PSMD4, PTEN, PTGS2, PTPN1, PTRH2, PVRL3, RAB27A, RAD23B, RAPGEF1, RASSF1, RASSF2, RBBP8, RBM15, RDH10, RGS10, RIF1, RPL6, RTN4, RUNX1, RXRB, SAFB, SDC4, SEPP1, SERTAD1, SGCD, SHISA2, SIAH1, SLC20A1, SLC25A19, SLC25A37, SLC2A1, SLC2A3, SLC5A3, SLC9A3R1, SMAD3, SNAI2, SOX4, SP1, SPEN, SPRY1,SPRY2,SPRY4, ST8SIA1,STAM, STAMBP, STARD13, STAT2,STIP1,STK3, SV2A, SV2B, SYNJ1,TDG, TFAP2A, TFAP2C, TFB1M, TFDP1, TFRC, TGFA, TGFBR2, TGIF1, THBS1, THBS2, TIMP3, TK2, TNFRSF1A, TOP1, TP53INP1, TRAF3IP2, TRIM63, TRPV2, TUBG1, TXNIP, UBD, UHRF1, ULK1, VAMP2, VEGFA, VGF, VWF, WDR77, XBP1, ZBTB20, ZEB2, ZNF148	371	yes
Cell Death and Survival	cell death of prostate cancer cell lines	1.66E-05	Increased	2.080	ABCE1, ABL1, ACACA, AKAP12, AKT1, ATM, BIRC5, DDIT3, DIABLO, DKK3, EGR1, ETS2, FASN, FN1, FOXO3, GADD45A, GDF15, HBEGF, HIF1A, HOXC6, HSPA1A/HSPA1B, HSPB8, ICMT, ID1, IGFBP3, IGFBP4, IGFBP5, IL6, MAP2K1, MAP2K3, MCL1, MET, ORAI1, PIM1, PMAIP1, PTEN, PTGS2, SH3RF1, TGFA, TOP1, TPD52	41	yes
Cell Death and Survival	apoptosis of prostate cancer cell lines	2.21E-05	Increased	2.068	ABCE1, ABL1, ACACA, AKAP12, AKT1, ATM, BIRC5, DIABLO, DKK3, EGR1, ETS2, FASN, FN1, FOXO3, GADD45A, GDF15, HBEGF, HIF1A, HOXC6, HSPA1A/HSPA1B, HSPB8, ID1, IGFBP3, IGFBP4, IGFBP5, IL6, MAP2K3, MCL1, MET, ORAI1, PIM1, PMAIP1, PTEN, PTGS2, SH3RF1, TGFA, TPD52	37	yes
Cellular Growth and Proliferation	cytostasis of tumor cell lines	4.83E-04	Increased	2.184	ABL1, ADRBK1, BCL6, BHLHE40, BIRC5,BMPR1A, CCND1, CCND3, CDCA8, CDKN1B, CEACAM1, CTNNB1,CYR61,EGR1,ETS1,FOXO3, G3BP1, IL6,LIF,MXI1,NME1,NOTCH1,NQO1,PPP1R15A, PTEN,RACGAP1, RXRB, SMAD3, TGFBR2, TOP1	30	yes
Cellular Growth and Proliferation	cytostasis	7.51E-04	Increased	2.369	ABL1, ADRBK1, BCL6, BHLHE40, BIRC5, BMPR1A, CBX2, CCND1, CCND3, CDCA8, CDKN1B, CDKN2C, CEACAM1, CEBPB, CTNNB1, CYR61, EGR1, ETS1, FOXO3, G3BP1, GBP2, HAS2, HAS3, HBP1, HSPA1A/HSPA1B, ID1, ID2, IL6, ING4, KIT, KLF6, KRAS, LATS2, LIF, MXI1, NME1, NOTCH1, NQO1, PPP1R15A, PRKCZ, PTEN, PTPN1, RACGAP1, RXRB, SAFB, SMAD3, STAMBP, TFAP2A, TGFBR2, TOP1	50	yes

Category	Functions Annotation	p-Value	Predicted Activation State	Activation z-score	Molecules	# Molecules	Shown in Fig. S4b
Cell Cycle	interphase	1.21E-07	Decreased	-2.145	ABL1, AHR, AKAP12, AKT1, ANXA2, ARRB1, ATF3, ATF5, ATM, BHLHE40, BID, BIRC5, BTG1, BTK, C11orf82, CABLES1, CBX2, CCND1, CCND3, CCNE1, CCNE2, CCNG2, CD44, CDC25A, CDC25B, CDC25C, CDK5RAP3, CDK6, CDKN1B, CDKN2C, CDKN3, CDT1, CEBPB, CEBPD, COPS2, CTLA4, CTNNB1, CYR61, DDIT3, DDX3X, DEGS1, DUSP1, E2F3, E2F4, E2F5, EGR1, EPOR, ETS1, FASN, FBXL2, FEN1, FGF2, FN1, FOXO3, GADD45A, GAS1, GRB2, HBEGF, HINFP, ID1, ID2, IL1B, IL6, ING4, KRAS, LSM10, MAP2K1, MCM10, MCMBP, MET, MXD3, MXD4, MXI1, NOTCH1, NPAT, PNPT1, RASSF1, RBBP8, RGCC, RUNX1, SH2B3, SKP2, SP1, SPHK1, SPRY2, SRPK2, SRSF2, ST8SIA1, TAF2, TAOK2, TBRG4, TFDP1, TFDP2, TFRC, TGFA, TGFBR2, TXNIP, UHRF1, VEGFA, YWHAG, ZEB2	126	yes
Cell Cycle	S phase	1.98E-07	Decreased	-2.823	ABL1, ATM, BHLHE40, BID, BIRC5, CBX2, CCND1, CCND3, CCNE1, CCNG2, CDC25A, CDC25C, CDK6, CDKN1B, CDKN2C, CDT1, CEBPB, CTLA4, DDX3X, E2F3, E2F4, E2F5, EPOR, FEN1, FGF2, FN1, FOXO3, GADD45A, GAS1, GRB2, HBEGF, HINFP, ID1, ID2, IL1B, IL6, ING4, KRAS, LSM10, MAP2K1, MCM10, MCMBP, MET, MXD3, MXD4, MXI1, NOTCH1, NPAT, PNPT1, RASSF1, RBBP8, RGCC, RUNX1, SH2B3, SKP2, ST8SIA1, TFDP1, TFDP2, TGFA, TGFBR2, UHRF1,VEGFA	62	yes
Cell Cycle	entry into S phase	1.49E-06	Decreased	-2.733	ABL1, ATM, BHLHE40, CBX2, CCND1, CCND3, CCNE1, CDC25A, CDKN1B, CDKN2C, CEBPB, CTLA4, DDX3X, E2F3, E2F4, E2F5, FGF2, FN1, GAS1, GRB2,HBEGF, HINFP,ID2, IL1B, IL6, KRAS, MCM10, MET,NPAT, RGCC, SKP2, ST8SIA1, TFDP1, TFDP2, UHRF1	35	yes
Cell Cycle	entry into interphase	2.04E-06	Decreased	-2.663	ABL1, AKT1, ATM,BHLHE40,CBX2, CCND1, CCND3, CCNE1, CDC25A, CDKN1B, CDKN2C, CEBPB, CTLA4, DDX3X, E2F3, E2F4, E2F5, EGR1,FGF2, FN1,GAS1,GRB2,HBEGF,HINFP,ID2, IL1B, IL6, KRAS, MCM10, MET, NPAT, RGCC, SKP2, ST8SIA1, TFDP1, TFDP2,UHRF1	37	yes
Cellular Movement	cell movement of fibroblast cell lines	2.45E-06	Decreased	-2.308	ABL1, ACP1, ACTR2, AKT1, AMD1, CD44, CDKN1B, CSK, CTNNB1, DDR1, DDX3X, ELK3, FBXW7, FGF2, FN1, FOSL1, GNG12, GRB2, HAS2, HAS3, HBEGF, IL8, ITGA5, KLF2, LIMA1, MARCKS, MST1, MYLK, PTEN, PTGS2, PTPN1, PVR, RASSF1, SKP2, TP53INP1,VEGFA	36	yes
Connective Tissue Development and Function	cell movement of fibroblast cell lines	2.45E-06	Decreased	-2.308	ABL1, ACP1, ACTR2, AKT1, AMD1, CD44, CDKN1B, CSK, CTNNB1, DDR1, DDX3X, ELK3, FBXW7, FGF2, FN1, FOSL1, GNG12, GRB2, HAS2, HAS3, HBEGF, IL8, ITGA5, KLF2, LIMA1, MARCKS, MST1, MYLK, PTEN, PTGS2, PTPN1, PVR, RASSF1, SKP2, TP53INP1,VEGFA	36	yes
Cell Cycle	re-entry into interphase	3.43E-06	Decreased	-2.442	CCND1, CCND3, CCNE1, CDC25A, CDC25C, CDKN1B, CEBPB, FN1, ID2, MAP2K1, RUNX1, SKP2, TFDP1, TGFA, VEGFA	15	yes
Cellular Development	proliferation of fibroblasts	4.59E-06	Decreased	-2.018	ABL1, ACTB, AHR,AKT1,ATF3, ATF4, ATM,CBX2, CBX7, CCND1, CCND3, CCNE1, CD44, CDK6, CDKN1B, CEBPB, CIRBP, CITED2, CTNNB1,DNM1L, DUSP1, FEN1, FGF2,FN1, FNDC3B, FOSL1, GADD45A, GRB2, GRN, HBEGF, HIF1A, HMMR, ICMT, IFNAR1, IGFBP3, IGFBP4, IL1B, IL6, IP6K2, ITGA5, JUND, KRAS, LDHA, LIF, MAP2K3, MCM8, MET, PA2G4, PHC2, PLAT, PPARD, PPAT, PSME3, PTEN, SAFB, SERTAD1, SKP2, SMAD3, SPHK1, SPRY2, STARD10, TGFBR2, TGIF1, TNFRSF1A, TPR,TXNIP	66	yes
Cellular Growth and Proliferation	proliferation of fibroblasts	4.59E-06	Decreased	-2.018	ABL1, ACTB, AHR,AKT1,ATF3, ATF4, ATM,CBX2, CBX7, CCND1, CCND3, CCNE1, CD44, CDK6, CDKN1B, CEBPB, CIRBP, CITED2, CTNNB1,DNM1L, DUSP1, FEN1, FGF2,FN1, FNDC3B, FOSL1, GADD45A, GRB2, GRN, HBEGF, HIF1A, HMMR, ICMT, IFNAR1, IGFBP3, IGFBP4, IL1B, IL6, IP6K2, ITGA5, JUND, KRAS, LDHA, LIF, MAP2K3, MCM8, MET, PA2G4, PHC2, PLAT, PPARD, PPAT, PSME3, PTEN, SAFB, SERTAD1, SKP2, SMAD3, SPHK1, SPRY2, STARD10, TGFBR2, TGIF1, TNFRSF1A, TPR,TXNIP	66	yes
Connective Tissue Development and Function	proliferation of fibroblasts	4.59E-06	Decreased	-2.018	ABL1, ACTB, AHR,AKT1,ATF3, ATF4, ATM,CBX2, CBX7, CCND1, CCND3, CCNE1, CD44, CDK6, CDKN1B, CEBPB, CIRBP, CITED2, CTNNB1,DNM1L, DUSP1, FEN1, FGF2,FN1, FNDC3B, FOSL1, GADD45A, GRB2, GRN, HBEGF, HIF1A, HMMR, ICMT, IFNAR1, IGFBP3, IGFBP4, IL1B, IL6, IP6K2, ITGA5, JUND, KRAS, LDHA, LIF, MAP2K3, MCM8, MET, PA2G4, PHC2, PLAT, PPARD, PPAT, PSME3, PTEN, SAFB, SERTAD1, SKP2, SMAD3, SPHK1, SPRY2, STARD10, TGFBR2, TGIF1, TNFRSF1A, TPR,TXNIP	66	yes
Cell Cycle	re-entry into S phase	6.05E-06	Decreased	-2.442	CCND1, CCND3, CCNE1, CDC25A, CDKN1B, CEBPB, FN1, ID2, MAP2K1, RUNX1, SKP2, TFDP1, TGFA, VEGFA	14	yes
Cellular Movement	migration of fibroblast cell lines	1.22E-05	Decreased	-2.300	ABL1, ACP1, CDKN1B, CSK, CTNNB1, DDR1, DDX3X, ELK3, FBXW7, FGF2, FN1, GNG12, HAS2, HAS3, HBEGF, IL8, ITGA5, KLF2, LIMA1, MARCKS, MYLK, PTEN, PTGS2, PVR, RASSF1, SKP2, TP53INP1, VEGFA	28	yes
Connective Tissue Development and Function	migration of fibroblast cell lines	1.22E-05	Decreased	-2.300	ABL1, ACP1, CDKN1B, CSK, CTNNB1, DDR1, DDX3X, ELK3, FBXW7, FGF2, FN1, GNG12, HAS2, HAS3, HBEGF, IL8, ITGA5, KLF2, LIMA1, MARCKS, MYLK, PTEN, PTGS2, PVR, RASSF1, SKP2, TP53INP1, VEGFA	28	yes
Cancer	tumorigenesis of malignant tumor	1.25E-05	Decreased	-2.565	AHR, AKT1, ANK3, ARID4B, ASXL2, ATM, BIRC5, BMF, CABLES1, CBX7, CCND1, CCND3, CCNDBP1, CDKN1B, CDKN2C, CHD9, CTLA4, DCBLD2, DDB2, DTNA, EGR1, ERRFI1, FBXO4, FEN1, FGF2, FNDC3B, GADD45A, GDF15, GRB2, ID1, IFNAR1,IFNAR2, IGFBP3, IL1B, IL6, ING2, KRAS, LTBR, MCL1, MET, MUC1, MXI1, NOTCH1,NQO1, ODC1, PPARD, PSME3, PTEN, PTGS2, PTPN1, PTPRE, RASSF1, RUNX1, SMAD3, SPHK1, STAT2, TGFBR2, THBS1, TPR, VEGFA, ZEB2,ZNF148	62	yes
Cancer	tumorigenesis of epithelial tumor	4.86E-05	Decreased	-2.022	AHR,AKT1,ATF5, BBC3, BIRC5,CABLES1, CBX7, CCND1,CCND3,CCNDBP1, CDKN1B,CDKN2C, CTLA4, DDB2, EGR1, ENG,ERRFI1,FBXO4, FOXO3, GADD45A, GDF15, GRB2,IGFBP3, IL6,KRAS, LTBR,MAP2K1, MET, MUC1, MXI1, NOTCH1, NQO1, ODC1, PPARD, PSME3, PTEN, PTGS2, PTPRE, RASSF1,SMAD3, SPHK1, TGFBR2, THBS1, THBS2, TNFRSF1A, TPR, VEGFA	47	yes
Gene Expression	binding of DNA	6.22E-05	Decreased	-2.123	ABL1, ADRB2, AHR, AKT1, ALYREF, APEX1, ATM, BMPR1A, BTAF1, BTK, CALM1 (includes others), CBFB, CCND1, CEBPB, CEBPD, CHUK, CTLA4, DDB2, DDIT3, DMAP1, EGR1, EPAS1, EPOR, ETS1, ETS2, FGF13, FGF2, FN1, FOSL1, FOXO3, FYB, GHR,HBEGF, HEY1,HEY2,HIF1A,HIPK2, HMGB2, HSPA1A/HSPA1B, ID1,ID2, IER3, IFNAR1,IGFBP3, IL1B, IL6, IL8, ING4,IP6K2, IRF9,ITGA5, JUND, JUP, KLF13, KLHDC2, KRAS, LIF, LPL, LTBR, LYN, MAP2K1, NCL, NFIC, NFKBIE, NKX2-5, NME1, NOTCH1, NR5A2, PAX3, PHB, PNPT1, POLG, PPARD, PPARGC1A, PSME3, PTEN, PTPN1, RASSF1, RGCC, RUNX1, RXRB, SMAD3, SP1, SP100, TFAP2A, TFDP1, TFF3, TGFA, TNFRSF1A, TRIB3, TSC22D3, UBE2N, UCN, UCN2, VEGFA, YWHAB, YWHAG	97	no
Cellular Growth and Proliferation	proliferation of connective tissue cells	8.24E-05	Decreased	-2.923	ABL1, ACTB, AHR, AKAP12, AKT1, ATF3, ATF4, ATM, BMPR1A, CBX2, CBX7, CCND1, CCND3, CCNE1, CCNG2, CD44, CDK6, CDKN1B, CEBPB, CHUK, CIRBP, CITED2, CSK, CTNNB1, CTSL2, DNM1L, DUSP1, EDNRB, EFNA1, FEN1, FGF13, FGF2,FGFR3, FN1, FNDC3B, FOSL1, GADD45A, GHR,GRB2, GRN, HBEGF, HIF1A,HMMR,HSPA1A/HSPA1B, HTR2B, ICMT,ID2, IFNAR1,IGFBP3, IGFBP4,IGFBP5, IL1B, IL6, IL8, IP6K2, ITGA5,JUND, JUP, KLF10, KRAS, LDHA, LIF, LIMA1, LRP5, MAP2K1, MAP2K3, MAP3K5, MCM8, MET,NOTCH1,NOTCH2, PA2G4, PHC2, PLAT, PPARD, PPAT, PSME3, PTEN, PTGS2, PTPN1, RAPGEF1, RUNX1, SAFB, SERTAD1, SKP2, SMAD3, SMAD6, SNAI2, SPHK1, SPRY2, STARD10, STC1, TGFA, TGFBR2, TGIF1, TNFRSF12A, TNFRSF1A, TPR, TXNIP, UBE2C	100	yes
Cancer	tumorigenesis of mammary tumor	1.04E-04	Decreased	-2.318	AKT1, CCND1, CDC25B, CHUK, CTLA4, CTNNB1, FBXO4, GADD45A, KRAS, MET, MUC1, PTEN, PTGS2, PTPN1, PTPRE, TGFA, TGFBR2, THBS1	18	yes
Reproductive System Disease	tumorigenesis of mammary tumor	1.04E-04	Decreased	-2.318	AKT1, CCND1, CDC25B, CHUK, CTLA4, CTNNB1, FBXO4, GADD45A, KRAS, MET, MUC1, PTEN, PTGS2, PTPN1, PTPRE, TGFA, TGFBR2, THBS1	18	yes
Cancer	growth of mammary tumor	1.54E-04	Decreased	-2.178	ABL1, AKT1, ATM, CTLA4, GADD45A, HIF1A, IGFBP5, IL12A, KRAS, PTEN, PTGS2	11	yes
Gene Expression	binding of protein binding site	1.54E-04	Decreased	-2.635	AHR, AKT1,APEX1, ATM,BMPR1A, BTK, CBFB, CCND1, CEBPB, CEBPD, CHUK, DDB2, DDIT3, EGR1, EPAS1, ETS1,ETS2, FGF2, FN1, FOXO3, GHR, HBEGF, HEY1,HEY2,HSPA1A/HSPA1B, ID1, ID2, IER3, IGFBP3, IL1B, IL6, IL8, ING4, IP6K2, JUP, KLF13, KRAS, LIF, LTBR, MAP2K1, NFIC, NOTCH1, NR5A2, PNPT1, PTEN, RGCC, RUNX1, SMAD3, SP1, SP100, TFAP2A, TFDP1, TFF3, TGFA, TNFRSF1A, TRIB3, VEGFA	57	no
Cancer	quantity of tumor	1.91E-04	Decreased	-2.081	AKT1, CCND1, CDKN1B, CDKN2C, CTNNB1, EDNRB, GJB1, HIF1A, HMMR, HPGD, IFNGR1, KIT, KLF6, KRAS, MAP2K1, MET, MST1, NQO1, ODC1, PPARD, PTEN, RUNX1, SPHK1, STK3, TGFA, TGFBR2, TP53INP1	27	no
Cancer	tumorigenesis of carcinoma	2.50E-04	Decreased	-2.758	AHR, AKT1, BIRC5, CABLES1, CBX7, CCND3, CCNDBP1, CDKN1B, CDKN2C, CTLA4, DDB2, EGR1, ERRFI1, FBXO4, GADD45A, GDF15, GRB2, IGFBP3, KRAS, LTBR, MET, MUC1, MXI1, NOTCH1, NQO1, ODC1, PPARD, PSME3, PTEN, PTGS2, PTPRE, RASSF1, SMAD3, SPHK1, TGFBR2, THBS1, TPR, VEGFA	38	yes
Developmental Disorder	runting	4.15E-04	Increased	2.236	IL6, INSIG1, INSIG2, NFIC, NLRP3, PTRH2	6	no
Cellular Movement	movement of vascular endothelial cells	5.77E-04	Decreased	-2.821	ADAMTS1, ADM, AKT1, ANXA2, CD151, CDKN1B, CYR61, EFNA1, FGF13, FGF2, FN1, FOXO3, HIF1A, HLX, HSPA5, ID1, IL8, KLF2, NRP1, PTEN, PTGS2, RTN4, SP100, SPRY4, TGFBR2, THBS1, THBS2, VEGFA	28	yes
Cardiovascular System Development and Function	movement of vascular endothelial cells	5.77E-04	Decreased	-2.821	ADAMTS1, ADM, AKT1, ANXA2, CD151, CDKN1B, CYR61, EFNA1, FGF13, FGF2, FN1, FOXO3, HIF1A, HLX, HSPA5, ID1, IL8, KLF2, NRP1, PTEN, PTGS2, RTN4, SP100, SPRY4, TGFBR2, THBS1, THBS2, VEGFA	28	yes
Cellular Movement	cell movement of endothelial cells	6.63E-04	Decreased	-2.815	ACP1, ADAMTS1, ADM, AKT1, ANGPTL4, ANXA2, ARHGAP24, CD151, CD36, CDKN1B, CEACAM1, CSPG4, CXCR4, CYR61,EFNA1, ENG, ENPP2, FGF13, FGF2, FN1,FOXO3, GRN, HAS3, HEY1, HIF1A, HLX, HMMR, HSPA5, ID1, IGFBP3, IL1B, IL8, ITGA3, ITGA4, KLF2, MAP2K1, MAP2K3, MAP2K5, MARCKS, NRP1, PIM1, PRKCZ, PTEN, PTGS2, RGCC, RTN4, SDC4, SP100, SPRY4, STC1, TGFBR2, THBS1, THBS2, TIMP3, TNFRSF12A, VEGFA, WARS	57	yes

Cardiovascular System Development and Function	cell movement of endothelial cells	6.63E-04	Decreased	-2.815	ACP1, ADAMTS1, ADM, AKT1, ANGPTL4, ANXA2, ARHGAP24, CD151, CD36, CDKN1B, CEACAM1, CSPG4, CXCR4, CYR61,EFNA1, ENG, ENPP2, FGF13, FGF2, FN1, FOXO3, GRN, HAS3, HEY1, HIF1A, HLX, HMMR, HSPA5, ID1, IGFBP3, IL1B, IL8, ITGA3, ITGA4, KLF2, MAP2K1, MAP2K3, MAP2K5, MARCKS, NRP1, PIM1, PRKCZ, PTEN, PTGS2, RGCC, RTN4, SDC4, SP100, SPRY4, STC1, TGFBR2, THBS1, THBS2, TIMP3, TNFRSF12A, VEGFA, WARS	57	yes
Cell Cycle	cell cycle progression of tumor cell lines	7.70E-04	Decreased	-2.320	ABL1, AHR, AKT1, APBB3, BCL6, BIRC5, CCND1, CCND3, CCNE1, CCNG2, CD44, CDC25B, CDC25C, CDK6, CDKN1B, CDKN2C, CEBPB, CHUK, CSNK2A2, DIABLO, DUSP1, EGR1, FOXO3, FRMD6, HBEGF, HIF1A, HPGD, IER3, IGFBP3, IL6, KRAS, LIF, LYN, MAFB, NOTCH1, PHB, PTEN, RASSF1, SLFN11, SRSF2, XBP1	41	yes
Post-Translational Modification	activation of protein	8.42E-04	Decreased	-2.195	ADM, AKT1, AMD1, BBC3, BID, CCNE1, FABP5, FGF2, IGFBP3, IL1B, IL6, KIT, LIF, ODC1, PMAIP1, PTEN, SPHK1, VEGFA	18	no
Cancer	mammary tumor	8.79E-04	Decreased	-2.430	ABL1, ACTA2, ADAMTS1, AGPAT6, AKAP12, AKT1, ALDH1A3, ALYREF, ANAPC13, ANG, ARHGAP19, ARHGDIA, ARHGEF2, ARNTL, ARRB1, ATF3, ATM, BEX1, BEX2, BHLHE40, BIRC5, C14orf159, C1QBP, CALM1 (includes others), CCNB2, CCND1, CCNE1, CCNE2, CD44, CDC25B, CDKN1B, CDT1, CEBPB, CEBPD, CENPA, CHD7, CHUK, CLDN1, CLTCL1, COL4A3BP, COPS2, CTDSPL, CTLA4, CTNNB1, CYR61, DDIT4, DUSP1, EGLN1, EGR1, EIF1, EIF5, ELOVL6, ENG, EPOR, ERI2, FAM107B, FAM198B, FAM49B, FAM72D, FASN, FBXO4, FBXW4, FBXW7, FEN1, FN1, FOXO3, FSTL3, FURIN, GADD45A, GRN, H3F3A/H3F3B, HBEGF, HBP1, HEY2, HIF1A, HK2, HMMR, HNRNPA1, HSPA5, HSPB8, IDH3A, IER3, IGFBP3, IGFBP5, IL12A, IL6, ING4, JUND, KIT, KLF10, KLF11, KLF6, KRAS, LETMD1, LIMA1, MCL1, MCM10, MET, MKKS, MT1F, MT1G, MT2A, MUC1, MUM1, MYBBP1A, MYCBP2, MYLK, NEK2, NME1, NOL12, NOP16, NOTCH1, NOTCH2, NQO1, NUP93, ODC1, PAK1IP1, PDK4, PHB, PKD1L2, PMAIP1, PPFIA1, PRAME, PRIM1, PSMD12, PTEN, PTGS2, PTPN1, PTPRE, QKI, RAD23B, RANBP1, RASSF1, RBM4B, RGS2, RPL6, RPS24, RRP12, RUNX1, SAFB2, SCHIP1, SDC1, SIDT2, SKP2, SLC27A1, SLC2A1, SLC9A3R1, SMAD3, SNAI2, SQLE, SRP19, SRPK1, SSPN, SV2A, TAF1D, TGFA, TGFBR2, THBS1, TPD52, TUBB2A, TUBB4B, TUBG1, UBE2C, UBE2G2, UHRF1, VEGFA, WWTR1, XRCC3, YPEL5, ZBTB20, ZNF318, ZNF703, ZYX	173	yes
Cell Death and Survival	neuronal cell death	9.93E-04	Decreased	-2.015	ABL1, ADRBK1, AGRN, AKT1, ATF3, ATM, ATXN3, BAG5, BBC3, BID, BIRC5, BNIP3, CD200, CDC25A, CDK6, CDKN1B, CHUK, CTNNB1, CTSL2, DDIT3, DIABLO, DNAJB2, DUSP1, DUSP6, E2F3, E2F4, EGLN1, EGR1, EHD4, EPOR, ETS2, FAIM, FBXW7, FGF2, FN1, FOXO3, FZD2, GAB2, GCLM, GDF15, HBEGF, HIF1A, HIPK2, HK2, HMGB2, HRK, HSPA5, HSPH1, ID2, IDE, IGFBP3, IL1B, IL6, IL8, ITGA5, KLF6, KRAS, LDHA, LIF, MAP2K1, MAP2K3, MAP3K12, MAP3K5, MBP, MEF2C, MEF2D, MET, MXD3, NCS1, NQO1, NRTN, P2RX7, PEX11B, PHB, PLAT, PLP1, PPARGC1A, PRNP, PSME3, PTEN, PTGS2, RASD2, RGS10, RNF19A, RUNX1, SH3RF1, SIAH1, SLC2A1, SOX4, SP1, SRPK2, ST8SIA1, STAM, STAMBP, TFB1M, TFDP1, TGFA, TMEM158, TNFRSF1A, TNFRSF21, TRIM2, UBE2V2, UCN, VEGFA, WFS1, YWHAB	106	no
Infectious Disease	Viral Infection	1.45E-03	Decreased	-2.495	ABCE1, ABL1, ABTB1, ACTB, ACTN1, ACTR2, ADRBK1, AFG3L1P, AHCTF1, AHR, AKT1, ALKBH8, ANXA2, AP1B1, APOBEC3F, ARNTL, ARRB1, ASXL2, ATF4, ATM, ATP6V0A4, BBC3, BCL9, BICD2, C15orf52, C1R, C1S, C20orf24, C3AR1, C4orf33, C6orf48, CALCOCO1, CAPN3, CBLB, CD200, CD44, CDKN1B, CEBPD, CHD1, CHMP1B, CHORDC1, CHST6, CHUK, CLTCL1, CNST, COASY, CTSL2, CXCR4, CYP2U1, DCBLD1, DCLK1, DDIT3, DDX3X, DHRS2, DHX15, DHX33, DHX58, DMAP1, DNAJA1, DNAJB2, DTX3, DUSP1, EGR1, EIF2C2, EIF2S1, EIF4A3, ENC1, EPAS1, EPOR, EPS15, ERI2, ETS2, EXOSC10, EXOSC3, F12, FN1, FOXF2, FURIN, FXR1, G3BP1, G3BP2, GAB2, GABARAPL1, GHR, GPT2, GRB2, GRK5, H3F3A/H3F3B, HIST1H2AC, HIST1H2BD, HIST2H2AA3/HIST2H2AA4, HLX, HMGCS1, HMGN2, HNRPDL, HPGD, HSPA5, HSPA6, HYAL2, IER3, IFI35, IFIT2, IFNAR1, IFNAR2, IFNGR1, IL12A, IL1B, IL6, IL8, IMPDH1, IRF4, IRF9, IRS2, ISG20, ISG20L2, ITGA3, ITGA4, ITGA5, ITK, ITPKA, KLF2, KLHDC2, LAMP2, LEF1, LIMK1, LPL, MAP2K1, MAP2K3, MAP2K5, MAP3K12, MAT2A, MED31, MGAT1, MGLL, MND1, MPHOSPH6, MR1, MRPL44, MT2A, MYOF, NCL, NOP56, NRP1, NTHL1, NUP155, OPTN, OSBPL6, OTUD1, P2RX7, PACSIN3, PARP9, PDE3B, PDE7B, PDXK, PDZD8, PGRMC2, PIK3CB, PKD1L2, PLAT, PMM1, POLG, POU3F1, PPARGC1A, PPP1R15A, PPP2R2A, PPP2R5E, PPP3R1, PRDM7, PRMT3, PRNP, PRSS35, PSMD12, PSMD4, PTGS2, PVR, RAB32, RAB5C, RAB9A, RABEPK, RACGAP1, RALB, RANBP1, RAPGEF1, RASSF1, RBM25, RNF144A, RNF150, RTN2, RUNX1, SAFB, SDC1, SEC14L1, SEC61G, SH2B3, SIGMAR1, SLC2A1, SLC2A3, SLC4A7, SLC9A3R1, SMAD3, SNRPA, SNRPA1, SNRPD3, SNRPF, SNX10, SNX6, SON, SOX4, SP100, SPAST, SPCS3, SPEN, SPHK1, SPRY2, SRPK1, SRPK2, SRSF2, SSR1, ST3GAL5, ST6GAL1, STAG3L1, STAT2, STIP1, SYNJ1, TCFL5, TFDP2, TFRC, TGFBR2, THOC2, TIAM2, TMC6, TMEM181, TNFRSF1A, TRAPPC8, TRMT6, TRPV2, TUBB2A, TUBB4B, TUBG1, TXNIP, UBE2C, ULK1, VEGFA, VWF, WIPF1, WWP2, XBP1, ZCCHC17, ZEB2, ZNF148, ZNF446, ZNF536, ZNF688, ZYX	254	yes
DNA Replication, Recombination, and Repair	quantity of centrosome	1.67E-03	Decreased	-2.491	CDC25B, CHMP1B, GADD45A, ID1, KIF23, LATS2, LMO4, MKS1, RASSF1, SKP2, TFDP1, TMEM67	12	yes
Cellular Assembly and Organization	quantity of centrosome	1.67E-03	Decreased	-2.491	CDC25B, CHMP1B, GADD45A, ID1, KIF23, LATS2, LMO4, MKS1, RASSF1, SKP2, TFDP1, TMEM67	12	no
Cellular Development	proliferation of ovarian cancer cell lines	1.79E-03	Decreased	-2.143	AKT1, ARHGEF2, ATF3, CCND1, CD44, CXCR4, DAB2, E2F3, FOSL1, FOXO3, GDF15, GRN, HAS2, HAS3, HBEGF, IL6, KLF2, NUMA1, SERTAD1, SKP2, TGFA, TGFBR2	22	yes
Cellular Growth and Proliferation	proliferation of ovarian cancer cell lines	1.79E-03	Decreased	-2.143	AKT1, ARHGEF2, ATF3, CCND1, CD44, CXCR4, DAB2, E2F3, FOSL1, FOXO3, GDF15, GRN, HAS2, HAS3, HBEGF, IL6, KLF2, NUMA1, SERTAD1, SKP2, TGFA, TGFBR2	22	yes
Developmental Disorder	hypoplasia of organ	1.80E-03	Increased	2.376	ABL1, ADRBK1, AHR, AKT1, ALDH1A3, ARHGDIA, ARID5B, ARRB1, ATF4, BAG3, BCL6, CBY1, CCND3, CCNE1, CCNE2, CDK6, CDKN1B, CTLA4, DHCR7, E2F3, E2F4, ECE2, EPOR, ETS1, FGF2, FGFRL1, GAS1, HBEGF, HLX, IFNGR1,ITGA3,KRAS, LIF, LYN, MAFF, MAP2K1, MET, NFAT5, NKX2-5, NKX3-1, NKX3-2, NOTCH2, PKNOX1, PRRX1, PSMC3IP, RASSF2, RDH10, RUNX1, SLC20A1, SMAD3, SOX4, SPEN, TDG, VEGFA, WIPF1, XBP1	56	no
Cancer	bone marrow cancer	2.53E-03	Increased	2.200	ABL1, ACTG1, AHI1, AKT1, ARID4B, ARID5B, ATM, BCL6, BCOR, BIRC5, C12orf5, CBFB, CCND1, CDC25A, CHUK, CTNNB1, DLEU1, DLEU2, DNM1L, E2F3, E2F4, ENC1, EPOR, FAIM3, FBXL2, FBXW7, FOXO3, GHR, HLX, HSPA1A/HSPA1B, ID4, IFNAR1, IFNAR2, IL1B, IL6, IL8, IMPDH1, IRF4, ITGA3, ITGA4, ITGA5, KIT, KRAS, LDHA, LYN, MSMO1, NOTCH1, NQO1, PDE3B, PDE7B, PDE9A, PPAT, PRIM1, PTEN, RBM15, RPL6, RPS24, RUNX1, RXRB, SNRPD3, SOX4, SRSF2, TUBB2A, TUBB4B, TUBG1, U2AF1, XRCC3	67	no
Hematological Disease	bone marrow cancer	2.53E-03	Increased	2.200	ABL1, ACTG1, AHI1, AKT1, ARID4B, ARID5B, ATM, BCL6, BCOR, BIRC5, C12orf5, CBFB, CCND1, CDC25A, CHUK, CTNNB1, DLEU1, DLEU2, DNM1L, E2F3, E2F4, ENC1, EPOR, FAIM3, FBXL2, FBXW7, FOXO3, GHR, HLX, HSPA1A/HSPA1B, ID4, IFNAR1, IFNAR2, IL1B, IL6, IL8, IMPDH1, IRF4, ITGA3, ITGA4, ITGA5, KIT, KRAS, LDHA, LYN, MSMO1, NOTCH1, NQO1, PDE3B, PDE7B, PDE9A, PPAT, PRIM1, PTEN, RBM15, RPL6, RPS24, RUNX1, RXRB, SNRPD3, SOX4, SRSF2, TUBB2A, TUBB4B, TUBG1, U2AF1, XRCC3	67	no
Cell Cycle	S phase of fibroblast cell lines	2.56E-03	Decreased	-3.130	ABL1, BID, CCND1, CCNE1, CDC25A, CDKN1B, DDX3X, E2F3, E2F4, GADD45A, GAS1, SKP2, TFDP1	13	yes
Connective Tissue Development and Function	S phase of fibroblast cell lines	2.56E-03	Decreased	-3.130	ABL1, BID, CCND1, CCNE1, CDC25A, CDKN1B, DDX3X, E2F3, E2F4, GADD45A, GAS1, SKP2, TFDP1	13	yes
Gene Expression	expression of gene	2.69E-03	Increased	2.032	ANK3, ARID4B, CD44, CITED1, CITED2, CTNNB1, FGF2, HINFP, ID2, IL1B, IL6, ITGA3, KIT, LEF1, MEF2C, MET, NKX2-5, PLP1, PLSCR1, POU3F1, QKI, RBM4B, SPRY2, SRPK2, TFAP2A, TLE1, VEGFA	27	no
Cellular Movement	migration of endothelial cells	2.72E-03	Decreased	-2.282	ACP1, ADAMTS1, ADM, AKT1, ANGPTL4, ANXA2, ARHGAP24, CD151, CDKN1B, CYR61, EFNA1, ENG, FGF13, FGF2, FN1, FOXO3, GRN, HAS3, HEY1, HIF1A, HLX, HMMR, HSPA5, ID1, IGFBP3, IL1B, IL8, ITGA3, ITGA4, KLF2, MAP2K1, MAP2K3, MARCKS, NRP1, PIM1, PRKCZ, PTEN, PTGS2, RGCC, RTN4, SDC4, SP100, SPRY4, STC1, TGFBR2, THBS1, TIMP3, TNFRSF12A, VEGFA, WARS	50	yes
Cardiovascular System Development and Function	migration of endothelial cells	2.72E-03	Decreased	-2.282	ACP1, ADAMTS1, ADM, AKT1, ANGPTL4, ANXA2, ARHGAP24, CD151, CDKN1B, CYR61, EFNA1, ENG, FGF13, FGF2, FN1, FOXO3, GRN, HAS3, HEY1, HIF1A, HLX, HMMR, HSPA5, ID1, IGFBP3, IL1B, IL8, ITGA3, ITGA4, KLF2, MAP2K1, MAP2K3, MARCKS, NRP1, PIM1, PRKCZ, PTEN, PTGS2, RGCC, RTN4, SDC4, SP100, SPRY4, STC1, TGFBR2, THBS1, TIMP3, TNFRSF12A, VEGFA, WARS	50	yes
Cellular Growth and Proliferation	proliferation of epithelial cells	2.80E-03	Decreased	-3.131	AKT1, ASIP, BMPR1A, CCND1, CCND3, CCNG2, CDC25A, CDC25B, CDK6, CDKN1B, CDKN2C, CEBPB, CHUK, CTNNB1, CTSL2, DLX5, EDNRB, EFNA1, FGF2, FGFR3, FN1, FOXF2, GAB2, GAS1, GDF15, GRN, HBEGF, ID1, ID2, IGFBP4, IL1B, IL6, IL8, ITGA3, JUP, KIT, KLF10, KRAS, LTBR, MAP2K1, MAP2K5, MAP3K5, MST1, NFIB, NKX3-1, NME1, NOTCH1, PAX3, POU3F2, PPARD, PTEN, PTGS2, PTK6, RRAS, RUNX1, SKP2, SMAD3, SNAI2, SPHK1, STMN1, TGFA, TGFBR2, TNFRSF1A, VEGFA	64	yes
Cancer	hyperplasia of breast	2.97E-03	Decreased	-2.170	CCND1, CDC25B, CDKN2C, CEBPB, CSNK2A2, CTNNB1, ING4, PTGS2, PTPRE, SDC1, TGFA	11	yes
Cell Cycle	entry into interphase of fibroblast cell lines	3.33E-03	Decreased	-2.449	ABL1, AKT1, CCND1, CDC25A, DDX3X, E2F3, GAS1, SKP2	8	yes
Cancer	hyperplasia of exocrine gland	3.33E-03	Decreased	-2.135	CCND1, CDKN2C, CSNK2A2, CTNNB1, CTSL2, PTGS2, PTPRE, SDC1	8	no

Table S4. Downstream effect analysis by IPA software of genes significantly modulated only by the association of TRAIL with AZD6244

Results shown here are based on the set of genes identified by the areas highlighted in fuchsia in **Fig. 4.12.**
See supplementary methods for the meaning of the p values and of the z score statistics.

Category	Functions Annotation	p-Value	Predicted Activation	Activation z-score	Molecules	# Molecules	Data shown in Fig. S5b
Cell Death and Survival	apoptosis of carcinoma cell lines	1.58E-04	Increased	2.907	ABCC1, AKT3, BAP1, BAX, BCL2, BCL2L11, BIRC5, CASP1, CCND1, CDKN1B, CDKN2C, DDIT3, DUSP1, ETS2, FADD, FAS, FBXL2, FGF2, FOXO3, HIF1A, HMGA1, ID3, IGFBP3, ING1, KIAA1967, KLF2, KRAS, KRT18, MAP3K7, MCL1, NFKBIA, PMAIP1, PMEPA1, PRKAR1A, PTGS2, RABGGTB, RARB, RBM4B, REPS2, RRM1, SPP1, SPRY2, SRC, TLR4, TNFSF10	45	yes
Cell Death and Survival	cell death of carcinoma cell lines	6.35E-05	Increased	2.396	ABCC1, AKT3, BAP1, BAX, BCL2, BCL2L11, BIRC5, CASP1, CCND1, CDKN1B, CDKN2C, CFH, DDIT3, DUSP1, ETS2, FADD, FAS, FBXL2, FGF2, FOXO3, GAB1, HIF1A, HK1, HMGA1, ID3, IGFBP3, ING1, JUN, KIAA1967, KLF2, KRAS, KRT18, MAP3K5, MAP3K7, MCL1, MYC, NEK2, NFKBIA, NQO1, PMAIP1, PMEPA1, PRKAR1A, PTGS2, RABGGTB, RARB, RBM4B, REPS2, RRM1, SPP1, SPRY2, SRC, TLR4, TNFSF10, TUBB3	54	yes
Cell Death and Survival	apoptosis of sarcoma cells	4.03E-04	Increased	2.308	ABL1, BAX, BCL2, BCL2L11, BTK, CASP1, CDK6, CDKN1B, CTLA4, FAS, FBXL2, HIF1A, KDR, LPAR1, NFKBIA, PIK3CD, PNP, PTEN, RARA, RUNX1, TNFSF10, TNFSF13B, TRIB1	23	yes
Tumor Morphology	apoptosis of sarcoma cells	4.03E-04	Increased	2.308	ABL1, BAX, BCL2, BCL2L11, BTK, CASP1, CDK6, CDKN1B, CTLA4, FAS, FBXL2, HIF1A, KDR, LPAR1, NFKBIA, PIK3CD, PNP, PTEN, RARA, RUNX1, TNFSF10, TNFSF13B, TRIB1	23	yes
Cell Death and Survival	apoptosis of leukemia cells	3.28E-04	Increased	2.153	ABL1, BAX, BCL2, BCL2L11, BTK, CASP1, CDK6, CDKN1B, CTLA4, FAS, FBXL2, HIF1A, LPAR1, NFKBIA, PIK3CD, PNP, PTEN, RARA, RUNX1, TNFSF10, TNFSF13B, TRIB1	22	yes
Tumor Morphology	apoptosis of leukemia cells	3.28E-04	Increased	2.153	ABL1, BAX, BCL2, BCL2L11, BTK, CASP1, CDK6, CDKN1B, CTLA4, FAS, FBXL2, HIF1A, LPAR1, NFKBIA, PIK3CD, PNP, PTEN, RARA, RUNX1, TNFSF10, TNFSF13B, TRIB1	22	yes
Cell Death and Survival	cell death of sarcoma cells	9.14E-04	Increased	2.082	ABL1, BAX, BCL2, BCL2L11, BTK, CASP1, CDK6, CDKN1B, CTLA4, FAS, FBXL2, HIF1A, HMOX1, KDR, LPAR1, NFKBIA, PIK3CD, PNP, PTEN, RARA, RUNX1, TNFSF10, TNFSF13B, TRIB1	24	yes
Tumor Morphology	cell death of sarcoma cells	9.14E-04	Increased	2.082	ABL1, BAX, BCL2, BCL2L11, BTK, CASP1, CDK6, CDKN1B, CTLA4, FAS, FBXL2, HIF1A, HMOX1, KDR, LPAR1, NFKBIA, PIK3CD, PNP, PTEN, RARA, RUNX1, TNFSF10, TNFSF13B, TRIB1	24	yes
Organismal Survival	organismal death	4.14E-07	Increased	2.020	ABCA1, ABCC1, ABCC4, ABI1, ABL1, ABL2, ABR, ACACA, ACSS1, ACVR1, ADAM19, ADAMTS1, ADCY3, ADD1, ADK, ADM, ADORA2B, ADRBK1, AFF1, AHR, AIM2, AKAP12, AKT3, ALDH1A3, ALX1, AMACR, AMPH, ANGPT1, ANGPT2, ANGPTL4, ANK3, ANO1, ANP32B, ANTXR2, ANXA1, AP2M1, APH1A, APOE, AQP11, ARAP3, ARID5B, ARNT, ASPA, ATF6, ATM, ATP1B1, ATP2A2, ATP2B1, ATP5J2, ATXN3, AURKB, BAG3, BAP1, BAX, BBS4, BCL2, BCL2L11, BCL3, BDNF, BECN1, BID, BIRC5, BMF, BMI1, BMP1, BMPR1A, BRCA1, C1GALT1, C3AR1, CA14, CADPS2, CALR, CASP1, CAV1, CBL, CBY1, CCDC86, CCNB2, CCND1, CCND2, CCR1, CD200, CD36, CD59, CD74, CDC25A, CDK5, CDK5R1, CDK6, CDKN1A, CDKN1B, CDKN2C, CEBPB, CEBPD, CFB, CFH, CHKA, CITED1, CKS1B, CLCN7, CLDN1, CLIC4, CLN3, CNTNAP1, COL5A2, COMMD1, COPS8, CPB2, CPOX, CR2, CREB3L2, CREB5, CRKL, CSDA, CSRNP1, CTC1, CTGF, CTLA4, CTNNBIP1, CTSF, CXCR4, DAB2, DBI, DCC, DDAH1, DDB2, DEFB4A/DEFB4B, DGCR8, DHCR7, DHX58, DICER1, DISP1, DKC1, DKK1, DLL3, DLX1, DMRT2, DNAJB4, DNAJC5, DNM3, DSP, DUSP1, DVL2, E2F2, E2F3, E2F5, ECE2, EDNRB, EEF1E1, EFNB2, EGLN1, EGR2, EGR3, EHD4, EIF2C2, EIF4A1, ELK3, ENPP2, EOMES, EPAS1, EPOR, ERCC5, ERRFI1, ESPL1, ETS1, ETS2, ETV1, EXTL3, F2R, F2RL1, FABP3, FADD, FAM20C, FANCL, FAS, FASN, FBN2, FBXO45, FCER1G, FEN1, FGF2, FGFR3, FGFRL1, FKBP4, FLI1, FNDC3B, FOS, FOSL1, FOXD3, FOXM1, FOXO1, FOXO3, FST, FSTL1, FTH1, FURIN, FYN, GAB1, GABPB1, GAS1, GATAD2A, GCLM, GHR, GJB1, GLCE, GLI2, GNA12, GNA13, GNAL, GNL3, GRIP1, GSTK1, GSTM1, H2AFX, HAS2, HAX1, HBEGF, HDAC7, HES1, HEXA, HEY1, HEY2, HHAT, HHEX, HIF1A, HIP1, HIPK1, HIPK2, HIST2H2AA3/HIST2H2AA4, HK2, HMBS, HMGA2, HMGCL, HMGCR, HMOX1, HNRNPD, HOXA5, HOXB2, HOXC13, HOXC4, HOXD11, HOXD13, HPGD, HS3ST1, HSP90AB1, HSPB8, HTR7, HTRA2, ICAM1, ID1, ID2, ID3, IDH1, IDS, IFNAR1, IFNAR2, IFT122, IGF2R, IGFBP3, IGFBP5, IL11RA, IL12A, IL1B, IL27RA, IL8, INCENP, ING1, ING4, INSIG2, IP6K2, IRAK1, IRF5, IRF9, IRS2, ITGA4, ITGA6, ITGB3, ITPKB, ITPR2, ITPR3, JAM3, JPH1, JUN, KAT2A, KCNAB1, KCNQ2, KDR, KIAA0586, KIDINS220, KIT, KLF2, KLF4, KLF9, KRAS, KRR1, LAMA2, LAMA4, LAMC1, LAMTOR2, LDB1, LEF1, LHX6, LIF, LIMK1, LIMS1, LMO4, LOX, LPAR1, LPL, LRP5, LRP8, LTBR, LYN, MACF1, MAF, MAFF, MAFG, MAL, MAN2A2, MAP2K1, MAP2K3, MAP2K5, MAP3K1, MAP3K12, MAP3K3, MAP3K7, MAPKAPK5, MARCKS, MARCKSL1, MCL1, MCM10, MCM2, MCOLN1, MED23, MEF2A, MEF2C, MERTK, MESP1, MGAT1, MITF, MMP16, MMP9, MNS1, MNT, MSN, MT1E, MTHFD2, MTHFR, MTSS1, MUT, MX1, MYB, MYC, NAT1, NDRG1, NFIA, NFIB, NFKBIA, NKX2-5, NLGN2, NLRP3, NOV, NPC1, NQO1, NR2F1, NR3C1, NR4A2, NR5A2, NRCAM, NRP1, NRXN2, NUDT1, NUSAP1, OCRL, OPHN1, OTX1, OVOL2, PAK4, PAPPA, PARP2, PAX3, PAXIP1, PCID2, PCSK1, PDE4B, PELI1, PER2, PES1, PEX11B, PEX2, PEX5, PHB, PHC2, PKDCC, PKNOX1, PLAT, PLCB4, PLCL1, PMS2, PNN, PNPLA8, PNPT1, POU3F1, POU3F2, PPAP2B, PPARGC1A, PPIF, PPIG, PPP1R14C, PPP1R15A, PPP1R3C, PPP1R9A, PRDX1, PRKAR1A, PRKD1, PRMT1, PRNP, PRRX1, PSMC2, PSMD4, PTEN, PTGES, PTGS2, PTK2, PTPN12, PVRL3, RAB27A, RAC2, RAD54B, RAD9A, RAPGEF1, RARA, RARB, RASA3, RASSF2, RBBP8, RBMS1, REV3L, RGMA, RHBDF2, RHEBL1, RIF1, RIMS2, RNASEL, RPL29, RPL6, RTN4, RUNX1, RUNX2, RXRA, RYK, SATB1, SCNN1A, SDC4, SEMA3A, SFRP1, SGCD, SHB, SHISA2, SIAH1, SIK3, SIM2, SLC11A2, SLC17A7, SLC20A1, SLC25A19, SLC25A37, SLC2A1, SLC2A3, SLC2A8, SLC3A2, SLC7A1, SMARCAL1, SMPD1, SMTN, SNAI2, SNAP23, SNX27, SOD2, SOX4, SOX6, SPEN, SPP1, SPRED1, SPRED2, SPRY1, SPRY2, SPRY4, SRC, SSBP2, ST8SIA1, STAM, STARD13, STAT2, STIM1, STIM2, STK4, STXBP1, STXBP5, SV2B, SYK, SYNJ1, TACC3, TAF4, TARBP2, TBX2, TCF4, TCF7L2, TEAD2, TERF1, TFAP2A, TFAP2C, TFB1M, TFDP1, TGFA, TGFBR2, TGFBR3, TGIF1, THBS1, THBS2, TIMP2, TIMP3, TIRAP, TJP2, TK1, TLR4, TMOD1, TNFRSF1A, TNFRSF1B, TNFSF10, TNFSF13B, TP53BP1, TP53INP1, TPH2, TPP2, TRAF3IP2, TRAFD1, TRIM63, TRO, TRPV2, TRRAP, TWIST1, TXNIP, UBD, UBR3, UHRF1, ULK1, UPF2, VAMP2, VASP, VDR, VEGFA, VGF, WASL, XBP1, XPC, ZBTB20, ZEB2, ZFP36, ZFP57, ZNF259	561	yes

Category	Functions Annotation	p-Value	Predicted Activation	Activation z-score	Molecules	# Molecules	Data shown in Fig. S5b
Cellular Movement	migration of connective tissue cells	1.60E-05	Decreased	-4.133	ABL1, ABL2, ANGPT1, APOE, ARID5B, CAV1, CBL, CCL2, CCNA2, CCND1, CDKN1A, CDKN1B, CTGF, CYTH2, F2R, FGF2, FOSL1, GNA12, GNA13, HBEGF, ITGB3, LIMA1, MAP2K1, MAP3K1, MRAS, MYC, PLAUR, PRKAR1A, PRKCE, PTK2, PTPRA, RAC2, RAP2A, RAPGEF1, SCHIP1, SDC4, SEMA3A, SMO, SNX17, SPP1, SRC, STMN1, TGFBR2, THBS1, TIMP2, VASP, ZFAND5, ZYX	48	yes
Cell Cycle	entry into interphase	2.63E-04	Decreased	-3.900	ABL1, ATM, BHLHE40, CCND1, CDC25A, CDC6, CDKN1A, CDKN1B, CDKN2C, CEBPB, CTLA4, E2F2, E2F3, E2F5, EGR1, FGF2, FOS, FOXM1, GAS1, GTF2I, HBEGF, HINFP, HMGA1, HMOX1, ID2, ID3, IL1B, ILKAP, JUN, KLF4, KRAS, MCM10, MEIS2, MYC, PAM16, PTPRA, RUNX2, SOD2, SRC, ST8SIA1, TFDP1, UHRF1, VPS18	43	yes
Cell Cycle	entry into S phase	2.60E-04	Decreased	-3.869	ABL1, ATM, BHLHE40, CCND1, CDC25A, CDC6, CDKN1A, CDKN1B, CDKN2C, CEBPB, CTLA4, E2F2, E2F3, E2F5, FGF2, FOS, FOXM1, GAS1, GTF2I, HBEGF, HINFP, HMGA1, HMOX1, ID2, ID3, IL1B, ILKAP, JUN, KLF4, KRAS, MCM10, MEIS2, MYC, PAM16, SOD2, SRC, ST8SIA1, TFDP1, UHRF1, VPS18	40	yes
Cellular Movement	migration of fibroblasts	3.43E-06	Decreased	-3.750	ABL1, ABL2, ANGPT1, APOE, ARID5B, CAV1, CCL2, CCNA2, CCND1, CDKN1A, CDKN1B, F2R, FGF2, GNA12, GNA13, HBEGF, ITGB3, MAP2K1, MAP3K1, MRAS, MYC, PLAUR, PRKAR1A, PRKCE, PTK2, PTPRA, RAC2, RAP2A, RAPGEF1, SCHIP1, SDC4, SMO, SNX17, SPP1, STMN1, TGFBR2, THBS1, TIMP2, VASP, ZFAND5, ZYX	41	yes
Connective Tissue Development and Function	migration of fibroblasts	3.43E-06	Decreased	-3.750	ABL1, ABL2, ANGPT1, APOE, ARID5B, CAV1, CCL2, CCNA2, CCND1, CDKN1A, CDKN1B, F2R, FGF2, GNA12, GNA13, HBEGF, ITGB3, MAP2K1, MAP3K1, MRAS, MYC, PLAUR, PRKAR1A, PRKCE, PTK2, PTPRA, RAC2, RAP2A, RAPGEF1, SCHIP1, SDC4, SMO, SNX17, SPP1, STMN1, TGFBR2, THBS1, TIMP2, VASP, ZFAND5, ZYX	41	yes
Cellular Movement	cell movement of endothelial cells	2.80E-07	Decreased	-3.603	ADAMTS1, ADM, ANGPT1, ANGPT2, ANGPTL4, ANXA2, APOE, ARHGAP24, ARHGEF6, ARNT, BDNF, CAV1, CCL2, CD36, CDKN1B, CEACAM1, CSPG4, CTGF, CXCR4, DICER1, DKK1, EFNA1, EFNB2, ENPP2, EYA3, F2RL1, FAP, FGF13, FGF2, FOXO1, FOXO3, GAB1, HAS3, HEY1, HHEX, HIF1A, HMMR, HSP90AB1, HSPB1, ICAM1, ID1, ID3, IGF2R, IGFBP3, IL1B, IL8, ITGA4, ITGB3, KDR, KLF2, KLHL20, MAP2K1, MAP2K3, MAP2K5, MAP2K6, MAP3K7, MAPKAPK5, MARCKS, MDK, MMP9, MTSS1, MYC, NOX4, NPTX1, NRP1, PAXIP1, PGF, PLAUR, PLXNA1, PRKCE, PRKD1, PTEN, PTGS2, PTK2, PTPRZ1, RTN4, SCG2, SDC4, SEMA3A, SEMA4D, SP100, SPP1, SPRY4, SRC, STC1, TGFBR2, THBS1, THBS2, TIMP2, TIMP3, TNFRSF12A, TNFSF10, VASP, VEGFA	94	yes
Cardiovascular System Development and Function	cell movement of endothelial cells	2.80E-07	Decreased	-3.603	ADAMTS1, ADM, ANGPT1, ANGPT2, ANGPTL4, ANXA2, APOE, ARHGAP24, ARHGEF6, ARNT, BDNF, CAV1, CCL2, CD36, CDKN1B, CEACAM1, CSPG4, CTGF, CXCR4, DICER1, DKK1, EFNA1, EFNB2, ENPP2, EYA3, F2RL1, FAP, FGF13, FGF2, FOXO1, FOXO3, GAB1, HAS3, HEY1, HHEX, HIF1A, HMMR, HSP90AB1, HSPB1, ICAM1, ID1, ID3, IGF2R, IGFBP3, IL1B, IL8, ITGA4, ITGB3, KDR, KLF2, KLHL20, MAP2K1, MAP2K3, MAP2K5, MAP2K6, MAP3K7, MAPKAPK5, MARCKS, MDK, MMP9, MTSS1, MYC, NOX4, NPTX1, NRP1, PAXIP1, PGF, PLAUR, PLXNA1, PRKCE, PRKD1, PTEN, PTGS2, PTK2, PTPRZ1, RTN4, SCG2, SDC4, SEMA3A, SEMA4D, SP100, SPP1, SPRY4, SRC, STC1, TGFBR2, THBS1, THBS2, TIMP2, TIMP3, TNFRSF12A, TNFSF10, VASP, VEGFA	94	yes
Cellular Movement	chemotaxis of cells	6.97E-04	Decreased	-3.587	ABCC1, ABL1, ADRBK1, ANGPT1, ANGPT2, ANGPTL2, ANXA1, ANXA2, APOE, ARAP3, BDNF, C3AR1, CALR, CASP1, CAV1, CBL, CCL2, CCL20, CCL28, CCND1, CCR1, CD36, CD74, CDKN1A, CEACAM1, CKLF, COL4A3BP, CTGF, CTSE, CXCL13, CXCL16, CXCR4, DEFB4A/DEFB4B, DUSP6, EDNRB, EFNA1, ENPP2, EPHA2, ETV4, F2R, F2RL1, FADD, FAS, FCER1G, FCGR2A, FGF2, FYN, GAB1, GNA12, GNA13, HBEGF, HDAC6, HMGB2, HSPD1, ICAM1, IGF2R, IL16, IL1B, IL8, ITGA4, ITGA6, ITGB3, JAM3, JUN, KDR, KIT, LEF1, LIF, LIMK1, LOX, LYN, MAP3K1, MAP3K5, MDK, MMP9, MPP1, MST1, MYLK, NEDD9, NOV, NPTX1, NRCAM, NRP1, PDE4B, PGF, PIK3CD, PLAUR, PLXNB1, PREX1, PRNP, PTEN, PTGES, PTGS2, PTK2, RAC2, RAP1GAP, RGS1, ROCK1, RTN4, SCG2, SEMA3A, SEMA4D, SPHK1, SPP1, SRC, SYK, TFF3, TGFA, THBS1, THBS2, TIRAP, TLR4, TNFRSF1A, TRAF3IP2, TRIB1, TRPV2, VEGFA, VEGFB, WASL, YARS	120	yes
Cellular Assembly and Organization	formation of cellular protrusions	5.98E-09	Decreased	-3.583	ABI1, ABL1, ABL2, ACACA, ADCY3, AHR, AKAP12, ANGPTL4, ANK3, APOE, ARAP1, ARHGAP24, ARHGAP33, ATF6, ATL1, ATP7A, ATXN1, BAIAP2, BBS4, BCL2, BDNF, BECN1, BSN, BTG3, BTK, CACNA1H, CAV1, CBY1, CCL2, CDC42EP1, CDC42EP4, CDK5, CDK5R1, CDKN1A, CDKN1B, CNTNAP1, CRKL, CTGF, CTLA4, CXCR4, CYFIP1, CYTH2, DCC, DCLK1, DCX, DDAH1, DGKG, DIAPH2, DIAPH3, DICER1, DKK3, DLG4, DNM3, DZIP1L, EFHD1, EFNA1, EFNB2, ENC1, EPHA2, EPHA4, EPS15, ETV4, EVI5L, F2RL1, FEZ1, FGF13, FGF2, FNBP1L, FOS, FYN, GAB1, GDPD5, GNA12, GNA13, HMGB2, HSPB1, HTR7, IFT122, IL11RA, IL1B, IL1RAP, ITGA4, ITGA6, ITGB3, JUN, KBTBD10, KDR, KIAA1598, KIDINS220, KIT, KLF9, LAMB1, LAMC1, LIMK1, LOX, LPAR1, LRP8, LRRC16A, LYN, LZTS1, MAP2K1, MAP3K1, MAP3K7, MARCKS, MATN2, MBP, MKS1, MRAS, MSN, MT2A, MTSS1, MYO10, MYO5A, NCKIPSD, NEO1, NFIA, NFIB, NFKBIA, NPHP3, NRCAM, NRP1, NRTN, ONECUT2, OPHN1, OPTN, P2RX7, PACSIN2, PAK4, PARVB, PCM1, PHLDB2, PI4KB, PLAT, PLXNB1, PMP22, POU3F1, POU3F2, PPP1R9A, PREX1, PRICKLE2, PRKCE, PRMT1, PRNP, PTEN, PTK2, PTPRE, PTPRM, PTPRZ1, PVR, PVRL3, RAB17, RAB3IP, RAC2, RALA, RALB, RANBP1, RAP1GAP, RAP2A, RIN1, RIT1, ROCK1, ROCK2, RTN4, RUFY3, RUNX3, RYK, SDC4, SEMA3A, SEMA4D, SLC11A2, SMPD1, SMPD2, SPHK1, SRC, SRGAP2, ST8SIA1, STMN1, STX3, STXBP5, SYK, TBC1D7, TGIF1, THBS1, TIAM2, TM4SF1, TMEM67, TNC, TNFRSF12A, TNFRSF1A, TRPV4, TTC8, TWIST1, ULK1, VANGL2, VASP, VEGFA, WASL, WIPF1, WISP2, WWTR1	200	yes
Cellular Function and Maintenance	formation of cellular protrusions	5.98E-09	Decreased	-3.583	ABI1, ABL1, ABL2, ACACA, ADCY3, AHR, AKAP12, ANGPTL4, ANK3, APOE, ARAP1, ARHGAP24, ARHGAP33, ATF6, ATL1, ATP7A, ATXN1, BAIAP2, BBS4, BCL2, BDNF, BECN1, BSN, BTG3, BTK, CACNA1H, CAV1, CBY1, CCL2, CDC42EP1, CDC42EP4, CDK5, CDK5R1, CDKN1A, CDKN1B, CNTNAP1, CRKL, CTGF, CTLA4, CXCR4, CYFIP1, CYTH2, DCC, DCLK1, DCX, DDAH1, DGKG, DIAPH2, DIAPH3, DICER1, DKK3, DLG4, DNM3, DZIP1L, EFHD1, EFNA1, EFNB2, ENC1, EPHA2, EPHA4, EPS15, ETV4, EVI5L, F2RL1, FEZ1, FGF13, FGF2, FNBP1L, FOS, FYN, GAB1, GDPD5, GNA12, GNA13, HMGB2, HSPB1, HTR7, IFT122, IL11RA, IL1B, IL1RAP, ITGA4, ITGA6, ITGB3, JUN, KBTBD10, KDR, KIAA1598, KIDINS220, KIT, KLF9, LAMB1, LAMC1, LIMK1, LOX, LPAR1, LRP8, LRRC16A, LYN, LZTS1, MAP2K1, MAP3K1, MAP3K7, MARCKS, MATN2, MBP, MKS1, MRAS, MSN, MT2A, MTSS1, MYO10, MYO5A, NCKIPSD, NEO1, NFIA, NFIB, NFKBIA, NPHP3, NRCAM, NRP1, NRTN, ONECUT2, OPHN1, OPTN, P2RX7, PACSIN2, PAK4, PARVB, PCM1, PHLDB2, PI4KB, PLAT, PLXNB1, PMP22, POU3F1, POU3F2, PPP1R9A, PREX1, PRICKLE2, PRKCE, PRMT1, PRNP, PTEN, PTK2, PTPRE, PTPRM, PTPRZ1, PVR, PVRL3, RAB17, RAB3IP, RAC2, RALA, RALB, RANBP1, RAP1GAP, RAP2A, RIN1, RIT1, ROCK1, ROCK2, RTN4, RUFY3, RUNX3, RYK, SDC4, SEMA3A, SEMA4D, SLC11A2, SMPD1, SMPD2, SPHK1, SRC, SRGAP2, ST8SIA1, STMN1, STX3, STXBP5, SYK, TBC1D7, TGIF1, THBS1, TIAM2, TM4SF1, TMEM67, TNC, TNFRSF12A, TNFRSF1A, TRPV4, TTC8, TWIST1, ULK1, VANGL2, VASP, VEGFA, WASL, WIPF1, WISP2, WWTR1	200	yes
Cell Morphology	formation of cellular protrusions	5.98E-09	Decreased	-3.583	ABI1, ABL1, ABL2, ACACA, ADCY3, AHR, AKAP12, ANGPTL4, ANK3, APOE, ARAP1, ARHGAP24, ARHGAP33, ATF6, ATL1, ATP7A, ATXN1, BAIAP2, BBS4, BCL2, BDNF, BECN1, BSN, BTG3, BTK, CACNA1H, CAV1, CBY1, CCL2, CDC42EP1, CDC42EP4, CDK5, CDK5R1, CDKN1A, CDKN1B, CNTNAP1, CRKL, CTGF, CTLA4, CXCR4, CYFIP1, CYTH2, DCC, DCLK1, DCX, DDAH1, DGKG, DIAPH2, DIAPH3, DICER1, DKK3, DLG4, DNM3, DZIP1L, EFHD1, EFNA1, EFNB2, ENC1, EPHA2, EPHA4, EPS15, ETV4, EVI5L, F2RL1, FEZ1, FGF13, FGF2, FNBP1L, FOS, FYN, GAB1, GDPD5, GNA12, GNA13, HMGB2, HSPB1, HTR7, IFT122, IL11RA, IL1B, IL1RAP, ITGA4, ITGA6, ITGB3, JUN, KBTBD10, KDR, KIAA1598, KIDINS220, KIT, KLF9, LAMB1, LAMC1, LIMK1, LOX, LPAR1, LRP8, LRRC16A, LYN, LZTS1, MAP2K1, MAP3K1, MAP3K7, MARCKS, MATN2, MBP, MKS1, MRAS, MSN, MT2A, MTSS1, MYO10, MYO5A, NCKIPSD, NEO1, NFIA, NFIB, NFKBIA, NPHP3, NRCAM, NRP1, NRTN, ONECUT2, OPHN1, OPTN, P2RX7, PACSIN2, PAK4, PARVB, PCM1, PHLDB2, PI4KB, PLAT, PLXNB1, PMP22, POU3F1, POU3F2, PPP1R9A, PREX1, PRICKLE2, PRKCE, PRMT1, PRNP, PTEN, PTK2, PTPRE, PTPRM, PTPRZ1, PVR, PVRL3, RAB17, RAB3IP, RAC2, RALA, RALB, RANBP1, RAP1GAP, RAP2A, RIN1, RIT1, ROCK1, ROCK2, RTN4, RUFY3, RUNX3, RYK, SDC4, SEMA3A, SEMA4D, SLC11A2, SMPD1, SMPD2, SPHK1, SRC, SRGAP2, ST8SIA1, STMN1, STX3, STXBP5, SYK, TBC1D7, TGIF1, THBS1, TIAM2, TM4SF1, TMEM67, TNC, TNFRSF12A, TNFRSF1A, TRPV4, TTC8, TWIST1, ULK1, VANGL2, VASP, VEGFA, WASL, WIPF1, WISP2, WWTR1	200	yes

Cellular Movement	chemotaxis	6.77E-04	Decreased	-3.578	ABCC1, ABL1, ADRBK1, ANGPT1, ANGPT2, ANGPTL2, ANXA1, ANXA2, APOE, ARAP3, BDNF, C3AR1, CALR, CASP1, CAV1, CBL, CCL2, CCL20, CCL28, CCND1, CCR1, CD36, CD74, CDKN1A, CEACAM1, CKLF, COL4A3BP, CTGF, CTSE, CXCL13, CXCL16, CXCR4, DEFB4A/DEFB4B, DUSP6, EDNRB, EFNA1, EFNB2, ENPP2, EPHA2, ETV4, F2R, F2RL1, FADD, FAS, FCER1G, FCGR2A, FGF2, FOSL1, FYN, GAB1, GNA12, GNA13, HBEGF, HDAC6, HMGB2, HSPD1, ICAM1, IGF2R, IL16, IL1B, IL8, ITGA4, ITGA6, ITGB3,JAM3, JUN, KDR, KIT, LEF1, LIF, LIMK1, LOX, LYN, MAP2K1, MAP3K1, MAP3K5, MDK, MMP9, MPP1, MST1, MYLK, NEDD9, NOV, NPTX1, NRCAM, NRP1, PDE4B, PGF, PIK3CD, PLAUR, PLXNB1, PREX1, PRNP, PTEN, PTGES, PTGS2, PTK2, RAC2, RALA, RAP1GAP, RGS1, ROCK1, RTN4, SCG2, SEMA3A,SEMA4D, SPHK1,SPP1, SRC, SYK, TFF3, TGFA, THBS1, THBS2, TIRAP, TLR4, TNFRSF1A, TRAF3IP2, TRIB1, TRPV2, VEGFA, VEGFB, WASL, YARS	124	yes
Cellular Assembly and Organization	organizatio	3.30E-10	Decreased	-3.532	ABCC1, ABI1, ABL1, ABL2, ABR, ACACA, ADCY3, ADD1, ADM, ADRBK1, AFAP1, AHR, AKAP11, AKAP12, ANGPT2, ANGPTL4, ANK3, APOE, ARAP1, ARAP3, ARHGAP24, ARHGAP33, ARHGEF1, ARHGEF17, ARHGEF2, ATF6, ATL1, ATP2B1, ATP7A, ATXN1, BAG3, BAIAP2, BAX, BBS4, BCL2, BDNF, BECN1, BIRC5, BSN, BTG3, BTK, CACNA1H, CALR, CAV1, CBL, CBY1, CCL2, CD2, CDC25B, CDC42EP1, CDC42EP4, CDK2AP2, CDK5, CDK5R1, CDK5RAP3, CDKN1A, CDKN1B, CEP350, CHAMP1, CHMP1B, CHN2, CKAP4, CLIP3, CNTNAP1, CRIPT, CRKL, CTGF, CTLA4, CXCR4, CYFIP1, CYTH2, DAPK1, DCC, DCLK1, DCX, DDAH1, DGKG, DIAPH2, DIAPH3, DICER1, DKK3, DLG4, DLGAP5, DNM3, DSP, DVL2, DYNC1LI2, DYNLL1, DZIP1L, EFHD1, EFNA1, EFNB2, ENC1, EPHA2, EPHA4, EPS15, ESPL1, ETS1, ETV4, EVI5L, F2R, F2RL1, FAS, FCGR2A, FEZ1, FGF13, FGF2, FKBP4, FNBP1L, FOS, FOXM1, FYN, GAB1, GALK2, GDPD5, GHR, GJB1, GLB1, GNA12, GNA13, GOLGA2, GPSM2, GRK5, GSTM1, HAS2, HBP1, HDAC6, HMGB2, HSPB1, HTR7, ICAM1, IFT122, IL11RA, IL1B, IL1RAP, IL8, ITGA4, ITGA6, ITGB3, ITK, JUN, KBTBD10, KDR, KIAA1598, KIDINS220, KIF11, KIF13B, KIF2C, KIF4A, KIT, KLF2, KLF9, KLHL20, KRAS, KRT18, LAMA2, LAMB1, LAMC1, LIMK1, LMCD1, LOX, LPAR1, LPIN1, LRP8, LRRC16A, LYN, LZTS1, MACF1, MAP2K1, MAP2K5, MAP3K1, MAP3K12, MAP3K7, MAP6D1, MAPKAPK5, MAPRE3, MARCKS, MATN2, MBP, MERTK, MIA, MID1, MKS1, MRAS, MSN, MT2A, MTSS1, MYB, MYO10, MYO5A, NCKIPSD, NDC80, NDRG1, NEK2, NEO1, NFIA, NFIB, NFKBIA, NPC1, NPHP3, NQO1, NR2F1, NRCAM, NRP1, NRTN, NUSAP1, ONECUT2, OPHN1, OPTN, P2RX7, PACSIN2, PAK4, PARVB, PCM1, PDLIM4, PHLDB2, PI4KB, PLAT, PLAUR, PLK1S1, PLXNB1, PMP22, POU3F1, POU3F2, PPP1R9A, PREX1, PRICKLE2, PRKCE, PRMT1, PRNP, PSRC1, PTEN, PTK2, PTPRE, PTPRM, PTPRZ1, PVR, PVRL3, RAB17, RAB2A, RAB3IP, RAC2, RACGAP1, RALA, RALB, RAN, RANBP1, RAP1GAP, RAP2A, RARRES3, RGS20, RHOJ, RIN1, RIT1, RND3, RNF19A, ROCK1, ROCK2, RRBP1, RTN4, RUFY3, RUNX3, RYK, SDC4, SEMA3A, SEMA4D, SFRP1, SIAH1, SLC11A2, SLC3A2, SMPD1, SMPD2, SORBS1, SPHK1, SPP1, SRC, SRGAP2, SSH1, ST8SIA1, STK24, STMN1, STRADB, STX3, STXBP5, SYK, SYNM, TACC2, TACC3, TBC1D7, TERF1, TGIF1, THBS1, TIAM2, TIMP3, TLR4, TM4SF1, TMEM67, TNC, TNFRSF12A, TNFRSF1A, TNFSF10, TPX2, TRPV4, TTC8, TTK, TUBB3, TWIST1, ULK1, VANGL2, VASP, VEGFA, WASL, WIPF1, WISP2, WWTR1, XPC	316	yes
Cellular Function and Maintenance	organizatio	3.30E-10	Decreased	-3.532	ABCC1, ABI1, ABL1, ABL2, ABR, ACACA, ADCY3, ADD1, ADM, ADRBK1, AFAP1, AHR, AKAP11, AKAP12, ANGPT2, ANGPTL4, ANK3, APOE, ARAP1, ARAP3, ARHGAP24, ARHGAP33, ARHGEF1, ARHGEF17, ARHGEF2, ATF6, ATL1, ATP2B1, ATP7A, ATXN1, BAG3, BAIAP2, BAX, BBS4, BCL2, BDNF, BECN1, BIRC5, BSN, BTG3, BTK, CACNA1H, CALR, CAV1, CBL, CBY1, CCL2, CD2, CDC25B, CDC42EP1, CDC42EP4, CDK2AP2, CDK5, CDK5R1, CDK5RAP3, CDKN1A, CDKN1B, CEP350, CHAMP1, CHMP1B, CHN2, CKAP4, CLIP3, CNTNAP1, CRIPT, CRKL, CTGF, CTLA4, CXCR4, CYFIP1, CYTH2, DAPK1, DCC, DCLK1, DCX, DDAH1, DGKG, DIAPH2, DIAPH3, DICER1, DKK3, DLG4, DLGAP5, DNM3, DSP, DVL2, DYNC1LI2, DYNLL1, DZIP1L, EFHD1, EFNA1, EFNB2, ENC1, EPHA2, EPHA4, EPS15, ESPL1, ETS1, ETV4, EVI5L, F2R, F2RL1, FAS, FCGR2A, FEZ1, FGF13, FGF2, FKBP4, FNBP1L, FOS, FOXM1, FYN, GAB1, GALK2, GDPD5, GHR, GJB1, GLB1, GNA12, GNA13, GOLGA2, GPSM2, GRK5, GSTM1, HAS2, HBP1, HDAC6, HMGB2, HSPB1, HTR7, ICAM1, IFT122, IL11RA, IL1B, IL1RAP, IL8, ITGA4, ITGA6, ITGB3, ITK, JUN, KBTBD10, KDR, KIAA1598, KIDINS220, KIF11, KIF13B, KIF2C, KIF4A, KIT, KLF2, KLF9, KLHL20, KRAS, KRT18, LAMA2, LAMB1, LAMC1, LIMK1, LMCD1, LOX, LPAR1, LPIN1, LRP8, LRRC16A, LYN, LZTS1, MACF1, MAP2K1, MAP2K5, MAP3K1, MAP3K12, MAP3K7, MAP6D1, MAPKAPK5, MAPRE3, MARCKS, MATN2, MBP, MERTK, MIA, MID1, MKS1, MRAS, MSN, MT2A, MTSS1, MYB, MYO10, MYO5A, NCKIPSD, NDC80, NDRG1, NEK2, NEO1, NFIA, NFIB, NFKBIA, NPC1, NPHP3, NQO1, NR2F1, NRCAM, NRP1, NRTN, NUSAP1, ONECUT2, OPHN1, OPTN, P2RX7, PACSIN2, PAK4, PARVB, PCM1, PDLIM4, PHLDB2, PI4KB, PLAT, PLAUR, PLK1S1, PLXNB1, PMP22, POU3F1, POU3F2, PPP1R9A, PREX1, PRICKLE2, PRKCE, PRMT1, PRNP, PSRC1, PTEN, PTK2, PTPRE, PTPRM, PTPRZ1, PVR, PVRL3, RAB17, RAB2A, RAB3IP, RAC2, RACGAP1, RALA, RALB, RAN, RANBP1, RAP1GAP, RAP2A, RARRES3, RGS20, RHOJ, RIN1, RIT1, RND3, RNF19A, ROCK1, ROCK2, RRBP1, RTN4, RUFY3, RUNX3, RYK, SDC4, SEMA3A, SEMA4D, SFRP1, SIAH1, SLC11A2, SLC3A2, SMPD1, SMPD2, SORBS1, SPHK1, SPP1, SRC, SRGAP2, SSH1, ST8SIA1, STK24, STMN1, STRADB, STX3, STXBP5, SYK, SYNM, TACC2, TACC3, TBC1D7, TERF1, TGIF1, THBS1, TIAM2, TIMP3, TLR4, TM4SF1, TMEM67, TNC, TNFRSF12A, TNFRSF1A, TNFSF10, TPX2, TRPV4, TTC8, TTK, TUBB3, TWIST1, ULK1, VANGL2, VASP, VEGFA, WASL, WIPF1, WISP2, WWTR1, XPC	316	yes
Gene Expression	binding	1.06E-06	Decreased	-3.529	AHR, ATM, BCL2, BMPR1A, BRCA1, BTK, CCND1, CD2, CEBPB, CEBPD, CHRM1, CSDA, DDB2, DDIT3, EGR1, EGR2, EPAS1, ETS1, ETS2, FAS, FGF2, FLI1, FOS, FOXO1, FOXO3, FZD6, GABPB1, GHR, GLRX, HBEGF, HEY1, HEY2, HIVEP2, HMGA1, HOXB13, ID1, ID2, ID3, IER3, IFI16, IGFBP3, IL1B, IL8, ING4, IP6K2, ITGB3, JUN, KLF13, KRAS, LIF, LMCD1, LTBR, MAP2K1, MAP2K6, MAP3K1, MYB, MYC, NFKBIA, NR2F1, NR3C1, NR5A2, PNPT1, PPP1CC, PRDX1, PRMT2, PTEN, PTK2, RARA, RARB, RUNX1, RUNX2, RXRA, SOAT1, SOD2, SP100, SRC, SSBP2, TFAP2A, TFDP1, TFF3, TGFA, TNFRSF1A, TNFRSF1B, TRADD, TRIB3, TXLNG, VEGFA, ZBTB17	88	no
Cellular Assembly and Organization	organizatio	4.45E-11	Decreased	-3.469	ABCA1, ABCC1, ABCD1, ABI1, ABL1, ABL2, ABR, ACACA, ADCY3, ADD1, ADM, ADRBK1, AFAP1, AHR, AKAP11, AKAP12, ANGPT2, ANGPTL4, ANK3, APOE, ARAP1, ARAP3, ARHGAP24, ARHGAP33, ARHGEF1, ARHGEF17, ARHGEF2, ATF6, ATL1, ATP2B1, ATP7A, ATXN1, BAG3, BAIAP2, BAX, BBS4, BCL2, BDNF, BECN1, BIRC5, BSN, BTG3, BTK, CACNA1H, CALR, CAV1, CBL, CBY1, CCL2, CD2, CDC25B, CDC42EP1, CDC42EP4, CDK2AP2, CDK5, CDK5R1, CDK5RAP3, CDKN1A, CDKN1B, CEP350, CHAMP1, CHMP1B, CHN2, CKAP4, CLIP3, CLN3, CLN5, CNTNAP1, COL4A3BP, CRIPT, CRKL, CROCC, CTGF, CTLA4, CXCR4, CYFIP1, CYTH2, DAPK1, DCC, DCLK1, DCX, DDAH1, DGKG, DIAPH2, DIAPH3, DICER1, DKK3, DLG4, DLGAP5, DNM3, DSP, DVL2, DYNC1LI2, DYNLL1, DZIP1L, EFHD1, EFNA1, EFNB2, ENC1, EPAS1, EPHA2, EPHA4, EPS15, ESPL1, ETS1, ETV4, EVI5L, F2R, F2RL1, FAS, FCGR2A, FEZ1, FGF13, FGF2, FKBP4, FNBP1L, FOS, FOXM1, FYN, GAB1, GALK2, GDPD5, GHR, GJB1, GLB1, GNA12, GNA13, GOLGA2, GORASP1, GPSM2, GRK5, GSTM1, HAS2, HAUS4, HBP1, HDAC6, HEXA, HMGB2, HMGCL, HPS4, HSPB1, HTR7, HTRA2, ICAM1, IFT122, IL11RA, IL1B, IL1RAP, IL8, ITGA4, ITGA6, ITGB3, ITK, JUN, KBTBD10, KDR, KIAA1598, KIDINS220, KIF11, KIF13B, KIF2C, KIF4A, KIT, KLF2, KLF9, KLHL20, KRAS, KRT18, LAMA2, LAMB1, LAMC1, LIMK1, LMCD1, LOX, LPAR1, LPIN1, LRP8, LRRC16A, LYN, LZTS1, MACF1, MAP2K1, MAP2K5, MAP3K1, MAP3K12, MAP3K7, MAP6D1, MAPKAPK5, MAPRE3, MARCKS, MATN2, MBP, MERTK, MFF, MIA, MID1, MKS1, MRAS, MSN, MT2A, MTSS1, MYB, MYO10, MYO5A, NCKIPSD, NDC80, NDRG1, NEK2, NEO1, NFIA, NFIB, NFKBIA, NPC1, NPHP3, NPLOC4, NQO1, NR2F1, NRCAM, NRP1, NRTN, NSFL1C, NUSAP1, ONECUT2, OPHN1, OPTN, P2RX7, PACSIN2, PAK4, PARVB, PCM1, PDLIM4, PEX11B, PEX16, PEX2, PEX5, PHLDB2, PI4KB, PLAT, PLAUR, PLEKHM2, PLK1S1, PLXNB1, PMP22, POU3F1, POU3F2, PPARGC1A, PPP1R9A, PREX1, PRICKLE2, PRKCE, PRKD1, PRMT1, PRNP, PSRC1, PTEN, PTK2, PTPRE, PTPRM, PTPRZ1, PVR, PVRL3, RAB17, RAB2A, RAB3IP, RAB5B, RAB6A, RAC2, RACGAP1, RALA, RALB, RAN, RANBP1, RAP1GAP, RAP2A, RARRES3, RGS20, RHOJ, RIN1, RIT1, RND3, RNF19A, ROCK1, ROCK2, RRBP1, RTN4, RUFY3, RUNX3, RYK, SDC4, SEMA3A, SEMA4D, SFRP1, SIAH1, SLC11A2, SLC3A2, SMPD1, SMPD2, SNX10, SOD2, SORBS1, SPHK1, SPP1, SRC, SRGAP2, SSH1, ST8SIA1, STK24, STMN1, STRADB, STX3, STXBP5, SYK, SYNJ2BP, SYNM, TACC2, TACC3, TBC1D7, TERF1, TGIF1, THBS1, TIAM2, TIMP3, TLR4, TM4SF1, TMEM67, TNC, TNFRSF12A, TNFRSF1A, TNFSF10, TPX2, TRPV4, TTC8, TTK, TUBB3, TWIST1, ULK1, VANGL2, VASP, VEGFA, VPS18, WASL, WIPF1, WISP2, WWTR1, XPC	345	yes
Cellular Function and Maintenance	organizatio	4.45E-11	Decreased	-3.469	ABCA1, ABCC1, ABCD1, ABI1, ABL1, ABL2, ABR, ACACA, ADCY3, ADD1, ADM, ADRBK1, AFAP1, AHR, AKAP11, AKAP12, ANGPT2, ANGPTL4, ANK3, APOE, ARAP1, ARAP3, ARHGAP24, ARHGAP33, ARHGEF1, ARHGEF17, ARHGEF2, ATF6, ATL1, ATP2B1, ATP7A, ATXN1, BAG3, BAIAP2, BAX, BBS4, BCL2, BDNF, BECN1, BIRC5, BSN, BTG3, BTK, CACNA1H, CALR, CAV1, CBL, CBY1, CCL2, CD2, CDC25B, CDC42EP1, CDC42EP4, CDK2AP2, CDK5, CDK5R1, CDK5RAP3, CDKN1A, CDKN1B, CEP350, CHAMP1, CHMP1B, CHN2, CKAP4, CLIP3, CLN3, CLN5, CNTNAP1, COL4A3BP, CRIPT, CRKL, CROCC, CTGF, CTLA4, CXCR4, CYFIP1, CYTH2, DAPK1, DCC, DCLK1, DCX, DDAH1, DGKG, DIAPH2, DIAPH3, DICER1, DKK3, DLG4, DLGAP5, DNM3, DSP, DVL2, DYNC1LI2, DYNLL1, DZIP1L, EFHD1, EFNA1, EFNB2, ENC1, EPAS1, EPHA2, EPHA4, EPS15, ESPL1, ETS1, ETV4, EVI5L, F2R, F2RL1, FAS, FCGR2A, FEZ1, FGF13, FGF2, FKBP4, FNBP1L, FOS, FOXM1, FYN, GAB1, GALK2, GDPD5, GHR, GJB1, GLB1, GNA12, GNA13, GOLGA2, GORASP1, GPSM2, GRK5, GSTM1, HAS2, HAUS4, HBP1, HDAC6, HEXA, HMGB2, HMGCL, HPS4, HSPB1, HTR7, HTRA2, ICAM1, IFT122, IL11RA, IL1B, IL1RAP, IL8, ITGA4, ITGA6, ITGB3, ITK, JUN, KBTBD10, KDR, KIAA1598, KIDINS220, KIF11, KIF13B, KIF2C, KIF4A, KIT, KLF2, KLF9, KLHL20, KRAS, KRT18, LAMA2, LAMB1, LAMC1, LIMK1, LMCD1, LOX, LPAR1, LPIN1, LRP8, LRRC16A, LYN, LZTS1, MACF1, MAP2K1, MAP2K5, MAP3K1, MAP3K12, MAP3K7, MAP6D1, MAPKAPK5, MAPRE3, MARCKS, MATN2, MBP, MERTK, MFF, MIA, MID1, MKS1, MRAS, MSN, MT2A, MTSS1, MYB, MYO10, MYO5A, NCKIPSD, NDC80, NDRG1, NEK2, NEO1, NFIA, NFIB, NFKBIA, NPC1, NPHP3, NPLOC4, NQO1, NR2F1, NRCAM, NRP1, NRTN, NSFL1C, NUSAP1, ONECUT2, OPHN1, OPTN, P2RX7, PACSIN2, PAK4, PARVB, PCM1, PDLIM4, PEX11B, PEX16, PEX2, PEX5, PHLDB2, PI4KB, PLAT, PLAUR, PLEKHM2, PLK1S1, PLXNB1, PMP22, POU3F1, POU3F2, PPARGC1A, PPP1R9A, PREX1, PRICKLE2, PRKCE, PRKD1, PRMT1, PRNP, PSRC1, PTEN, PTK2, PTPRE, PTPRM, PTPRZ1, PVR, PVRL3, RAB17, RAB2A, RAB3IP, RAB5B, RAB6A, RAC2, RACGAP1, RALA, RALB, RAN, RANBP1, RAP1GAP, RAP2A, RARRES3, RGS20, RHOJ, RIN1, RIT1, RND3, RNF19A, ROCK1, ROCK2, RRBP1, RTN4, RUFY3, RUNX3, RYK, SDC4, SEMA3A, SEMA4D, SFRP1, SIAH1, SLC11A2, SLC3A2, SMPD1, SMPD2, SNX10, SOD2, SORBS1, SPHK1, SPP1, SRC, SRGAP2, SSH1, ST8SIA1, STK24, STMN1, STRADB, STX3, STXBP5, SYK, SYNJ2BP, SYNM, TACC2, TACC3, TBC1D7, TERF1, TGIF1, THBS1, TIAM2, TIMP3, TLR4, TM4SF1, TMEM67, TNC, TNFRSF12A, TNFRSF1A, TNFSF10, TPX2, TRPV4, TTC8, TTK, TUBB3, TWIST1, ULK1, VANGL2, VASP, VEGFA, VPS18, WASL, WIPF1, WISP2, WWTR1, XPC	345	yes
Cellular Development	plasma projections	5.89E-04	Decreased	-3.384	ABL1, ABL2, ADCY3, AHR, ANK3, APOE, ARHGAP24, ARHGAP33, ATF6, ATL1, ATP7A, ATXN1, BAIAP2, BBS4, BCL2, BDNF, BSN, BTG3, CACNA1H, CAV1, CDK5, CDK5R1, CDKN1A, CNTNAP1, CYTH2, DCC, DCLK1, DCX, DDAH1, DICER1, DLG4, EFHD1, EFNA1, EFNB2, ENC1, EPHA4, ETV4, FEZ1, FGF13, FGF2, FNBP1L, FOS, FYN, GDPD5, HMGB2, IL11RA, IL1B, IL1RAP, ITGB3, JUN, KDR, KIAA1598, KIDINS220, KLF9, LAMB1, LAMC1, LIMK1, LOX, LRP8, LYN, LZTS1, MAP2K1, MATN2, MBP, MSN, MT2A, MYO5A, NFIA, NFIB, NFKBIA, NRCAM, NRP1, NRTN, OPHN1, OPTN, P2RX7, PAK4, PARVB, PLAT, PLXNB1, PMP22, POU3F1, POU3F2, PPP1R9A, PREX1, PRICKLE2, PRKCE, PRMT1, PRNP, PTEN, PTK2, PTPRE, PTPRM, PTPRZ1, RAB17, RAC2, RALA, RALB, RAP2A, RIT1, ROCK1, ROCK2, RTN4, RUFY3, RUNX3, RYK, SEMA3A, SEMA4D, SLC11A2, SMPD1, SMPD2, SRC, SRGAP2, ST8SIA1, STMN1, STX3, STXBP5, TIAM2, TNC, TRPV4, ULK1, VASP, WASL, WISP2	124	yes
Cellular Assembly and Organization	plasma projections	5.89E-04	Decreased	-3.384	ABL1, ABL2, ADCY3, AHR, ANK3, APOE, ARHGAP24, ARHGAP33, ATF6, ATL1, ATP7A, ATXN1, BAIAP2, BBS4, BCL2, BDNF, BSN, BTG3, CACNA1H, CAV1, CDK5, CDK5R1, CDKN1A, CNTNAP1, CYTH2, DCC, DCLK1, DCX, DDAH1, DICER1, DLG4, EFHD1, EFNA1, EFNB2, ENC1, EPHA4, ETV4, FEZ1, FGF13, FGF2, FNBP1L, FOS, FYN, GDPD5, HMGB2, IL11RA, IL1B, IL1RAP, ITGB3, JUN, KDR, KIAA1598, KIDINS220, KLF9, LAMB1, LAMC1, LIMK1, LOX, LRP8, LYN, LZTS1, MAP2K1, MATN2, MBP, MSN, MT2A, MYO5A, NFIA, NFIB, NFKBIA, NRCAM, NRP1, NRTN, OPHN1, OPTN, P2RX7, PAK4, PARVB, PLAT, PLXNB1, PMP22, POU3F1, POU3F2, PPP1R9A, PREX1, PRICKLE2, PRKCE, PRMT1, PRNP, PTEN, PTK2, PTPRE, PTPRM, PTPRZ1, RAB17, RAC2, RALA, RALB, RAP2A, RIT1, ROCK1, ROCK2, RTN4, RUFY3, RUNX3, RYK, SEMA3A, SEMA4D, SLC11A2, SMPD1, SMPD2, SRC, SRGAP2, ST8SIA1, STMN1, STX3, STXBP5, TIAM2, TNC, TRPV4, ULK1, VASP, WASL, WISP2	124	yes
Cellular Function and Maintenance	plasma projections	5.89E-04	Decreased	-3.384	ABL1, ABL2, ADCY3, AHR, ANK3, APOE, ARHGAP24, ARHGAP33, ATF6, ATL1, ATP7A, ATXN1, BAIAP2, BBS4, BCL2, BDNF, BSN, BTG3, CACNA1H, CAV1, CDK5, CDK5R1, CDKN1A, CNTNAP1, CYTH2, DCC, DCLK1, DCX, DDAH1, DICER1, DLG4, EFHD1, EFNA1, EFNB2, ENC1, EPHA4, ETV4, FEZ1, FGF13, FGF2, FNBP1L, FOS, FYN, GDPD5, HMGB2, IL11RA, IL1B, IL1RAP, ITGB3, JUN, KDR, KIAA1598, KIDINS220, KLF9, LAMB1, LAMC1, LIMK1, LOX, LRP8, LYN, LZTS1, MAP2K1, MATN2, MBP, MSN, MT2A, MYO5A, NFIA, NFIB, NFKBIA, NRCAM, NRP1, NRTN, OPHN1, OPTN, P2RX7, PAK4, PARVB, PLAT, PLXNB1, PMP22, POU3F1, POU3F2, PPP1R9A, PREX1, PRICKLE2, PRKCE, PRMT1, PRNP, PTEN, PTK2, PTPRE, PTPRM, PTPRZ1, RAB17, RAC2, RALA, RALB, RAP2A, RIT1, ROCK1, ROCK2, RTN4, RUFY3, RUNX3, RYK, SEMA3A, SEMA4D, SLC11A2, SMPD1, SMPD2, SRC, SRGAP2, ST8SIA1, STMN1, STX3, STXBP5, TIAM2, TNC, TRPV4, ULK1, VASP, WASL, WISP2	124	yes
Cell Morphology	plasma projections	5.89E-04	Decreased	-3.384	ABL1, ABL2, ADCY3, AHR, ANK3, APOE, ARHGAP24, ARHGAP33, ATF6, ATL1, ATP7A, ATXN1, BAIAP2, BBS4, BCL2, BDNF, BSN, BTG3, CACNA1H, CAV1, CDK5, CDK5R1, CDKN1A, CNTNAP1, CYTH2, DCC, DCLK1, DCX, DDAH1, DICER1, DLG4, EFHD1, EFNA1, EFNB2, ENC1, EPHA4, ETV4, FEZ1, FGF13, FGF2, FNBP1L, FOS, FYN, GDPD5, HMGB2, IL11RA, IL1B, IL1RAP, ITGB3, JUN, KDR, KIAA1598, KIDINS220, KLF9, LAMB1, LAMC1, LIMK1, LOX, LRP8, LYN, LZTS1, MAP2K1, MATN2, MBP, MSN, MT2A, MYO5A, NFIA, NFIB, NFKBIA, NRCAM, NRP1, NRTN, OPHN1, OPTN, P2RX7, PAK4, PARVB, PLAT, PLXNB1, PMP22, POU3F1, POU3F2, PPP1R9A, PREX1, PRICKLE2, PRKCE, PRMT1, PRNP, PTEN, PTK2, PTPRE, PTPRM, PTPRZ1, RAB17, RAC2, RALA, RALB, RAP2A, RIT1, ROCK1, ROCK2, RTN4, RUFY3, RUNX3, RYK, SEMA3A, SEMA4D, SLC11A2, SMPD1, SMPD2, SRC, SRGAP2, ST8SIA1, STMN1, STX3, STXBP5, TIAM2, TNC, TRPV4, ULK1, VASP, WASL, WISP2	124	yes
Cellular Assembly and Organization	microtubule dynamics	9.05E-11	Decreased	-3.297	ABCC1, ABI1, ABL1, ABL2, ACACA, ADCY3, ADM, AHR, AKAP11, AKAP12, ANGPT2, ANGPTL4, ANK3, APOE, ARAP1, ARHGAP24, ARHGAP33, ARHGEF2, ATF6, ATL1, ATP2B1, ATP7A, ATXN1, BAIAP2, BAX, BBS4, BCL2, BDNF, BECN1, BIRC5, BSN, BTG3, BTK, CACNA1H, CAV1, CBL, CBY1, CCL2, CD2, CDC25B, CDC42EP1, CDC42EP4, CDK2AP2, CDK5, CDK5R1, CDK5RAP3, CDKN1A, CDKN1B, CEP350, CHAMP1, CHMP1B, CHN2, CKAP4, CLIP3, CNTNAP1, CRIPT, CRKL, CTGF, CTLA4, CXCR4, CYFIP1, CYTH2, DAPK1, DCC, DCLK1, DCX, DDAH1, DGKG, DIAPH2, DIAPH3, DICER1, DKK3, DLG4, DLGAP5, DNM3, DSP, DVL2, DYNC1LI2, DYNLL1, DZIP1L, EFHD1, EFNA1, EFNB2, ENC1, EPHA2, EPHA4, EPS15, ETV4, EVI5L, F2R, F2RL1, FAS, FEZ1, FGF13, FGF2, FKBP4, FNBP1L, FOS, FOXM1, FYN, GAB1, GALK2, GDPD5, GHR, GJB1, GLB1, GNA12, GNA13, GOLGA2, GRK5, GSTM1, HDAC6, HMGB2, HSPB1, HTR7, ICAM1, IFT122, IL11RA, IL1B, IL1RAP, IL8, ITGA4, ITGA6, ITGB3, JUN, KBTBD10, KDR, KIAA1598, KIDINS220, KIF13B, KIF2C, KIF4A, KIT, KLF2, KLF9, KRT18, LAMA2, LAMB1, LAMC1, LIMK1, LMCD1, LOX, LPAR1, LRP8, LRRC16A, LYN, LZTS1, MACF1, MAP2K1, MAP3K1, MAP3K12, MAP3K7, MAP6D1, MAPRE3, MARCKS, MATN2, MBP, MIA, MID1, MKS1, MRAS, MSN, MT2A, MTSS1, MYB, MYO10, MYO5A, NCKIPSD, NDRG1, NEK2, NEO1, NFIA, NFIB, NFKBIA, NPC1, NPHP3, NQO1, NR2F1, NRCAM, NRP1, NRTN, NUSAP1, ONECUT2, OPHN1, OPTN, P2RX7, PACSIN2, PAK4, PARVB, PCM1, PHLDB2, PI4KB, PLAT, PLXNB1, PMP22, POU3F1, POU3F2, PPP1R9A, PREX1, PRICKLE2, PRKCE, PRMT1, PRNP, PSRC1, PTEN, PTK2, PTPRE, PTPRM, PTPRZ1, PVR, PVRL3, RAB17, RAB2A, RAB3IP, RAC2, RACGAP1, RALA, RALB, RAN, RANBP1, RAP1GAP, RAP2A, RARRES3, RGS20, RIN1, RIT1, RNF19A, ROCK1, ROCK2, RRBP1, RTN4, RUFY3, RUNX3, RYK, SDC4, SEMA3A, SEMA4D, SLC11A2, SMPD1, SMPD2, SPHK1, SRC, SRGAP2, ST8SIA1, STK24, STMN1, STX3, STXBP5, SYK, TACC2, TACC3, TBC1D7, TERF1, TGIF1, THBS1, TIAM2, TIMP3, TLR4, TM4SF1, TMEM67, TNC, TNFRSF12A, TNFRSF1A, TPX2, TRPV4, TTC8, TUBB3, TWIST1, ULK1, VANGL2, VASP, VEGFA, WASL, WIPF1, WISP2, WWTR1, XPC	277	yes
Cellular Function and Maintenance	microtubule dynamics	9.05E-11	Decreased	-3.297	ABCC1, ABI1, ABL1, ABL2, ACACA, ADCY3, ADM, AHR, AKAP11, AKAP12, ANGPT2, ANGPTL4, ANK3, APOE, ARAP1, ARHGAP24, ARHGAP33, ARHGEF2, ATF6, ATL1, ATP2B1, ATP7A, ATXN1, BAIAP2, BAX, BBS4, BCL2, BDNF, BECN1, BIRC5, BSN, BTG3, BTK, CACNA1H, CAV1, CBL, CBY1, CCL2, CD2, CDC25B, CDC42EP1, CDC42EP4, CDK2AP2, CDK5, CDK5R1, CDK5RAP3, CDKN1A, CDKN1B, CEP350, CHAMP1, CHMP1B, CHN2, CKAP4, CLIP3, CNTNAP1, CRIPT, CRKL, CTGF, CTLA4, CXCR4, CYFIP1, CYTH2, DAPK1, DCC, DCLK1, DCX, DDAH1, DGKG, DIAPH2, DIAPH3, DICER1, DKK3, DLG4, DLGAP5, DNM3, DSP, DVL2, DYNC1LI2, DYNLL1, DZIP1L, EFHD1, EFNA1, EFNB2, ENC1, EPHA2, EPHA4, EPS15, ETV4, EVI5L, F2R, F2RL1, FAS, FEZ1, FGF13, FGF2, FKBP4, FNBP1L, FOS, FOXM1, FYN, GAB1, GALK2, GDPD5, GHR, GJB1, GLB1, GNA12, GNA13, GOLGA2, GRK5, GSTM1, HDAC6, HMGB2, HSPB1, HTR7, ICAM1, IFT122, IL11RA, IL1B, IL1RAP, IL8, ITGA4, ITGA6, ITGB3, JUN, KBTBD10, KDR, KIAA1598, KIDINS220, KIF13B, KIF2C, KIF4A, KIT, KLF2, KLF9, KRT18, LAMA2, LAMB1, LAMC1, LIMK1, LMCD1, LOX, LPAR1, LRP8, LRRC16A, LYN, LZTS1, MACF1, MAP2K1, MAP3K1, MAP3K12, MAP3K7, MAP6D1, MAPRE3, MARCKS, MATN2, MBP, MIA, MID1, MKS1, MRAS, MSN, MT2A, MTSS1, MYB, MYO10, MYO5A, NCKIPSD, NDRG1, NEK2, NEO1, NFIA, NFIB, NFKBIA, NPC1, NPHP3, NQO1, NR2F1, NRCAM, NRP1, NRTN, NUSAP1, ONECUT2, OPHN1, OPTN, P2RX7, PACSIN2, PAK4, PARVB, PCM1, PHLDB2, PI4KB, PLAT, PLXNB1, PMP22, POU3F1, POU3F2, PPP1R9A, PREX1, PRICKLE2, PRKCE, PRMT1, PRNP, PSRC1, PTEN, PTK2, PTPRE, PTPRM, PTPRZ1, PVR, PVRL3, RAB17, RAB2A, RAB3IP, RAC2, RACGAP1, RALA, RALB, RAN, RANBP1, RAP1GAP, RAP2A, RARRES3, RGS20, RIN1, RIT1, RNF19A, ROCK1, ROCK2, RRBP1, RTN4, RUFY3, RUNX3, RYK, SDC4, SEMA3A, SEMA4D, SLC11A2, SMPD1, SMPD2, SPHK1, SRC, SRGAP2, ST8SIA1, STK24, STMN1, STX3, STXBP5, SYK, TACC2, TACC3, TBC1D7, TERF1, TGIF1, THBS1, TIAM2, TIMP3, TLR4, TM4SF1, TMEM67, TNC, TNFRSF12A, TNFRSF1A, TPX2, TRPV4, TTC8, TUBB3, TWIST1, ULK1, VANGL2, VASP, VEGFA, WASL, WIPF1, WISP2, WWTR1, XPC	277	yes

Cellular Movement	cell movement of connective tissue cells	3.52E-06	Decreased	-3.246	ABL1, ABL2, ANGPT1, ANGPT2, APOE, ARID5B, CAV1, CBL, CCL2, CCNA2, CCND1, CDKN1A, CDKN1B, CTGF, CYTH2, ENPP2, F2R, FGF2, FOS, FOSL1, GNA12, GNA13, HBEGF, HMMR, IGF2R, IL16, IL1B, ITGB3, JUN, LIMA1, LIMK1, LPAR1, MAP2K1, MAP3K1, MRAS, MYC, NOV, PLAUR, PRKAR1A, PRKCE, PTEN, PTK2, PTPRA, RAC2, RAP2A, RAPGEF1, SCHIP1, SDC4, SEMA3A, SMO, SNX17, SPP1, SRC, STMN1, TGFA, TGFBR2, THBS1, TIMP2, VASP, ZFAND5, ZYX	61	yes
Cellular Growth and Proliferation	proliferation of epithelial cells	1.91E-04	Decreased	-3.241	ASIP, BAX, BMPR1A, BRCA1, CCND1, CCND2, CCNG2, CDC25A, CDC25B, CDK6, CDKN1A, CDKN1B, CDKN2C, CEBPB, DCC, DKK1, EDNRB, EFNA1, EPHA2, FGF2, FGFR3, FOS, FOXM1, FST, FYN, FZD7, GAS1, GDF15, GLI2, HBEGF, HOXA5, HOXB13, HSF4, ID1, ID2, IL1B, IL8, ITGA6, ITGB3, JUN, KDR, KIT, KLF4, KRAS, LAMB1, LAMC1, LRIG1, LTBP4, LTBR, MAGED1, MAP2K1, MAP2K5, MAP3K5, MAP3K7, MC1R, MCC, MMP9, MST1, MYB, MYC, NFIB, NFKBIA, NKX3-1, NR3C1, OVOL2, PAX3, PEX2, POU3F2, PPP1R13L, PTEN, PTGS2, PTK2, PTPN12, PTPRZ1, RARA, RRAS, RUNX1, RUNX3, RXRA, SEMA4D, SFRP1, SMO, SNAI2, SOX2, SPHK1, SPP1, STMN1, TCF4, TCF7L2, TGFA, TGFBR2, TGFBR3, TIMELESS, TNFRSF1A, TNFSF10, TWIST1, VDR, VEGFA	98	yes
Cellular Movement	homing of cells	6.72E-05	Decreased	-3.233	ABCC1, ABL1, ADRBK1, ANGPT1, ANGPT2, ANGPTL2, ANXA1, ANXA2, APOE, ARAP3, BCL2, BDNF, C3AR1, CALR, CASP1, CAV1, CBL, CCL2, CCL20, CCL28, CCND1, CCR1, CD36, CD74, CDKN1A, CEACAM1, CHST2, CKLF, COL4A3BP, CRKL, CTGF, CTSE, CXCL13, CXCL16, CXCR4, DEFB4A/DEFB4B, DUSP6, EDNRB, EFNA1, ENPP2, EPHA2, ETV4, F2R, F2RL1, FADD, FAS, FCER1G, FCGR2A, FGF2, FOXO1, FYB, FYN, GAB1, GNA12, GNA13, HBEGF, HDAC6, HMGB2, HSPD1, ICAM1, IGF2R, IGFBP3, IL16, IL1B, IL8, ITGA4, ITGA6, ITGB3, JAM3, JUN, KDR, KIT, LEF1, LIF, LIMK1, LOX, LTBR, LYN, MAP3K1, MAP3K5, MDK, MMP9, MPP1, MST1, MYB, MYLK, NEDD9, NOV, NPTX1, NQO1, NRCAM, NRP1, PDE4B, PGF, PIK3CD, PLAUR, PLXNB1, PREX1, PRNP, PTEN, PTGES, PTGS2, PTK2, PTPRA, PTPRZ1, RAC2, RAP1GAP, RGS1, ROCK1, RTN4, RUNX1, SCG2, SEMA3A, SEMA4D, SNAI2, SPHK1, SPP1, SRC, SYK, TFF3, TGFA, THBS1, THBS2, TIRAP, TLR4, TNFRSF1A, TRAF3IP2, TRIB1, TRPV2, VEGFA, VEGFB, WASL, YARS	133	yes
Cellular Movement	homing	5.72E-05	Decreased	-3.229	ABCC1, ABL1, ADRBK1, ANGPT1, ANGPT2, ANGPTL2, ANXA1, ANXA2, APOE, ARAP3, BCL2, BDNF, C3AR1, CALR, CASP1, CAV1, CBL, CCL2, CCL20, CCL28, CCND1, CCR1, CD36, CD74, CDKN1A, CEACAM1, CHST2, CKLF, COL4A3BP, CRKL, CTGF, CTSE, CXCL13, CXCL16, CXCR4, DEFB4A/DEFB4B, DUSP6, EDNRB, EFNA1, EFNB2, ENPP2, EPHA2, ETV4, F2R, F2RL1, FADD, FAS, FCER1G, FCGR2A, FGF2, FOSL1, FOXO1, FYB, FYN, GAB1, GNA12, GNA13, HBEGF, HDAC6, HMGB2, HSPD1, ICAM1, IGF2R, IGFBP3, IL16, IL1B, IL8, ITGA4, ITGA6, ITGB3, JAM3, JUN, KDR, KIT, LEF1, LIF, LIMK1, LOX, LTBR, LYN, MAP2K1, MAP3K1, MAP3K5, MDK, MMP9, MPP1, MST1, MYB, MYLK, NEDD9, NOV, NPTX1, NQO1, NRCAM, NRP1, PDE4B, PGF, PIK3CD, PLAUR, PLXNB1, PREX1, PRNP, PTEN, PTGES, PTGS2, PTK2, PTPRA, PTPRZ1, RAC2, RALA, RAP1GAP, RGS1, ROCK1, RTN4, RUNX1, SCG2, SEMA3A, SEMA4D, SNAI2, SPHK1, SPP1, SRC, SYK, TFF3, TGFA, THBS1, THBS2, TIRAP, TLR4, TNFRSF1A, TRAF3IP2, TRIB1, TRPV2, VEGFA, VEGFB, WASL, YARS	137	yes
Organismal Development	formation of vessel	3.92E-04	Decreased	-3.137	ADAMTS1, AHR, ANGPT1, ANGPT2, APOE, CCL2, CTGF, CXCR4, DGCR8, EFNB2, ENPP2, EPAS1, F12, FGF2, FOXM1, FOXO3, GAB1, IL1B, ING4, ITGB3, JUN, KDR, LTBR, MEF2C, MMP9, NRP1, PLAUR, SEMA4D, SRC, TGFBR3, TIMP2, VEGFA	32	yes
Cellular Movement	movement of vascular endothelial cells	1.79E-06	Decreased	-3.060	ADAMTS1, ADM, ANGPT1, ANGPT2, ANXA2, ARHGEF6, CDKN1B, DICER1, DKK1, EFNA1, EFNB2, F2RL1, FGF13, FGF2, FOXO1, FOXO3, GAB1, HHEX, HIF1A, HSP90AB1, ID1, ID3, IL8, ITGB3, KDR, KLF2, KLHL20, MAP3K7, MAPKAPK5, MDK, MMP9, NRP1, PTEN, PTGS2, PTPRZ1, RTN4, SP100, SPRY4, SRC, TGFBR2, THBS1, THBS2, TIMP2, TNFSF10, VEGFA	45	yes
Cardiovascular System Development and Function	movement of vascular endothelial cells	1.79E-06	Decreased	-3.060	ADAMTS1, ADM, ANGPT1, ANGPT2, ANXA2, ARHGEF6, CDKN1B, DICER1, DKK1, EFNA1, EFNB2, F2RL1, FGF13, FGF2, FOXO1, FOXO3, GAB1, HHEX, HIF1A, HSP90AB1, ID1, ID3, IL8, ITGB3, KDR, KLF2, KLHL20, MAP3K7, MAPKAPK5, MDK, MMP9, NRP1, PTEN, PTGS2, PTPRZ1, RTN4, SP100, SPRY4, SRC, TGFBR2, THBS1, THBS2, TIMP2, TNFSF10, VEGFA	45	yes
Cellular Movement	cell movement of muscle cells	2.09E-05	Decreased	-3.010	ADM, ANGPT2, APOE, CBL, CCL2, CCND1, CDKN1B, CLIC4, DUSP1, ENPP2, F2R, FGF2, FOXO1, FOXO4, FURIN, FZD4, GAB1, HBEGF, HMOX1, IGFBP5, IL1B, IL8, ITGB5, KDR, LOX, LPAR1, MMP9, MYC, NEO1, NOV, NQO1, PAPPA, PAX3, PLAT, PLAUR, PTGS2, PTK2, RCAN1, ROCK1, RTN4, SDC4, SIX4, SPP1, THBS1, TLR4, TNFSF10, TRIB1, VCAN, WISP2	49	yes
Cellular Movement	cell movement of smooth muscle cells	3.88E-05	Decreased	-2.991	ADM, ANGPT2, APOE, CBL, CCL2, CCND1, CDKN1B, CLIC4, DUSP1, ENPP2, F2R, FGF2, FOXO4, FZD4, HBEGF, HMOX1, IGFBP5, IL1B, IL8, ITGB5, KDR, LOX, LPAR1, MMP9, MYC, NEO1, NOV, NQO1, PAPPA, PLAT, PLAUR, PTGS2, PTK2, RCAN1, ROCK1, RTN4, SDC4, SPP1, THBS1, TLR4, TNFSF10, TRIB1, VCAN, WISP2	44	yes
Skeletal and Muscular System Development and Function	cell movement of smooth muscle cells	3.88E-05	Decreased	-2.991	ADM, ANGPT2, APOE, CBL, CCL2, CCND1, CDKN1B, CLIC4, DUSP1, ENPP2, F2R, FGF2, FOXO4, FZD4, HBEGF, HMOX1, IGFBP5, IL1B, IL8, ITGB5, KDR, LOX, LPAR1, MMP9, MYC, NEO1, NOV, NQO1, PAPPA, PLAT, PLAUR, PTGS2, PTK2, RCAN1, ROCK1, RTN4, SDC4, SPP1, THBS1, TLR4, TNFSF10, TRIB1, VCAN, WISP2	44	yes
Cellular Development	epithelial-mesenchymal transition	1.91E-05	Decreased	-2.972	ABL1, CAV1, CLIC4, DICER1, EFNA1, ESRP1, ETV5, FGF2, FOXO1, FTH1, HAS2, HEY1, HEY2, HHEX, HIF1A, HMGA2, HNRNPAB, ID1, KRAS, LEF1, LOXL3, MAP3K3, MCAM, MESP1, MRAS, NDRG1, NFKBIA, NRP1, PAX3, PLAUR, PRNP, PTEN, PTPN14, RUNX3, SNAI2, STMN1, TGFBR2, TGFBR3, TWIST1, VEGFA, ZEB2	41	yes
Cellular Movement	cell movement of fibroblasts	2.77E-07	Decreased	-2.940	ABL1, ABL2, ANGPT1, ANGPT2, APOE, ARID5B, CAV1, CCL2, CCNA2, CCND1, CDKN1A, CDKN1B, ENPP2, F2R, FGF2, FOS, GNA12, GNA13, HBEGF, HMMR, IGF2R, IL16, IL1B, ITGB3, JUN, LIMK1, LPAR1, MAP2K1, MAP3K1, MRAS, MYC, NOV, PLAUR, PRKAR1A, PRKCE, PTEN, PTK2, PTPRA, RAC2, RAP2A, RAPGEF1, SCHIP1, SDC4, SMO, SNX17, SPP1, SRC, STMN1, TGFA, TGFBR2, THBS1, TIMP2, VASP, ZFAND5, ZYX	55	yes
Connective Tissue Development and Function	cell movement of fibroblasts	2.77E-07	Decreased	-2.940	ABL1, ABL2, ANGPT1, ANGPT2, APOE, ARID5B, CAV1, CCL2, CCNA2, CCND1, CDKN1A, CDKN1B, ENPP2, F2R, FGF2, FOS, GNA12, GNA13, HBEGF, HMMR, IGF2R, IL16, IL1B, ITGB3, JUN, LIMK1, LPAR1, MAP2K1, MAP3K1, MRAS, MYC, NOV, PLAUR, PRKAR1A, PRKCE, PTEN, PTK2, PTPRA, RAC2, RAP2A, RAPGEF1, SCHIP1, SDC4, SMO, SNX17, SPP1, SRC, STMN1, TGFA, TGFBR2, THBS1, TIMP2, VASP, ZFAND5, ZYX	55	yes
Cardiovascular System Development and Function	formation of blood vessel	3.01E-04	Decreased	-2.867	ADAMTS1, ANGPT1, APOE, CCL2, CTGF, CXCR4, DGCR8, EFNB2, ENPP2, F12, FGF2, FOXM1, FOXO3, GAB1, IL1B, ING4, ITGB3, JUN, KDR, MEF2C, MMP9, NRP1, PLAUR, SEMA4D, SRC, TGFBR3, TIMP2, VEGFA	28	yes
Organismal Development	formation of blood vessel	3.01E-04	Decreased	-2.867	ADAMTS1, ANGPT1, APOE, CCL2, CTGF, CXCR4, DGCR8, EFNB2, ENPP2, F12, FGF2, FOXM1, FOXO3, GAB1, IL1B, ING4, ITGB3, JUN, KDR, MEF2C, MMP9, NRP1, PLAUR, SEMA4D, SRC, TGFBR3, TIMP2, VEGFA	28	yes
Cellular Movement	migration of fibroblast cell lines	1.57E-04	Decreased	-2.865	ABL1, BDNF, CCNA2, CDKN1A, CDKN1B, CLIC4, CRKL, ELK3, FGF2, GNG12, HAS2, HAS3, HBEGF, IL8, KLF2, LIMA1, MARCKS, MMP9, MYLK, NOX4, PLAUR, PRKD1, PTEN, PTGDS, PTGS2, PTK2, PTPN12, PTPRA, PVR, RAC2, SPP1, SRC, TP53INP1, VEGFA	34	yes
Connective Tissue Development and Function	migration of fibroblast cell lines	1.57E-04	Decreased	-2.865	ABL1, BDNF, CCNA2, CDKN1A, CDKN1B, CLIC4, CRKL, ELK3, FGF2, GNG12, HAS2, HAS3, HBEGF, IL8, KLF2, LIMA1, MARCKS, MMP9, MYLK, NOX4, PLAUR, PRKD1, PTEN, PTGDS, PTGS2, PTK2, PTPN12, PTPRA, PVR, RAC2, SPP1, SRC, TP53INP1, VEGFA	34	yes
Cellular Movement	migration of smooth muscle cells	5.45E-05	Decreased	-2.846	ADM, ANGPT2, APOE, CBL, CCL2, CDKN1B, CLIC4, DUSP1, F2R, FGF2, FOXO4, FZD4, HBEGF, HMOX1, IGFBP5, IL1B, IL8, ITGB5, KDR, LPAR1, MMP9, MYC, NEO1, NOV, NQO1, PAPPA, PLAT, PLAUR, PTGS2, PTK2, RCAN1, ROCK1, RTN4, SDC4, SPP1, THBS1, TLR4, TNFSF10, VCAN, WISP2	40	yes
Skeletal and Muscular System Development and Function	migration of smooth muscle cells	5.45E-05	Decreased	-2.846	ADM, ANGPT2, APOE, CBL, CCL2, CDKN1B, CLIC4, DUSP1, F2R, FGF2, FOXO4, FZD4, HBEGF, HMOX1, IGFBP5, IL1B, IL8, ITGB5, KDR, LPAR1, MMP9, MYC, NEO1, NOV, NQO1, PAPPA, PLAT, PLAUR, PTGS2, PTK2, RCAN1, ROCK1, RTN4, SDC4, SPP1, THBS1, TLR4, TNFSF10, VCAN, WISP2	40	yes
Cellular Movement	homing of endothelial cells	1.88E-04	Decreased	-2.835	ANGPT1, ANGPT2, CCL2, CD36, CEACAM1, CXCR4, EFNA1, ENPP2, FGF2, IGF2R, IGFBP3, IL8, KDR, NPTX1, PTGS2, SEMA4D, THBS1, THBS2, VEGFA	19	yes
Cardiovascular System Development and Function	homing of endothelial cells	1.88E-04	Decreased	-2.835	ANGPT1, ANGPT2, CCL2, CD36, CEACAM1, CXCR4, EFNA1, ENPP2, FGF2, IGF2R, IGFBP3, IL8, KDR, NPTX1, PTGS2, SEMA4D, THBS1, THBS2, VEGFA	19	yes
Gene Expression	binding of DNA	3.97E-05	Decreased	-2.801	ABL1, AHR, ARNT, ATF6B, ATM, BCL2, BCL3, BMPR1A, BRCA1, BTK, CALM1 (includes others), CALR, CAV1, CCND1, CD2, CDKN1A, CEBPB, CEBPD, CHRM1, CSDA, CTLA4, DDB2, DDIT3, EGR1, EGR2, EPAS1, EPOR, ERCC5, ETS1, ETS2, FADD, FAS, FGF13, FGF2, FLI1, FOS, FOSL1, FOXM1, FOXO1, FOXO3, FYB, FZD6, GABPB1, GFPT1, GHR, GLRX, GTF2B, HBEGF, HEY1, HEY2, HIF1A, HIPK2, HIVEP2, HMGA1, HMGB2, HOXB13, ID1, ID2, ID3, IER3, IFI16, IFNAR1, IGFBP3, IL1B, IL8, ING1, ING4, IP6K2, IRF9, ITGB3, JUN, JUND, KDR, KLF13, KLHDC2, KRAS, LIF, LMCD1, LOX, LPL, LTBR, LYN, MAP2K1, MAP2K6, MAP3K1, MYB, MYC, NCL, NFKBIA, NFKBIE, NKX2-5, NR2F1, NR3C1, NR5A2, OAS1, PAX3, PBXIP1, PELI1, PHB, PNPT1, PPARGC1A, PPP1CC, PRDX1, PRKCE, PRMT2, PTEN, PTK2, RARA, RARB, RUNX1, RUNX2, RXRA, SOAT1, SOCS2, SOD2, SP100, SPP1, SRC, SSBP2, TCF4, TCF7L2, TFAP2A, TFDP1, TFF3, TGFA, TNFRSF1A, TNFRSF1B, TNFSF13B, TRADD, TRIB3, TSC22D3, TXLNG, UCN2, VDR, VEGFA, XPC, YWHAG, ZBTB17, ZBTB5	139	yes
Cellular Movement	migration of muscle cells	1.42E-05	Decreased	-2.750	ADM, ANGPT2, APOE, CBL, CCL2, CDKN1B, CLIC4, DUSP1, F2R, FGF2, FOXO1, FOXO4, FURIN, FZD4, GAB1, HBEGF, HMOX1, IGFBP5, IL1B, IL8, ITGB5, KDR, LPAR1, MMP9, MYC, NEO1, NOV, NQO1, PAPPA, PAX3, PLAT, PLAUR, PTGS2, PTK2, RCAN1, ROCK1, RTN4, SDC4, SIX4, SPP1, THBS1, TLR4, TNFSF10, VCAN, WISP2	45	yes
Skeletal and Muscular System Development and Function	migration of muscle cells	1.42E-05	Decreased	-2.750	ADM, ANGPT2, APOE, CBL, CCL2, CDKN1B, CLIC4, DUSP1, F2R, FGF2, FOXO1, FOXO4, FURIN, FZD4, GAB1, HBEGF, HMOX1, IGFBP5, IL1B, IL8, ITGB5, KDR, LPAR1, MMP9, MYC, NEO1, NOV, NQO1, PAPPA, PAX3, PLAT, PLAUR, PTGS2, PTK2, RCAN1, ROCK1, RTN4, SDC4, SIX4, SPP1, THBS1, TLR4, TNFSF10, VCAN, WISP2	45	yes
Cancer	metastasis	1.18E-06	Decreased	-2.744	ABL1, ACTA2, ADAMTS1, AHR, AKAP12, AKT3, ANGPT2, ANGPTL2, ANGPTL4, ANK3, ANXA1, APOE, BIRC5, BMPR1A, C1R, CASP1, CAV1, CBR1, CCL2, CCND2, CD36, CD97, CDC25A, CDK5, CDK5RAP3, CDKN1A, CDKN2C, CEACAM1, CEBPD, CREB3L4, CRYZ, CTGF, CTLA4, CXCR4, DAPK1, DCC, DDB2, DGCR6L, DKK1, DLGAP5, DUSP6, EDNRB, ENPP2, EPAS1, EPHA2, F2R, FABP5, FBN2, FGF2, FOXM1, FST, FSTL3, FYN, FZD7, GART, GDF15, GLRX, GNA12, GREB1, GYG2, HIF1A, HMGB2, HMMR, HMOX1, HOXC6, ICAM1, ID2, IFNAR1, IFNAR2, IGFBP5, IL12A, IL1B, ING4, ITGA6, ITGB3, ITPR3, KDR, KIAA1199, KIDINS220, KIF20A, KIT, KRAS, KRT18, LETMD1, LMCD1, LRRC17, LRRC26, LTBR, MAP2K1, MAP3K5, MCAM, MITF, MLPH, MMP9, MYC, NCAPG, NDRG1, NEDD9, NFKBIA, NQO1, NR2F1, NT5E, NUAK1, PAPPA, PDLIM3, PDZRN3, PGF, PLAT, PLAUR, POLE, PPAP2B, PRNP, PROM1, PRRX1, PTEN, PTGS2, PTK2, PTPRA, RALB, REV3L, RRM1, RUNX2, SEMA4D, SLC16A3, SLC38A6, SMO, SPP1, SSTR2, STEAP3, TGFA, TGFBR2, TGFBR3, THBS1, TIMP3, TM4SF1, TP53BP1, TRIM9, TUBA1C, TUBB3, TUBB4A, TWIST1, TXNIP, VCAN, VEGFA, VEGFB, ZNF536	146	yes
Cancer	germ cell and embryonal neoplasm	2.35E-04	Decreased	-2.736	ABCC1, ABCC4, ARMCX3, ATM, BAX, BCL2, BMI1, BRCA1, CCDC41, CCND1, CDK6, CDKN1A, CDKN2C, CXCR4, DHRS4, FOXD3, FOXO3, FOXO4, FYN, GEMIN5, GLDC, GLI2, H2AFX, IDH1, ING4, KHDRBS3, KIF11, KIT, KRAS, LOXL3, MAP2K1, MDK, MMP9, MYC, NPTX1, OLIG1, PTEN, SFRP1, SMO, SOX2, ST7, STAT2, TUBA1C, TUBB3, TUBB4A, VEGFA, ZBTB17	47	no
Reproductive System Disease	germ cell and embryonal neoplasm	2.35E-04	Decreased	-2.736	ABCC1, ABCC4, ARMCX3, ATM, BAX, BCL2, BMI1, BRCA1, CCDC41, CCND1, CDK6, CDKN1A, CDKN2C, CXCR4, DHRS4, FOXD3, FOXO3, FOXO4, FYN, GEMIN5, GLDC, GLI2, H2AFX, IDH1, ING4, KHDRBS3, KIF11, KIT, KRAS, LOXL3, MAP2K1, MDK, MMP9, MYC, NPTX1, OLIG1, PTEN, SFRP1, SMO, SOX2, ST7, STAT2, TUBA1C, TUBB3, TUBB4A, VEGFA, ZBTB17	47	no
Cellular Movement	migration of breast cancer cell lines	2.11E-06	Decreased	-2.707	ACSL4, ANGPT2, ANKS1A, ANXA1, BCAR3, BHLHE41, CAV1, CCL2, CDKN1B, CHN2, CTSL1, CXCR4, DBF4, EPHA2, EPOR, ETS1, FGF2, FHOD1, FOSL1, FOXO3, GAB1, HIF1A, HMMR, ID1, IGFBP3, IL8, ITGA6, ITGB3, JUN, MAP2K1, MAP4K4, MCAM, MCF2L, MMP9, NDRG1, NRP1, PLAUR, PLXNA1, PPM1F, PRKD1, PTK2, RAB21, RAP1GAP, RNF144A, RUVBL1, SEMA3A, SEMA4D, SLC16A4, SNAI2, SPP1, SRC, SSH1, TFAP2A, TFAP2C, TGFA, TIMP2, VASP, VEGFA, WWTR1	59	yes
Cellular Movement	migration of endothelial cells	2.12E-06	Decreased	-2.697	ADAMTS1, ADM, ANGPT1, ANGPT2, ANGPTL4, ANXA2, APOE, ARHGAP24, ARHGEF6, ARNT, BDNF, CAV1, CCL2, CDKN1B, CTGF, DICER1, DKK1, EFNA1, EFNB2, EYA3, F2RL1, FAP, FGF13, FGF2, FOXO1, FOXO3, GAB1, HAS3, HEY1, HHEX, HIF1A, HMMR, HSP90AB1, HSPB1, ICAM1, ID1, ID3, IGF2R, IGFBP3, IL1B, IL8, ITGA4, ITGB3, KDR, KLF2, KLHL20, MAP2K1, MAP2K3, MAP2K6, MAP3K7, MAPKAPK5, MARCKS, MDK, MMP9, MYC, NOX4, NRP1, PAXIP1, PGF, PLAUR, PLXNA1, PRKCE, PRKD1, PTEN, PTGS2, PTK2, PTPRZ1, RTN4, SCG2, SDC4, SEMA3A, SP100, SPP1, SPRY4, SRC, STC1, TGFBR2, THBS1, TIMP2, TIMP3, TNFRSF12A, TNFSF10, VASP, VEGFA	84	yes
Cardiovascular System Development and Function	migration of endothelial cells	2.12E-06	Decreased	-2.697	ADAMTS1, ADM, ANGPT1, ANGPT2, ANGPTL4, ANXA2, APOE, ARHGAP24, ARHGEF6, ARNT, BDNF, CAV1, CCL2, CDKN1B, CTGF, DICER1, DKK1, EFNA1, EFNB2, EYA3, F2RL1, FAP, FGF13, FGF2, FOXO1, FOXO3, GAB1, HAS3, HEY1, HHEX, HIF1A, HMMR, HSP90AB1, HSPB1, ICAM1, ID1, ID3, IGF2R, IGFBP3, IL1B, IL8, ITGA4, ITGB3, KDR, KLF2, KLHL20, MAP2K1, MAP2K3, MAP2K6, MAP3K7, MAPKAPK5, MARCKS, MDK, MMP9, MYC, NOX4, NRP1, PAXIP1, PGF, PLAUR, PLXNA1, PRKCE, PRKD1, PTEN, PTGS2, PTK2, PTPRZ1, RTN4, SCG2, SDC4, SEMA3A, SP100, SPP1, SPRY4, SRC, STC1, TGFBR2, THBS1, TIMP2, TIMP3, TNFRSF12A, TNFSF10, VASP, VEGFA	84	yes
Cellular Movement	chemotaxis of endothelial cells	3.34E-04	Decreased	-2.689	ANGPT1, ANGPT2, CCL2, CD36, CEACAM1, CXCR4, EFNA1, ENPP2, FGF2, IGF2R, IL8, KDR, NPTX1, PTGS2, SEMA4D, THBS1, THBS2, VEGFA	18	yes
Cardiovascular System Development and Function	chemotaxis of endothelial cells	3.34E-04	Decreased	-2.689	ANGPT1, ANGPT2, CCL2, CD36, CEACAM1, CXCR4, EFNA1, ENPP2, FGF2, IGF2R, IL8, KDR, NPTX1, PTGS2, SEMA4D, THBS1, THBS2, VEGFA	18	yes
Cellular Movement	invasion of cells	5.52E-12	Decreased	-2.651	ABL1, ABL2, ACAT1, ACSL4, ADAMTS1, ADM, AKT3, AMD1, ANG, ANGPT2, ANXA1, ARAP3, ATP6V0A4, B4GALT5, BATF3, BAX, BCAN, BCAR3, BCL2, BDNF, BHLHE40, BHLHE41, CALR, CAV1, CBL, CCL2, CCNA2, CCND1, CCR1, CD97, CDC25B, CDK5, CDK5R1, CDK5RAP3, CDKN1B, CEACAM1, CHD1, CITED1, CLCA2, CLDN1, CMTM8, CSPG4, CTGF, CTSK, CTSL1, CXCR4, DAB2, DIAPH2, DIAPH3, DKK1, DKK3, DNAJB4, E2F5, EDNRB, EFNA1, ENPP2, EPHA2, ETS1, ETS2, ETV1, ETV4, ETV5, F2R, FABP5, FAS, FGF13, FGF2, FHOD1, FOSL1, FOXD3, FOXM1, FOXO3, FST, FSTL1, FURIN, FYN, GAB1, GBP1, GDF15, GJB1, GNA12, GNAL, HAS2, HAS3, HAX1, HBEGF, HBP1, HHEX, HIF1A, HIPK2, HMGA1, HMMR, HMOX1, ID1, ID2, IER3, IL1B, IL8, IRS2, ITGA4, ITGA6, ITGB3, JAM3, JUN, JUND, KLF4, KRAS, LAMC1, LDLRAP1, LEF1, LGMN, LIMK1, LOX, LPAR1, LRIG1, LRP5, LYN, MAP2K1, MAP2K5, MAP2K6, MAP3K11, MAP4K4, MARCKS, MCAM, MIA, MITF, MMP16, MMP9, MRAS, MST1, MYC, MYLK, NAMPT, NCOA4, NDRG1, NEDD9, NFKBIA, NOV, NQO1, NRCAM, NRP1, NUAK1, PA2G4, PAK4, PAPPA, PARVB, PLAT, PLAUR, PLGRKT, PLXNB1, POU3F2, PPM1F, PRKCE, PTEN, PTGS2, PTK2, PTP4A1, PTP4A2, RALA, RAP1GAP, RND3, RNF144A, ROCK1, RPRD1A, RUNX2, RUNX3, RUVBL1, SDC4, SEMA4D, SFRP1, SIM2, SLC2A1, SNAI2, SOD2, SP100, SPHK1, SPP1, SPRY2, SRC, SSTR2, ST8SIA1, STMN1, SYK, TBX2, TFAP2A, TFAP2C, TFF3, TGFA, TGFBR2, TGFBR3, THBS1, THBS2, TIMP2, TIMP3, TNFSF10, TWIST1, VASP, VCAN, VDR, VEGFA, VEGFB, WISP2, WWTR1, ZEB2	204	yes

Cell Cycle	S phase	6.17E-06	Decreased	-2.618	ABL1, ANGPT1, ANP32B, ATM, BCL2, BHLHE40, BID, BIRC5, BRCA1, CAV1, CCNA2, CCND1, CCND2, CCNG2, CDC25A, CDC25C, CDC6, CDK6, CDKN1A, CDKN1B, CDKN2C, CEBPB, CTLA4, DBF4, E2F2, E2F3, E2F5, EPOR, FEN1, FGF2, FOS, FOXM1, FOXO3, GAB1, GAS1, GTF2I, HBEGF, HINFP, HMGA1, HMOX1, ID1, ID2, ID3, IL1B, ILKAP, ING4, JUN, KLF4, KRAS, LZTS1, MAP2K1, MCM10, MCMBP, MEIS2, MIA, MXD3, MXD4, MXI1, MYC, NRIP1, PAM16, PMEPA1, PNPT1, RBBP8, REV3L, RUNX1, SH2B3, SLBP, SOD2, SRC, ST8SIA1, TFDP1, TGFA, TGFBR2, TIMELESS, TP53BP1, UHRF1, VEGFA, VPS18	79	yes
Cellular Movement	migration of vascular endothelial cells	1.19E-05	Decreased	-2.574	ADAMTS1, ADM, ANGPT1, ANGPT2, ANXA2, ARHGEF6, CDKN1B, DICER1, DKK1, EFNA1, EFNB2, F2RL1, FGF13, FGF2, FOXO1, FOXO3, GAB1, HHEX, HIF1A, HSP90AB1, ID1, ID3, ITGB3, KDR, KLF2, KLHL20, MAP3K7, MAPKAPK5, MDK, MMP9, NRP1, PTEN, PTGS2, PTPRZ1, RTN4, SP100, SPRY4, SRC, TGFBR2, TIMP2, TNFSF10, VEGFA	42	yes
Cardiovascular System Development and Function	migration of vascular endothelial cells	1.19E-05	Decreased	-2.574	ADAMTS1, ADM, ANGPT1, ANGPT2, ANXA2, ARHGEF6, CDKN1B, DICER1, DKK1, EFNA1, EFNB2, F2RL1, FGF13, FGF2, FOXO1, FOXO3, GAB1, HHEX, HIF1A, HSP90AB1, ID1, ID3, ITGB3, KDR, KLF2, KLHL20, MAP3K7, MAPKAPK5, MDK, MMP9, NRP1, PTEN, PTGS2, PTPRZ1, RTN4, SP100, SPRY4, SRC, TGFBR2, TIMP2, TNFSF10, VEGFA	42	yes
Cellular Movement	invasion of tumor cell lines	9.91E-12	Decreased	-2.567	ABL1, ABL2, ACAT1, ACSL4, ADAMTS1, ADM, AKT3, ANXA1, ARAP3, ATP6V0A4, BATF3, BCAN, BCAR3, BCL2, BDNF, BHLHE41, CALR, CAV1, CBL, CCL2, CCNA2, CCR1, CD97, CDC25B, CDK5, CDK5R1, CDK5RAP3, CDKN1B, CHD1, CMTM8, CSPG4, CTGF, CTSK, CXCR4, DAB2, DIAPH2, DIAPH3, DKK1, DKK3, DNAJB4, E2F5, EFNA1, ENPP2, EPHA2, ETS1, ETS2, ETV1, ETV4, ETV5, FABP5, FAS, FGF2, FHOD1, FOSL1, FOXD3, FOXM1, FURIN, GDF15, GJB1, GNA12, GNAL, HAS2, HAS3, HAX1, HBEGF, HBP1, HIF1A, HIPK2, HMGA1, HMMR, HMOX1, ID1, ID2, IL8, IRS2, ITGA4, ITGB3, JAM3, JUN, JUND, KLF4, KRAS, LDLRAP1, LEF1, LIMK1, LOX, LPAR1, LRIG1, LRP5, LYN, MAP4K4, MARCKS, MCAM, MIA, MITF, MMP16, MMP9, MST1, NAMPT, NDRG1, NFKBIA, NOV, NRP1, NUAK1, PA2G4, PAK4, PAPPA, PARVB, PLAT, PLAUR, PLGRKT, PLXNA1, PLXNB1, POU3F2, PPM1F, PRKCE, PTEN, PTGS2, PTK2, PTP4A2, RALA, RAP1GAP, RND3, RNF144A, ROCK1, RUVBL1, SDC4, SFRP1, SIM2, SLC2A1, SNAI2, SOD2, SP100, SPHK1, SPP1, SPRY2, SRC, SSTR2, ST8SIA1, STMN1, TFAP2A, TFAP2C, TFF3, TGFA, TGFBR2, TIMP2, TIMP3, TNFSF10, TWIST1, VCAN, VEGFA, VEGFB, WWTR1, ZEB2	153	yes
Cancer	neoplasia of cells	1.06E-07	Decreased	-2.536	ABL1, ADAMTS1, ADAMTS9, ANG, ANGPT2, ANGPTL4, ARMC10, BAP1, BAX, BCDIN3D, BCL2, BCL3, BECN1, BMPR1A, CAV1, CBR1, CCL2, CCND1, CDC25A, CDKN1A, CKS1B, CREB3L4, CSNK1E, CTSL1, CXCR4, DAPK1, DCC, DGCR8, DICER1, DKK1, DNAJB4, DYNLL1, EGR1, ENPP2, EPAS1, ETS1, ETV1, F2R, FABP5, FADD, FGF2, FOS, FYN, HAS2, HIF1A, HMOX1, IFNAR1, IL27RA, IL8, ING1, KIT, KRAS, LRRC26, LZTS1, MAP2K1, MCAM, MMP9, MYC, NFKBIA, NOX4, NUPR1, PLAUR, PPAP2A, PPAP2B, PRKAR1A, PRNP, PROM1, PTEN, PTGES, PTK2, PTPRA, RALA, RALB, RIT1, RRM1, RUNX1, RUNX2, RUNX3, RYK, SEMA4D, SMO, SNAI2, SOD2, SOX2, SPHK1, SPRY2, TGFA, TGFBR2, THBS1, TIMP3, TP53BP1, TPD52, TWIST1, TXNIP, VEGFA	95	no
Cellular Movement	migration of tumor cell lines	3.89E-11	Decreased	-2.483	ACSL4, AFAP1, AKAP11, AKT3, ANGPT2, ANKS1A, ANXA1, ANXA2, AP2M1, BCAR3, BHLHE41, CAV1, CCL2, CCL20, CD36, CD97, CDC25B, CDK5, CDKN1B, CHN2, CKLF, CMTM8, CRKL, CTGF, CTSL1, CXCR4, DAB2, DBF4, DCBLD2, DEFB4A/DEFB4B, DGCR6L, E2F5, EGR1, ENPP2, EPHA2, EPOR, ETS1, ETV4, F2RL1, FBXL2, FGF2, FHOD1, FOSL1, FOXD3, FOXM1, FOXO3, FYN, GAB1, GNA13, GOLGA2, HAS2, HAS3, HAX1, HBEGF, HDAC6, HIF1A, HMMR, HMOX1, ID1, IGFBP3, IL8, ING4, ITGA4, ITGA6, ITGB3, JUN, KANK1, KDR, KIDINS220, KLF2, KLF4, KRAS, LAMB3, LIMK1, LMCD1, LOX, LPAR1, LYN, MAP2K1, MAP3K1, MAP3K7, MAP4K4, MC1R, MCAM, MCF2L, MDK, MERTK, MITF, MMP9, MSN, MST1, MYO10, NDRG1, NEDD9, NFKBIA, NOV, NREP, NRP1, PHB, PIK3C2B, PLAUR, PLCL1, PLGRKT, PLXNA1, PLXNB1, PPFIA1, PPM1F, PREX1, PRKD1, PRNP, PTEN, PTGS2, PTK2, PTP4A2, PTPN12, PTPRM, PTPRZ1, PVR, RAB21, RALA, RALB, RAP1GAP, RARRES1, RGS1, RNF144A, RUNX2, RUVBL1, SCNN1A, SEMA3A, SEMA4D, SH3PXD2B, SHC4, SLC16A4, SLC2A1, SNAI2, SOD2, SPHK1, SPP1, SPRY2, SRC, SSH1, ST6GAL1, STMN1, SYK, SYNM, TFAP2A, TFAP2C, TGFA, THBS1, THBS2, TIMP2, TLR4, TNC, TNFSF10, TP53INP1, TRIP6, TWIST1, VASP, VEGFA, VEGFB, VPS28, WWTR1, ZYX	163	yes
Cellular Development	branching of endothelial cell lines	3.94E-04	Decreased	-2.425	ADM, ETS1, FADD, FGF2, LAMA4, VEGFA	6	yes
Cell Morphology	branching of endothelial cell lines	3.94E-04	Decreased	-2.425	ADM, ETS1, FADD, FGF2, LAMA4, VEGFA	6	yes
Cardiovascular System Development and Function	branching of endothelial cell lines	3.94E-04	Decreased	-2.425	ADM, ETS1, FADD, FGF2, LAMA4, VEGFA	6	yes
Cancer	neoplasia of stomach	4.05E-04	Decreased	-2.425	ABL1, AHR, AIM2, ANXA1, APOE, ARAP3, BAX, BIRC5, BRCA1, CASP1, CAV1, CCND1, CD58, CDKN1A, CDKN1B, CDKN2C, COBLL1, DAPK1, DKK1, EPOR, ETV4, FOXM1, GSTM1, HMGA2, HMGCR, IGF2R, IGFBP3, IL1B, IL8, KDR, KRAS, LZTS1, MAL, MDK, MIA, MMP9, MTHFR, MYC, NAMPT, NQO1, NR3C1, NRIP1, NUDT1, PA2G4, PDK4, PHB, PTEN, PTGS2, RNF103, SEC31A, SIAH1, SIRT2, SLC16A4, SOX2, SPP1, TGFBR2, TLR4, TTK, TUBA1C, TUBB3, TUBB4A, UBE2C, UGT2B7	63	no
Gastrointestinal Disease	neoplasia of stomach	4.05E-04	Decreased	-2.425	ABL1, AHR, AIM2, ANXA1, APOE, ARAP3, BAX, BIRC5, BRCA1, CASP1, CAV1, CCND1, CD58, CDKN1A, CDKN1B, CDKN2C, COBLL1, DAPK1, DKK1, EPOR, ETV4, FOXM1, GSTM1, HMGA2, HMGCR, IGF2R, IGFBP3, IL1B, IL8, KDR, KRAS, LZTS1, MAL, MDK, MIA, MMP9, MTHFR, MYC, NAMPT, NQO1, NR3C1, NRIP1, NUDT1, PA2G4, PDK4, PHB, PTEN, PTGS2, RNF103, SEC31A, SIAH1, SIRT2, SLC16A4, SOX2, SPP1, TGFBR2, TLR4, TTK, TUBA1C, TUBB3, TUBB4A, UBE2C, UGT2B7	63	no
Cancer	growth of tumor	2.03E-07	Decreased	-2.414	ABCC1, ABL1, ADAMTS1, ADM, AHR, AKT3, ANG, ANGPT2, ANGPTL4, ANXA2, ATM, BCL2, BECN1, BIRC5, BMI1, BRCA1, CALR, CASP1, CCL2, CCR1, CD36, CD59, CDK5, CDKN1A, CDKN1B, CEACAM1, CENPA, CTLA4, DAB2IP, DAPK1, DKK1, EFNA1, EFNB2, EPAS1, EPHA2, F2R, FADD, FAS, FCER1G, FGF2, FGFR3, FOS, FOXD3, FOXM1, FOXO1, FRMD6, FTH1, GJB1, HBEGF, HIF1A, HMGA1, HMGCR, HMMR, HMOX1, IFNAR1, IGFBP5, IL12A, IL1B, IL27RA, ITGB3, ITGB5, JAM3, KDR, KIDINS220, KRAS, LAMA4, LAMB1, LIF, LTBR, MAP2K1, MAPKAPK5, MCL1, MMP9, MYB, MYC, NCAPG, NDRG1, NEDD9, NFKBIA, NOLC1, NRP1, NT5E, NUAK1, PGF, PTEN, PTGES, PTGS2, RAB27A, RALB, RUNX1, RUNX2, SAT1, SLC16A3, SMO, SOD2, SPP1, SRC, SSTR2, TACC2, TCF4, TGFBR2, THBS1, TIMP2, TLR4, TNC, TNFSF10, TPR, TPX2, TSC22D1, TUBB3, VEGFA	111	no
Cancer	Pancreatic Cancer and Tumors	8.10E-05	Decreased	-2.414	ADAMTS1, AHR, ANXA1, BAX, BIRC5, BNIP3, BRCA1, CASP1, CASP4, CCND1, CD59, CD74, CDK5, CDK5R1, CDKN1A, CDKN1B, CDKN2C, CXCR4, DCLK1, DKK1, EPHA2, FBN2, FXYD3, GDF15, HBEGF, HIF1A, HLA-DRA, HOXB2, ID1, IGFBP3, IL1B, KDR, KIT, KRAS, LAMA4, MMP9, MYB, MYC, NPTX1, NR5A2, PDK4, PLAT, PLAUR, POLE, PRKD1, PROM1, PTEN, PTGES, PTGS2, PTK2, RARA, RRM1, SPP1, SRC, SSTR2, TLR4, TP53INP1, TPM2, TTLL1, TWIST1, VEGFA	61	no
Gastrointestinal Disease	Pancreatic Cancer and Tumors	8.10E-05	Decreased	-2.414	ADAMTS1, AHR, ANXA1, BAX, BIRC5, BNIP3, BRCA1, CASP1, CASP4, CCND1, CD59, CD74, CDK5, CDK5R1, CDKN1A, CDKN1B, CDKN2C, CXCR4, DCLK1, DKK1, EPHA2, FBN2, FXYD3, GDF15, HBEGF, HIF1A, HLA-DRA, HOXB2, ID1, IGFBP3, IL1B, KDR, KIT, KRAS, LAMA4, MMP9, MYB, MYC, NPTX1, NR5A2, PDK4, PLAT, PLAUR, POLE, PRKD1, PROM1, PTEN, PTGES, PTGS2, PTK2, RARA, RRM1, SPP1, SRC, SSTR2, TLR4, TP53INP1, TPM2, TTLL1, TWIST1, VEGFA	61	no
Endocrine System Disorders	Pancreatic Cancer and Tumors	8.10E-05	Decreased	-2.414	ADAMTS1, AHR, ANXA1, BAX, BIRC5, BNIP3, BRCA1, CASP1, CASP4, CCND1, CD59, CD74, CDK5, CDK5R1, CDKN1A, CDKN1B, CDKN2C, CXCR4, DCLK1, DKK1, EPHA2, FBN2, FXYD3, GDF15, HBEGF, HIF1A, HLA-DRA, HOXB2, ID1, IGFBP3, IL1B, KDR, KIT, KRAS, LAMA4, MMP9, MYB, MYC, NPTX1, NR5A2, PDK4, PLAT, PLAUR, POLE, PRKD1, PROM1, PTEN, PTGES, PTGS2, PTK2, RARA, RRM1, SPP1, SRC, SSTR2, TLR4, TP53INP1, TPM2, TTLL1, TWIST1, VEGFA	61	no
Cellular Movement	migration of cells	2.68E-11	Decreased	-2.406	ABCA1, ABCC1, ABL1, ABL2, ABR, ACSL4, ACVR1, ADAM19, ADAMTS1, ADD1, ADM, ADORA2B, ADRBK1, AFAP1, AHR, AKAP11, AKT3, ANGPT1, ANGPT2, ANGPTL2, ANGPTL4, ANKS1A, ANXA1, ANXA2, AP2M1, APOE, ARAP3, ARHGAP24, ARHGEF1, ARHGEF6, ARID5B, ARNT, ATM, BAG3, BAX, BCAR3, BCL2, BDNF, BHLHE40, BHLHE41, BID, BMPR1A, BRCA1, BTK, C1GALT1, C2, C3AR1, CADPS2, CALR, CASP1, CAV1, CBL, CCL2, CCL20, CCL28, CCNA2, CCNB2, CCND1, CCR1, CD2, CD200, CD276, CD36, CD58, CD74, CD97, CD99L2, CDC25B, CDK5, CDK5R1, CDKN1A, CDKN1B, CDKN2C, CEACAM1, CFB, CFH, CHN2, CHST2, CKLF, CLCA2, CLIC4, CMTM8, COL4A3BP, CPB2, CR2, CRKL, CSPG4, CTGF, CTLA4, CTSE, CTSL1, CXCL13, CXCL16, CXCR4, CYTH2, DAB2, DBF4, DCBLD2, DCC, DCLK1, DCX, DEFB4A/DEFB4B, DGCR6L, DIAPH2, DICER1, DKK1, DLX1, DUSP1, E2F3, E2F5, EDNRB, EFNA1, EFNB2, EGLN1, EGR1, EGR2, ELK3, ENPP2, EPAS1, EPHA2, EPOR, ERRFI1, ETS1, ETV4, ETV5, EYA3, F2R, F2RL1, FAP, FAS, FBXL2, FBXO45, FCER1G, FCGR2A, FGF13, FGF2, FHOD1, FKBP4, FOSL1, FOXD3, FOXM1, FOXO1, FOXO3, FOXO4, FTH1, FURIN, FYB, FYN, FZD4, GAB1, GAL3ST1, GJB1, GLI2, GLRX, GNA12, GNA13, GNG12, GOLGA2, GPR183, GTPBP4, HAS2, HAS3, HAX1, HBEGF, HDAC6, HEY1, HHEX, HIF1A, HMMR, HMOX1, HOXB2, HSP90AB1, HSPB1, HSPD1, ICAM1, ID1, ID2, ID3, IFNAR1, IGF2R, IGFBP3, IGFBP5, IL11RA, IL12A, IL16, IL1B, IL27RA, IL8, ING4, IRF5, IRS2, ITGA4, ITGA6, ITGB3, ITGB5, ITK, JAM3, JUN, KANK1, KDR, KIDINS220, KIT, KLF2, KLF4, KLHL20, KRAS, LAMA2, LAMB1, LAMB3, LAMC1, LEF1, LGMN, LHX6, LIMA1, LIMK1, LMCD1, LMO4, LOX, LPAR1, LRP5, LRP8, LTBR, LYN, MAP2K1, MAP2K3, MAP2K5, MAP2K6, MAP3K1, MAP3K12, MAP3K5, MAP3K7, MAP4K4, MAPKAPK5, MARCKS, MARCKSL1, MATN2, MC1R, MCAM, MCF2L, MCM2, MDK, MERTK, MESP1, MGLL, MIA, MITF, MLLT11, MMP9, MPP1, MRAS, MSN, MST1, MYC, MYLK, MYO10, MYO9A, NAMPT, NCKIPSD, NCL, NDRG1, NEDD9, NEO1, NFIA, NFKBIA, NLRP3, NOV, NOX4, NPC1, NQO1, NR2F1, NR4A2, NREP, NRP1, NRTN, NT5E, ONECUT2, OVOL2, P2RX7, PA2G4, PACSIN2, PAK4, PAPPA, PAX3, PAXIP1, PDE4B, PEX11B, PEX2, PEX5, PGF, PHB, PIK3C2B, PIK3CD, PIK3IP1, PLAT, PLAUR, PLCL1, PLGRKT, PLP1, PLXNA1, PLXNB1, PMP22, POU3F2, PPAP2A, PPAP2B, PPFIA1, PPM1F, PPP1R15A, PRDX1, PREX1, PRKAR1A, PRKCE, PRKD1, PRMT2, PRNP, PTEN, PTGDS, PTGES, PTGS2, PTK2, PTP4A1, PTP4A2, PTPN12, PTPN14, PTPRA, PTPRM, PTPRZ1, PVR, RAB21, RAB27A, RAC2, RALA, RALB, RAP1GAP, RAP2A, RAPGEF1, RARA, RARRES1, RCAN1, REPS2, RGS1, RNF144A, ROCK1, ROCK2, RPRD1A, RRAS, RTN4, RUNX1, RUNX2, RUNX3, RUVBL1, RXRA, SARS, SCG2, SCHIP1, SCNN1A, SCPEP1, SDC3, SDC4, SEMA3A, SEMA3C, SEMA4D, SEMA6A, SFRP1, SH2B3, SH3BP1, SH3PXD2B, SHC4, SIX4, SLC16A4, SLC2A1, SLC3A2, SMO, SMPD1, SMPD2, SNAI2, SNX17, SOD2, SORBS3, SORT1, SOX8, SP100, SPHK1, SPP1, SPRY2, SPRY4, SRC, SRGAP1, SSH1, ST3GAL4, ST3GAL6, ST6GAL1, STC1, STIM1, STK24, STK4, STMN1, SYK, SYNM, TFAP2A, TFAP2C, TGFA, TGFBR2, THBS1, THBS2, TIAM2, TIMP2, TIMP3, TIRAP, TLR4, TM4SF1, TNC, TNFRSF12A, TNFRSF1A, TNFRSF1B, TNFSF10, TNFSF13B, TNS3, TP53INP1, TRAF3IP2, TRIM32, TRIP6, TRPV2, TUBB2B, TWIST1, TXK, VASP, VCAN, VDR, VEGFA, VEGFB, VPS18, VPS28, WASL, WISP2, WWTR1, YARS, ZBTB24, ZEB2, ZFAND5, ZP3, ZYX	441	yes
Cell Cycle	entry into S phase of connective tissue cells	2.64E-04	Decreased	-2.356	ATM, CCND1, CDKN1A, CDKN1B, E2F2, E2F3, E2F5, FGF2, ID3, MYC, TFDP1	11	yes
Cancer	quantity of tumor	4.98E-04	Decreased	-2.342	CCND1, CDKN1A, CDKN1B, CDKN2C, DCC, EDNRB, FOXM1, GJB1, HIF1A, HIP1, HIPK1, HMMR, HPGD, ITGB3, JUN, KIT, KRAS, MAP2K1, MMP9, MST1, MYC, NQO1, NT5E, PARP4, PRKCE, PTEN, RARA, RUNX1, SAT1, SPHK1, TAF4, TGFA, TGFBR2,	35	no
Connective Tissue Development and Function	quantity of fibroblast cell lines	7.12E-04	Decreased	-2.333	BECN1, CAV1, CCNA2, CCND1, CDKN1A, DYNLL1, ERRFI1, FAS, GNA12, NOX4, PTGS2, RBBP8, SPHK1, TNFSF10	14	no
Tissue Morphology	quantity of fibroblast	7.12E-04	Decreased	-2.333	BECN1, CAV1, CCNA2, CCND1, CDKN1A, DYNLL1, ERRFI1, FAS, GNA12, NOX4, PTGS2, RBBP8, SPHK1, TNFSF10	14	no
Cell Morphology	cell spreading	1.70E-04	Decreased	-2.312	ANGPT1, ARAP1, ARHGAP24, ATRN, BTK, CBL, CRKL, CSPG4, DAB2, DIAPH2, EDNRB, EFNA1, EPHA2, ETS1, FCGR2A, FGF2, IGF2R, IGFBP5, IL8, ING4, IRAK1, ITGA4, ITGB3, LAMA2, LPAR1, LPXN, LYN, MARCKS, MMP9, MYO10, NEDD9, PACSIN2, PAK4, PARVB, PMP22, PPFIA1, PRKCE, PRKD1, PRNP, PTBP1, PTK2, PTPN12, PTPN14, PTPRA, PVR, RAP1GAP, RAP2A, RAPGEF1, RRBP1, RTN4, SDC4, SEMA3A, SMPD1, SMPD2, SNAI2, SORBS1, SORBS3, SPHK1, SPP1, SPRY2, SRC, SYK, SYNM, THBS1, THBS2, TNC, VASP, VEGFA, WASL, ZYX	70	yes
Cellular Movement	cell movement of prostate cancer cell lines	3.22E-04	Decreased	-2.307	AFAP1, ANXA2, CAV1, CXCR4, DBF4, EFNA1, EPHA2, GDF15, HMOX1, ID1, IL8, ITGB3, KDR, LAMB3, MAP4K4, NDRG1, NRP1, PA2G4, PHB, PRKCE, PRKD1, RALB, RARRES1, TBXAS1, TNFSF10, TWIST1, VEGFA	27	yes
Cellular Movement	cell movement of fibroblast cell lines	1.08E-05	Decreased	-2.303	ABL1, AMD1, BDNF, CCNA2, CDKN1A, CDKN1B, CLIC4, CRKL, ELK3, FGF2, FOS, FOSL1, GAB1, GNA13, GNG12, HAS2, HAS3, HAX1, HBEGF, IL8, KLF2, LIMA1, LOX, MARCKS, MMP9, MST1, MTSS1, MYLK, NOX4, NRCAM, PLAUR, PRKD1, PTEN, PTGDS, PTGS2, PTK2, PTPN12, PTPRA, PVR, RAC2, SPP1, SRC, TP53INP1, TRIM32, VEGFA, WASL	46	yes
Connective Tissue Development and Function	cell movement of fibroblast cell lines	1.08E-05	Decreased	-2.303	ABL1, AMD1, BDNF, CCNA2, CDKN1A, CDKN1B, CLIC4, CRKL, ELK3, FGF2, FOS, FOSL1, GAB1, GNA13, GNG12, HAS2, HAS3, HAX1, HBEGF, IL8, KLF2, LIMA1, LOX, MARCKS, MMP9, MST1, MTSS1, MYLK, NOX4, NRCAM, PLAUR, PRKD1, PTEN, PTGDS, PTGS2, PTK2, PTPN12, PTPRA, PVR, RAC2, SPP1, SRC, TP53INP1, TRIM32, VEGFA, WASL	46	yes

Cellular Development	differentiation ofcells	5.84E-09	Decreased	-2.293	ABCC4, ABI1, ABL1, ABL2, ACACA, ACVR1, ADAMTS9, ADD1, ADK, ADM, ADORA2B, ADRBK1, AFF1, AHCTF1, AHR, AMD1, ANG, ANGPT1, ANGPT2, ANGPTL2, ANKRD54, ANXA1, ANXA2, ARID2, ARID5B, ARL4A, ARNT, ASPA, ATM, ATP7A, BAIAP2,BATF, BATF3, BAX, BCL2, BCL2L11, BCL3, BDNF, BECN1, BHLHE40, BHLHE41, BMI1, BMP1, BMPR1A, BNIP3, BRCA1, BTG1, BTG3, BTK, C14orf169, C3AR1, CADPS2, CALR, CAV1, CBL, CBY1, CCL2, CCND1, CCR1, CD2, CD200, CD276, CD36, CD74, CDC25A, CDK5, CDK5R1, CDK5RAP3, CDK6, CDKN1A, CDKN1B, CDKN2C, CEACAM1, CEBPB, CEBPD, CHD1, CHD7, CHKA, CITED1, CLIC1, CLIC4, CMTM8, COL11A2, CR2, CREB3L2, CREB5, CSDA, CTDSPL, CTGF, CTHRC1, CTLA4, CTNNBIP1, CTSE, CTSK, CXCR4, CYTL1, DAB2, DCX, DDIT3, DEDD, DEF6, DHCR7, DICER1, DISP1, DKK1, DLK2, DLL3, DLX1, DSP, DUSP1, DUSP5, DVL2, DYRK3, E2F2, EDNRB, EFNA1, EFNB2, EGR1, EGR2, EGR3, ELF1, ELK4, ENC1, EOMES, EPAS1, EPHA2, EPHA4, EPOR, ERO1L, ERRFI1, ETS1, ETS2, ETV4, ETV5, EXOC6, EXTL1, FABP5, FADD, FAM20C, FAS, FCER1G, FEZ1, FGF2, FGFR3, FLI1, FNDC3B, FOS, FOSL1, FOXD3, FOXM1, FOXO1, FOXO3, FOXO4, FST, FSTL3, FYN, FZD1, FZD2, FZD7, GAB1, GAS1, GDPD5, GHR, GJA3, GLI2, GNA12, GNA13, GNA15, GNAL, GNL3, GPC4, GPSM2, GRAP2, HAS2, HBEGF, HBP1, HDAC7, HES1, HEY1, HEY2, HHEX, HIF1A, HINFP, HIST1H4A (includes others), HIVEP2, HMG20B, HMGA2, HMGB2, HMGB3, HMOX1, HOXA5, HOXB13, HOXB2, HOXD11, HPS4, HSF4, HSP90AB1, HSPA2, HSPD1, HTR7, ICAM1, ID1, ID2, ID3, IFI16, IFNAR1, IFNGR2, IGF2R, IGFBP3, IGFBP5, IKZF4, IL11RA, IL12A, IL17D, IL1B, IL1RAP, IL1RAPL1, IL27RA, IL7R, IL8, IRF4, IRF5, IRS2, IRX3, ITGA6, ITGB3, ITGB5, ITK, ITPKB, JAM3, JUN, JUND, KBTBD10, KDR, KIT, KLF13, KLF15, KLF4, KLF9, KRAS, L3MBTL1, LAMA2, LAMA4, LAMB3, LAMC1, LDB1, LEF1, LIF, LIMK1, LIMS1, LMO4, LPIN1, LRIG1, LRP5, LRP8, LRRC17, LTBP4, LTBR, LYN, MAF, MAFF, MAFG, MAGED1, MAL, MALT1, MAP2K1, MAP2K3, MAP2K6, MAP3K12, MAP3K5, MAP3K7, MBP, MC1R, MCC, MCL1, MDK, MEF2C, MERTK, MESP1, MITF, MKS1, MLLT11, MLPH, MMP9, MRAS, MST1, MVK, MXD3, MYB, MYC, MYO5A, N4BP2L2, NAMPT, NDRG1, NFIA, NFIB, NFKBIA, NKX2-5, NMRK2, NOC3L, NOV, NOX4, NR2F1, NR3C1, NR4A2, NREP, NRP1, NRTN, OCA2, OLIG1, ONECUT2, OSBPL9, OTX1, OVOL2, PA2G4, PAK4, PARP2, PAX3, PBXIP1, PCSK1, PDK4, PER3, PEX11B, PGF, PIK3CD, PIM3, PKDCC, PKNOX1, PLAT, PLAUR, PLCL1, PLP1, PMP22, PNP, POU3F1, POU3F2, PPARGC1A, PPP1CC, PPP1R13L, PRAME, PRKAR1A, PRKD1, PRMT5, PRNP, PTEN, PTGDS, PTGS2, PTK2, PTPRA, PTPRE, PTPRZ1, QKI, RAB27A, RAC2, RACGAP1, RARA, RARB, RARRES3, RASA3, RASSF2, RBM38, RIT1, RND3, ROCK1, ROCK2, ROGDI, RQCD1, RRAS, RTN4, RUNX1, RUNX2, RUNX3, RXRA, RYK, SACS, SARS, SATB1, SDC3, SELENBP1, SEMA3A, SEMA4D, SFRP1, SFXN1, SH2B3, SH3PXD2A, SH3PXD2B, SHB, SIK3, SLC3A2, SMAD6, SMARCA1, SMO, SNAI2, SOCS2, SOD2, SORT1, SOX2, SOX4, SOX6, SOX8, SPEN, SPHK1, SPP1, SPRED1, SPRED2, SPRY1, SPRY2, SPRY4, SRC, SSBP2, ST8SIA1, STAT2, STC1, STIM1, STK39, STK4, STMN1, SYK, TACC3, TBX2, TCF4, TCF7L2, TFAP2A, TGFA, TGFBR2, TGIF1, THBS1, THBS2, TIMP2, TIMP3, TIRAP, TLR4, TMEM67, TNC, TNFRSF12A, TNFRSF1A, TNFRSF1B, TNFSF10, TNFSF13B, TRIB3, TRIM24, TRIM32, TRPM1, TSC22D3, TUBB3, TWIST1, TXK, TXNIP, TYRP1, UBD, ULK1, UPK1A, VASP, VCAN, VDR, VEGFA, VGF, WWTR1, XBP1, YWHAG, ZBTB17, ZFP36, ZIC2, ZNF536	465	yes
Cancer	head and neck cancer	4.90E-07	Decreased	-2.293	ABL1, ACTA2, ADAMTS1, ADAMTS9, ADSL, AKT3, ALAD, ANGPT2, ANO1, ANXA1, ANXA2, ARHGEF2, ATM, BAX, BCCIP, BCL2, BCL3, BDNF, BMI1, BRCA1, CALCOCO2, CASP4, CAV1, CCDC41, CCNB2, CCND1, CDK6, CDKN1A, CDKN1B, CDKN2C, CEBPD, CHKA, CHRM1, CHRNB1, CXCL16, CXCR4, DAPK1, DHRS4, DKC1, DVL2, E2F3, ECE2, EFNB2, EGR1, EIF2C2, ENC1, EPHA2, EPS15, ETS1, FABP3, FABP5, FADD, FASN, FOS, FOXM1, FOXO3, FOXO4, FTH1, FURIN, FZD7, GEMIN5, GLI2, GNA12, GNB4, GSTM1, HIPK2, HMGA1, HMGA2, HMGB2, HMOX1, HSP90AB1, ID1, IDH1, IGFBP3, IGFBP5, IL8, ING1, JUN, KDR, KHDRBS3, KIT, KRAS, KRT18, LAMA4, LAMB3, LMO4, LPAR1, LTBR, LYN, MAP4K4, MARCKS, MCL1, MCM2, MIA, MINPP1, MMP9, MSMO1, MTHFR, MYC, NCOA4, NFIB, NPTX1, NQO1, NR3C1, NRIP1, NUSAP1, NXT1, OLIG1, PAM16, PCM1, PGF, PINK1, PLAT, PPFIA1, PPIL1, PRKAR1A, PRKCE, PROM1, PTEN, PTGS2, PTPRM, RAC2, RAP1GAP, RUNX2, RXRG, SEMA4D, SFRP1, SLC2A1, SMO, SOX2, SP110, SPHK1, SPP1, SRC, STAT2, SYK, TERF1, TFAP2A, TFF3, TGFA, TGFBR2, THBS1, TIMP3, TLR4, TMEM45A, TNC, TNFRSF1A, TRIM24, TRIM32, TUBA1C, TUBB3, TUBB4A, TWIST1, UBE2C, ZEB2, ZNF185	156	no
Cancer	central nervous system tumor	4.59E-05	Decreased	-2.283	ABL1, ACTA2, ADAM19, AKT3, ALAD, ANXA1, ANXA2, ARHGEF2, B4GALT5, BAX, BCL2, BCL3, BDNF, BIRC5, BMI1, CAV1, CCDC41, CCNB2, CCND1, CDK6, CDKN1B, CDKN2C, CEBPD, CHKA, CHRNB1, CIC, CXCL16, DAPK1, DHRS4, DKC1, DVL2, E2F3, EGR1, ENC1, EPHA2, ETV4, FGF2, FOXM1, FOXO3, FOXO4, FURIN, GEMIN5, GLI2, GNB4, H3F3A/H3F3B, HBEGF, HIPK2, HMGA1, HMGA2, HMGB2, HMOX1, ID1, ID2, IDH1, ING4, KDR, KHDRBS3, KRAS, LAMA4, LAMB1, LAMB3, LPAR1, MAP4K4, MARCKS, MCL1, MIA, MMP9, MYC, NFIB, NPTX1, NR3C1, NRIP1, NUSAP1, OLIG1, PAM16, PINK1, PROM1, PTEN, PTPRM, RAC2, RHPN2, SEMA4D, SFRP1, SMO, SNAI2, SOX2, SPHK1, SRC, STAT2, TERF1, TFAP2A, TGFA, TNC, TNFRSF1A, TUBB4A, UBE2C, ZEB2	97	no
Neurological Disease	central nervous system tumor	4.59E-05	Decreased	-2.283	ABL1, ACTA2, ADAM19, AKT3, ALAD, ANXA1, ANXA2, ARHGEF2, B4GALT5, BAX, BCL2, BCL3, BDNF, BIRC5, BMI1, CAV1, CCDC41, CCNB2, CCND1, CDK6, CDKN1B, CDKN2C, CEBPD, CHKA, CHRNB1, CIC, CXCL16, DAPK1, DHRS4, DKC1, DVL2, E2F3, EGR1, ENC1, EPHA2, ETV4, FGF2, FOXM1, FOXO3, FOXO4, FURIN, GEMIN5, GLI2, GNB4, H3F3A/H3F3B, HBEGF, HIPK2, HMGA1, HMGA2, HMGB2, HMOX1, ID1, ID2, IDH1, ING4, KDR, KHDRBS3, KRAS, LAMA4, LAMB1, LAMB3, LPAR1, MAP4K4, MARCKS, MCL1, MIA, MMP9, MYC, NFIB, NPTX1, NR3C1, NRIP1, NUSAP1, OLIG1, PAM16, PINK1, PROM1, PTEN, PTPRM, RAC2, RHPN2, SEMA4D, SFRP1, SMO, SNAI2, SOX2, SPHK1, SRC, STAT2, TERF1, TFAP2A, TGFA, TNC, TNFRSF1A, TUBB4A, UBE2C, ZEB2	97	no
Cellular Movement	cell movement	7.71E-12	Decreased	-2.277	ABCA1, ABCC1, ABL1, ABL2, ABR, ACSL4, ACVR1, ADAM19, ADAMTS1, ADD1, ADM, ADORA2B, ADRBK1, AFAP1, AHR, AKAP11, AKT3, AMD1, ANGPT1, ANGPT2, ANGPTL2, ANGPTL4, ANKS1A, ANXA1, ANXA2, AP2M1, APOE, ARAP3, ARHGAP24, ARHGEF1, ARHGEF6, ARID5B, ARNT, ARPC1B, ATM, ATP2B4, BAG3, BAX, BCAN, BCAR3, BCL2, BDNF, BHLHE40, BHLHE41, BID, BMPR1A, BRCA1, BTK, C1GALT1, C2, C3AR1, CADPS2, CALR, CASP1, CAV1, CBL, CCL2, CCL20, CCL28, CCNA2, CCNB2, CCND1, CCR1, CD2, CD200, CD276, CD36, CD58, CD59, CD74, CD97, CD99L2, CDC25B, CDK5, CDK5R1, CDKN1A, CDKN1B, CDKN2C, CEACAM1, CEBPD, CFB, CFH, CHN2, CHST2, CKLF, CLCA2, CLIC4, CMTM8, COL4A3BP, CPB2, CR2, CRKL, CSPG4, CTGF, CTLA4, CTSE, CTSL1, CXCL13, CXCL16, CXCR4, CYTH2, DAB2, DBF4, DCBLD2, DCC, DCLK1, DCX, DEFB4A/DEFB4B, DGCR6L, DIAPH2, DICER1, DKK1, DKK3, DLX1, DNAJB4, DUSP1, DUSP6, E2F2, E2F3, E2F5, EDNRB, EFNA1, EFNB2, EGLN1, EGR1, EGR2, ELK3, ENPP2, EPAS1, EPHA2, EPHA4, EPOR, ERRFI1, ETS1, ETV4, ETV5, EYA3, F2R, F2RL1, FADD, FAP, FAS, FBXL2, FBXO45, FCER1G, FCGR2A, FGF13, FGF2, FHOD1, FKBP4, FNBP1L, FOS, FOSL1, FOXD3, FOXM1, FOXO1, FOXO3, FOXO4, FST, FTH1, FURIN, FYB, FYN, FZD4, GAB1, GAL3ST1, GDF15, GEMIN5, GJB1, GLI2, GLRX, GNA12, GNA13, GNG12, GOLGA2, GPR183, GTPBP4, HAS2, HAS3, HAX1, HBEGF, HDAC6, HEY1, HEY2, HHEX, HIF1A, HIPK2, HMGB2, HMMR, HMOX1, HOXB2, HSP90AB1, HSPB1, HSPD1, ICAM1, ID1, ID2, ID3, IFNAR1, IGF2R, IGFBP3, IGFBP5, IL11RA, IL12A, IL16, IL1B, IL27RA, IL8, ING4, IRF5, IRS2, ITGA4, ITGA6, ITGB3, ITGB5, ITK, JAM3, JUN, KANK1, KDR, KIDINS220, KIT, KLF2, KLF4, KLHL20, KRAS, LAMA2, LAMB1, LAMB3, LAMC1, LEF1, LGMN, LHX6, LIF, LIMA1, LIMK1, LIMS1, LMCD1, LMO4, LOX, LPAR1, LRIG1, LRP5, LRP8, LTBR, LYN, MAP2K1, MAP2K3, MAP2K5, MAP2K6, MAP3K1, MAP3K12, MAP3K5, MAP3K7, MAP4K4, MAPKAPK5, MARCKS, MARCKSL1, MATN2, MBP, MC1R, MCAM, MCF2L, MCM2, MDK, MERTK, MESP1, MGLL, MIA, MITF, MLLT11, MMP9, MPP1, MRAS, MSN, MST1, MTSS1, MYB, MYC, MYLK, MYO10, MYO9A, NAMPT, NCKIPSD, NCL, NCOA4, NDRG1, NEDD9, NEO1, NFIA, NFKBIA, NLRP3, NOV, NOX4, NPC1, NPTX1, NQO1, NR2F1, NR4A2, NRCAM, NREP, NRP1, NRTN, NT5E, ONECUT2, OVOL2, P2RX7, PA2G4, PACSIN2, PAK4, PAPPA, PAX3, PAXIP1, PDE4B, PEX11B, PEX2, PEX5, PGF, PHB, PIK3C2B, PIK3CD, PIK3IP1, PLAT, PLAUR, PLCL1, PLGRKT, PLP1, PLXNA1, PLXNB1, PMP22, POU3F2, PPAP2A, PPAP2B, PPFIA1, PPM1F, PPP1R15A, PPP1R9A, PPP3CC, PRDX1, PREX1, PRKAR1A, PRKCE, PRKD1, PRMT2, PRNP, PTEN, PTGDS, PTGES, PTGS2, PTK2, PTP4A1, PTP4A2, PTPN12, PTPN14, PTPRA, PTPRM, PTPRZ1, PVR, RAB21, RAB27A, RAC2, RALA, RALB, RAP1GAP, RAP2A, RAPGEF1, RARA, RARRES1, RCAN1, REPS2, RGS1, RIN1, RNF144A, ROCK1, ROCK2, ROPN1B, RPRD1A, RRAS, RTN4, RUNX1, RUNX2, RUNX3, RUVBL1, RXRA, SARS, SCG2, SCHIP1, SCNN1A, SCPEP1, SDC3, SDC4, SEMA3A, SEMA3C, SEMA4D, SEMA6A, SFRP1, SH2B3, SH3BP1, SH3PXD2A, SH3PXD2B, SHC4, SIX4, SLC16A4, SLC2A1, SLC2A8, SLC3A2, SMO, SMPD1, SMPD2, SNAI2, SNX17, SNX27, SOCS2, SOD2, SORBS3, SORD, SORT1, SOX8, SP100, SPHK1, SPP1, SPRY2, SPRY4, SRC, SRGAP1, SSH1, ST3GAL4, ST3GAL5, ST3GAL6, ST6GAL1, STARD13, STC1, STIM1, STK24, STK4, STMN1, SYK, SYNM, TBXAS1, TFAP2A, TFAP2C, TFF3, TGFA, TGFBR2, TGFBR3, THBS1, THBS2, TIAM2, TIMP2, TIMP3, TIRAP, TLR4, TM4SF1, TNC, TNFRSF12A, TNFRSF1A, TNFRSF1B, TNFSF10, TNFSF13B, TNS3, TP53INP1, TPR, TPST2, TRAF3IP2, TRIB1, TRIM32, TRIP6, TRPV2, TUBA1C, TUBB2B, TWIST1, TXK, VASP, VCAN, VDR, VEGFA, VEGFB, VPS18, VPS28, WASL, WISP2, WWTR1, YARS, ZBTB24, ZEB2, ZFAND5, ZP3, ZYX	488	yes
Cellular Development	T cell development	1.12E-03	Decreased	-2.273	ABL1, AFF1, AHR, ANXA1, ATM, ATP7A, BATF, BAX, BCL2, BCL2L11, BCL3, BHLHE40, BHLHE41, BIRC5, BRCA1, C3AR1, CASP1, CBL, CCND1, CD2, CD74, CDKN1A, CDKN1B, CEBPB, CHD7, CTLA4, CXCR4, DEF6, DICER1, DKK1, E2F2, EFNA1, EFNB2, EGR1, EGR2, EGR3, ELK4, EOMES, EPHA2, EPHA4, ETS1, ETS2, FADD, FAS, FCER1G, FCGR2A, FOXO1, FOXO3, FYN, FZD7, GRAP2, HIF1A, HIVEP2, HSPD1, ICAM1, ID1, ID2, ID3, IFNAR1, IFNAR2, IFNGR2, IGF2R, IL12A, IL1B, IL27RA, IL7R, IRF4, IRF5, ITGA4, ITK, ITPKB, KDR, KIT, KLF4, LEF1, LIF, MAF, MALT1, MAP2K1, MAP3K7, MBP, MCL1, MLLT11, MNT, MYB, NFKBIA, PCSK1, PHLPP1, PIK3CD, PKNOX1, PLP1, PNP, PRKD1, PRNP, PTGS2, RUNX1, RUNX2, RUNX3, SATB1, SLC3A2, SNAI2, SOX4, SPP1, STAT2, SYK, TCF4, TGFBR2, TNFRSF1A, TNFRSF1B, TNFSF10, TNFSF13B, TXK, VEGFA, WASL, ZBTB17	115	no
Cellular Function and Maintenance	T cell development	1.12E-03	Decreased	-2.273	ABL1, AFF1, AHR, ANXA1, ATM, ATP7A, BATF, BAX, BCL2, BCL2L11, BCL3, BHLHE40, BHLHE41, BIRC5, BRCA1, C3AR1, CASP1, CBL, CCND1, CD2, CD74, CDKN1A, CDKN1B, CEBPB, CHD7, CTLA4, CXCR4, DEF6, DICER1, DKK1, E2F2, EFNA1, EFNB2, EGR1, EGR2, EGR3, ELK4, EOMES, EPHA2, EPHA4, ETS1, ETS2, FADD, FAS, FCER1G, FCGR2A, FOXO1, FOXO3, FYN, FZD7, GRAP2, HIF1A, HIVEP2, HSPD1, ICAM1, ID1, ID2, ID3, IFNAR1, IFNAR2, IFNGR2, IGF2R, IL12A, IL1B, IL27RA, IL7R, IRF4, IRF5, ITGA4, ITK, ITPKB, KDR, KIT, KLF4, LEF1, LIF, MAF, MALT1, MAP2K1, MAP3K7, MBP, MCL1, MLLT11, MNT, MYB, NFKBIA, PCSK1, PHLPP1, PIK3CD, PKNOX1, PLP1, PNP, PRKD1, PRNP, PTGS2, RUNX1, RUNX2, RUNX3, SATB1, SLC3A2, SNAI2, SOX4, SPP1, STAT2, SYK, TCF4, TGFBR2, TNFRSF1A, TNFRSF1B, TNFSF10, TNFSF13B, TXK, VEGFA, WASL, ZBTB17	115	no
Hematological System Development and Function	T cell development	1.12E-03	Decreased	-2.273	ABL1, AFF1, AHR, ANXA1, ATM, ATP7A, BATF, BAX, BCL2, BCL2L11, BCL3, BHLHE40, BHLHE41, BIRC5, BRCA1, C3AR1, CASP1, CBL, CCND1, CD2, CD74, CDKN1A, CDKN1B, CEBPB, CHD7, CTLA4, CXCR4, DEF6, DICER1, DKK1, E2F2, EFNA1, EFNB2, EGR1, EGR2, EGR3, ELK4, EOMES, EPHA2, EPHA4, ETS1, ETS2, FADD, FAS, FCER1G, FCGR2A, FOXO1, FOXO3, FYN, FZD7, GRAP2, HIF1A, HIVEP2, HSPD1, ICAM1, ID1, ID2, ID3, IFNAR1, IFNAR2, IFNGR2, IGF2R, IL12A, IL1B, IL27RA, IL7R, IRF4, IRF5, ITGA4, ITK, ITPKB, KDR, KIT, KLF4, LEF1, LIF, MAF, MALT1, MAP2K1, MAP3K7, MBP, MCL1, MLLT11, MNT, MYB, NFKBIA, PCSK1, PHLPP1, PIK3CD, PKNOX1, PLP1, PNP, PRKD1, PRNP, PTGS2, RUNX1, RUNX2, RUNX3, SATB1, SLC3A2, SNAI2, SOX4, SPP1, STAT2, SYK, TCF4, TGFBR2, TNFRSF1A, TNFRSF1B, TNFSF10, TNFSF13B, TXK, VEGFA, WASL, ZBTB17	115	no
Hematopoiesis	T cell development	1.12E-03	Decreased	-2.273	ABL1, AFF1, AHR, ANXA1, ATM, ATP7A, BATF, BAX, BCL2, BCL2L11, BCL3, BHLHE40, BHLHE41, BIRC5, BRCA1, C3AR1, CASP1, CBL, CCND1, CD2, CD74, CDKN1A, CDKN1B, CEBPB, CHD7, CTLA4, CXCR4, DEF6, DICER1, DKK1, E2F2, EFNA1, EFNB2, EGR1, EGR2, EGR3, ELK4, EOMES, EPHA2, EPHA4, ETS1, ETS2, FADD, FAS, FCER1G, FCGR2A, FOXO1, FOXO3, FYN, FZD7, GRAP2, HIF1A, HIVEP2, HSPD1, ICAM1, ID1, ID2, ID3, IFNAR1, IFNAR2, IFNGR2, IGF2R, IL12A, IL1B, IL27RA, IL7R, IRF4, IRF5, ITGA4, ITK, ITPKB, KDR, KIT, KLF4, LEF1, LIF, MAF, MALT1, MAP2K1, MAP3K7, MBP, MCL1, MLLT11, MNT, MYB, NFKBIA, PCSK1, PHLPP1, PIK3CD, PKNOX1, PLP1, PNP, PRKD1, PRNP, PTGS2, RUNX1, RUNX2, RUNX3, SATB1, SLC3A2, SNAI2, SOX4, SPP1, STAT2, SYK, TCF4, TGFBR2, TNFRSF1A, TNFRSF1B, TNFSF10, TNFSF13B, TXK, VEGFA, WASL, ZBTB17	115	no
Lymphoid Tissue Structure and Development	T cell development	1.12E-03	Decreased	-2.273	ABL1, AFF1, AHR, ANXA1, ATM, ATP7A, BATF, BAX, BCL2, BCL2L11, BCL3, BHLHE40, BHLHE41, BIRC5, BRCA1, C3AR1, CASP1, CBL, CCND1, CD2, CD74, CDKN1A, CDKN1B, CEBPB, CHD7, CTLA4, CXCR4, DEF6, DICER1, DKK1, E2F2, EFNA1, EFNB2, EGR1, EGR2, EGR3, ELK4, EOMES, EPHA2, EPHA4, ETS1, ETS2, FADD, FAS, FCER1G, FCGR2A, FOXO1, FOXO3, FYN, FZD7, GRAP2, HIF1A, HIVEP2, HSPD1, ICAM1, ID1, ID2, ID3, IFNAR1, IFNAR2, IFNGR2, IGF2R, IL12A, IL1B, IL27RA, IL7R, IRF4, IRF5, ITGA4, ITK, ITPKB, KDR, KIT, KLF4, LEF1, LIF, MAF, MALT1, MAP2K1, MAP3K7, MBP, MCL1, MLLT11, MNT, MYB, NFKBIA, PCSK1, PHLPP1, PIK3CD, PKNOX1, PLP1, PNP, PRKD1, PRNP, PTGS2, RUNX1, RUNX2, RUNX3, SATB1, SLC3A2, SNAI2, SOX4, SPP1, STAT2, SYK, TCF4, TGFBR2, TNFRSF1A, TNFRSF1B, TNFSF10, TNFSF13B, TXK, VEGFA, WASL, ZBTB17	115	no
Cell-mediated Immune Response	T cell development	1.12E-03	Decreased	-2.273	ABL1, AFF1, AHR, ANXA1, ATM, ATP7A, BATF, BAX, BCL2, BCL2L11, BCL3, BHLHE40, BHLHE41, BIRC5, BRCA1, C3AR1, CASP1, CBL, CCND1, CD2, CD74, CDKN1A, CDKN1B, CEBPB, CHD7, CTLA4, CXCR4, DEF6, DICER1, DKK1, E2F2, EFNA1, EFNB2, EGR1, EGR2, EGR3, ELK4, EOMES, EPHA2, EPHA4, ETS1, ETS2, FADD, FAS, FCER1G, FCGR2A, FOXO1, FOXO3, FYN, FZD7, GRAP2, HIF1A, HIVEP2, HSPD1, ICAM1, ID1, ID2, ID3, IFNAR1, IFNAR2, IFNGR2, IGF2R, IL12A, IL1B, IL27RA, IL7R, IRF4, IRF5, ITGA4, ITK, ITPKB, KDR, KIT, KLF4, LEF1, LIF, MAF, MALT1, MAP2K1, MAP3K7, MBP, MCL1, MLLT11, MNT, MYB, NFKBIA, PCSK1, PHLPP1, PIK3CD, PKNOX1, PLP1, PNP, PRKD1, PRNP, PTGS2, RUNX1, RUNX2, RUNX3, SATB1, SLC3A2, SNAI2, SOX4, SPP1, STAT2, SYK, TCF4, TGFBR2, TNFRSF1A, TNFRSF1B, TNFSF10, TNFSF13B, TXK, VEGFA, WASL, ZBTB17	115	no
Cellular Development	development of leukocytes	2.73E-04	Decreased	-2.266	ABL1, ADM, AFF1, AHR, ANXA1, ATM, ATP7A, BATF, BAX, BCL2, BCL2L11, BCL3, BHLHE40, BHLHE41, BIRC5, BRCA1, BTK, C3AR1, CASP1, CBL, CCND1, CD2, CD74, CDKN1A, CDKN1B, CEBPB, CHD7, CR2, CTLA4, CXCR4, DEF6, DICER1, DKK1, E2F2, EFNA1, EFNB2, EGR1, EGR2, EGR3, ELK4, EOMES, EPHA2, EPHA4, EPOR, ETS1, ETS2, FADD, FAS, FCER1G, FCGR2A, FGF2, FOS, FOXO1, FOXO3, FYN, FZD7, GRAP2, HIF1A, HIVEP2, HSPD1, ICAM1, ID1, ID2, ID3, IFNAR1, IFNAR2, IFNGR2, IGF2R, IL11RA, IL12A, IL1B, IL27RA, IL7R, IRF4, IRF5, ITGA4, ITGB3, ITK, ITPKB, KDR, KIT, KLF2, KLF4, KRAS, LEF1, LIF, LTBR, LYN, MAF, MALT1, MAP2K1, MAP3K7, MBP, MCL1, MDK, MERTK, MLLT11, MNT, MYB, NFKBIA, NQO1, PCSK1, PGF, PHLPP1, PIK3CD, PKNOX1, PLEKHA2, PLP1, PNP, PRKD1, PRNP, PTGS2, RALA, RALB, RARA, RUNX1, RUNX2, RUNX3, SATB1, SLC3A2, SMO, SNAI2, SOX4, SPP1, STAT2, SYK, TCF4, TGFBR2, TNFRSF1A, TNFRSF1B, TNFSF10, TNFSF13B, TP53BP1, TXK, VEGFA, WASL, XBP1, ZBTB17	138	no
Hematological System Development and Function	development of leukocytes	2.73E-04	Decreased	-2.266	ABL1, ADM, AFF1, AHR, ANXA1, ATM, ATP7A, BATF, BAX, BCL2, BCL2L11, BCL3, BHLHE40, BHLHE41, BIRC5, BRCA1, BTK, C3AR1, CASP1, CBL, CCND1, CD2, CD74, CDKN1A, CDKN1B, CEBPB, CHD7, CR2, CTLA4, CXCR4, DEF6, DICER1, DKK1, E2F2, EFNA1, EFNB2, EGR1, EGR2, EGR3, ELK4, EOMES, EPHA2, EPHA4, EPOR, ETS1, ETS2, FADD, FAS, FCER1G, FCGR2A, FGF2, FOS, FOXO1, FOXO3, FYN, FZD7, GRAP2, HIF1A, HIVEP2, HSPD1, ICAM1, ID1, ID2, ID3, IFNAR1, IFNAR2, IFNGR2, IGF2R, IL11RA, IL12A, IL1B, IL27RA, IL7R, IRF4, IRF5, ITGA4, ITGB3, ITK, ITPKB, KDR, KIT, KLF2, KLF4, KRAS, LEF1, LIF, LTBR, LYN, MAF, MALT1, MAP2K1, MAP3K7, MBP, MCL1, MDK, MERTK, MLLT11, MNT, MYB, NFKBIA, NQO1, PCSK1, PGF, PHLPP1, PIK3CD, PKNOX1, PLEKHA2, PLP1, PNP, PRKD1, PRNP, PTGS2, RALA, RALB, RARA, RUNX1, RUNX2, RUNX3, SATB1, SLC3A2, SMO, SNAI2, SOX4, SPP1, STAT2, SYK, TCF4, TGFBR2, TNFRSF1A, TNFRSF1B, TNFSF10, TNFSF13B, TP53BP1, TXK, VEGFA, WASL, XBP1, ZBTB17	138	no
Hematopoiesis	development of leukocytes	2.73E-04	Decreased	-2.266	ABL1, ADM, AFF1, AHR, ANXA1, ATM, ATP7A, BATF, BAX, BCL2, BCL2L11, BCL3, BHLHE40, BHLHE41, BIRC5, BRCA1, BTK, C3AR1, CASP1, CBL, CCND1, CD2, CD74, CDKN1A, CDKN1B, CEBPB, CHD7, CR2, CTLA4, CXCR4, DEF6, DICER1, DKK1, E2F2, EFNA1, EFNB2, EGR1, EGR2, EGR3, ELK4, EOMES, EPHA2, EPHA4, EPOR, ETS1, ETS2, FADD, FAS, FCER1G, FCGR2A, FGF2, FOS, FOXO1, FOXO3, FYN, FZD7, GRAP2, HIF1A, HIVEP2, HSPD1, ICAM1, ID1, ID2, ID3, IFNAR1, IFNAR2, IFNGR2, IGF2R, IL11RA, IL12A, IL1B, IL27RA, IL7R, IRF4, IRF5, ITGA4, ITGB3, ITK, ITPKB, KDR, KIT, KLF2, KLF4, KRAS, LEF1, LIF, LTBR, LYN, MAF, MALT1, MAP2K1, MAP3K7, MBP, MCL1, MDK, MERTK, MLLT11, MNT, MYB, NFKBIA, NQO1, PCSK1, PGF, PHLPP1, PIK3CD, PKNOX1, PLEKHA2, PLP1, PNP, PRKD1, PRNP, PTGS2, RALA, RALB, RARA, RUNX1, RUNX2, RUNX3, SATB1, SLC3A2, SMO, SNAI2, SOX4, SPP1, STAT2, SYK, TCF4, TGFBR2, TNFRSF1A, TNFRSF1B, TNFSF10, TNFSF13B, TP53BP1, TXK, VEGFA, WASL, XBP1, ZBTB17	138	no

Lymphoid Tissue Structure and Development	development of leukocytes	2.73E-04	Decreased	-2.266	ABL1, ADM, AFF1, AHR, ANXA1, ATM, ATP7A, BATF, BAX, BCL2, BCL2L11, BCL3, BHLHE40, BHLHE41, BIRC5, BRCA1, BTK, C3AR1, CASP1, CBL, CCND1, CD2, CD74, CDKN1A, CDKN1B, CEBPB, CHD7, CR2, CTLA4, CXCR4, DEF6, DICER1, DKK1, E2F2, EFNA1, EFNB2, EGR1, EGR2, EGR3, ELK4, EOMES, EPHA2, EPHA4, EPOR, ETS1, ETS2, FADD, FAS, FCER1G, FCGR2A, FGF2, FOS, FOXO1, FOXO3, FYN, FZD7, GRAP2, HIF1A, HIVEP2, HSPD1, ICAM1, ID1, ID2, ID3, IFNAR1, IFNAR2, IFNGR2, IGF2R, IL11RA, IL12A, IL1B, IL27RA, IL7R, IRF4, IRF5, ITGA4, ITGB3, ITK, ITPKB, KDR, KIT, KLF2, KLF4, KRAS, LEF1, LIF, LTBR, LYN, MAF, MALT1, MAP2K1, MAP3K7, MBP, MCL1, MDK, MERTK, MLLT11, MNT, MYB, NFKBIA, NQO1, PCSK1, PGF, PHLPP1, PIK3CD, PKNOX1, PLEKHA2, PLP1, PNP, PRKD1, PRNP, PTGS2, RALA, RALB, RARA, RUNX1, RUNX2, RUNX3, SATB1, SLC3A2, SMO, SNAI2, SOX4, SPP1, STAT2, SYK, TCF4, TGFBR2, TNFRSF1A, TNFRSF1B, TNFSF10, TNFSF13B, TP53BP1, TXK, VEGFA, WASL, XBP1, ZBTB17	138	no
Cancer	brain cancer	1.84E-05	Decreased	-2.254	ABL1, ACTA2, AKT3, ALAD, ANXA1, ANXA2, ARHGEF2, BAX, BCL2, BCL3, BDNF, BMI1, CAV1, CCDC41, CCNB2, CCND1, CDK6, CDKN1B, CDKN2C, CEBPD, CHKA, CHRNB1, CXCL16, DAPK1, DHRS4, DKC1, DVL2, E2F3, EGR1, ENC1, EPHA2, FOXM1, FOXO3, FOXO4, FURIN, GEMIN5, GLI2, GNB4, HIPK2, HMGA1, HMGA2, HMGB2, HMOX1, ID1, IDH1, KDR, KHDRBS3, KRAS, LAMB3, LPAR1, MAP4K4, MARCKS, MCL1, MIA, MMP9, MYC, NFIB, NPTX1, NR3C1, NRIP1, NUSAP1, OLIG1, PAM16, PINK1, PROM1, PTEN, PTPRM, RAC2, SEMA4D, SFRP1, SMO, SOX2, SPHK1, SRC, STAT2, TERF1, TFAP2A, TGFA, TNC, TNFRSF1A, TUBB4A, UBE2C, ZEB2	83	no
Neurological Disease	brain cancer	1.84E-05	Decreased	-2.254	ABL1, ACTA2, AKT3, ALAD, ANXA1, ANXA2, ARHGEF2, BAX, BCL2, BCL3, BDNF, BMI1, CAV1, CCDC41, CCNB2, CCND1, CDK6, CDKN1B, CDKN2C, CEBPD, CHKA, CHRNB1, CXCL16, DAPK1, DHRS4, DKC1, DVL2, E2F3, EGR1, ENC1, EPHA2, FOXM1, FOXO3, FOXO4, FURIN, GEMIN5, GLI2, GNB4, HIPK2, HMGA1, HMGA2, HMGB2, HMOX1, ID1, IDH1, KDR, KHDRBS3, KRAS, LAMB3, LPAR1, MAP4K4, MARCKS, MCL1, MIA, MMP9, MYC, NFIB, NPTX1, NR3C1, NRIP1, NUSAP1, OLIG1, PAM16, PINK1, PROM1, PTEN, PTPRM, RAC2, SEMA4D, SFRP1, SMO, SOX2, SPHK1, SRC, STAT2, TERF1, TFAP2A, TGFA, TNC, TNFRSF1A, TUBB4A, UBE2C, ZEB2	83	no
Cancer	brain tumor	3.00E-05	Decreased	-2.254	ABL1, ACTA2, ADAM19, AKT3, ALAD, ANXA1, ANXA2, ARHGEF2, BAX, BCL2, BCL3, BDNF, BMI1, CAV1, CCDC41, CCNB2, CCND1, CDK6, CDKN1B, CDKN2C, CEBPD, CHKA, CHRNB1, CXCL16, DAPK1, DHRS4, DKC1, DVL2, E2F3, EGR1, ENC1, EPHA2, FGF2, FOXM1, FOXO3, FOXO4, FURIN, GEMIN5, GLI2, GNB4, HIPK2, HMGA1, HMGA2, HMGB2, HMOX1, ID1, IDH1, KDR, KHDRBS3, KRAS, LAMB3, LPAR1, MAP4K4, MARCKS, MCL1, MIA, MMP9, MYC, NFIB, NPTX1, NR3C1, NRIP1, NUSAP1, OLIG1, PAM16, PINK1, PROM1, PTEN, PTPRM, RAC2, SEMA4D, SFRP1, SMO, SOX2, SPHK1, SRC, STAT2, TERF1, TFAP2A, TGFA, TNC, TNFRSF1A, TUBB4A, UBE2C, ZEB2	85	no
Neurological Disease	brain tumor	3.00E-05	Decreased	-2.254	ABL1, ACTA2, ADAM19, AKT3, ALAD, ANXA1, ANXA2, ARHGEF2, BAX, BCL2, BCL3, BDNF, BMI1, CAV1, CCDC41, CCNB2, CCND1, CDK6, CDKN1B, CDKN2C, CEBPD, CHKA, CHRNB1, CXCL16, DAPK1, DHRS4, DKC1, DVL2, E2F3, EGR1, ENC1, EPHA2, FGF2, FOXM1, FOXO3, FOXO4, FURIN, GEMIN5, GLI2, GNB4, HIPK2, HMGA1, HMGA2, HMGB2, HMOX1, ID1, IDH1, KDR, KHDRBS3, KRAS, LAMB3, LPAR1, MAP4K4, MARCKS, MCL1, MIA, MMP9, MYC, NFIB, NPTX1, NR3C1, NRIP1, NUSAP1, OLIG1, PAM16, PINK1, PROM1, PTEN, PTPRM, RAC2, SEMA4D, SFRP1, SMO, SOX2, SPHK1, SRC, STAT2, TERF1, TFAP2A, TGFA, TNC, TNFRSF1A, TUBB4A, UBE2C, ZEB2	85	no
Cancer	neoplasia of tumor cells	2.39E-04	Decreased	-2.244	ABL1, CAV1, CBR1, CDC25A, CREB3L4, CTSL1, CXCR4, DCC, DGCR8, DICER1, KRAS, LZTS1, MCAM, MMP9, PTEN, PTK2, PTPRA, RRM1, RUNX2, SPHK1, TGFA, TGFBR2, TP53BP1, VEGFA	24	no
Cell Cycle	interphase of breast cell	1.10E-03	Decreased	-2.236	CDC25C, CDKN1A, CDKN1B, FADD, ID1, KDM5B, LEF1, MYC	8	yes
Cancer	genital tumor	2.55E-06	Decreased	-2.222	ABCC1, ABCC4, ABL1, ACAD8, ACO1, ACRC, ADAMTS9, AFAP1, ALPK1, AMACR, AMD1, ANAPC1/ANAPC1P1, ANGPT1, ANTXR2, ANXA2, APOE, ARAP3, ARG2, ARMCX3, ATM, ATP10B, ATXN1, AURKB, BAX, BCL2, BECN1, BHLHE40, BIRC5, BMI1, BMPR1A, BRCA1, BSDC1, BTG3, C11orf9, C1R, CALCOCO2, CAV1, CCDC41, CCL2, CCNB2, CCND1, CCND2, CD74, CDC25A, CDC25B, CDC25C, CDC42EP1, CDK6, CDKN1A, CDKN1B, CDKN2C, CFB, CFH, CHD1, CHRM1, CHST2, CIRBP, CMTM8, COL15A1, CROCC, CTDSPL, CTGF, CTLA4, CXCL16, CXCR4, DAB2, DAB2IP, DGCR8, DHRS4, DICER1, DTNA, DUSP1, DUSP4, DYNLRB1, E2F2, E2F3, EDNRB, EFNB2, EIF2C2, ELK4, EPHA4, EPOR, ESRP1, ETV1, ETV4, ETV5, F2R, FAM136A, FAM13A, FAM222B, FAS, FASN, FBXL13, FEN1, FGF2, FGFR3, FHOD3, FOS, FOSL1, FOXD3, FOXO3, FOXO4, FRMD6, FYCO1, FYN, GDF15, GEMIN5, GLDC, GLI2, GNA12, GPR101, GPR183, GPRC5A, GSTM1, GTF2I, GUCY1A2, H2AFX, HILPDA, HIP1, HIPK2, HIST2H2AA3/HIST2H2AA4, HMGA1, HMGA2, HMOX1, HOXA5, HOXB13, HOXB2, HOXC4, HOXC6, HOXD11, HSP90AB1, ID1, IDH1, IER3, IFNGR2, IGF2BP3, IGFBP3, IL1RAPL1, IL7R, IL8, ING4, IRS2, ITK, ITPR3, JUN, KCNS3, KDR, KHDRBS3, KIAA1147, KIAA1211, KIF11, KIT, KRAS, LARP1B, LCTL, LEF1, LOXL3, LPAR1, LRIG1, LRP5, LRP8, LTBR, MAMLD1, MAP2K1, MCAM, MCL1, MCM2, MDK, MMP9, MSMB, MST1, MTHFD2, MXI1, MYC, MYLK, NCL, NFKBIA, NKX2-5, NKX3-1, NPIPL2 (includes others), NPTX1, NR3C1, NT5E, OLIG1, PDCD2L, PDK4, PDLIM4, PGF, PGM5, PI15, PLAUR, PLGLB1/PLGLB2, PLXNB1, POLE, PPAP2A, PPAT, PPP3CC, PRAME, PRKCE, PROM1, PSAT1, PSMD4, PTEN, PTGDS, PTGES, PTGS2, PTK2, PTPRA, QKI, RACGAP1, RARB, RARRES1, RCAN2, RCBTB2, RNASEL, RNF144A, RNF144B, RNF145, RPL29, RPS6KC1, RRAS, RRM1, RUNX2, RUNX3, SAT1, SEC14L1, SECISBP2L, SEMA3C, SEMA4D, SFRP1, SH3PXD2A, SIM2, SLC16A3, SLC2A1, SLC7A1, SLC7A6, SMO, SNAI2, SOD2, SON, SORT1, SOX2, SPOP, SPP1, SPRED2, SPRY1, SPRY2, SRC, SRGAP1, SSTR2, ST7, STAT2, STC1, STIM1, STK4, SUN3, SYNPO2, TBC1D14, TFF3, TGFBR2, TIMP3, TK1, TNS3, TP53INP1, TPD52, TRADD, TRIM48, TRIOBP, TRO, TRRAP, TTK, TUBA1C, TUBB2B, TUBB3, TUBB4A, TUBB6, TUBB8, TXNIP, UBE2C, UGT2B17, VCAN, VEGFA, VEGFB, WDR19, WIPF1, XPC, YEATS2, ZBTB17, ZBTB20, ZBTB22, ZC3H15, ZDHHC11, ZFP36, ZFYVE26, ZNF827, ZWINT	296	no
Reproductive System Disease	genitaltumor	2.55E-06	Decreased	-2.222	ABCC1, ABCC4, ABL1, ACAD8, ACO1, ACRC, ADAMTS9, AFAP1, ALPK1, AMACR, AMD1, ANAPC1/ANAPC1P1, ANGPT1, ANTXR2, ANXA2, APOE, ARAP3, ARG2, ARMCX3, ATM, ATP10B, ATXN1, AURKB, BAX, BCL2, BECN1, BHLHE40, BIRC5, BMI1, BMPR1A, BRCA1, BSDC1, BTG3, C11orf9, C1R, CALCOCO2, CAV1, CCDC41, CCL2, CCNB2, CCND1, CCND2, CD74, CDC25A, CDC25B, CDC25C, CDC42EP1, CDK6, CDKN1A, CDKN1B, CDKN2C, CFB, CFH, CHD1, CHRM1, CHST2, CIRBP, CMTM8, COL15A1, CROCC, CTDSPL, CTGF, CTLA4, CXCL16, CXCR4, DAB2, DAB2IP, DGCR8, DHRS4, DICER1, DTNA, DUSP1, DUSP4, DYNLRB1, E2F2, E2F3, EDNRB, EFNB2, EIF2C2, ELK4, EPHA4, EPOR, ESRP1, ETV1, ETV4, ETV5, F2R, FAM136A, FAM13A, FAM222B, FAS, FASN, FBXL13, FEN1, FGF2, FGFR3, FHOD3, FOS, FOSL1, FOXD3, FOXO3, FOXO4, FRMD6, FYCO1, FYN, GDF15, GEMIN5, GLDC, GLI2, GNA12, GPR101, GPR183, GPRC5A, GSTM1, GTF2I, GUCY1A2, H2AFX, HILPDA, HIP1, HIPK2, HIST2H2AA3/HIST2H2AA4, HMGA1, HMGA2, HMOX1, HOXA5, HOXB13, HOXB2, HOXC4, HOXC6, HOXD11, HSP90AB1, ID1, IDH1, IER3, IFNGR2, IGF2BP3, IGFBP3, IL1RAPL1, IL7R, IL8, ING4, IRS2, ITK, ITPR3, JUN, KCNS3, KDR, KHDRBS3, KIAA1147, KIAA1211, KIF11, KIT, KRAS, LARP1B, LCTL, LEF1, LOXL3, LPAR1, LRIG1, LRP5, LRP8, LTBR, MAMLD1, MAP2K1, MCAM, MCL1, MCM2, MDK, MMP9, MSMB, MST1, MTHFD2, MXI1, MYC, MYLK, NCL, NFKBIA, NKX2-5, NKX3-1, NPIPL2 (includes others), NPTX1, NR3C1, NT5E, OLIG1, PDCD2L, PDK4, PDLIM4, PGF, PGM5, PI15, PLAUR, PLGLB1/PLGLB2, PLXNB1, POLE, PPAP2A, PPAT, PPP3CC, PRAME, PRKCE, PROM1, PSAT1, PSMD4, PTEN, PTGDS, PTGES, PTGS2, PTK2, PTPRA, QKI, RACGAP1, RARB, RARRES1, RCAN2, RCBTB2, RNASEL, RNF144A, RNF144B, RNF145, RPL29, RPS6KC1, RRAS, RRM1, RUNX2, RUNX3, SAT1, SEC14L1, SECISBP2L, SEMA3C, SEMA4D, SFRP1, SH3PXD2A, SIM2, SLC16A3, SLC2A1, SLC7A1, SLC7A6, SMO, SNAI2, SOD2, SON, SORT1, SOX2, SPOP, SPP1, SPRED2, SPRY1, SPRY2, SRC, SRGAP1, SSTR2, ST7, STAT2, STC1, STIM1, STK4, SUN3, SYNPO2, TBC1D14, TFF3, TGFBR2, TIMP3, TK1, TNS3, TP53INP1, TPD52, TRADD, TRIM48, TRIOBP, TRO, TRRAP, TTK, TUBA1C, TUBB2B, TUBB3, TUBB4A, TUBB6, TUBB8, TXNIP, UBE2C, UGT2B17, VCAN, VEGFA, VEGFB, WDR19, WIPF1, XPC, YEATS2, ZBTB17, ZBTB20, ZBTB22, ZC3H15, ZDHHC11, ZFP36, ZFYVE26, ZNF827, ZWINT	296	no
Cellular Movement	cell movement of vascular smooth muscle cells	5.60E-04	Decreased	-2.216	ADM, ANGPT2, CCND1, CDKN1B, CLIC4, FGF2, FOXO4, FZD4, HMOX1, IGFBP5, IL1B, IL8, ITGB5, KDR, NEO1, NOV, NQO1, PAPPA, PLAUR, PTGS2, RCAN1, ROCK1, RTN4, SDC4, SPP1, THBS1, TLR4, TNFSF10, TRIB1, WISP2	30	yes
Skeletal and Muscular System Development and Function	cell movement of vascular smooth muscle cells	5.60E-04	Decreased	-2.216	ADM, ANGPT2, CCND1, CDKN1B, CLIC4, FGF2, FOXO4, FZD4, HMOX1, IGFBP5, IL1B, IL8, ITGB5, KDR, NEO1, NOV, NQO1, PAPPA, PLAUR, PTGS2, RCAN1, ROCK1, RTN4, SDC4, SPP1, THBS1, TLR4, TNFSF10, TRIB1, WISP2	30	yes
Cellular Movement	cell movement of breast cancer cell lines	2.37E-08	Decreased	-2.214	ACSL4, ANGPT2, ANKS1A, ANXA1, ARPC1B, BCAR3, BHLHE41, CAV1, CCL2, CDKN1B, CHN2, COL4A3BP, CTSL1, CXCR4, DBF4, EPHA2, EPOR, ETS1, FGF2, FHOD1, FOS, FOSL1, FOXO3, FURIN, GAB1, GEMIN5, HIF1A, HMMR, ID1, IGFBP3, IL8, ITGA6, ITGB3, JUN, LIMK1, LPAR1, LRIG1, MAP2K1, MAP4K4, MCAM, MCF2L, MMP9, NDRG1, NFKBIA, NRP1, PIK3CD, PLAUR, PLXNA1, PPM1F, PRKD1, PTK2, RAB21, RAB27A, RAP1GAP, RNF144A, RUVBL1, SEMA3A, SEMA4D, SLC16A4, SNAI2, SPHK1, SPP1, SRC, SSH1, SYK, TFAP2A, TFAP2C, TGFA, TIMP2, TUBA1C, VASP, VEGFA, WWTR1	73	yes
Cellular Development	proliferation of muscle cells	3.80E-05	Decreased	-2.209	ABCC2, ABCC4, ADM, ANG, ANGPT2, APOE, ATP2B1, BDNF, BIRC5, CAV1, CBL, CCL2, CDKN1A, CDKN1B, CEBPD, CTNNBIP1, CXCL16, DGCR8, DUSP1, E2F3, FGF2, FOS, FOXK1, FOXM1, FOXO1, FZD4, HBEGF, HEY1, HEY2, HIF1A, HMGA2, HMGCR, HMOX1, HSPD1, ID2, ID3, IGFBP3, IGFBP5, IL12A, IL1B, IL8, IRAK1, ITGA6, ITGB3, JUN, KIT, KLF4, KRAS, LIF, LPAR1, MAP2K1, MMP9, MYB, MYC, NAMPT, NOV, NOX4, NQO1, NR4A2, PAPPA, PLAT, PLAUR, PRKAR1A, PRNP, PRRX1, PTEN, PTGDS, PTGS2, PTK2, RARA, ROCK1, RXRA, SDC4, SPP1, ST8SIA1, TCF4, TGFBR2, TGFBR3, THBS1, TLR4, TNC, TNFRSF12A, TNFRSF1A, TNFRSF1B, TNFSF10, TRIB1, VCAN, VEGFA, WISP2	89	no
Cellular Growth and Proliferation	proliferation of muscle cells	3.80E-05	Decreased	-2.209	ABCC2, ABCC4, ADM, ANG, ANGPT2, APOE, ATP2B1, BDNF, BIRC5, CAV1, CBL, CCL2, CDKN1A, CDKN1B, CEBPD, CTNNBIP1, CXCL16, DGCR8, DUSP1, E2F3, FGF2, FOS, FOXK1, FOXM1, FOXO1, FZD4, HBEGF, HEY1, HEY2, HIF1A, HMGA2, HMGCR, HMOX1, HSPD1, ID2, ID3, IGFBP3, IGFBP5, IL12A, IL1B, IL8, IRAK1, ITGA6, ITGB3, JUN, KIT, KLF4, KRAS, LIF, LPAR1, MAP2K1, MMP9, MYB, MYC, NAMPT, NOV, NOX4, NQO1, NR4A2, PAPPA, PLAT, PLAUR, PRKAR1A, PRNP, PRRX1, PTEN, PTGDS, PTGS2, PTK2, RARA, ROCK1, RXRA, SDC4, SPP1, ST8SIA1, TCF4, TGFBR2, TGFBR3, THBS1, TLR4, TNC, TNFRSF12A, TNFRSF1A, TNFRSF1B, TNFSF10, TRIB1, VCAN, VEGFA, WISP2	89	no
Skeletal and Muscular System Development and Function	proliferation of muscle cells	3.80E-05	Decreased	-2.209	ABCC2, ABCC4, ADM, ANG, ANGPT2, APOE, ATP2B1, BDNF, BIRC5, CAV1, CBL, CCL2, CDKN1A, CDKN1B, CEBPD, CTNNBIP1, CXCL16, DGCR8, DUSP1, E2F3, FGF2, FOS, FOXK1, FOXM1, FOXO1, FZD4, HBEGF, HEY1, HEY2, HIF1A, HMGA2, HMGCR, HMOX1, HSPD1, ID2, ID3, IGFBP3, IGFBP5, IL12A, IL1B, IL8, IRAK1, ITGA6, ITGB3, JUN, KIT, KLF4, KRAS, LIF, LPAR1, MAP2K1, MMP9, MYB, MYC, NAMPT, NOV, NOX4, NQO1, NR4A2, PAPPA, PLAT, PLAUR, PRKAR1A, PRNP, PRRX1, PTEN, PTGDS, PTGS2, PTK2, RARA, ROCK1, RXRA, SDC4, SPP1, ST8SIA1, TCF4, TGFBR2, TGFBR3, THBS1, TLR4, TNC, TNFRSF12A, TNFRSF1A, TNFRSF1B, TNFSF10, TRIB1, VCAN, VEGFA, WISP2	89	no
Cellular Assembly and Organization	quantity of membrane ruffles	2.13E-05	Decreased	-2.189	ADD1, ARHGEF2, CDC42EP1, IL8, PTEN, ROCK2, SORBS2	7	no
Cellular Growth and Proliferation	proliferation of connective tissue cells	6.89E-05	Decreased	-2.171	ABL1, AHR, AKAP12, AKT3, ATM, BAX, BCL2, BMI1, BMPR1A, CAV1, CBL, CCL2, CCNA2, CCND1, CCND2, CCNG2, CD74, CDK6, CDKN1A, CDKN1B, CEBPB, CIRBP, CTC1, CTGF, CTHRC1, DICER1, DKK1, DUSP1, EDNRB, EFNA1, EPHA2, ESPL1, F2R, F2RL1, FADD, FAS, FEN1, FGF13, FGF2, FGFR3, FLI1, FNDC3B, FOS, FOSL1, FOXO1, FOXO4, FST, FTH1, FYN, GHR, GLI2, HBEGF, HIF1A, HMMR, HMOX1, HOXA5, HOXB13, ID2, IFNAR1, IGFBP3, IGFBP5, IL1B, IL8, IP6K2, ITGB3, JUN, JUND, KLF4, KRAS, LIF, LIMA1, LOX, LPAR1, LRIG1, LRP5, LZTS1, MAP2K1, MAP2K3, MAP2K6, MAP3K1, MAP3K5, MAP3K7, MCF2L, MMP9, MYC, NFKBIA, NOX4, NR3C1, NUPR1, OVOL2, PA2G4, PEX2, PGF, PHC2, PHLPP1, PLAT, PLAUR, PMS2, PPAT, PPP1R13L, PSMD10, PTEN, PTGES, PTGS2, PTK2, PTPRZ1, RAPGEF1, RARA, RIT1, RPL29, RRM1, RUNX1, RUNX2, RXRA, SFRP1, SIRT2, SLC3A2, SMAD6, SMARCAL1, SMO, SNAI2, SOD2, SOX8, SPHK1, SPP1, SPRY2, SRC, STARD10, STC1, TAF4, TGFA, TGFBR2, TGIF1, TNFRSF12A, TNFRSF1A, TNFSF10, TPR, TWIST1, TXNIP, UBE2C, VCAN, VDR, WASL	143	yes
Cellular Development	branching of cells	2.60E-04	Decreased	-2.163	ABL1, ADM, ANG, ANGPT1, ANGPT2, ANGPTL2, ANXA2, BCL2, BDNF, CDK5R1, DCX, DICER1, EFNA1, ETS1, FADD, FGF2, GAB1, HOXD11, JUN, KDR, KRAS, LAMA2, LAMA4, MKS1, MMP9, MST1, NFKBIA, PIM3, RND3, RRAS, RTN4, RUNX2, SARS, SEMA4D, SPP1, TGFA, TIMP2, TMEM67, TNC, VEGFA	40	no
Cell Cycle	entry into S phase of fibroblasts	8.24E-04	Decreased	-2.138	ATM, CCND1, CDKN1A, CDKN1B, E2F2, E2F3, E2F5, ID3, MYC, TFDP1	10	yes
Connective Tissue Development and Function	entry into S phase of fibroblasts	8.24E-04	Decreased	-2.138	ATM, CCND1, CDKN1A, CDKN1B, E2F2, E2F3, E2F5, ID3, MYC, TFDP1	10	yes
Cancer	neoplasia of cancer cells	5.77E-04	Decreased	-2.137	ABL1, CBR1, CREB3L4, CTSL1, CXCR4, DCC, DGCR8, DICER1, KRAS, LZTS1, MCAM, PTEN, RRM1, TGFA, TGFBR2, VEGFA	16	no
Cellular Development	proliferation of tumor cells	3.45E-06	Decreased	-2.086	ABL1, ADRBK1, AFAP1L2, ANXA2, ATM, ATP2A2, BAX, BCAN, BCL2, BECN1, BIRC5, BMI1, CASP1, CAV1, CCND1, CDC25A, CDK5, CDK6, CDKN1A, CDKN1B, CDKN2C, CXCR4, DCC, DDIT3, DGCR8, DICER1, DKK1, DUSP1, DVL2, EFNA1, EGR1, EPHA2, F2R, F2RL1, FAS, FASN, FGF2, FOS, FOSL1, FOXM1, FOXO3, FST, GDF15, GREB1, HBEGF, HDAC6, HIF1A, HMGA2, HMGCR, HMMR, HMOX1, ID1, ID2, ID3, IGFBP3, IGFBP5, IL12A, IL1B, IL8, KDR, KIT, KRAS, LZTS1, LZTS2, MAP2K1, MAP2K3, MAP2K5, MAP2K6, MCAM, MMP9, MST1, MYB, MYC, NFKBIA, NKX3-1, NOV, NOX4, NR4A2, NRP1, PLAT, PLAUR, POU3F2, PPP1R13L, PRKCE, PTEN, PTGS2, PTPRA, PTPRE, RARB, RCAN1, RUVBL1, RXRA, SEC14L2, SEMA4D, SFRP1, SLC3A2, SMO, SNAI2, SPHK1, SPP1, SRC, SSTR2, TAX1BP3, TCF7L2, TFF3, TGFA, TGFBR2, THBS1, TIAM2, TIMP2, TIMP3, TLE1, TNFSF10, TNFSF13B, TP53BP1, TPD52, TWIST1, TXNIP, USP10, VCAN, VEGFA, XBP1, ZMAT3	123	yes
Cellular Growth and Proliferation	proliferation of tumor cells	3.45E-06	Decreased	-2.086	ABL1, ADRBK1, AFAP1L2, ANXA2, ATM, ATP2A2, BAX, BCAN, BCL2, BECN1, BIRC5, BMI1, CASP1, CAV1, CCND1, CDC25A, CDK5, CDK6, CDKN1A, CDKN1B, CDKN2C, CXCR4, DCC, DDIT3, DGCR8, DICER1, DKK1, DUSP1, DVL2, EFNA1, EGR1, EPHA2, F2R, F2RL1, FAS, FASN, FGF2, FOS, FOSL1, FOXM1, FOXO3, FST, GDF15, GREB1, HBEGF, HDAC6, HIF1A, HMGA2, HMGCR, HMMR, HMOX1, ID1, ID2, ID3, IGFBP3, IGFBP5, IL12A, IL1B, IL8, KDR, KIT, KRAS, LZTS1, LZTS2, MAP2K1, MAP2K3, MAP2K5, MAP2K6, MCAM, MMP9, MST1, MYB, MYC, NFKBIA, NKX3-1, NOV, NOX4, NR4A2, NRP1, PLAT, PLAUR, POU3F2, PPP1R13L, PRKCE, PTEN, PTGS2, PTPRA, PTPRE, RARB, RCAN1, RUVBL1, RXRA, SEC14L2, SEMA4D, SFRP1, SLC3A2, SMO, SNAI2, SPHK1, SPP1, SRC, SSTR2, TAX1BP3, TCF7L2, TFF3, TGFA, TGFBR2, THBS1, TIAM2, TIMP2, TIMP3, TLE1, TNFSF10, TNFSF13B, TP53BP1, TPD52, TWIST1, TXNIP, USP10, VCAN, VEGFA, XBP1, ZMAT3	123	yes

Tumor Morphology	proliferation		or cells	3.45E-06	Decreased	-2.086	ABL1, ADRBK1, AFAP1L2, ANXA2, ATM, ATP2A2, BAX, BCAN, BCL2, BECN1, BIRC5, BMI1, CASP1, CAV1, CCND1, CDC25A, CDK5, CDK6, CDKN1A, CDKN1B, CDKN2C, CXCR4, DCC, DDIT3, DGCR8, DICER1, DKK1, DUSP1, DVL2, EFNA1, EGR1, EPHA2, F2R, F2RL1, FAS, FASN, FGF2, FOS, FOSL1, FOXM1, FOXO3, FST, GDF15, GREB1, HBEGF, HDAC6, HIF1A, HMGA2, HMGCR, HMMR, HMOX1, ID1, ID2, ID3, IGFBP3, IGFBP5, IL12A, IL1B, IL8, KDR, KIT, KRAS, LZTS1, LZTS2, MAP2K1, MAP2K3, MAP2K5, MAP2K6, MCAM, MMP9, MST1, MYB, MYC, NFKBIA, NKX3-1, NOV, NOX4, NR4A2, NRP1, PLAT, PLAUR, POU3F2, PPP1R13L, PRKCE, PTEN, PTGS2, PTPRA, PTPRE, RARB, RCAN1, RUVBL1, RXRA, SEC14L2, SEMA4D, SFRP1, SLC3A2, SMO, SNAI2, SPHK1, SPP1, SRC, SSTR2, TAX1BP3, TCF7L2, TFF3, TGFA, TGFBR2, THBS1, TIAM2, TIMP2, TIMP3, TLE1, TNFSF10, TNFSF13B, TP53BP1, TPD52, TWIST1, TXNIP, USP10, VCAN, VEGFA, XBP1, ZMAT3	123	yes
Cellular Movement	invasion of b cell lines				sed	-2.049	ABL1, ABL2, ACSL4, ADAMTS1, ATP6V0A4, BCAR3, BHLHE41, CALR, CAV1, CBL, CCNA2, CDKN1B, CTSK, CXCR4, DIAPH2, DIAPH3, FAS, FGF2, FHOD1, FURIN, HAS2, HBP1, HIF1A, HMMR, ID1, ID2, IRS2, ITGB3, JUN, LIMK1, LOX, MCAM, MMP9, MST1, NAMPT, NFKBIA, PAK4, PARVB, PLAUR, PPM1F, PTGS2, PTK2, RNF144A, RUVBL1, SIM2, SP100, SPP1, SRC, STMN1, TFAP2A, TFAP2C, TGFBR2, TNFSF10, TWIST1, WWTR1, ZEB2	56	yes
Cancer	pulmonary a				sed	-2.041	BECN1, CDKN1B, CDKN2C, FOXM1, FOXO3, FOXO4, LZTS1, MYC, NUDT1, SSBP2, XPC	11	no
Respiratory Disease	pulmonary a				sed	-2.041	BECN1, CDKN1B, CDKN2C, FOXM1, FOXO3, FOXO4, LZTS1, MYC, NUDT1, SSBP2, XPC	11	no
Cancer	tumorigene tumor	sis of ma	lignant	5.73E-06	Decreased	-2.032	AFF1, AHR, ANK3, ASXL2, ATM, ATP2A2, AURKB, BCL2, BECN1, BIN3, BIRC5, BMF, BRCA1, CABLES1, CCND1, CDKN1A, CDKN1B, CDKN2C, CTLA4, DCBLD2, DCC, DDB2, DKC1, DTNA, E2F2, EGR1, ERRFI1, FEN1, FGF2, FNDC3B, FOS, FOXM1, GDF15, GLI2, GSTM1, H2AFX, HIP1, HMGA2, ID1, IFNAR1, IFNAR2, IGFBP3, IL1B, ING1, ING2, JARID2, JUN, KIF11, KRAS, LTBR, LZTS1, MCL1, MT1E, MXI1, MYB, MYC, NFIA, NFKBIA, NQO1, NUDT1, PIM2, PLAUR, PMS2, PRDX1, PRICKLE2, PRKAR1A, PRKCE, PTEN, PTGS2, PTPRE, ROCK2, RUNX1, RUNX3, SIRT2, SPHK1, SRC, SSBP2, STAT2, TGFBR2, THBS1, TNFSF10, TP53BP1, TPR, TRIM24, VEGFA, XPC, ZEB2	87	no
Tissue Development	myelination of nervous			3.22E-04	Decreased	-2.031	ADAM19, BDNF, DICER1, EGR2, FYN, GJB1, IL11RA, IL1B, LAMC1, MAL, MBP, MYO5A, P2RX7, PMP22, POU3F1, PTPRE, RTN4	17	no
Nervous System Development and Function	myelination tissue	of nerv	ous	3.22E-04	Decreased	-2.031	ADAM19, BDNF, DICER1, EGR2, FYN, GJB1, IL11RA, IL1B, LAMC1, MAL, MBP, MYO5A, P2RX7, PMP22, POU3F1, PTPRE, RTN4	17	no
Cellular Assembly and of	formation		ress	5.41E-05	Decreased	-2.027	ABL2, AKAP13, ARAP1, ARHGAP18, ARHGEF1, ARHGEF11, ARHGEF17, ARHGEF2, ARHGEF3, BOP1, C3AR1, CAV1, CDKN1A, CHRM1, CNTNAP1, CTGF, DAB2, DIAPH3, F2R, FGF2, FHOD1, FYN, GNA12, GNA13, GNG12, HAX1, HDAC6, IL8, KANK2, KDR, KLF2, KRAS, LIMK1, LMCD1, LPAR1, MAP2K1, MCF2L, MYLK, NCKIPSD, NOX4, PAK4, PLAT, PPM1F, PRKCE, PTK2, PTPRA, RND3, ROCK1, ROCK2, SDC4, SEMA4D, SORBS1, SORBS3, SPRY2, SRC, STARD13, TNC, TNS3, VASP, VEGFA, ZYX	61	no
Cellular Function and of	formation		ress	5.41E-05	Decreased	-2.027	ABL2, AKAP13, ARAP1, ARHGAP18, ARHGEF1, ARHGEF11, ARHGEF17, ARHGEF2, ARHGEF3, BOP1, C3AR1, CAV1, CDKN1A, CHRM1, CNTNAP1, CTGF, DAB2, DIAPH3, F2R, FGF2, FHOD1, FYN, GNA12, GNA13, GNG12, HAX1, HDAC6, IL8, KANK2, KDR, KLF2, KRAS, LIMK1, LMCD1, LPAR1, MAP2K1, MCF2L, MYLK, NCKIPSD, NOX4, PAK4, PLAT, PPM1F, PRKCE, PTK2, PTPRA, RND3, ROCK1, ROCK2, SDC4, SEMA4D, SORBS1, SORBS3, SPRY2, SRC, STARD13, TNC, TNS3, VASP, VEGFA, ZYX	61	yes
Tissue Development	formation of		ress	5.41E-05	Decreased	-2.027	ABL2, AKAP13, ARAP1, ARHGAP18, ARHGEF1, ARHGEF11, ARHGEF17, ARHGEF2, ARHGEF3, BOP1, C3AR1, CAV1, CDKN1A, CHRM1, CNTNAP1, CTGF, DAB2, DIAPH3, F2R, FGF2, FHOD1, FYN, GNA12, GNA13, GNG12, HAX1, HDAC6, IL8, KANK2, KDR, KLF2, KRAS, LIMK1, LMCD1, LPAR1, MAP2K1, MCF2L, MYLK, NCKIPSD, NOX4, PAK4, PLAT, PPM1F, PRKCE, PTK2, PTPRA, RND3, ROCK1, ROCK2, SDC4, SEMA4D, SORBS1, SORBS3, SPRY2, SRC, STARD13, TNC, TNS3, VASP, VEGFA, ZYX	61	yes
Cancer	pituitary car				sed	-2.021	ACTA2, ANXA2, ARHGEF2, BCL3, BDNF, CCNB2, CCND1, CDKN1B, CDKN2C, CEBPD, CHKA, CHRNB1, DAPK1, DKC1, E2F3, EGR1, FOXO3, FOXO4, GNB4, HMGA1, HMGA2, HMGB2, HMOX1, ID1, LAMB3, MIA, MMP9, NFIB, NR3C1, NRIP1, NUSAP1, PAM16, PTPRM, RAC2, SEMA4D, SOX2, TFAP2A, TGFA, TUBB4A	39	no
Reproductive System Disease	pituitary can				sed	-2.021	ACTA2, ANXA2, ARHGEF2, BCL3, BDNF, CCNB2, CCND1, CDKN1B, CDKN2C, CEBPD, CHKA, CHRNB1, DAPK1, DKC1, E2F3, EGR1, FOXO3, FOXO4, GNB4, HMGA1, HMGA2, HMGB2, HMOX1, ID1, LAMB3, MIA, MMP9, NFIB, NR3C1, NRIP1, NUSAP1, PAM16, PTPRM, RAC2, SEMA4D, SOX2, TFAP2A, TGFA, TUBB4A	39	no
Neurological Disease	pituitary car				sed	-2.021	ACTA2, ANXA2, ARHGEF2, BCL3, BDNF, CCNB2, CCND1, CDKN1B, CDKN2C, CEBPD, CHKA, CHRNB1, DAPK1, DKC1, E2F3, EGR1, FOXO3, FOXO4, GNB4, HMGA1, HMGA2, HMGB2, HMOX1, ID1, LAMB3, MIA, MMP9, NFIB, NR3C1, NRIP1, NUSAP1, PAM16, PTPRM, RAC2, SEMA4D, SOX2, TFAP2A, TGFA, TUBB4A	39	no
Endocrine System Disorders	pituitary can				sed	-2.021	ACTA2, ANXA2, ARHGEF2, BCL3, BDNF, CCNB2, CCND1, CDKN1B, CDKN2C, CEBPD, CHKA, CHRNB1, DAPK1, DKC1, E2F3, EGR1, FOXO3, FOXO4, GNB4, HMGA1, HMGA2, HMGB2, HMOX1, ID1, LAMB3, MIA, MMP9, NFIB, NR3C1, NRIP1, NUSAP1, PAM16, PTPRM, RAC2, SEMA4D, SOX2, TFAP2A, TGFA, TUBB4A	39	no
Cellular Movement	cell movement lines		mor cell	2.41E-10	Decreased	-2.006	ABL1, ACSL4, AFAP1, AKAP11, AKT3, ANGPT2, ANKS1A, ANXA1, ANXA2, AP2M1, ARAP3, ARPC1B, BCAN, BCAR3, BHLHE41, CALR, CAV1, CCL2, CCL20, CD36, CD97, CDC25B, CDK5, CDKN1B, CHN2, CKLF, CMTM8, COL4A3BP, CRKL, CTGF, CTSL1, CXCL13, CXCR4, DAB2, DBF4, DCBLD2, DEFB4A/DEFB4B, DGCR6L, DKK3, DNAJB4, E2F5, EFNA1, EGR1, ENPP2, EPHA2, EPOR, ETS1, ETV4, ETV5, F2RL1, FADD, FBXL2, FGF2, FHOD1, FOS, FOSL1, FOXD3, FOXM1, FOXO3, FURIN, FYN, GAB1, GDF15, GEMIN5, GNA13, GOLGA2, HAS2, HAS3, HAX1, HBEGF, HDAC6, HIF1A, HIPK2, HMMR, HMOX1, ID1, IGFBP3, IL8, ING4, ITGA4, ITGA6, ITGB3, JUN, KANK1, KDR, KIDINS220, KIT, KLF2, KLF4, KRAS, LAMB3, LIF, LIMK1, LMCD1, LOX, LPAR1, LRIG1, LRP5, LYN, MAP2K1, MAP3K1, MAP3K7, MAP4K4, MC1R, MCAM, MCF2L, MDK, MERTK, MITF, MMP9, MSN, MST1, MYB, MYO10, NDRG1, NEDD9, NFKBIA, NOV, NRCAM, NREP, NRP1, PA2G4, PGF, PHB, PIK3C2B, PIK3CD, PLAUR, PLCL1, PLGRKT, PLXNA1, PLXNB1, PPFIA1, PPM1F, PREX1, PRKCE, PRKD1, PRNP, PTEN, PTGS2, PTK2, PTP4A2, PTPN12, PTPRM, PTPRZ1, PVR, RAB21, RAB27A, RALA, RALB, RAP1GAP, RARRES1, RGS1, RNF144A, RUNX2, RUVBL1, SCNN1A, SEMA3A, SEMA4D, SH3PXD2B, SHC4, SLC16A4, SLC2A1, SNAI2, SNX27, SOD2, SPHK1, SPP1, SPRY2, SRC, SSH1, ST3GAL5, ST6GAL1, STARD13, STMN1, SYK, SYNM, TBXAS1, TFAP2A, TFAP2C, TGFA, THBS1, THBS2, TIMP2, TLR4, TNC, TNFSF10, TP53INP1, TRIP6, TUBA1C, TWIST1, VASP, VEGFA, VEGFB, VPS28, WASL, WWTR1, ZYX	197	yes

Table S5. Upstream regulator analysis, by IPA software, of genes significantly modulated by the association of TRAIL with AZD6244

Results shown here are based on the set of genes identified by areas highlighted in fuchsia in Fig. S8A.
See supplementary methods for the meaning of the p values and of the z score statistics.

Upstream Regulator	Log Ratio	Molecule Type	Predicted Activation State	Activation z-score	p-value of overlap	Target molecules in dataset
MITF	0.442	transcription regulator	Activated	4.882	3.09E-14	ACO2, APOE, ATP6V1B2, ATP6V1C1, BCL2, BEST1, CA14, CAPN3, CCNG2, CDK5R1, CHKA, CLCN7, CTSK, DAPK1, DSTYK, EDNRB, ESRP1, FAM53B, FOS, GMPR, GREB1, GYG2, HIF1A, HPGD, HPS4, IL8, IRF4, ITGA4, ITPKB, KCNN2, KIAA1598, KIT, MBP, MC1R, MDH1, MICAL1, MITF, MLANA, NR3C1, PHACTR1, PIR, PLA1A, PPM1H, QDPR, RAB27A, SEMA6A, SORT1, SOX6, ST3GAL6, STX7, STXBP1, TBC1D16, TBX2, TFAP2A, TMC6, TMCC2, TRPM1, TXNIP, TYRP1, USP48, VAT1
HNF4A		transcription regulator	Activated	2.058	3.90E-06	ANKRA2, ANKZF1, APH1A, APOE, ARG2, ARHGEF19, AS3MT, ATAT1, ATF6B, ATP6V1H, AVPI1, BAZ1A, BCCIP, BMI1, BPGM, BRD8, BSDC1, BTG1, C11orf1, C11orf71, C12orf52, C1orf123, C1S, C2, C21orf59, C22orf28, C2orf44, C4orf19, CAV1, CCDC115, CCDC41, CCDC53, CCNA2, CCND1, CCNG2, CD3EAP, CD55, CDC25A, CDC6, CDK2AP2, CDK5, CDK5RAP3, CDKN1A, CDKN1B, CEBPB, CEBPD, CEP95, CES2, CETN3, CHERP, CHMP1B, CIAO1, CLDN1, CLTCL1, COPS7B, COPS8, CPB2, CRADD, CRIPT, CRKL, CROT, CRYZ, CYP27A1, CYTH2, DBP, DCAF13, DDX10, DDX18, DHDDS, DHRS4, DLG4, DNAJB4, DPH5, DSN1, DUSP3, DUSP6, E2F5, EGR1, EIF4G1, EIF5, ELP5, EMC2, EMG1, ENC1, EPHA2, EPM2AIP1, ERCC5, ERI2, ERLIN1, ERO1L, EXOSC2, F12, FAM107B, FAM216A, FAM46A, FAS, FEM1B, FEN1, FGF13, FKBPL, FOXO1, FOXRED1, FTSJ1, FURIN, FXYD6, FYCO1, FZD1, G3BP2, GAB1, GALM, GAS1, GDF15, GJB1, GLCE, GNL3, GOLGA2, GPR137, GPR37, GSPT1, GSTA4, GSTK1, GSTO1, GTF2B, GTF2I, GTPBP3, GUSB, HADHB, HBP1, HDAC6, HEXA, HEY1, HIF1A, HIST1H2BD, HIST1H4A , HIST2H2AA3/HIST2H2AA4, HIST2H2BE , HLA-F, HMGB2, HPS5, HTRA2, IER5, IFNAR1, IFT122, IL11RA, IL1RAP, INCENP, ING4, INTS7, IPO13, ISOC1, ISOC2, ITGA6, JUN, KCNN2, KIF20A, KLF15, KLHL20, KRR1, LAMTOR2, LARS2, LDB1, LHX6, LIMS1, LPCAT3, LPGAT1, LRP5, MAP2K5, MAP3K3, MAP3K7, MCEE, MDH1, MED23, MGEA5, MGST1, MICU1, MID1, MINA, MOCOS, MPP1, MRPL3, MRPL32, MRPL44, MRPS12, MRPS18C, MRTO4, MSMB, MST1, MT1X, MT2A, MTHFS, MUT, MYC, N4BP2L2, NAMPT, NARS2, NCBP2, NCOA4, NDC80, NDRG1, NDUFB3, NEURL2, NOC3L, NOLC1, NOP16, NR2F1, NR5A2, NUAK1, NUCB1, NUDT2, NUDT6, NUP54, OTUD6B, PAAF1, PAGR1, PAN2, PARP4, PCDH20, PDK4, PELO, PEPD, PEX11B, PEX16, PFKFB4, PHB, PI4KB, PIK3R3, PINK1, PITPNB, PNMA1, PNO1, PNP, POLR1B, POLR1C, POLR3E, POLR3G, PPARGC1A, PPFIBP1, PPIL1, PPP1R12B, PPP1R3C, PPP2R3C, PRCP, PRELID2, PRICKLE4, PRKCE, PRMT1, PROM1, PRPF38B, PSAT1, PSMB5, PSMD10, PTGDS, PTK2, PTPRE, QTRTD1, RAB2A, RABEPK, RAP1GAP, RARA, RARB, RBM23, RHPN2, RIOK1, RNASE4, ROCK1, RPS6KC1, RQCD1, RRM1, RTCA, RTFDC1, RXRA, SAMM50, SAT2, SEC31A, SEMA3C, SEPSECS, SERPINB8, SETDB2, SIRT2, SLC16A6, SLC22A18AS, SLC25A19, SLC25A20, SLC25A40, SLC30A7, SLC38A1, SNAI2, SNAP23, SNAPC1, SNX17, SNX5, SPATA5L1, SPCS2, SPP1, SRPRB, SRSF2, SSU72, STAM, STARD10, STIM1, STK19, STK24, STOML1, STX18, SUCLG1, SULT1A3/SULT1A4, SYNJ2BP, TAOK3, TBC1D15, TBC1D16, TCF7L2, TEX10, TFB1M, TFB2M, TIMM21, TIMP3, TMC6, TMEM140, TMEM187, TMEM216, TMEM59, TMEM63A, TMEM87B, TMUB2, TNC, TOM1, TOR2A, TPP2, TPX2, TRAIP, TRAPPC6A, TRIM24, TRIM4, TRMT1L, TRPC4AP, TSPAN14, TTC19, TUBB4A, TUFT1, TXNIP, UBQLN2, UCHL5, UGT2B11, UPF3B, UQCC, UTP23, VIPAS39, WASL, WDR12, ZC3H10, ZC3H15, ZCCHC9, ZDHHC6, ZFYVE19, ZKSCAN5, ZNF193
KLF2	-0.211	transcription regulator	Activated	2.748	2.10E-03	ADM, ANGPT2, BCL3, CCL2, CD55, CDKN1A, CTGF, CXCR4, EFNA1, EPAS1, HIF1A, ID1, ID3, IL1B, IL8, ITGB3, ITGB5, KCNN4, KDR, MAP3K5, MT2A, MYC, NDRG1, NFKBIA, NQO1, PGF, PPAP2B, PTGDS, PTGS2, RALA, RUNX2, SLC2A1, TCF4, THBS1
MEOX2		transcription regulator	Activated	2.138	2.73E-03	ANGPT1, CCL2, CCL20, CDKN1A, EFNA1, FGF2, HBEGF, ICAM1, ID1, ID3, IL8, ITGB3, ITGB5
TFEB		transcription regulator	Activated	2.395	2.65E-02	ATP6V1H, CLCN7, CTSF, HEXA, MCOLN1, SCPEP1, TMEM55B, TYRP1, VEGFA
SOX9		transcription regulator	Activated	2.198	3.13E-02	BMI1, CDKN1A, CTGF, CXCR4, FOS, KIT, MIA, MITF, PTGDS, RUNX2, SNAI2, SOX8, TCF7L2, VEGFA
CIITA		transcription regulator	Activated	2.172	7.71E-02	CCND1, CD74, GCNT2, HLA-DPA1, HLA-DRA, HLA-DRB1, MMP9
FOXA1		transcription regulator	Activated	2.021	2.08E-01	ACTA2, ACTG2, ANXA1, CD58, EFHD1, ELK3, FNDC3B, FSTL1, HK1, LHFP, LYN, MALT1, NR4A2, NRIP1, PRNP, TFF3, TPM2, TRIM2, UGT2B17, XBP1
MYOCD		transcription regulator	Activated	2.383	3.26E-01	ACTA2, ATP2A2, CDKN1A, FOS, MEF2C, MYLK, VCAN
IKZF1		transcription regulator	Activated	2.615	3.52E-01	ADAM19, CCND2, CDKN1B, EPOR, FGF13, FGFR3, HES1, HNRPLL, KIT, LHFP, LHFPL2, MYC, PPP1R9A, PRNP, RAI14, SASH1, SLC27A3
GATA6		transcription regulator	Activated	2.069	4.62E-01	ACTA2, CAV1, CDKN1A, DAB2, MEF2C, MYLK, SEMA3C, TNFSF10

Upstream Regulator	Log Ratio	Molecule Type	Predicted Activation State	Activation z-score	p-value of overlap	Target molecules in dataset
TGFB1		growth factor	Inhibited	-3.235	4.82E-20	ABCA1, ABCC2, ABCD1, ABCE1, ABL1, ACAA2, ACSL3, ACSS1, ACTA2, ACTG2, ACTN1, ACVR1, ADAM19, ADK, ADM, ADORA2B, AHNAK, AHR, AIF1L, AIM2, ALDH18A1, AMD1, ANGPT1, ANGPTL4, ANXA2, APOE, AQP11, ARHGEF19, ARID5B, ARL4A, ASNS, ATM, ATXN1, B3GALT2, BAX, BCL2, BCL2L11, BCL3, BDNF, BECN1, BHLHE40, BIRC5, BMF, BMI1, BMP1, BTG1, C1S, C2, C20orf24, CALCOCO2, CALM1 , CAMK2G, CASP1, CASP4, CAV1, CCL2, CCL20, CCNA2, CCNB2, CCND1, CCND2, CCNG2, CCR1, CD36, CD55, CD59, CDC25A, CDC25C, CDC42EP4, CDK5R1, CDKN1A, CDKN1B, CDKN2C, CEBPB, CELF2, CENPA, CKS1B, CLCA2, CLIC4, CMTM5, CNIH, COL16A1, CRYGS, CSPG4, CSRP2, CTGF, CTLA4, CTPS1, CTSH, CTSK, CXCR4, CYB561, DAB2, DAPK1, DDB2, DDIT4, DDX21, DKC1, DKK3, DLL3, DNAJB4, DSP, DUSP1, DUSP4, DYNLL1, DYRK2, EDNRB, EGLN1, EGR1, EGR2, EGR3, EIF4A3, ELK3, EOMES, EPHA2, ERCC5, ESPL1, ESRP1, ETS1, F2R, F2RL1, FABP5, FAM3C, FAM53B, FAS, FCER1G, FGF12, FGF2, FLI1, FNDC3B, FOS, FOXO1, FOXO3, FSTL3, FTH1, FTL, FURIN, FXYD6, FYN, FZD1, FZD2, GALM, GAS1, GBP1, GDF15, GDPD5, GLCE, GLI2, GLRX2, GMPR, GNA13, GNB4, GPR19, GPR83, GPRC5A, GUSB, H1FX, HAS2, HAS3, HBEGF, HES1, HEXA, HEY1, HIF1A, HLA-DRB1, HMGA1, HMGA2, HMOX1, HNMT, HOXD1, HPGD, HSD17B10, HSPB1, ICAM1, ID1, ID2, ID3, IER3, IFI16, IGFBP3, IGFBP5, IL12A, IL17D, IL1B, IL8, ING1, ITGA4, ITGA6, ITGB3, ITGB5, ITPR2, JUN, JUND, KCNG1, KDELR3, KDM5B, KDR, KIAA1199, KIT, KLF15, KLF2, KLF4, KLF9, KRAS, KRT18, LAMB3, LAMC1, LDB1, LIF, LIMS1, LOX, LPCAT3, LPL, MAF, MAP2K1, MAP2K3, MAP3K11, MBNL2, MCM2, MEF2C, MGEA5, MID1, MITF, MMP9, MPP6, MSMB, MSMO1, MSN, MTHFD2, MTRR, MXD3, MXD4, MXI1, MYB, MYC, MYLK, MYO10, NAMPT, NCAPG, NDC80, NEDD9, NEK2, NFIB, NFKBIA, NLRP3, NNMT, NOC3L, NOP58, NOV, NOX4, NPAS2, NR4A2, NRP1, NT5E, NUAK1, NUPR1, OARD1, OPN3, P4HA1, PA2G4, PAPPA, PDLIM4, PDLIM5, PDXK, PHLDA2, PIK3CD, PINK1, PLA1A, PLAT, PLAUR, PLCL1, PMEPA1, PMM1, PNO1, PNP, PPP1R13B, PPP1R3C, PPP2R5A, PRODH, PROM1, PTEN, PTGDS, PTGES, PTGS2, PTK2, RAB6A, RAB9A, RACGAP1, RALB, RARA, RBMS1, RIN1, RUNX1, RUNX2, RUNX3, RXRA, SCCPDH, SDC4, SELENBP1, SEMA3A, SFRP1, SLC16A3, SLC20A1, SLC2A1, SLC2A3, SLC39A14, SLC39A8, SLC7A1, SLC7A5, SMAD6, SMTN, SNAI2, SNTB2, SOD2, SOX4, SPHK1, SPOCK1, SPP1, SPRY1, SRC, SRI, SRM, SRSF2, SSTR2, ST3GAL5, STC2, TACC2, TAX1BP3, TCN2, TGFA, TGFBR2, TGFBR3, TGIF1, THBS1, TIMP2, TIMP3, TJP2, TLE4, TLR4, TNC, TNFRSF12A, TNFSF13B, TPM2, TPST2, TRIM2, TRIM9, TSC22D1, TSC22D3, TUBB3, TWIST1, TXNIP, UCK2, UST, VASP, VAT1, VCAN, VDR, VEGFA,
MYC	-1.011	transcription regulator	Inhibited	-2.033	1.85E-18	ABCE1, ACAT1, ACSL4, ACTN1, ADD1, ADK, ADM, AIMP2, AK2, AKAP12, ALDH18A1, AMD1, ANGPT1, ANGPT2, ASNS, AURKB, BAX, BCKDHB, BCL2, BDNF, BIRC5, BMI1, BOP1, BRCA1, CASP1, CAV1, CCNA2, CCNB2, CCND1, CCND2, CCNG2, CDC25A, CDC25B, CDC25C, CDK6, CDKN1A, CDKN1B, CEBPD, CHKA, CHRNB1, CLIC4, CLUH, COL15A1, COL5A2, CSDA, CSPG4, CSRP2, DBI, DDB2, DDIT3, DDX18, DDX21, DKC1, DKK1, DUSP1, DUSP6, E2F2, E2F3, EGLN1, EGR2, EIF4A1, EIF4G1, F2R, FABP5, FAM129A, FAP, FAS, FASN, FBN2, FOS, FOSL1, FOXM1, FSTL1, FTH1, GART, GAS1, GCLM, GFPT1, GOLGA2, GRPEL1, GSR, GTF2F2, HAS2, HIF1A, HIST1H4A , HIVEP2, HK2, HMGA1, HMOX1, HNRNPAB, HNRNPD, HSPB1, HSPD1, ICAM1, ID1, ID2, ID3, IER3, IL1RAP, IL8, IMPA2, IRF9, ITGA6, JARID2, KDR, KLF4, KRAS, LAMB3, LGMN, LIMA1, LIMS1, LOX, LXN, MAPKAPK5, MBP, ME2, METAP1, MGAT1, MINA, MITF, MMP9, MNT, MRPL12, MSN, MT1E, MTHFR, MYC, NCL, NDRG1, NOLC1, NOP56, NOP58, NUCB1, NUDC, OAS1, OLIG1, PFAS, PFKFB3, PHB, PHF20, PLA1A, PLAUR, PLP1, PMAIP1, PMP22, PNO1, POLR1B, PPAT, PPP1CC, PPP1R15A, PRMT1, PRODH, PSAT1, PTEN, RAB40B, RANBP1, RARA, RARRES1, ROCK1, ROCK2, RPL6, RPL7, RPS7, RRP1B, RRS1, RTN2, RUVBL1, SAT1, SCPEP1, SERBP1, SFRP1, SFXN1, SLC16A3, SLC1A5, SLC25A19, SLC2A1, SLC2A3, SLC38A1, SLC3A2, SLC7A5, SNHG12, SNRPC, SOD2, SOX2, SOX6, SPP1, SRM, SRSF2, ST3GAL1, ST3GAL4, STMN1, TFDP1, TGFBR2, THBS1, THBS2, TIMM23, TIMP2, TLE1, TLE4, TNC, TNS3, TP53I3, TPD52, TPP2, TXNIP, UBE2C,

ERBB2		kinase	Inhibited	-2.222	2.76E-16	ABL1, ACAA2, ACSL4, ACTA2, ADAM19, ADIPOR2, AHNAK, ALAD, ANG, ANGPTL2, ANGPTL4, ANXA2, ATP1B3, BAG2, BCKDHB, BCL2, BCL3, BHLHE40, BIRC5, BMP1, BNIP3, CCL20, CCNA2, CCNB2, CCND1, CCND2, CD36, CD59, CDC25A, CDC25C, CDK6, CDKN1A, CDKN1B, CDKN2C, CENPA, CHST2, CKS1B, COL5A2, CRADD, CTGF, CYB561, DDIT3, DECR1, DUSP6, EGR1, ELF2, ELK3, EPS15, ESPL1, ETV1, ETV4, ETV5, F2R, FAM134B, FASN, FEN1, FOS, FOXO1, FSTL1, FSTL3, FZD4, G3BP1, GHR, GNAI1, HADHB, HAS2, HES1, HIF1A, HIST1H4A , HMGA2, HMGB2, HSPB1, HSPB8, ID1, ID2, IDH1, IGF2R, IGFBP3, IGFBP5, IL1B, IL8, IRX3, ITGA6, ITGB3, ITPR2, JUN, KCNN4, KDM5B, KDR, KIT, KLF4, LAMB1, LXN, MACF1, MAP2K3, MARCKS, MITF, MMP9, MSMB, MXD3, MXI1, MYC, MYO10, NCAPG, NDC80, NDRG1, NEDD9, NEK2, NFIB, NNMT, NOX4, NRP1, PDE8A, PDK4, PDLIM4, PFKFB3, PHLDA2, PHLDB1, PHYH, PIK3CD, PINK1, PLAT, PLAUR, PMEPA1, PPP2R2B, PPP2R5A, PTEN, PTGES, PTGS2, QKI, RALB, RASA3, RNF149, SEC61A1, SFRP1, SLC2A1, SMTN, SNAI2, SORBS1, SOX4, SPAG1, SPOCK1, SQLE, SRC, ST3GAL4, ST3GAL6, STK17B, TAX1BP3, TFAP2C, TGFA, TGIF1, THBS1, TIMP3, TNC, TPD52, TSC22D1, TUBB4A, UBE2C, UCK1, VCAN, VDR, VEGFA, WBP5, WFS1, WISP2, WWC1, XBP1, ZNF703, ZWINT
NUPR1	0.299	transcription regulator	Inhibited	-6.095	1.29E-15	ABL2, ACSS1, ADM, AEN, AKAP12, ANK3, AP5M1, AS3MT, AVPI1, BNIP3, BRCA1, BRI3BP, BTG1, C2orf44, C3orf58, C8orf58, CCDC77, CCNA2, CCNB2, CDC25C, CDCA3, CDCA8, CDKN1B, CEBPB, CENPL, CHMP1B, CHTF8, CNPY4, COQ10A, CREB5, CROT, CTPS2, CXCR4, DDIT3, DGCR8, DSN1, DUSP5, EGLN1, EME1, ESPL1, ETS1, ETV1, FAM111B, FAM115C, FOXO3, FUCA1, GCNT2, GDF15, GPSM2, GRAMD3, GSTA4, GTSE1, HBEGF, HILPDA, HIST1H4A , HK2, HSPA2, IFIT2, IGF2BP3, IL13RA1, IL8, ING2, IP6K2, IPP, IRS2, ITPR3, KANK2, KIF11, KIF20A, KIF2C, KLF4, LARS2, LHFPL2, LIF, LRP8, LRRC16A, LRRC33, MAFG, MCM10, MEGF9, MGLL, MT1X, MTFMT, MYC, NAPEPLD, NCKIPSD, NDRG1, NFIB, NT5DC3, NUP50, NUPR1, OSGEPL1, PER3, PFKFB3, PFKFB4, PHLDA1, PM20D2, PMP22, PPP1R15A, PRELID2, PRNP, PXDC1, RAB17, RAB32, RAB38, RBMS1, RCL1, RFTN2, RILPL2, RIMKLA, RNF122, RNF19B, SAMD4A, SAT1, SH2D5, SHPK, SIX4, SLC16A10, SLC16A6, SLC25A20, SLC2A1, SLC39A8, SRGAP2, STX3, SUOX, TCEANC2, TFAP2A, TMEM158, TMEM167B, TMEM19, TMEM194A, TNS3, TOLLIP, TP53BP1, TRAFD1, TRIB1, TRIB3, UAP1, UBIAD1, UPP1, VPS45, WDR91, XBP1,
HGF		growth factor	Inhibited	-3.636	3.22E-15	ACTA2, ADAMTS1, AHR, AIMP2, AKAP12, AKAP13, ANGPT2, ANGPTL2, ANGPTL4, ANK3, ASNS, ATM, AURKB, BAG2, BCL2, BIRC5, CALM1 , CASP1, CAV1, CCL2, CCND1, CCNG2, CD3EAP, CDC25A, CDC25B, CDC25C, CDC6, CDKN1A, CDKN1B, CDKN2C, CKS1B, CTGF, CTSK, CXCR4, DBF4, DDIT3, DDX21, DIAPH2, DKC1, DUSP4, DUSP6, DYNLL1, EFNB2, EGR1, EPHA4, ERRFI1, ETS1, FAM3C, FASTK, FEN1, FOS, FOSL1, FOXM1, GAB1, GNA13, GPSM2, GRK5, HBEGF, HES1, HK1, HK2, HMMR, HMOX1, HTR7, ICAM1, IGFBP3, IL1B, IL27RA, IL8, ISG20, ITGA6, ITPR3, KIF11, KIF2C, KRR1, KRT18, LGMN, LRP8, MAP2K3, MCL1, MCM2, MERTK, MID1, MMP9, MYC, NAMPT, NDC80, NEK2, NEK3, NOLC1, NOP2, NPC1, NR4A2, NR5A2, NRCAM, NRIP1, NRP1, PEX5, PGF, PHB, PHLDA1, PHLDA2, PIM2, PLAUR, PMP22, PPAN, PPAP2A, PPAP2B, PTGS2, PVR, RGS20, RIN1, RNF103, RUNX2, SEMA3A, SFRP1, SLC20A1, SLC7A1, SLK, SOCS2, SOX2, SPP1, SPRY2, STC1, STK10, TGFA, TGFBR2, THBS1, TIMP3, TMEM158, TNFRSF1A, TPX2, TRAIP, TRIB1, TRIP13, TTK, UBE2C, VDR, VEGFA
RAF1		kinase	Inhibited	-2.961	5.67E-13	AKAP12, AMD1, ANXA1, BCL2, BCL2L11, BECN1, BTG1, C22orf28, CCND1, CD74, CDC25A, CDC42EP1, CDC6, CDKN1A, CDKN1B, CLDN1, CTSH, CTSL1, DCBLD2, DHRS3, DUSP4, DUSP5, DUSP6, EGR1, EGR3, FAM13A, FAS, FOS, HBEGF, HIF1A, HMGA2, HMGB3, HNRNPAB, HPCAL1, HSPB1, ID3, IER3, IGFBP3, IL12A, IL1B, ITGB3, ITGB5, JUN, LIF, LPGAT1, MCF2L, MGLL, MMP9, MYC, NOP56, PHLDA1, PHLDA2, PLAT, PLAUR, PNP, PTGS2, RAN, RGS1, RND3, SCNN1A, SEC14L2, SELENBP1, SMAGP, SPRY2, SQLE, ST3GAL4, ST6GALNAC2, TOMM40, TPM2, TSC22D1, TXNIP, VEGFA, WISP2, YPEL5
EGF		growth factor	Inhibited	-3.078	1.94E-12	ABI1, ACSL4, ACTN1, ANGPT1, ARHGEF2, ATM, ATP2A2, AURKB, B4GALT5, BCL2, BIRC5, BRCA1, CASP1, CAV1, CCND1, CCND2, CDC25C, CDC42EP1, CDK5, CDKN1A, CDKN1B, CEBPB, CEBPD, CPB2, CTGF, CXCR4, DDIT3, DUSP1, DUSP4, DUSP5, DUSP6, E2F3, EGR1, EGR2, EGR3, EPAS1, EPHA2, EPS15, ERRFI1, ETS1, ETS2, FASN, FGF2, FOS, FOSL1, FST, FSTL1, GAL3ST1, GAS1, GFPT1, GSTA4, HAS2, HAS3, HBEGF, HES1, HIF1A, HMOX1, ICAM1, ID1, ID2, IDH1, IDS, IER3, IGFBP3, IGFBP5, IL1B, IL7R, IL8, ITGB3, JUN, JUND, KRAS, LPCAT3, MCL1, MMP9, MST1, MYC, NCL, NR4A2, NRP1, PDK4, PHLDA2, PLAT, PLAUR, PPAP2B, PTGES, PTGS2, PTPN12, RALA, RRM1, RUNX1, RXRA, SCG2, SH2B3, SNAI2, SOX4, SPP1, SPRY2, SPRY4, ST3GAL1, ST3GAL4, TFAP2A, TFDP1, TGFA, TGFBR2, TGIF1, THBS1, TIMP3, TNC, TNFRSF12A, TWIST1, UGT2B17, ULK1, VAMP2, VASP, VCAN, VDR, VEGFA, ZFP36
TNF		cytokine	Inhibited	-4.265	7.22E-12	ABCA1, ABCC1, ABCC2, ABR, ABTB2, ACACA, ACADS, ADM, ADORA2B, AK2, AKAP12, ALAD, ALDH1A3, ANGPT1, ANGPT2, ANGPTL4, APOE, ARSI, ATP2A2, ATP2B1, BAX, BCKDHB, BCL2, BCL2L11, BCL2L13, BCL3, BDNF, BHLHE40, BHLHE41, BID, BIRC5, BMPR1A, BTG1, BTG3, CALR, CASP1, CASP4, CAV1, CCL2, CCL20, CCL28, CCND1, CCND2, CCR1, CCRN4L, CD36, CD55, CDC25C, CDC42EP4, CDK5R1, CDKN1A, CDKN2C, CEBPB, CEBPD, CFB, CHST2, CHSY3, CLIC4, CLTCL1, COL15A1, COL16A1, CRADD, CTGF, CTLA4, CTSF, CXCL13, CXCL16, CXCR4, CYP27A1, CYTH3, DBI, DDIT3, DEFB4A/DEFB4B, DHRS3, DKK1, DLX1, DUSP1, DUSP14, DUSP5, DUSP6, EDNRB, EFNA1, EFNB2, EGR1, EGR2, ELK3, ENPP2, EPHA2, ETS1, F2RL1, FABP5, FADD, FADS1, FAS, FASN, FCER1G, FGF2, FGFRL1, FOS, FOSL1, FOXO4, FST, FTH1, GAB1, GBP1, GCLM, GDF15, GHR, GNAI1, GNB4, GSPT1, GSTM2, GUSB, HBEGF, HERC1, HES1, HEXA, HIF1A, HIPK2, HK2, HLA-DRA, HLA-F, HMGCR, HMOX1, HPGD, HSP90AB1, HSPD1, ICAM1, ID1, IER3, IFNAR2, IFNGR2, IGFBP3, IGFBP5, IL12A, IL16, IL1B, IL7R, IL8, IRF4, IRF5, ITGA4, ITGA6, ITGB3, ITPR2, JARID2, JUN, JUND, KDR, KIF20A, KIT, KLF2, KLF4, KYNU, LAMA4, LAMB3, LAMC1, LIF, LOX, LPL, LSS, LTBR, LXN, LYN, MAFF, MAP2K3, MAP2K6, MAP3K7, MARCKSL1, MBP, MC1R, MCAM, MCL1, MGST1, MIA, MMP16, MMP9, MNT, MST1, MT1A, MT1E,, MYC,, MYLK,, NAMPT,, NEDD9,, NFKBIA,, NFKBIE,, NLRP3,, NNMT,, NOV,, NQO1,, NR3C1,, NR4A2,, NR5A2,, NRIP1,, NRP1,, NUAK1,, OAS1,, OGN,, OLFML2B,, OPTN,, P2RX5,, PAPPA,, PCDH7,, PDE4B PHLDA1, PLAT, PLAUR, PLIN2, PLP1, PMAIP1, PNPLA8, PPAP2A, PPARGC1A, PPIF, PPP1R15A, PPP1R3C, PTEN, PTGES, PTGS2, PTPN12, QKI, RAB32, RARA, RARRES3, RASSF7, RCAN1, RGS1, RGS20, RNASE4, RND3, RNF149, RRM1, RUNX2, RXRA, SAMD4A, SAT1, SCNN1A, SDC4, SEMA3C, SERPINB8, SFRP1, SLC20A1, SLC2A1, SLC7A1, SMPD1, SMPD2, SNN, SOAT1, SOD2, SORBS1, SOX4, SPHK1, SPP1, SPSB1, SQLE, ST3GAL5, ST3GAL6, ST6GAL1, STMN1, SUPT4H1, SVIL, TBXAS1, TFAP2A, TFAP2C, TGFA, TGFBR2, TGIF1, THBS1, THBS2, TIMP2, TIMP3, TK1, TLR4, TM4SF1, TNC, TNFRSF1A, TNFRSF1B, TNFSF10, TNFSF13B, TP53I3, TP53INP1, TPP2, TPST1, TRADD, TRAFD1, TRIM63, TSC22D3, TWIST1, TXN2, TXNIP, UBD, UBE2H, UBQLN2, UCK1, VASP, VDR, VEGFA, WISP2, YWHAG, ZFP36,
VEGFA	-0.581	growth factor	Inhibited	-2.983	4.54E-11	ADAMTS1, AK4, ANGPT2, ARG2, ATP5J2, BAX, BCL2, BIRC5, BTK, CAV1, CCL2, CCND1, CD55, CDC25C, CDKN1A, CDKN1B, CEACAM1, CLIC4, CTGF, CXCR4, DECR1, DUSP4, DUSP5, E2F2, E2F3, EFNB2, EGR1, ETS1, ETS2, ETV4, ETV5, FGF2, FOS, GART, GBP1, HBEGF, HK1, HMOX1, ICAM1, ID1, ID3, IGFBP5, IL8, KDR, LDB1, MCL1, ME2, MEF2C, MMP9, MRPL3, MRPS12, PLAT, PPA1, PPAP2B, PPARGC1A, PTGS2, RCAN1, RUNX1, RUNX2, SDHB, SMTN, SNAI2, SOD2, STARD8, STC1, SYNM, THBS1, TJP2, TOMM20, TXN2, VEGFA
HIF1A	-0.809	transcription regulator	Inhibited	-2.673	8.15E-11	ACO1, ACTA2, ADAMTS1, ADM, ADORA2B, AKAP12, ANGPTL4, ASNS, ATP2A2, BCL2, BHLHE40, BHLHE41, BID, BIRC5, BNIP3, BRCA1, CAV1, CDKN1A, CDKN1B, CHKA, CTPS1, CXCR4, EGLN1, EPAS1, EPOR, ERO1L, ETS1, FAM13A, FOS, FURIN, GHR, H2AFX, HIF1A, HILPDA, HIST1H2AC, HIST1H2AG , HIST1H4A , HIST2H2AC, HK2, HMGCL, HMOX1, ID2, IGFBP3, IGFBP5, IL1B, IL8, IRS2, ITGB3, JUN, KIAA1199, KRT18, LOX, MAFF, MCL1, MEF2C, MITF, MMP9, MYC, NDRG1, NOV, NOX4, NT5E, P4HA1, PFKFB3, PFKFB4, PGF, PLAUR, PMAIP1, PPFIA4, PTGS2, QKI, SCG2, SDC4, SIRT2, SLC16A4, SLC25A37, SLC29A1, SLC2A1, SLC2A3, SLC40A1, SPHK1, ST3GAL1, STC2, TCF4, TGFA, TMEM19, TMEM45A, VASP, VEGFA
IL2		cytokine	Inhibited	-3.174	3.66E-10	ABCC1, ADCY3, AHR, ATM, BAX, BCCIP, BCL2, BHLHE40, CAPN5, CASP1, CCL2, CCND1, CCND2, CCNG2, CD2, CD58, CD59, CDC25A, CDC6, CDK5R1, CDK6, CDKN1A, CDKN1B, CDKN2C, CEACAM1, CLSPN, CSRNP1, CTLA4, CTPS1, CXCR4, CYP27A1, DAPK1, DDX21, DKC1, DUSP4, DUSP5, DUSP6, EEF1E1, ELF1, ENPP2, EOMES, ETS1, FAIM3, FAS, FCER1G, FGF2, FOS, FOXO1, FOXO3, FYN, GART, GDF15, GNL3, HK2, HSPD1, ICAM1, IER3, IFNGR2, IL1B, IL27RA, IL7R, IL8, ING4, IP6K2, IRF4, ISG20, ITGA4, ITK, JUN, JUND, KIT, KLF13, LIF, MAF, MAP2K1, MAP2K6, MMP9, MYB, MYC, NOP2, PDCD2L PHB, PHLDA1, PHLDA2, PIK3R3, PIM2, PMAIP1, PNP, POLR1B, POLR1C, PPAT, PPP2R2B, PTGS2, PUS1, SATB1, SESN1, SESN3, SLC30A1, SNAP23, SOCS2, SPP1, SPRED1, SPRED2, STAM, STK17B, TNFRSF12A, TNFRSF1A, TNFRSF1B, TNFSF10, TP53INP1, TRAF5, TRIB3, UCK2, UPP1, VEGFA, XBP1, YARS, ZHX1
AGT		growth factor	Inhibited	-2.514	5.90E-10	ACTA2, ADD3, ADM, ADORA2B, ANGPT1, ANGPT2, ANK3, ARHGEF11, ARID2, ATP1B1, ATP2B1, BAX, BCL2, BECN1, BRCA1, CALR, CAV1, CCL2, CCND1, CCND2, CD36, CDC25A, CDKN1A, CDKN1B, COL11A2, CREB5, CTGF, CYTH3, DAB2, DUSP1, EDNRB, EFNB2, EGR1, ERRFI1, ETS1, ETV1, FASN, FGF13, FGF2, FOS, FOXO3, FRAT2, GAS2, GFPT1, GRK5, HAS2, HBEGF, HES1, HEY1, HIF1A, HMGB2, HMGCR, HMOX1, HSPB1, ICAM1, ID3, IDH1, IGFBP3, IGFBP5, IL8, ITGB3, ITGB5, ITPKB, JUN, LAMB1, LIF, LSS, MATN2, MGST1, MMP9, MSMO1, MXD4, MYB, MYC, NCALD, NCL, NDRG1, NOX4, NR4A2, NREP, PGF, PIR, PNKD, PPFIBP1, PPP1R3C, PTEN, PTGS2, RCAN1, RRAS, SCNN1A, SEMA6A, SGCD, SLC2A1, SOD2, SOX4, SOX6, SPP1, SPRY1, STC1, TBX2, TGFA, TGFBR2, TNFRSF12A, TUBB3, TXNIP, VEGFA, WASL, ZEB2, ZFP36
KRAS	0.529	enzyme	Inhibited	-2.271	1.82E-09	ABCC4, AHR, AMPH, ATP1B1, BCL2, BMI1, BNIP3, CASP1, CCND1, CD74, CDKN1A, CDKN1B, DCLK1, DDAH1, DDIT3, DUSP4, DUSP5, DUSP6, E2F5, EFNA1, EIF5, ERO1L, ETV1, ETV5, FOS, FOSL1, FSTL1, FTH1, GAS1, GNA13, GTF2I, HADHB, HEXA, HIF1A, HLA-DRB1, HMGA2, ID1, IER3, IGF2BP2, IL1B, IL8, IP6K2, IRF9, ITGB3, KRAS, LAMB3, LOX, LTBP4, MAP2K1, MCAM, MICB, MTRR, MYLK, NPC1, NQO1, NR3C1, NR5A2, NT5E, OAS1, PHC2, PLA1A, PLAT, PMAIP1, PPFIBP1, PTEN, PTGS2, PTK2, RNASE4, ROCK1, SDC4, SLC3A2, SOAT1, SORT1, SP100, SPRY2, STAT2, TEAD2, TGFBR2, THBS1, TIMP2, TNC, TPM2, UPP1, VCAN, VEGFA
IFNG		cytokine	Inhibited	-2.168	3.24E-09	ABCA1, ABI1, ACO1, ACSS1, ADM, ADORA2B, ADRBK1, AHR, AIF1L, AIM2, ALDH1A3, ANGPTL4, ANKS1A, AQP11, ARG2, ATP2A2, BAX, BCAN, BCL2, BCL2L11, BDNF, BECN1, BID, BMF, BTG1, C1R, CALCOCO2, CAPN3, CASP1, CASP4, CAV1, CCL2, CCL20, CCL28, CCNA2, CCND1, CCND2, CCR1, CD2, CD200, CD276, CD36, CD55, CD74, CDK5R1, CDKN1A, CDKN1B, CEACAM1, CEBPB, CEBPD, CFB, CHAC1, CIRBP, CLIC4, COL5A2, CTGF, CTSH, CTSK, CXCL16, CXCR4, CYB561, CYP27A1, DAPK1, DBP, DDB2, DDIT3, DECR1, DEFB4A/DEFB4B, DKK1, DUSP1, DUSP5, E2F2, E2F5, EDNRB, EGR1, EGR2, EGR3, EPOR, ETS2, F2R, F2RL1, FABP5, FAS, FASN, FCER1G, FCGR2A, FGF12, FGF2, FOS, FTH1, FTL, FZD1, FZD2, GAL3ST1, GART, GBP1, GDF15, GLIPR2, GMPR, GNA13, GNB4, GPR19, GPR83, GUSB, HAS2, HBEGF, HIF1A, HK2, HLA-DRA, HLA-DRB1, HLA-F, HMGCR, HMOX1, HSP90AB1, HSPB1, HSPD1, ICAM1, ID1, IER3, IFI16, IFIT2, IFNGR2, IL12A, IL17D, IL1B, IL7R, IL8, IRAK1, IRF4, IRF5, IRF9, IRS2, ISG20, ITGA6, ITGB3, ITPKB, JUN, JUND, KDR, KLF2, KLF4, KRAS, KYNU, LAMC1, LARGE, LGALS3BP, LIF, LIMK1, LOX, LPL, LYN, LZTS1, MAP2K1, MARCKSL1, MITF, MLANA, MMP9, MRAS, MT1E, MTMR3, MYC, NAMPT, NCALD, NEDD9, NFKBIA, NQO1, NUPR1, OAS1, OPN3, OPTN, PANX1, PAPPA, PCSK1, PELI1, PHACTR1, PHLDA1, PI4KB, PIM2, PIM3, PLAUR, PMAIP1, PRAME, PRNP, PTGES, PTGS2, RAB27A, RAB38, RAC2, RARRES1, RARRES3, RTP4, RUNX2, SCLY, SCNN1A, SDC4, SHB, SLC11A2, SLC29A1, SLC2A1, SLC40A1, SLC7A5, SLFN5, SMAGP, SMTN, SNAI2, SOAT1, SOCS2, SOD2, SP100, SP110, SPP1, SQLE, STAT2, SYNM, TBXAS1, TCF7L2, TFDP1, TGFBR2, TGFBR3, TGIF1, THBS1, TLR4, TMEM158, TMOD1, TNFRSF12A, TNFRSF1A, TNFRSF1B, TNFSF10, TNFSF13B, TRAFD1, TXK, TYRP1, UBD, VDR, VEGFA, ZFP36, ZYX

FGF2	-0.341	growth factor	Inhibited	-2.373	5.36E-08	ACTA2, AGAP3, ANG, ANGPT1, ANGPT2, BAX, BCL2, BDNF, BIRC5, CAV1, CCL2, CCND1, CCND2, CDC25A, CDKN1A, CDKN1B, CTSK, CTSL1, CXCR4, DDIT3, EDNRB, EFNB2, EGR1, ENPP2, EPAS1, EPOR, ERRFI1, ETS1, FAS, FGF2, FGFR3, FOS, FOSL1, FOXO1, FOXO3, FOXO4, FTH1, GBP1, HAS2, HBEGF, HIF1A, ICAM1, ID3, IGFBP3, IGFBP5, IL1B, JUN, KDR, KRAS, LOX, MBP, MITF, MMP9, NOV, NR3C1, NR4A2, PLAT, PLAUR, PRKCE, PTGS2, PTPRE, RUNX1, RUNX2, SCG2, SFRP1, SLC20A1, SLC2A1, SPP1, SPRY1, SPRY2, SPRY4, ST3GAL1, ST3GAL4, TGFBR3, THBS1, TIMP3, TNFRSF12A, TNFSF10, TWIST1, UGT2B17, VEGFA, VGF, ZFP57
BRAF		enzyme	Inhibited	-2.218	1.20E-07	BCL2L11, BMF, CCND1, CDKN1A, CDKN1B, CEBPB, DUSP4, EGR1, EPAS1, FOXD3, HIF1A, IL1B, IL8, MMP9, MYC, POU3F2, RND3, THBS1, TSC22D1
EPAS1	0.797	transcription regulator	Inhibited	-2.295	2.17E-07	ACACA, ADM, AKAP12, ANGPT2, ANGPTL4, BHLHE40, BNIP3, CAV1, CCND1, CHKA, CXCR4, DDIT3, FAM13A, FASN, FOS, GAL3ST1, HIF1A, HILPDA, HIST1H2AC, HOXA5, IGFBP3, IGFBP5, IRS2, ITGB3, KDR, KIAA1199, LOX, MAFF, MYOM2, NDRG1, PAN2, PFKFB3, PGF, PLIN2, PTPRZ1, SLC11A2, SLC16A4, SLC29A1, SLC2A1, SLC2A3, SOD2, SPHK1, STC2, TGFA, TMEM45A, TPP2, UGP2, VEGFA, WISP2
CSF1		cytokine	Inhibited	-3.495	2.28E-07	APOE, BAX, BCL2, BCL2L11, BIRC5, CBL, CCL2, CCND1, CCND2, CD97, CDKN1A, CTSK, DUSP1, DUSP5, EGR1, EGR3, ETS2, F2R, F2RL1, FAS, FCER1G, FCGR2A, FOS, GDF15, GRAP2, IL11RA, IL12A, IL1B, IRF4, IRF5, ITGA4, ITGB3, ITGB5, JUN, MAP3K3, MERTK, MMP16, MMP9, MYC, NKIRAS1, RUNX1, SFRP1, SLC29A1, STX3, TNFRSF1A, TNFRSF1B, TRAIP, VEGFA
NRG1		growth factor	Inhibited	-2.902	2.66E-07	ACTN1, ANGPT1, ARHGEF2, BCL2, BNIP3, BRCA1, CCND1, CCND2, CDC42EP1, CDKN1A, CDKN1B, CTGF, DDIT3, DNAJB2, DUSP1, DUSP4, DUSP6, EGR1, EGR2, EGR3, EPHA2, ERRFI1, FOS, FSTL1, G3BP1, HES1, HIF1A, HK2, HMGA1, HMGCR, HMOX1, ID1, IER3, IL8, ITGB3, ITGB5, JUND, LMO4, LPCAT3, MBP, MCL1, MMP9, MST1, MYC, PLAUR, POU3F1, PTGS2, RUNX1, SLC2A1, SLC2A3, SOX4, VEGFA, ZFP36
OSM		cytokine	Inhibited	-2.234	5.30E-07	ABCA1, ABCC1, ABCC4, ADAMTS1, AHCYL1, AHR, AMACR, ANGPT2, ANXA1, ANXA2, ARHGEF2, ARL4A, ASNS, ATP2B4, ATP9A, BAIAP2, BHLHE40, BMI1, BRD8, C1R, C1S, CASP4, CCL2, CCL20, CCND1, CCND2, CCNG2, CDC42EP4, CDKN1A, CDKN1B, CEBPD, CHD1, CTSH, CTSL1, DAPK1, DEFB4A/DEFB4B, DHRS3, DYRK3, ETS2, EXOSC10, FGF2, FOS, GAB1, GART, GBP1, GFPT1, GLE1, GMPR, GOLGA2, HBEGF, HIF1A, HK2, HLA-F, HMG20B, HMOX1, HSF4, HSPA2, ICAM1, ID1, ID2, IL13RA1, IL1B, IL8, IRAK1, IRF9, ISG20, ITPKB, JMJD1C, JUN, KCNG1, KRR1, LARGE, LIF, MARCKS, MGLL, MLLT11, MMP9, MOAP1, MT1X, MT2A, MYC, NAMPT, NUAK1, OAS1, PDLIM5, PEPD, PFKFB3, PLCB4, PLLP, PPP3CC, PTEN, PTGES, PTP4A1, PTPRZ1, QKI, RAP2A, RNASE4, RUNX1, RYK, SERPINB8, SLC16A3, SLC16A6, SMPD1, SON, SORD, SRPK1, ST8SIA1, STK4, TIMP3, TM4SF1, TNC, TOM1, TPX2, TRRAP, TULP3, UAP1, UBQLN2, UPK1A, VDR, VEGFA, ZNF266, ZNF330
TREM1		transmembrane receptor	Inhibited	-3.706	8.72E-07	ABL2, ACSL3, ADORA2B, ARRDC4, ASNS, ATP1B1, BRE, CCL20, CEBPB, CFB, DEFB4A/DEFB4B, DUSP14, DUSP4, EGR1, EGR2, EGR3, EPM2AIP1, ETS2, FABP3, FOSL1, GCLM, GPRC5A, HBEGF, HES1, IFIT2, IL1B, IL8, KANK1, LIF, LPL, MAFF, MCOLN2, MOAP1, MT1E, NFKBIA, NPC1, NR4A2, NT5E, PHLDA1, PHLDA2, PIM2, PPAP2B, PTGS2, RCAN1, RGS1, RHOBTB3, SNAPC1, SPP1, SPRY2, SYNJ2, TBC1D7, THBS1, TLR4, TMEM158, WBP5, YRDC
STAT3		transcription regulator	Inhibited	-2.591	1.51E-06	ADM, ANGPT2, ANGPTL4, ARG2, BATF, BCL2, BCL2L11, BCL3, BIRC5, CASP1, CCL2, CCL20, CCND1, CCND2, CCR1, CD74, CDC25A, CDKN1A, CDKN1B, CEACAM1, CEBPB, CEBPD, CFB, CTSL1, CXCL13, DDIT3, EGR1, EGR2, EGR3, EME1, EPAS1, FAS, FASN, FCER1G, FGF2, FOS, HAS2, HIF1A, HIST2H2AA3/HIST2H2AA4, HK2, HLA-DRB1, HMOX1, ICAM1, ID2, IFI16, IGFBP5, IL1B, IL8, IRF4, ISG20, KDR, KLF4, LIF, LTBR, MAF, MAP2K5, MCL1, MITF, MMP9, MRAS, MT1E, MYB, MYC, NAMPT, NDRG1, OAS1, PAX3, PCSK1, PHB, PHLDA1, PIM2, PLAUR, PMAIP1, PPARGC1A, PTGS2, RAB27A, SLFN5, SMAD6, SOD2, SP110, STC2, TCF4, TFF3, THBS1, TNFRSF1B, TNFSF10, TWIST1, VCAN, VEGFA, ZFP36
IKBKB		kinase	Inhibited	-2.431	2.88E-06	ABCA1, AURKB, BCL2, BRCA1, CCL2, CCL20, CCNA2, CCND1, CCR1, CCRN4L, CDC25B, CDC6, CDKN1A, CEBPB, CEBPD, CKS1B, CTSF, CTSK, CXCR4, DUSP6, EGR1, ENPP2, FAS, FASN, FOS, FOXM1, FOXO3, FYN, GRK5, H2AFX, HIF1A, HK2, HMOX1, ICAM1, IL1B, IL8, ITGB3, ITGB5, KIF20A, MBP, MMP9, MT1E, MYC, MYO1D, NFKBIA, OGN, PCDH7, PTEN, PTGS2, RCAN1, SEMA3C, SFRP1, SOCS2, SOD2, TIMP2, TIMP3, TNFRSF1B, TPM2, TRIM63, TWIST1, VCAN, VEGFA
IL6		cytokine	Inhibited	-2.908	3.21E-06	ABCA1, ABCC1, ABCC2, ADAMTS1, ADRBK1, AHNAK, AHR, ANG, ANXA1, APOE, ATP2A2, BATF, BAX, BCL2, BCL2L11, BCL3, BDNF, BIRC5, BMI1, CASP1, CCL2, CCL20, CCNA2, CCNB2, CCND1, CCR1, CD36, CD74, CD97, CDC25C, CDC6, CDKN1A, CDKN1B, CEACAM1, CEBPB, CEBPD, CENPA, CES2, CPB2, CTGF, CTSK, CXCR4, DEFB4A/DEFB4B, DUSP1, DUSP6, E2F2, EGR1, ENPP2, EOMES, ETS2, F12, FAS, FLI1, FOS, FOXM1, GLRX, GSTA4, HIF1A, HLA-DRB1, HMOX1, HOMER3, HPGD, ICAM1, ID1, ID2, IFI16, IFIT2, IGFBP3, IGFBP5, IL12A, IL7R, IL8, IRF4, IRF9, ITGB3, ITGB5, JUN, JUND, KDR, KIF11, KIF2C, KIT, KRT18, LARGE, LIF, LPL, MAF, MAP2K1, MCL1, MERTK, MMP9, MRAS, MT1E, MYB, MYC, NAMPT, NFKBIA, OSBPL1A, PHB, PLAT, PPP1R15A, PPRC1, PRNP, PROM1, PTGES, PTGS2, SCNN1A SLC39A14, SMOX, SNX10, SOCS2, SOD2, SP110, SPP1, SRC, SV2B, TBC1D9, TBXAS1, THBS1, TK1, TLR4, TNFRSF1A, TNFRSF1B, TRAIP, TTK, TWIST1, UBE2C, VASP, VEGFA, XBP1
MAPK9		kinase	Inhibited	-2.769	3.58E-06	BAX, BCL2, BCL2L11, BMP1, CAV1, CCL2, CDKN1A, CDKN1B, CEBPB, CHERP, EGR1, FOS, FOSL1, GSTM1, HIF1A, HMGA1, IFI16, IL12A, IL1B, IL8, IRF9, ISG20, JUN, JUND, LGALS3BP, LIF, MARCKSL1, MMP9, MYC, NCL, PLA1A, PLAT, PPP1R15A, PTEN, PTGES, RILPL1, SOD2, VDR, ZFP36, ZYX
MAP2K1	-0.339	kinase	Inhibited	-2.436	3.93E-06	ABCC1, ACTA2, AHR, APOE, BCL2, BCL2L11, BRCA1, CAPN3, CCL2, CCND1, CDKN1A, CDKN1B, CTGF, DAB2, DKK1, DUSP1, DUSP5, DUSP6, EGR2, ETV5, F2R, FASN, FGF2, FOS, FOSL1, FURIN, GUSB, HIF1A, IL8, ITGB3, JUN, JUND, MITF, MMP9, MYC, NFKBIA, PLAUR, PTGS2, RAB38, RAP1GAP, SNAI2, THBS1, TNC, TWIST1, VEGFA
ITGB1		transmembrane receptor	Inhibited	-2.184	4.33E-06	ABCC1, ACTA2, APOE, BCL2, CCL2, CDKN1A, CDKN1B, FGFR3, FOS, GAS1, ICAM1, IL1B, IL8, ITGB3, JUN, LAMB1, LAMC1, LIMS1, MMP9, MYC, PTK2, RAC2, TCF4, THBS1, TIMP2, VEGFA
IL5		cytokine	Inhibited	-3.038	8.75E-06	ACAA2, ANXA2, ASNS, ATP1B1, ATXN1, BCL2, BCL3, BNIP3, CASP4, CCL2, CCND2, CCR1, CD55, CEACAM1, CKAP4, CXCR4, DDX21, DUSP5, DUSP6, EGLN1, EGR1, EGR2, EGR3, ERO1L, FAM65B, FAS, GCLM, GLIPR2, HBEGF, HIF1A, HMGCR, HMMR, HSPA6, ICAM1, IER3, IL8, KIAA1147, KLHDC2, MMP9, MYC, NDRG1, NEK2, P4HA1, PDE4B, PMP22, PPIF, PSAT1, RAB21, RAP1GAP, SLC16A3, SLC1A5, SLC2A1, SLC39A8, SLC7A5, SNAP23, SNTB1, SOCS2, SPCS2, SRI, ST7, STK39, TUBB2B, UCK2, UPP1, XBP1, ZYX
ZBTB17	0.295	transcription regulator	Inhibited	-2.183	1.00E-05	BCL2, BHLHE40, BTG3, CCND1, CDKN1A, DDB2, DDIT3, EGR1, IER3, LRRN3, PMAIP1, ZFP36
IL3		cytokine	Inhibited	-4.289	1.42E-05	AKR1A1, ARHGEF1, BCL2, BCL2L11, CALR, CCL2, CCND1, CCND2, CD97, CDKN1A, CDKN1B, COPS4, CTLA4, CXCR4, DDIT3, EGR1, EGR2, EGR3, ELK4, F2R, FAS, FASN, FCGR2A, FOS, FOXD3, GART, GNA13, HBEGF, HK1, HK2, HSPA2, ICAM1, IL1B, IL8, ITGB3, JUN, KLF13, KLF9, LIF, LYN, MCL1, MID1, MKI67IP, MT1E, MYC, NCL, NEDD9, NOV, NRP1, PIM2, PPM1G, RALA, RAN, RANBP1, RPL29, RPL6, RPL7, RPS7, SH3BP1, SLC2A1, SLC2A3, SLC3A2, SOX4, SPEN, TK1, TLR4, TNFSF10, TPD52, VASP, VEGFA, XBP1, YWHAG, ZBTB17, ZFAND5, ZSCAN21
PTGS2	-0.734	enzyme	Inhibited	-2.168	1.65E-05	ANG, ANGPT1, ANGPT2, ANXA1, ANXA2, BAX, BCL2, BRCA1, CCL2, CCND1, CDK5, CDKN1A, CDKN1B, CDKN2C, CTSK, CXCR4, DUSP1, DYNLL1, EGR1, FOS, ICAM1, IGFBP3, IL12A, IL1B, IL8, ITGA6, KDR, MCL1, MMP9, MYC, NOP2, NR4A2, PPA1, PTGS2, RUNX2, TNFSF10, VEGFA
CCL5		cytokine	Inhibited	-3.077	1.95E-05	AHR, CCL2, CCR1, CD97, DUSP1, DUSP6, F2R, F2RL1, FOS, HMGA1, IL12A, IL1B, IL8, LIMS1, MMP9, NAMPT, PLAUR, PNP, PPIF, PTGDS, SQLE, TLR4, VASP, ZFP36
NRIP1	-0.295	transcription regulator	Inhibited	-2.36	2.45E-05	ACAA2, ACACA, ACO2, CCNB2, CCND1, CCNG2, CDC6, CDKN1A, FASN, HADHB, HAS2, IL1B, PDK4, PTGS2, RARB, SDHB, SLC16A10, SLC25A19, SLC25A20, SMAD6, SUOX, TK1
HRAS		enzyme	Inhibited	-2.002	3.66E-05	ADM, ALDH1A3, AMACR, ANXA2, ASNS, ATP2A2, ATXN1, AURKB, B4GALT3, BCL2, BCL2L11, BIRC5, BMP1, BNIP3, CAV1, CCNA2, CCND1, CCND2, CD97, CDC25A, CDKN1A, CDKN1B, CEBPB, CEBPD, CECR5, CFB, COL5A2, CSRP2, CTGF, DDIT3, DUSP1, DUSP6, EGR1, ELK3, ETS1, F2R, FABP3, FAM167A, FAS, FGF2, FOS, FOSL1, FRMD6, FSTL1, FSTL3, FURIN, FZD1, FZD2, GNA13, GUSB, HAS2, HIF1A, HMOX1, HSPB1, ICAM1, ID2, IGFBP5, IL13RA1, IL1B, IL8, ITGA4, ITGA6, ITGB5, JUN, KRAS, KRT18, LRRC17, LXN, MCAM, MMP9, MRPL12, MSMO1, MYC, NFKBIA, NOP58, NQO1, NRP1, NSFL1C, PAFAH1B3, PDLIM5, PGF, PLAUR, PMEPA1, PRNP, PTEN, PTGS2, RAD9A, RAP1GAP, RARB, RASA3, RNF19B, RTN4, SASH1, SCNN1A, SESN1, SESN3, SOAT1, SORBS1, SOX4, SPP1, SPRY2, SQLE, STK10, TACC3, THBS1, TIMP3, TK1, TOM1, TOX2, TPM2, TSC22D1, TWIST1, UBASH3B, VCAN, VEGFA
IL1B	-0.471	cytokine	Inhibited	-3.529	3.99E-05	ABCC2, ACTA2, ADAMTS1, ADM, ANGPT1, ANGPTL4, ANXA1, APOE, ATP2A2, BAX, BCL2, BCL3, BDNF, BMF, C1R, CASP4, CCL2, CCL20, CCL28, CCR1, CCRN4L, CD55, CD74, CDKN1A, CEBPB, CEBPD, CFB, CPB2, CSRNP1, CTSF, CXCR4, DAB2, DBP, DDIT3, DDIT4, DEFB4A/DEFB4B, DUSP1, DUSP5, E2F2, EFNA1, EGR1, ENPP2, EPAS1, ERRFI1, F2RL1, FABP5, FAM129A, FAS, FGF2, FGFR3, FOS, FOSL1, FOXO1, FST, GBP1, GDF15, GHR, GUSB, HAS2, HBEGF, HES1, HEXA, HIF1A, HK2, HLA-DRA, HMGA1, HMOX1, HSPB1, ICAM1, ID3, IER3, IGFBP3, IGFBP5, IL12A, IL16, IL1B, IL1RAP, IL8, IRAK1, IRS2, ISG20, ITGB3, ITPKB, JUN, KDR, LAMB3, LIF, LOX, MAP2K6, MARCKSL1, MCL1, MIA, MMP9, MT1E, MT2A, MYC, NAMPT, NFKBIA, NQO1, NR4A2, P2RX7, PAPPA, PCDH7, PCSK1, PDE4B, PHLDA1, PIM3, PLAT, PLXDC2, PPARGC1A, PTGDS, PTGES, PTGS2, PTP4A1, RAC2, RARA, RASA2, RCAN1, RRS1, RUNX2, RXRA, SCLY, SCNN1A, SDC4, SESN1, SLC11A2, SLC20A1, SLC2A1, SOCS2, SOD2, SPP1, TGFBR2, THBS1, TIMP2, TIMP3, TK1, TLR4, TNFRSF1B, TNFSF10, TRAFD1, TSC22D3, TWIST1, UAP1, UBD, VASP, VCAN, VDR, VEGFA, XYLT1, ZFP36, ZYX
ELK1		transcription regulator	Inhibited	-2.569	6.62E-05	CDKN1A, CDKN1B, EGR1, EGR2, FOS, FOSL1, JUN, MCL1, MMP9, MYLK, PTGS2, RUNX2, SLC2A1, SPP1, ZFP36

EGR1	-1.389	transcription regulator	Inhibited	-2.105	8.87E-05	ATP2A2, BAX, BCL2L11, CACNA1H, CAV1, CCL2, CCND1, CCND2, CCR1, CDK5R1, CDKN1A, DUSP4, EGR1, EGR2, FAS, FGF2, FOSL1, FTL, GDF15, HMGCR, HMOX1, ICAM1, IL1B, IL8, JUN, JUND, MMP9, MYB, MYC, NDRG1, PTEN, PTGES, PTGS2, SOD2, SQLE, TGFBR2, THBS1, TLR4, TNFSF10, VEGFA
F2R	-0.373	G-protein coupled	Inhibited	-2.825	1.00E-04	ANGPT1, ANGPT2, CCL2, CCND1, CD55, CTGF, DUSP1, EGR1, F2R, FOS, HMOX1, ICAM1, IL1B, IL8, KDR, PTGS2, THBS1, VEGFA
PDGFB		growth factor	Inhibited	-3.34	1.00E-04	ACTA2, EGR1, FOS, FOXO1, FOXO3, FOXO4, ICAM1, IL8, KLF2, MMP9, MYC, NOV, PHLDA1, PTEN, PTGS2, SPP1, THBS1, TNC
CD40LG		cytokine	Inhibited	-2.831	1.21E-04	AHR, AKAP13, ALG3, BATF3, BAX, BCL2, BNIP3, BTG1, BTG3, CASP1, CCL2, CCL20, CCNG2, CCR1, CDC25B, CDK6, CDKN1A, CDKN1B, CELF2, CLUH, CSDA, CTGF, CXCL13, CXCR4, DECR1, DUSP1, DUSP4, DUSP5, E2F2, EGR1, FAS, FOS, FURIN, GPR183, HIF1A, HK2, ICAM1, ID2, ID3, IFIT2, IL12A, IL13RA1, IL1B, IL1RAP, IL7R, IL8, IRF4, ITGA4, JUN, JUND, MAP2K3, MARCKS, MARCKSL1, MCL1, METAP1, MT1E, MT1G, MT2A, MYC, NAMPT, NFKBIA, NFKBIE, ORC5, PLAUR, PMAIP1, PTGS2, PTPN12, PVR, RAB9A, RASSF2, RGS1, RUNX3, SEMA4D, SLC29A1, SMG7, SOD2, STK4, TGIF1, TNFSF10, TRADD, TRAF5, UBD, VEGFA, ZZZ3
EDN1		cytokine	Inhibited	-4.167	1.56E-04	ACTA2, ADAM19, ANXA1, ARHGEF11, ATF6, ATP2A2, BAG2, BCL2, CCND1, CDC25A, CDKN1B, CTGF, EDNRB, EGR1, ERRFI1, FGF2, FOS, FOSL1, FST, HEY1, HIF1A, ICAM1, IL8, ITGB3, JUN, MAP2K1, MARCKSL1, MBP, MCAM, MITF, MMP9, MSN, MYC, NUPR1, PLAUR, PLCB4, PRKCE, PTGS2, SLC2A1, THBS1, TIMP3, TPM2, VCAN, VEGFA
PRKCE	0.191	kinase	Inhibited	-3.09	1.97E-04	ACTA2, BAX, BCL2, BIRC5, CAV1, CCND1, CD55, CDKN1A, CEBPB, EGR1, FOS, HSP90AB1, IL1B, IL8, JUN, MMP9, MYC, PRKCE, PRKD1, PTGS2, VEGFA
STAT5A		transcription regulator	Inhibited	-2.112	2.48E-04	ARNT, ATM, BAX, BCL2, CASP4, CCND1, CCND2, CDC25C, CDK6, CDKN1A, CDKN1B, CEBPB, EPAS1, EPOR, FAS, FASN, FCER1G, FOS, GJB1, ICAM1, ID1, ID2, LTBR, MAF, MCL1, MYC, NR4A2, RIMKLA, SLC2A1, SOCS2, TNFRSF1A, UGP2, YWHAG, ZFP36, ZP3
MAPK1		kinase	Inhibited	-2.465	2.58E-04	ACO1, APBB3, APOE, ATP1B1, B3GALT4, BCL2, BDNF, BIRC5, C1S, CCND1, CDK5R1, CDKN1A, CDKN1B, CFB, CHST2, DAB2, DUSP1, EGR1, EGR2, ENDOD1, EXOC2, FAIM3, FOS, GBP1, GFOD1, GPR83, HMOX1, IFI16, IFIT2, IGF2BP3, IL1B, IRF9, ISG20, ITGB3, ITPR2, JUN, JUND, L3MBTL1, LAMA4, LGALS3BP, LIF, LZTS2, MBP, MCL1, MMP9, MNS1, NRP1, NT5E, NUPR1, OAS1, OSBPL3, PARP12, PDLIM3, PTGS2, QKI, SCNN1A, SOCS2, SP100, SP110, SPOCK1, SPP1, SPRY2, SPRY4, SPSB1, STAT2, SUOX, TMEM158, TNFRSF1B, TNFSF10, UBE2C, VDR, WIPF1
MAPK3		kinase	Inhibited	-3.611	2.66E-04	B4GALT5, BCL2L11, CCND1, DUSP4, EGR1, FOS, FOSL1, FURIN, IL8, JUN, MCL1, MMP9, MYC, PLAUR, PPARGC1A, PTGES, PTGS2, SPP1, THBS1
IL15		cytokine	Inhibited	-3.129	3.10E-04	ACADS, ACTG2, AHR, ANXA1, BCL2, BCL2L11, BTG1, CALM1, CCL2, CCND2, CCR1, CD2, CD55, CD59, CD74, CDK6, CEACAM1, CKS1B, CTGF, CXCR4, DDX18, DHRS4, DUSP14, DUSP5, EGR2, ELK3, ETS1, FAS, FYB, FYN, GABPB1, GLDC, GNL2, GPRC5A, HIST2H2AA3/HIST2H2AA4, HNRNPF, IL1RAP, IL7R, IL8, ITGB5, JUN, LEF1, LIF, LYN, MAF, MCL1, MICB, MST1, MT1G, MYC, NFKBIA, NUDT1, OGN, PA2G4, PAFAH1B3, PDE4B, PMAIP1, PNP, PTP4A1, PTP4A2, RAC2, RBBP8, SOCS2, SP100, SRSF7, TGFBR2, TJP2, TNFRSF1A, TNFSF10, UPP1, VDR, XBP1, YARS, ZFP36
PPRC1	-0.393	transcription regulator	Inhibited	-3.622	3.50E-04	CCL20, CLDN1, DDIT4, DUSP5, ERRFI1, FBXL13, GDF15, HK2, IL8, LAMB3, NAMPT, PHLDA1, PTGS2, RND3, SPRR2D, SUN3, TMEM154
IGF1		growth factor	Inhibited	-2.106	4.24E-04	ACACA, ACTA2, ADM, ANGPT2, BAX, BCL2, BDNF, BHLHE40, BIRC5, BRCA1, CCNA2, CCND1, CCND2, CDKN1A, CDKN1B, CSDA, CTGF, DDIT3, DDIT4, DEFB4A/DEFB4B, EFNB2, EGR1, EGR2, EPAS1, FASN, FOS, FOXO1, GHR, H2AFX, HIF1A, HMGCR, HMOX1, ICAM1, ID2, IER3, IFNGR2, IGFBP3, IGFBP5, IL16, IL1B, IL8, IRS2, ITGB5, JUN, LPL, MAFG, MAK16, MBP, MCL1, MYB, MYC, NFKBIA, NOX4, OSBPL7, PHLDA1, PLAUR, PLP1, PTEN, RARB, RUNX2, SLC20A1, SLC2A1, SNAI2, SOX2, SPP1, SQLE, THBS1, TK1, TLR4, TNFRSF12A, TUBB3, TWIST1, VEGFA
MIF		cytokine	Inhibited	-2.96	4.63E-04	ACTA2, C3AR1, CCL2, CCND1, CDKN1B, DUSP1, F2R, F2RL1, FASN, FOS, ICAM1, IL1B, IL8, ITIH5, JUN, MMP9, PTGS2, TLR4, TPH2
CREB1		transcription regulator	Inhibited	-2.941	6.18E-04	ABCA1, ADM, ANGPTL2, APOE, BCL2, BDNF, BHLHE40, CCNA2, CCND1, CEBPB, CEBPD, CR2, CSRNP1, CSRP2, DUSP1, DUSP14, EGR1, EGR2, ERRFI1, FASN, FOS, FRMD6, GPR19, HAS2, HLA-DRA, HMGCR, HMOX1, ID1, IL1B, IRS2, JUN, LSS, MCL1, MNS1, MSMO1, MVK, MYC, NDUFA10, NR4A2, PCSK1, PDXK, PER2, PIM3, PITPNB, PPARGC1A, PPP1R15A, PTGS2, SLC2A3, SMAD6, SOD2, SRPK2, TFAP2A, TOM1, UPP1, VEGFA, ZFP36
HBEGF	-0.161	growth factor	Inhibited	-2.892	6.88E-04	BCL2, CCND1, CCND2, CXCR4, FGF2, HK2, MMP9, NRP1, PDK4, PTGS2, TGFA, VEGFA
GRP		growth factor	Inhibited	-2.689	7.06E-04	CCND1, CDKN1B, FOS, IL8, JUN, MYC, PTGS2, PTK2, RRM1, VEGFA
BCL2	-0.394	transporter	Inhibited	-2.464	7.15E-04	ABCC1, ATP2A2, BAX, BCL2, BCL2L11, BNIP3, CCND1, CDKN1A, CDKN1B, CTSH, FAS, FOS, HIF1A, ICAM1, IL1B, IL8, MCAM, MCL1, MMP9, NDRG1, NFKBIA, PLAUR, PTEN, SPHK1, TIMP2, VEGFA
SYVN1		transporter	Inhibited	-4	8.12E-04	ABCC4, ACSL3, AHR, ATP1B3, BHLHE40, CALM1 , CCND1, CSPG4, CTPS1, CYB561, DAB2, DUSP1, EPHA2, FASN, GPRC5A, HSPB1, IL7R, ITGA6, KCNN4, LGALS3BP, MCAM, NDFIP2, PPAP2B, PTBP1, SLC1A5, SLC20A1, SLC27A3, SLC2A1, SLC2A3, SLC30A1, SLC39A10, SLC3A2, SLC43A3, SLC4A7, SLC7A5, SNAP23
HMGA1	-0.234	transcription regulator	Inhibited	-2.267	8.42E-04	ATM, BCL2, BRCA1, CAV1, CCND1, DAB2, DHCR7, HMGCR, ID3, KIT, MIA, MMP9, MVK, PTGS2, TWIST1
SRC	-0.181	kinase	Inhibited	-3.12	1.22E-03	CAV1, CBL, CCL2, CCND1, CCND2, CDKN1A, DUSP1, F2R, FOS, FOSL1, HAS2, HIF1A, HMOX1, ICAM1, ID1, IL8, JUN, KRT18, MCL1, MMP9, MYC, NQO1, PLAUR, PRKCE, PTGS2, SPP1, SRC, VEGFA
DDX17		enzyme	Inhibited	-2.176	1.67E-03	CCND1, CDKN1A, FOSL1, JUN, MYC
NGF		growth factor	Inhibited	-2.78	1.97E-03	ANXA2, BAX, BCL2, BCL2L11, BDNF, CAV1, CCND1, CDK5R1, CDKN1A, CDKN1B, DLG4, DUSP1, DUSP4, E2F2, EGR1, EGR2, EHD4, EPAS1, FAS, FOS, FOSL1, HMOX1, ID1, JUN, MAP3K11, MAP3K12, MMP9, MT1A, MYC, PLAUR, PPP2R2B, PTEN, SCG2, SLC40A1, TFAP2A, TNFRSF12A, TRPV4, VEGFA, VGF
TNFSF13B	-0.432	cytokine	Inhibited	-2.861	2.04E-03	BAX, BCL2, BCL2L11, CCND2, CR2, DUSP5, ICAM1, IL8, MCL1, MMP9, MYC, NAMPT, PIM2
SPHK1	-0.429	kinase	Inhibited	-2.478	2.66E-03	BCL2L11, CCND1, CDKN1A, CTGF, DEFB4A/DEFB4B, EGR1, IL1B, JUN, MAP2K6, PTGES, PTGS2
ARNT	0.203	transcription regulator	Inhibited	-3.13	3.25E-03	ADM, AHR, BHLHE40, BHLHE41, BNIP3, CAV1, CCND2, ERO1L, FURIN, GAS1, HIF1A, ID2, IRS2, ITGB3, KIF20A, MACF1, MPP1, NQO1, RANBP1, SLC2A1, UBE2C, VEGFA
PTK2	-0.306	kinase	Inhibited	-2.021	3.27E-03	ACTA2, CCND1, CDKN1A, CDKN1B, CSPG4, DSP, FOS, KRT18, MMP9, P4HA1, PRRX1, PTK2, THBS1, TIMP3, TNC
PRKCB		kinase	Inhibited	-2.761	3.27E-03	BAX, CCND1, CDKN1A, EGR1, FASN, FOS, ICAM1, IRS2, JUN, MMP9, MYC, PPARGC1A, PTGS2, SOD2, TGFBR2
CHRM1	0.171	G-protein coupled	Inhibited	-2.412	3.76E-03	CHRM1, EGR1, EGR2, EGR3, FOS, JUN
SMAD3		transcription regulator	Inhibited	-2.454	4.01E-03	ACTA2, BCL2, BCL2L11, CCL2, CCND1, CCND2, CCNG2, CDKN1A, CTGF, DAPK1, DUSP4, EGR1, FOS, FST, FSTL3, GLI2, HAS2, HBEGF, HEY1, HMOX1, ID1, IL1B, ITGB5, JUN, JUND, MMP9, MYC, NOV, RUNX2, SOX2, SPP1, SSTR2, TGFA, THBS1, TIMP3, TNC, TPM2, VDR, VEGFA, ZFP36, ZYX
IL7		cytokine	Inhibited	-2.531	4.25E-03	AHR, BAX, BCL2, BCL2L11, CCND2, CD2, CDK6, CDKN1A, CDKN1B, CEACAM1, CXCR4, DUSP5, FAS, GSR, IL7R, KLF2, LEF1, LIF, MAF, MCL1, MYC, PIM2, PMAIP1, RUNX2, SLC2A1, TNFSF10, UPP1, XBP1
TCF4	0.632	transcription regulator	Inhibited	-2.397	5.21E-03	BIRC5, CCND1, CDKN1A, DKK1, ID2, JUN, MIA, MITF, MYB, MYC, PSD3, SSTR2, TCF7L2, TYRP1, VCAN
E2F3	-0.184	transcription regulator	Inhibited	-2.18	5.33E-03	BIRC5, BMI1, CCNA2, CCND1, CDC25A, CDC6, CDCA4, CDKN1A, E2F2, E2F3, FGF2, MCM10, MCM2, MT1G, MYB, MYC, PPP1R13B, RRM1, TK1
MAP3K1	-0.479	kinase	Inhibited	-2.421	5.92E-03	CCND1, DUSP1, EGR1, FAS, FOS, HMOX1, HSPB1, IL8, JUN, LOXL3, NOV, PLAUR, PRDX1, PTGS2, THBS1, TNC
MAX		transcription regulator	Inhibited	-2.393	6.07E-03	BAX, CCND2, CCNG2, CDC25A, CDKN1A, CDKN1B, DDIT3, DKC1, E2F2, FTH1, HMGA1, ID1, ID2, JARID2, LRRN3, MYC, NCL, RBBP8, SCPEP1, TXNIP, UBE2C
NOTCH1		transcription regulator	Inhibited	-2.133	7.18E-03	ACTA2, ADAM19, ANGPT1, BCL2, CCND1, CCND2, CDKN1A, CDKN1B, CEBPD, CTGF, EFNB2, EPHA4, FGF2, FOS, FOSL1, GLI2, HES1, HEY1, HEY2, ICAM1, ID1, IGFBP3, IL8, ITGA6, LEF1, LOX, MCAM, MYC, PTEN, PTGDS, PTGS2, RLBP1, RUNX2, RUNX3, SPP1, TGFBR2, TGFBR3
GRN		growth factor	Inhibited	-2.201	7.55E-03	ANGPT1, BCL2, CCND1, FZD2, VEGFA

CXCL12		cytokine	Inhibited	-3.021	8.25E-03	ACTA2, BAX, BCL2, BCL3, BMP1, CCL2, CCND1, CD36, CTSK, CXCR4, EGR1, FOS, FYN, GAS2, GSR, HNRNPD, ICAM1, IFNAR2, IFNGR2, IL8, ITGB3, JMJD1C, JUN, MAPRE3, MARCKS, MMP9, MYC, PPEF1, PTGS2, ROCK1, RUNX3, SORBS3, TNFRSF1B, TNFSF10
FOXL2		transcription regulator	Inhibited	-2.001	8.79E-03	CCL20, FOS, FST, ICAM1, IER3, IL12A, LIF, MAFF, NR5A2, PPARGC1A, PPP1R15A, PTGS2, SMAD6, SOD2, SOX4, SPRY1
CSF2RB		transmembrane receptor	Inhibited	-2.219	1.05E-02	BCL2, CCND2, FOS, JUN, MYC, SNAP23
HDAC5		transcription regulator	Inhibited	-2.646	1.11E-02	CDKN1A, DAPK1, HES1, HK2, HLA-DRA, MAP3K3, MEF2C, MYC, PPARGC1A, PTEN, TNFRSF1A
MAP3K3	0.492	kinase	Inhibited	-2.2	1.24E-02	ADSSL1, BCL2, FOS, HAS2, IL8, JUN, SNAI2, TGFBR3
EPHB1		kinase	Inhibited	-2.224	1.31E-02	EGR1, EGR2, FOS, JUN, PTGS2
RHOA		enzyme	Inhibited	-2.491	1.34E-02	ACTA2, BAX, BCL2, CCND1, CDKN1A, CDKN1B, CEBPB, CTGF, FOS, GDF15, ICAM1, IL8, JUN, MMP9, RND3, RUNX2, SNAI2
IL17A		cytokine	Inhibited	-2.206	1.49E-02	BCL2, CCL2, CCL20, CEBPB, CEBPD, CTGF, CXCL13, CYTH3, DEFB4A/DEFB4B, DLX1, FAS, FOS, GUSB, HBEGF, HSPB8, ICAM1, IL16, IL1B, IL8, ITPR2, JUN, LOX, MMP9, NRP1, PTGS2, SPSB1, TIMP2, TLR4, VEGFA, YWHAG
CR2	0.122	transmembrane receptor	Inhibited	-2	1.54E-02	BCL2, CR2, FAS, IL1B
DNMT3B		enzyme	Inhibited	-2.688	1.63E-02	ABCD1, AHCTF1, BATF3, CDC25C, CDKN1A, EMILIN2, EPM2AIP1, HOXB13, IRF5, KDELR3, LONRF1, LXN, MAPRE3, MGST1, MID1, PRUNE2, RPP25, SLC30A1
MAP2K5	0.296	kinase	Inhibited	-2.411	1.68E-02	CCND1, FOS, JUN, KLF2, MEF2A, MMP9, PTGS2
FGFR1		kinase	Inhibited	-2.418	1.85E-02	BIRC5, CCND1, CCND2, CDKN1A, DNAJC1, EIF4G1, EIF5B, FGF2, FGFR3, FOS, HES1, JUN, MYC, PCSK1, PLAUR, PTGS2, PTPRA
TGFA	-1.34	growth factor	Inhibited	-2.907	1.94E-02	BIRC5, CASP1, CCL2, CCND1, CDKN1A, CEBPB, CTGF, ERRFI1, FOS, GJB1, ICAM1, IL8, MMP9, NR4A2, PLAT, PRNP, PTGS2, TGFA, VEGFA
IL1A		cytokine	Inhibited	-2.467	2.07E-02	ABCC2, ADAMTS1, ADORA2B, ALDH1A3, BCL2, BCL3, CCL2, CCL20, CDKN1A, DEFB4A/DEFB4B, F2RL1, FAS, FGF2, FOS, FTH1, GBP1, GNB4, HMOX1, ICAM1, IFNGR2, IGFBP5, IL1B, IL8, IRAK1, ITGB3, JUN, KIT, LIF, LOX, MCAM, MMP9, MT2A, MYC, NFKBIA, NR3C1, PTGES, PTGS2, SOD2, SPP1, TK1, UGT2B1
F3		transmembrane receptor	Inhibited	-2.611	2.22E-02	ANGPT1, CCL2, CTGF, EGR1, IL1B, IL8, MMP9, VEGFA
CXCR1		G-protein coupled	Inhibited	-2	2.69E-02	BAX, BCL2, CCND1, IL8
RELA		transcription regulator	Inhibited	-3.239	2.93E-02	APOE, BCL2, BCL3, BECN1, BIRC5, CAV1, CCL2, CCL20, CCND1, CDKN1A, CDKN1B, CEBPB, CFB, CR2, CXCR4, DDIT3, DEFB4A/DEFB4B, DGCR6, DUSP1, EGR1, FAS, FGF2, FOS, GDF15, GLI2, GRK5, HAS2, HES1, HIF1A, HMOX1, ICAM1, IER3, IFNGR2, IL12A, IL1B, IL7R, IL8, IRF4, JUN, KIT, LYN, MIA, MMP9, MYB, MYC, NAMPT, NFKBIA, NFKBIE, PTEN, PTGDS, PTGES, PTGS2, SDC4, SOD2, STIM1, TWIST1, UBE2H, VASP, VEGFA
IRS2	0.543	enzyme	Inhibited	-2.096	2.98E-02	ACACA, CDKN1B, EGR1, FASN, FOS, HMGCR, LPL, PPARGC1A, SLC2A1, VEGFA
LCK		kinase	Inhibited	-2.2	3.98E-02	ANXA1, CCNA2, CD2, FOS, JUN, KRT18, SOX2
PLAUR	-0.456	transmembrane receptor	Inhibited	-2.592	4.07E-02	ANG, CCL2, CCND1, ITGA6, ITGB3, KDR, MMP9, MYC, PLAUR
A2M		transporter	Inhibited	-3	4.07E-02	ATF6, BCL2, CCND1, DDIT3, EIF2A, FOXO1, MAP3K5, PPP1R15A, XBP1
THPO		cytokine	Inhibited	-2.241	4.37E-02	AURKB, BAX, BIRC5, CCNA2, CCND1, CCND2, FOS, ITGB3, KDR, MYC
CXCR4	-0.78	G-protein coupled	Inhibited	-2.736	4.37E-02	CCL2, CCND1, CXCR4, EGR1, ID1, ID2, IL8, MYC, RUNX2, TNFSF10
CSF2RA		transmembrane receptor	Inhibited	-2.216	4.42E-02	CCND2, FOS, JUN, MYC, SNAP23
TLR4	-0.247	transmembrane receptor	Inhibited	-2.804	4.99E-02	ADM, ADRBK1, ATM, BATF, BCL2, CCL2, CCND2, CD200, CDK6, CEBPD, CFB, CTSK, DAB2, DEFB4A/DEFB4B, E2F5, HBEGF, HHEX, HMOX1, ICAM1, IFIT2, IL12A, IL1B, IL8, ISG20, LMO4, MERTK, METTL1, MMP9, MYC, NFKBIA, PELI1, PLA1A, PLAT, PTGES, PTGS2, RGS1, RILPL1, RXRA, SLC6A12, SLCO3A1, SPP1, ST3GAL1, STAT2, TCF4, TIMELESS, TLR4, TNFSF10, TSC22D1, XBP1
CTNNB1		transcription regulator	Inhibited	-2.799	5.10E-02	ABCC1, ACTA2, ADSS, AHR, AKAP13, ALG3, ANXA1, ARL4A, ATM, BCL2, BIRC5, BMP1, CALM1, CASC4, CCNA2, CCND1, CCND2, CDKN1A, CEACAM1, CTDSPL, CTGF, DIAPH3, DKK1, EOMES, ETV4, F2R, FAS, FCER1G, FEN1, FOS, FOSL1, FSTL3, FZD7, GHR, GJB1, GLI2, GNA12, HHEX, HMG20B, HOXA5, ID2, ID3, IGFBP5, IL1B, IL8, IRF4, ITGA6, JUN, LAMB1, LEF1, LPL, MAP3K11, MCL1, MITF, MMP16, MMP9, MYC, MYLK, NPTX1, NRCAM, PAX3, PDE4B, PHLDA2, PLAUR, PMP22, POU3F2, PTGS2, RAI14, RCN1, RUNX2, SEC61A1, SEMA3C, SFRP1, SIM2, SLC1A5, SMAD6, SNAI2, SORBS3, SOX2, SOX4, SPP1, STXBP1, SYK, SYNM, TCF4, TCF7L2, TGFA, TIMP3, TLE4, TMEM2, TNC, TSC22D1, TWIST1, VCAN, VEGFA, ZNF624
MYCN		transcription regulator	Inhibited	-2.051	5.22E-02	ABCC1, ARPC1B, BAX, BID, BIRC5, BMI1, CAV1, CCND1, CCND2, CDKN1A, CDKN1B, CKAP4, COL5A2, CTGF, DKK3, E2F2, E2F5, EIF4A1, FRMD6, HK2, HMGA1, HSP90AB1, HSPD1, ID2, JARID2, LRRN3, MXI1, NCL, NUCB1, OLIG1, PHB, PTK2, RPL29, RPL6, RPL7, RPL9, RPS7, SLC25A19, SLC2A1, SORD, TIMP2, TNFRSF1A, WAC, ZEB2, ZFAND5, ZYX
FHL2		transcription regulator	Inhibited	-2	8.77E-02	ACTA2, BCL2L11, CCND1, IL8, MITF, SPP1
LRP1		transmembrane receptor	Inhibited	-2.425	1.07E-01	C1R, C1S, DDIT3, MMP9, PLIN2, PTGS2
C5		cytokine	Inhibited	-2.128	1.13E-01	BCL2, CCL2, CCND1, EFNB2, EGR1, FCGR2A, GDF15, ICAM1, IFNGR2, IL12A, IL1B, IL8, NFKBIA, PLAT, PPP1R15A, SLC25A15, ST6GAL1, VEGFA, ZFP36
IKBKE		kinase	Inhibited	-2.485	1.81E-01	BCL2, CCND1, CDKN1B, IFIT2, IL8, MMP9, MYC, NFKBIA, PTGS2
GHRL		growth factor	Inhibited	-2.195	2.01E-01	ACACA, BCL2, BDNF, FASN, FOS, IL1B, LPL, PTGS2, SPP1
TLR7		transmembrane receptor	Inhibited	-2.06	2.14E-01	BCL2, CCL2, CCL20, CREB5, FAIM3, FAM19A4, FGF2, HIVEP2, ICAM1, IER3, IL1B, IL8, NFKBIA, PLAT, TMEM154
TBK1		kinase	Inhibited	-2.288	2.35E-01	ATM, ICAM1, IFIT2, IL12A, IL1B, IL8, ISG20, PLA1A, PTGS2, RILPL1, SLCO3A1, TSC22D1, VEGFA
HSPD1	-0.238	enzyme	Inhibited	-2.219	2.39E-01	BAX, HSPD1, ICAM1, IL12A, IL1B
CARM1		transcription regulator	Inhibited	-2	2.39E-01	EGR3, ICAM1, MYC, PTGES, STC2
GDNF		growth factor	Inhibited	-2.184	3.01E-01	BDNF, CCND1, CDKN1B, EGR1, EGR2, ITGA6, KIT, SPHK1, STC1, TUBB4A, VASP
IL6ST		transmembrane receptor	Inhibited	-2.579	3.07E-01	ATP2A2, CCND1, EGR1, JUN, MYC, PIM2, TNFRSF1A, TNFRSF1B
HDAC6	0.174	transcription regulator	Inhibited	-2	3.17E-01	BIRC5, HIF1A, JUN, MYC, SRSF2, TPH2
TLR2		transmembrane receptor	Inhibited	-2.012	3.36E-01	CCL2, CCR1, CEBPB, CEBPD, DEFB4A/DEFB4B, DUSP1, HLA-DRB1, HMOX1, ICAM1, IL1B, IL8, IRAK1, ITGA4, KLF2, MMP9, PTGS2, TLR4, VDR, XBP1
IL18		cytokine	Inhibited	-2.131	4.02E-01	BCL2, CCL2, CCL20, CXCL16, FAS, ICAM1, IL12A, IL1B, IL8, IRF9, JUN, MMP9, PTEN, PTGS2, TGFBR2, TLR4, TXK, VEGFA
IL22		cytokine	Inhibited	-3.095	5.01E-01	ACTA2, BCL2, CCND1, DEFB4A/DEFB4B, HMOX1, HSPB1, IL1B, IL8, MCL1, MYC
TLR5		transmembrane receptor	Inhibited	-2.2	5.07E-01	CCL20, DEFB4A/DEFB4B, ICAM1, IL1B, IL8
DNMT1		enzyme	Inhibited	-2.189	1.00E+00	ASIP, BIRC5, CDC25C, CDKN1A, CDKN1B, MT1E